CHEMISTRY HALL LIBRARY

OHIO STATE UNIVERSITY
OCT 23 1959
LIBRARY

BULLETIN
OF THE
CHEMICAL SOCIETY OF JAPAN

Vol. 32 No. 9 September 1959

CONTENTS

General and Physical

T. MORITA: Bond Localization and the Hyperconjugative Effect in the Aromatic Carbonium Ions. II. Electronic Structures of the Carbonium Ions of Isomeric Xylenes 893

H. CHIHARA and S. SEKI: Studies on Crystal Hydrates. IV. Dehydration and Rehydration, Stable and Metastable Equilibria and Transition between Hydrate Modifications of Potassium Mercury(II) Chloride Monohydrate, $K_2HgCl_4 \cdot H_2O$ 897

H. CHIHARA and K. NAKATSU: Studies on Crystal Hydrates. V. Zeolitic Dehydration of DL-Tris-ethylenediamine-cobalt(III) Chloride Hydrate, DL-$[Co\ en_3]Cl_3 \cdot nH_2O$. Sorption and Desorption of Water Vapor. A Preliminary Study of the Dielectric Properties. 903

H. CHIHARA: Studies on Crystal Hydrates. VI. Thermodynamics of Dehydration of Crystal Hydrates. A New Criterion for the Continuous Zeolitic Dehydration. Capillary Condensation of Water Vapor into Exactly Uniform Pores and an Experimental Test of the Kelvin Equation. Case of DL-Tris-ethylenediamine-cobalt(III) Chloride Hydrate. 908

I. YASUMORI: Quantum-Mechanical Considerations of Chemical Reaction Rates. II. The Transmission through Curved Reaction Path. 913

H. IMAI, S. INOUYE and S. CHAKI: Studies on the Vibrated Dropping Mercury Electrode. I. The Theory of the Limiting Current and its Application to the Electrocapillarity. . . 994

T. ABE: Visible and Ultraviolet Absorption Spectra of Red Complexes of 1,3,5-Trinitrobenzene and its Derivatives with Ammonium Hydroxide 997

Analytical and Inorganic

S. HASHIMOTO: The Reaction of the Aquopentamminechromium(III) Complex Ion in Aqueous Solution. I. Substitution Reaction of a Coordinated Water with a Chloride Ion 945

S. KIDA: Investigation on Mixed Complexes. II. Cyano Complexes of Copper and Nickel. 981

Organic and Biological

S. TAKEMURA: Hydrazinolysis of Nucleic Acids. I. The Formation of Deoxyribopyrimidinic Acid from Herring Sperm Deoxyribonucleic Acid 920

S. TAKEMURA and M. MIYAZAKI: Hydrazinolysis of Nucleic Acids. II. The Formation of Ribo-apyrimidinic Acid from Yeast Ribonucleic Acid 926

T. OKUDA: Amino Acid Synthesis from Nitromalonic Ester. III. Note on the Synthesis of Glutamic Acid 931

Y. IZUMI: Studies on the Silk-Palladium Catalyst. I. Preparation and Stability 932

Y. IZUMI: Studies on the Silk-Palladium Catalyst. II. General Properties 936

Y. IZUMI: Studies on the Silk-Palladium Catalyst. III. Physicochemical Characterization . 942

(Continued on inside cover)

Published by the Chemical Society of Japan

THE CHEMICAL SOCIETY OF JAPAN

(NIPPON KAGAKUKAI)

Founded in 1948

Successor to the former Chemical Society of Japan founded in 1878 and to the Society of Chemical Industry, Japan founded in 1898.

OFFICERS

Munio KOTAKE, *President*, Osaka University, Osaka
Jurô HORIUTI, *Vice-President*, Hokkaido University, Sapporo
Teiji ICHIKAWA, *Vice-President*, Hiroshima University, Hiroshima
Eiichi IWASE, *Vice-President*, Institute of Physical and Chemical Research, Tokyo
Kenichi YAMAMOTO, *Vice-President*, Waseda University, Tokyo

BULLETIN OF THE CHEMICAL SOCIETY OF JAPAN

Editor: Yoshiyuki URUSHIBARA, The University of Tokyo, Tokyo
Assistant Editor: Saburo NAGAKURA, The University of Tokyo, Tokyo
Editorial Board:

Toshio ANDO	Kei MATSUZAKI	Tadao SHIBA
Genjiro HAZATO	Koji NAKANISHI	Osamu SIMAMURA
Kenichi HONDA	Shigeo OKUMURA	Tadashi SUEHIRO
Isao ICHISHIMA	Kazuo SAITO	Kenzi TAMARU
Masaji KUBO	Naoyasu SATA	Takeo WATASE
Hisao KUROYA	Tetsuro SEIYAMA	Tsuneo YOSHINO

(*Continued from outside cover*)

M. ŌKI and H. IWAMURA: Intramolecular Interaction between Hydroxyl Group and π-Electrons. IV. Rotational Isomers of Alcohols and Shift of ν_{O-H} Absorptions in Phenyl Substituted Alcohols 950

M. ŌKI and H. IWAMURA: Intramolecular Interaction between Hydroxyl Group and π-Electrons. V. Electronic Effect in Arylcarbinols and a Preliminary Note on the Interaction in Benzylaniline Derivatives 955

Y. TSUNO, T. IBATA and Y. YUKAWA: Resonance Effect in Hammett Relationship. I. The Substituent Effect in the Acid Catalyzed Decompositions of ω-Diazoacetophenones in Acetic Acid 960

Y. YUKAWA and Y. TSUNO: Resonance Effect in Hammett Relationship. II. Sigma Constants in Electrophilic Reactions and their Intercorrelation 965

Y. YUKAWA and Y. TSUNO: Resonance Effect in Hammett Relationship. III. The Modified Hammett Relationship for Electrophilic Reactions 971

T. TAKESHITA and M. KITAJIMA: Stereoisomers of 2,3-Camphane Diols 985

N. YATA: Decomposition Temperature of Urea Adducts. 991

Short Communications

S. MURAHASHI, B. RYUTANI and K. HATADA: Infrared Spectroscopic Study on Hydrogen Bond Formation between Acetylene and Donor Solvents. 1001

T. FUENO, K. ASADA, K. MOROKUMA and J. FURUKAWA: Polarographic Half-Wave Reduction Potentials of Vinyl Compounds and their Molecular Orbital Computation. 1003

K FUJITA: The Abnormal Relation between the Viscosities and the Temperatures of Sodium Carbonate Solution 1004

T. MASAMUNE and M. KOSHI: The Syntheses and Exhaustive Methylation of *cis*- and *trans*-1,2,3,4,5,6,4a,4b-Octahydrobenzo(f)quinoline 1005

K. HARADA: Thermal Homopolymerization of Lysine and Copolymerization with Neutral and Acidic Amino Acids. 1007

CHEMISTRY HALL LIBRARY

Bond Localization and the Hyperconjugative Effect in the Aromatic Carbonium Ions. II[1]*. Electronic Structures of the Carbonium Ions of Isomeric Xylenes*

By Toshifumi MORITA

(Received October 2, 1958)

Concerning the basic character of unsaturated hydrocarbons, there are several theoretical investigations[2-7] which have their theoretical standpoints on the localization of the C–H_2 bond of their carbonium ions. There are no reasons, however, for fixing the electronic structure of carbonium ions to only the bond localization one; in general, hyperconjugation of H_2 quasi-atom should also be taken into account. In this paper, the need for introduction of hyperconjugation will be revealed for protonated compounds of isomeric xylenes on the basis of the experimental basicity constants[8].

Dependence of Basicity of Isomeric Hydrocarbons on the π-Electron Energies of their Carbonium Ions

Gold and Tye[2], and also Heilbronner and Simonetta[3] have shown that the equilibrium constant K for carbonium ion formation is expressed as

$$-\boldsymbol{RT}\ln K = E_{BH^+} - E_B + \text{constant} \qquad (1)$$

where E_{BH^+} and E_B are π-electron energies of the aromatic carbonium ion, BH^+, and of the parent base, B, respectively. From Eq. 1, the following equation for the ratio of two K's is obtained:

$$K^{I}/K^{II} = \exp(-A/\boldsymbol{RT}) \qquad (2)$$

where

$$A = (E^{I}_{BH^+} - E^{II}_{BH^+}) - (E^{I}_{B} - E^{II}_{B}) \qquad (3)$$

Here superscripts I and II refer to either of the two isomeric types of a particular hydrocarbon.

In the case of xylene isomers, $E^{I}_{B} - E^{II}_{B}$ will be estimated from the empirical hyperconjugation energies obtained by Coulson and Crawford[9]. They have indicated that the empirical hyperconjugation energies per methyl group are 1.48, 1.39 and 1.27 kcal./mol. for *m*-, *p*- and *o*-xylenes, respectively. This shows that *m*-xylene is more stable than *p*-xylene by 0.18 kcal./mol., and *o*-xylene is less stable than *p*-xylene by 0.24 kcal./mol.

Now, from the evaluation of π-electron energies of protonated compounds, the basic strengths of *m*- and *o*-xylenes relative to that of *p*-xylene will be estimated by the use of Eqs. 2 and 3.

Consideration of Basicity of Isomeric Xylenes from the Standpoint of Bond Localization Model of their Carbonium Ions

There are several available points of proton attack in each isomer, and the position of highest proton affininity will be determined as that which makes the π-electron energy of the carbonium ion minimum. Now it will be indicated in the following discussion that only by the bond localization hypothesis the basic behaviors of isomeric xylenes can not be understandable. π-Electron energies of carbonium ions necessary for these considerations are calculated for all possible models with respect to the positions of proton attack on the basis of the bond localization hypothesis, using the semi-empirical LCAO MO method and solving numerically the secular equations constructed by the usual variational method. Several assumptions adopted in these calculations are as follows:

(1) the overlaps between the nearest neighboring atomic orbitals are included; (2) the resonance integral including overlap is proportional to the corresponding

1) Part I, T. Morita, This Bulletin, **31**, 322 (1958).
2) V. Gold and F. L. Tye, *J. Chem. Soc.*, **1952**, 2184.
3) E. Heilbronner and M. Simonetta, *Helv. Chim. Acta*, **35**, 1049 (1952).
4) E. L. Mackor, G. Dallinga, J. H. Kruizinga and A. Hofstra, *Rec. trav. chim.*, **75**, 836 (1956).
5) G. Dallinga, A. A. V. Stuart, P. J. Smit and E. L. Mackor, *Z. Elektrochem.*, **61**, 1019 (1957).
6) E. L. Mackor, A. Hofstra and J. H. van der Waals, *Trans. Faraday Soc.*, **54**, 66 (1958).
7) E. L. Mackor, A. Hofstra and J. H. van der Waals, ibid., **54**, 186 (1958).
8) M. Kilpatrick and F. E. Luborsky, *J. Am. Chem. Soc.*, **75**, 577 (1953).
9) C. A. Coulson and V. A. Crawford, *J. Chem. Soc.*, **1953**, 2052.

overlap integral: $\beta_{C\text{-}H_2}=\beta_{C\text{-}H_3}=2.19\beta$ and $\beta_{C(ring)\text{-}C(methyl)}=0.8\beta$, where $\beta_{C\text{-}H_2}$ is the resonance integral between H_2 quasi-atom and the ring carbon atom connecting with it, $\beta_{C\text{-}H_3}$ is that between H_3 quasi-atom and carbon atom in the methyl group, $\beta_{C(ring)\text{-}C(methyl)}$ is that between the ring- and the methyl- carbon atoms, and β is that between the neighboring atoms in the benzene molecule; the other resonance integrals are taken to be β; (3) the Coulomb integral of H_2 or H_3 quasi-atom is taken as $\alpha_{H_2}=\alpha_{H_3}=\alpha-0.3\beta$, and that of the carbon atom next to H_2- or H_3-group is taken as $\alpha_{C(-H_2)}=\alpha_{C(-H_3)}=\alpha-0.1\beta$, where α is the Coulomb integral of a carbon atom of benzene molecule; the other Coulomb integrals are taken to be α.

Computational results are shown in Table I and in Fig. 1. Charge distributions of parent bases calculated by Crawford[10] are 1.0093, 1.0081 and 0.9995 at the positions 2, 4 and 5 in *m*-xylene (1,3-dimethylbenzene) and 1.0044 and 1.0035 at the positions 3 and 4 in *o*-xylene (1,2-dimethylbenzene), respectively. Inspection of these charge distributions predict the order of proton acceptance. Between this order of proton affinity and stabilities of protonated compounds (Table I), a parallel relation exists. This correlation agrees with experimental reactivity of electrophilic substitution except for the position 2 of *m*-xylene, which may be supposed to have low proton affinity because of the steric effect of two neighboring methyl groups, although it is theoretically the most active toward a proton. From their hydrogen isotope exchange reaction studies, Lauer et al.[11] have indicated that relative reactivity of the position 2 to 4 of *m*-xylene is 0.58 : 1.0. We must take such a fact into account. In *m*-xylene, numbers of position of proton attack will be 2.58 and the energy of its probable carbonium ion will be weighted mean of energies of Models I and I′. For *o*-xylene carbonium ion, the stabilities of Models III and III′ are identical, being in agreement with experimental reactivity, halogenation or nitration of *o*-xylene. We assume the energy of protonated *o*-xylene to be the mean of Models III and III′.

TABLE I. π-ELECTRON ENERGIES OF THE CARBONIUM IONS OF XYLENE ISOMERS (BOND LOCALIZATION MODELS)

Carbonium ions	Models	π-Electron energies (units of $-\beta$)
m-Xylene-	I	−11.4819
	I′	−11.5342
	I″	−11.4444
p-Xylene-	II	−11.4905
o-Xylene-	III	−11.4914
	III′	−11.4806

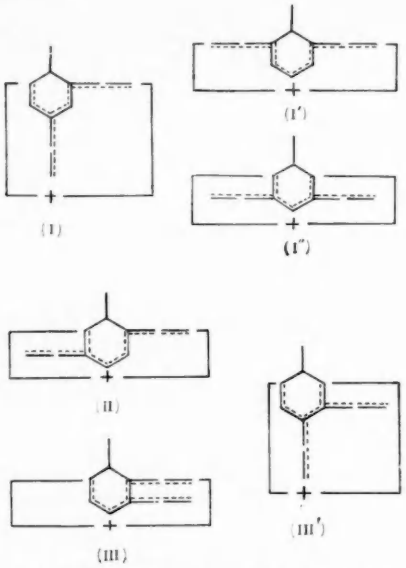

Fig. 1. Models of xylene carbonium ions.
I, I′ and I″: *m*-xylene carbonium ion
II : *p*-xylene carbonium ion
III, III′ : *o*-xylene carbonium ion

The ratio of basicity constants of *m*- and *o*-xylenes to that of *p*-xylene is estimated to be respectively 26 and 1.1 at 20°C from the measurement on the mixtures of these substances with anhydrous hydrogen fluoride[8]. In comparing these values experimentally observed with those theoretically calculated, it must be noticed that the number (Z) of positions of the highest proton affinity of *m*-, *o*- and *p*-xylenes are different from one another. For *m*-xylene, from our treatment mentioned above, $Z=2.58$. For *o*- and *p*-xylenes $Z=4$. Taking these Z values into consideration, the experimentally observed ratio of the reduced basicity constant[6] of *m*-xylene to that of *p*-xylene becomes 40.3 instead of 26, which is in disagreement with the theoretically calculated value, 1.0, using Eqs. 2 and 3. In the case of *o*-xylene, the experimental and theoretical values of K^{III}/K^{II} are 1.1 and 1.0, respectively, so the agreement between these two values

10) V. A. Crawford, ibid., **1953**, 2058.
11) W. M. Lauer, G. W. Matson and G. Stedman, *J. Am. Chem. Soc.*, **80**, 6437 (1958); see also, E. L. Mackor, P. J. Smit and J. H. van der Waals, *Trans. Faraday Soc.*, **53**, 1309 (1957).

is satisfactory[12]. Thus, basic behavior of isomeric xylenes is not understood by the bond localization hypothesis alone. It is natural to take hyperconjugation further into consideration, as is seen in the following section.

π-Electron Structures of Isomeric Xylene Carbonium Ions

In the following, as an example, the relative basicity of *m*-xylene compared to *p*-xylene will be discussed. From Eq. 3, A can be written as follows:

$$A=\{E^{I}_{BH^+}-(E^{I,0}_{BH^+}+0.18)\}$$
$$-\{E^{II}_{BH^+}-E^{II,0}_{BH^+}\}-\{E^{I}_{B}-E^{II}_{B}\} \quad (4)$$

where, $E^{I}_{BH^+}$ is the π-electron energy for the actual state of the *m*-xylene carbonium ion, $E^{II}_{BH^+}$ is the similar quantity for the *p*-xylene carbonium ion; $E^{I,0}_{BH^+}$ and $E^{II,0}_{BH^+}$ are the π-electron energies for the bond localization models of protonated *m*- and *p*-xylenes, respectively; E^{I}_{B} and E^{II}_{B} are the π-electron energies of *m*- and *p*-xylenes, respectively; the numerical value 0.18 in the right hand side of Eq. 4 is necessary for making $(E^{I,0}_{BH^+}+0.18)=E^{II,0}_{BH^+}$. This value, which is expressed in the unit of kcal./mol. by the use of $\beta=-60$kcal./mol.[12], estimated by comparing the weighted mean of π-electron energies of types I and I′ for protonated *m*-xylene with the energy of type II for protonated *p*-xylene. Taking $E^{I}_{B}-E^{II}_{B}=0.18$ kcal./mol., Eq. 4 becomes as follows:

$$A=-x+c \quad (5)$$

where

$$-x=E^{I}_{BH^+}-E^{I,0}_{BH^+} \quad (6)$$

and

$$-c=E^{II}_{BH^+}-E^{II,0}_{BH^+} \quad (7)$$

The quantities x and c indicate respectively the stabilization energies through hyperconjugation of H_2 quasi-atom in the actual states of *m*- and *p*-xylene carbonium ions compared with their bond localization models. Experiments show $K^{I}/K^{II}=40.3$[13] at 20°C, consequently from Eqs. 2, 3 and 5, we obtain

$$x=c+8.2 \quad (8)$$

Eq. 8 shows that, if the difference of hyperconjugation energies between protonated *m*- and *p*-xylenes is about eight kcal./mol., the experimentally observed basic behavior of *m*- and *p*-xylenes is understandable. A similar consideration suggests that no change in the hyperconjugation energies exists between *o*- and *p*-xylene carbonium ions. Indeed,

$$x=c+0.09$$

Here it will be noticed that the hyperconjugation energy of protonated *m*-xylene is the weighted mean of hyperconjugation energies by the methylene group for models I and I′, and that of protonated *o*-xylene is the weighted mean for the models III and III′. The value, 8.2 kcal./mol., of change in hyperconjugation energies between protonated *m*- and *p*-xylenes seems too great at first sight. This large difference may not be unreasonable, however, since the substances in question are the so-called "strongly hyperconjugated" systems[14,15].

Discussion

Brown and Brady[16] have shown that change in solvolysis rates between meta- and para-methyl substituted phenyldimethylcarbinyl chloride is explained reasonably, though qualitatively, in terms of valence bond structures. On the stabilities of the protonated isomeric xylenes also, treatment by means of valence bond structures may not be overlooked, and will be tried in the following way.

Model I of protonated *m*-xylene can resonate among three A (AI, AI_1 and AI_2), one B and one C structures (Fig. 2), according to Brown and Brady[16]. However, additional hyperconjugated structures by the two methyl substituents should be taken into account, such as four D, six E, one F, one G and five H structures. The number of resonance structures is altogether twenty-two (Fig. 2). For the models I′, I″, II, III and III′ similar types of resonance structures are considered. Numbers of resonance structures belonging to these types are indicated in Table II. Inspection of Table II suggests that model I is as stable as model I′, model I″ being less stable, and model III will possibly be more stable than model III′. Model I will probably be stable to almost

12) In these calculations, the unit of energy is expressed in kcal./mol. by the use of $\beta=-60$ kcal./mol. See, C. C. J. Roothan and R. S. Mulliken, *J. Chem. Phys.*, **16**, 118 (1948).

13) Here K means the reduced basicity constant.

14) N. Muller and R. S. Mulliken, *J. Am. Chem. Soc.*, **80**, 3489 (1958).

15) N. Muller, L. W. Pickett and R. S. Mulliken, ibid., **76**, 4770 (1954).

16) H. C. Brown and J. D. Brady, ibid., **74**, 3570 (1952).

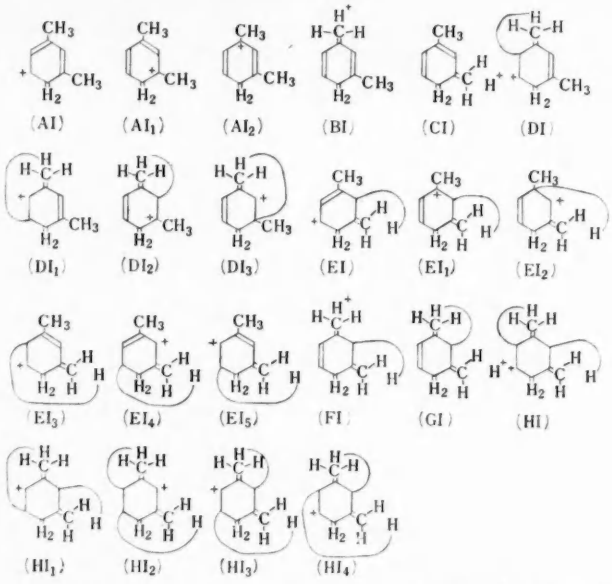

Fig. 2. Valence bond structures of model I of protonated *m*-xylene.

TABLE II. NUMBERS OF THE VALENCE BOND STRUCTURES

Models	A	B	C	D	E	F	G	H	Total
I	3	1	1	4	6	1	1	5	22
I'	3	1	1	5	6	2	2	3	23
I''	3	0	0	0	0	0	0	5	8
II	3	0	1	4	4	1	1	5	19
III	3	0	1	4	7	2	2	3	22
III'	3	1	0	4	4	1	1	2	12

the same extent as model III, which will be more stable than model II. These results are partly in disagreement with experiments. It may be said, however, that the difference of the stability of protonated compounds of xylene isomers will be attributable to that of numbers of hyperconjugation structures by the methyl group, irrespective of hyperconjugation or localization of the methylene.

From their electron spin resonance measurements of isomeric xylene negative ions, Tuttle, Jr. and Weissman[17] have indicated that methyl groups show hyperconjugation in a different manner among these substances and are more hyperconjugated in the *m*-xylene than in the *o*- and *p*-xylene negative ions. As has been hitherto accepted, the hyperconjugation phenomenon seems not so simple but complicated. At all events, it may be likely that the manner in which hyperconjugation occurs depends greatly on the environment of a methyl group.

17) T. R. Tuttle, Jr. and S. I. Weissman, ibid., **80**, 5342 (1958).

Summary

By means of the LCAO MO method, the π-electron energies of xylene carbonium ions are calculated, for all possible models, with respect to the positions of proton attack, on the basis of the bond localization hypothesis. It is indicated that the explanation of the basic behaviors of isomeric xylenes is impossible merely by the bond localization theory of their carbonium ions, and hyperconjugation should be taken into account.

It is indicated that, when the difference of hyperconjugation energies between protonated *m*- and *p*-xylene is about eight kcal./mol., the experimentally observed basic behavior of *m*- and *p*-xylenes is understandable.

The author wishes to thank Professor T. Titani (Tokyo Metropolitan University) for his interest, and Professor A. Kotera (Tokyo University of Education) for his guidance and instructive discussion.

Department of Chemistry
Tokyo Metropolitan University
Setagaya-ku, Tokyo

Studies on Crystal Hydrates. IV. Dehydration and Rehydration, Stable and Metastable Equilibria and Transition between Hydrate Modifications of Potassium Mercury(II) Chloride Monohydrate, $K_2HgCl_4 \cdot H_2O$*

By Hideaki CHIHARA and Syûzô SEKI

(Received February 13, 1959)

Numerous reports may be found in the literature of the subject as to the dehydration and rehydration of crystal hydrates, but there are few investigations based on the exact thermodynamical precautions. Atomistic interpretation of the phenomena related to the behavior of water molecules in the dehydration reaction seems to have insufficient ground to advance. One of the principal reasons for this seems to be that there are complexities which enable us to obtain a material at the well-defined thermodynamical as well as molecular state only with extreme difficulty. Dehydration can frequently produce amorphous or colloidal material which gradually changes to stable crystalline solids[1]. Different methods of preparation sometimes produce materials of different free energy[2].

Many hydrates undergo phase transitions prior to dehydration in the heating experiments[3]. A study of the mechanism of such transitions will assist in understanding the law governing the dehydration reaction.

In the present paper, another example of the difficulty of obtaining the true equilibrium will be presented. It was inferred that $K_2HgCl_4 \cdot H_2O$ might undergo "zeolitic" dehydration, from its crystal structure[4], in which water molecules are packed in channel-like interstices. Although the direct evidence of such type of dehydration was not obtained, a consideration of the entropy of dehydration let us conclude that this is the case. An X-ray diffraction study of the phase transition and the rehydration will be briefly reported.

* The Report III may be found in This Bulletin, **30**, 674 (1957).

1) H. Chihara and S. Seki, This Bulletin, **30**, 674 (1957); G. B. Erost, K. A. Moon and E. H. Tompkins, *Can. J. Chem.*, **29**, 604 (1951); H. W. Quinn, R. W. Missen and G. B. Frost, ibid., **33**, 286 (1955); R. C. W. Wheeler and G. B. Frost, ibid., **33**, 546 (1955).

2) W. F. Giauque, *J. Am. Chem. Soc.*, **71**, 3192 (1949).

3) H. Chihara and S. Seki, This Bulletin, **26**, 88 (1953).

4) C. H. MacGillavry, J. H. de Wilde and J. M. Bijvoet, *Z. Krist.*, **100**, 212 (1938).

Experimental

Material. — KCl: Takeda Co., first grade. Purified by recrystallization from water.

$HgCl_2$: Takeda Co., analytical grade. Recrystallized from water. $K_2HgCl_4 \cdot H_2O$: Crystals were prepared according to the phase diagram[5] of the system KCl-$HgCl_2$-H_2O which is reproduced in Fig. 1. Because amorphous samples were often obtained depending on the method of preparation as will be described later, the following procedure was found most satisfactory by analogy of the system $MnCl_2$-NH_4Cl[6]. A saturated solution corresponding to the point a in Fig. 1 (25°C) was

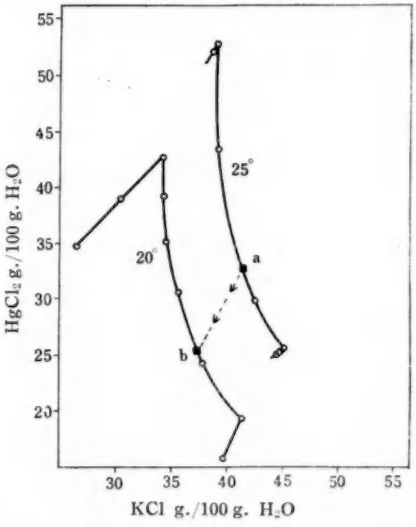

Fig. 1. Solution equilibrium diagram of the system KCl-$HgCl_2$-H_2O. Only a portion corresponding to the solid composition $K_2HgCl_4 \cdot H_2O$ is shown.

slowly cooled down to 20°C. A calculation shows that the solution changes its composition along the line a→b. The precipitate was filtered with a glass filter, pulverized, and then returned to

5) A. Seidell, "Solubilities of Inorganic and Metal Organic Compounds", 3rd Ed., Vol. 1, D. Van Nostrand Co., New York (1940), p. 624.

6) A. L. Greenberg and G. H. Walden, Jr., *J. Chem. Phys.*, **8**, 645 (1940); A. Grenall, ibid., **17**, 1036 (1949).

the mother solution for ten days in a closed vessel, being occasionally shaken. The X-ray photograph of the precipitate finally filtered was entirely consistent with the reported crystal structure[4].

Measurements of the Dehydration Pressures.—The dehydration pressures were measured by a simple mercury-in-glass manometer with the help of a traveling microscope to within ±0.01 mmHg. The water thermostat was kept at constant temperatures to within 0.005°C. In the experiment of the isothermal dehydration, the water vapor was trapped into a small capillary and weighed. The amount dehydrated was corrected for the mercury vapor condensing from the manometer into the trap.

Dehydration Equilibrium

The dehydration pressures of the crystalline $K_2HgCl_4 \cdot H_2O$ were measured between 26 and 40°C and the results are plotted in Fig. 2 by squares. The pressure equation is

$$\log P(\text{mmHg}) = 8.538 - (2161/T) \qquad (1)$$

The heating and cooling data were perfectly coincident within the experimental error and it was ascertained that equilibrium was attained with no hysteresis effect. The heat, the entropy, and the free energy of dehydration are given in Table I.

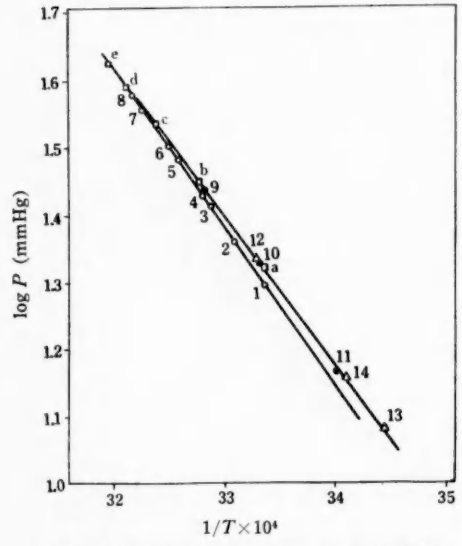

Fig. 2. Dehydration pressures of $K_2HgCl_4 \cdot H_2O$; □, crystalline hydrate (equilibrium data) (a-e); ○, heating direction of partly amorphous hydrate (1-8); ●, cooling direction of partly amorphous hydrate (9-11); △, subsequent heating and cooling measurements with partly amorphous hydrate (12-14).

TABLE I. CHANGES OF THE HEAT CONTENT, THE ENTROPY AND THE FREE ENERGY BY DEHYDRATION OF $K_2HgCl_4 \cdot H_2O$

ΔH kcal./mol.	ΔS cal./mol. deg.	ΔG at 25°C kcal./mol.
9.50	25.9	2.18

Results for Partly Amorphous Samples.—KCl 12.227 g. and $HgCl_2$ 15.459 g. were mixed with water 20 cc. and the solid was dissolved completely at high temperature by preventing evaporation. The solution was then cooled down to and kept at 20°C. It was deeply supercooled and no precipitation occurred before the entire solution reached 20°C. The solid precipitate after a few hours had the composition corresponding to $K_2HgCl_4 \cdot H_2O$ and the solution contained KCl 7.11 g. and $HgCl_2$ 6.13 g. The X-ray powder photograph of the solid thus prepared, however, showed that it was partly amorphous. The Debye rings, though faint, were consistent with the reported crystal structure of the hydrate[4]. The dehydration pressure of the partly amorphous hydrate showed a hysteresis phenomenon according to the pressure equations:

$$\log P(\text{mmHg}) = 9.139 - (2359/T)$$
in heating direction (2)

$$\log P(\text{mmHg}) = 8.595 - (2180/T)$$
in cooling direction (3)

The results are shown by open circles (heating direction) and by solid circles (cooling direction) in Fig. 2. The results of the subsequent heating and cooling experiments are indicated by triangles. It took about 20 days to reach an apparent dehydration equilibrium as compared with a few minutes in the case of the crystalline sample at 24.03°C.

The experiments of isothermal dehydration were made at 34.13°C. The initial formula of the hydrate was $K_2HgCl_4 \cdot 0.997 H_2O$. The constant value of the dehydration pressure was reached only after about 280 days (see Fig. 3). The calculated pressure from Eq. 2 was 31.09 mmHg and the apparent coincidence was good. The second equilibration with the composition $K_2HgCl_4 \cdot 0.965H_2O$ (water 0.032 mol. was taken from the original hydrate) was much slower than the first and then it was felt that further dehydration might accelerate the approach to the equilibrium. The third run, however, was even slower,

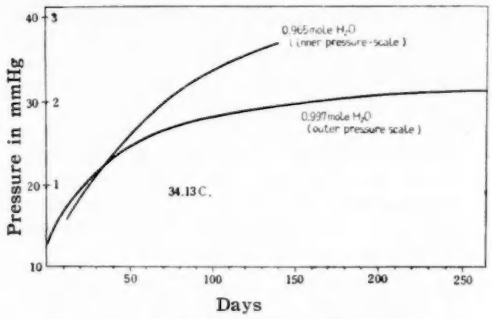

Fig. 3. Approach to the apparent equilibrium of isothermal dehydration of partly amorphous sample.

with 0.809 mol. of water per formula weight. The sample used in this experiment was taken out of the apparatus and examined by the X-rays. It was still partly amorphous but the crystallization seemed to have proceeded during the pressure measurements (longer than two and half years).

The differential thermal analysis of the partly amorphous sample gave only ill-defined peaks in comparison with the result for the crystalline sample which will be discussed below.

These results show that the crystallization of an amorphous solid is a very slow reaction at room temperature and that care must be exercised in the preparation of the solid substances, because an inadequate method of preparation sometimes produces materials of higher free energy than the one for the equilibrium product**.

Entropy of Dehydration

The value of entropy may be assigned to water molecules in the hydrate crystal by subtracting the experimental entropy of dehydration from the standard entropy of water vapor 45.1 cal./deg. mol. This method gives for the present case 19.2 cal./deg. mol. which amounts to roughly twice as large a value as in average hydrate crystals and shows that the dehydration is "zeolitic".

Transition and Dehydration in Air

The results of the differential thermal analysis are given in Fig. 4 which shows two heat-absorption peaks at 114 and 123°C, with a fine structure in the former peak. The shoulder at 107°C always appeared in several runs but one at 117.6°C was not always reproducible.

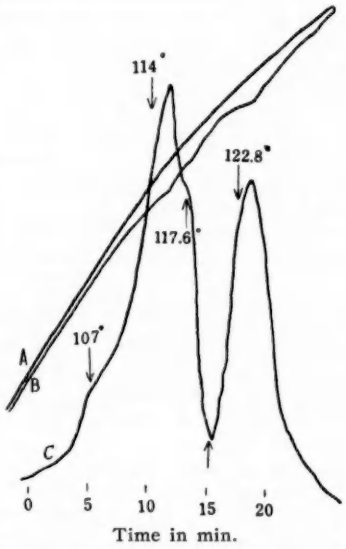

Fig. 4. Differential thermal analysis of crystalline $K_2HgCl_4 \cdot H_2O$; curve A, temperature of the reference NaCl powder; curve B temperature of the sample; curve C the temperature difference.

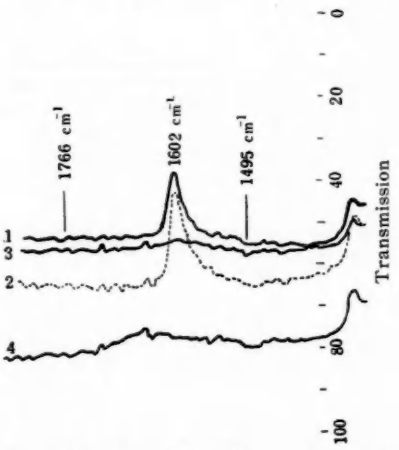

Fig. 5. Infrared spectra. (1) Room-temperature phase, (2) heated to 118°C, (3) heated to 130°C, (4) daifloil background.

There are evidences for the fact that the first peak at 114°C is due to a transition between two hydrate modifications

** A similar case is the dehydration and transition of $NiSO_4$ hexahydrate as reported by Simon and Knauer (*Z. anorg. u. allgem. Chem.*, 242, 375 (1939)).

7) Full discussion of the entropy of dehydration is given in Part VI (This Bulletin, 32, 908 (1959)).

and the second peak at 123°C is due to dehydration. There occurred no detectable evaporation and condensation of water in the apparatus of the thermal analysis[3] at the temperature between the two peaks, and also the infrared absorption spectrum*** of the hydrate crystals quenched from 118°C, at which the first heat effect completed its peak, retained the 6-micron absorption band of water (Fig. 5). The hydrate heated beyond the second heat-absorption temperature was not absorbed in this wavelength region; the heat absorption at 123°C is apparently due to dehydration.

An X-ray study was made of the transition of $K_2HgCl_4 \cdot H_2O$ at 114°C. The crystals were heated to 117°C in the apparatus of the differential thermal analysis (the transition was observed) and was rapidly cooled to room temperature and examined by the Norelco X-ray diffractometer. The scanning of the goniometer started about ten minutes after the sample was taken out of the heating vessel, with the scanning rate $2\theta = 0.5°$/min. The scanning was repeated according to the following succession:

12—61°, 35—46, 10—42, 10—35, 34—27 (reversely), 26—34, 10—14, 23—26, 28—31, 45—47, in 2θ values.

It took about 5.5 hr. for this series of scanning. The scanning was then repeated every day for the following six days. The change in the diffraction patterns with time was bewildering during the first few hours. Some of the typical results are reproduced in Fig. 6. The diffraction

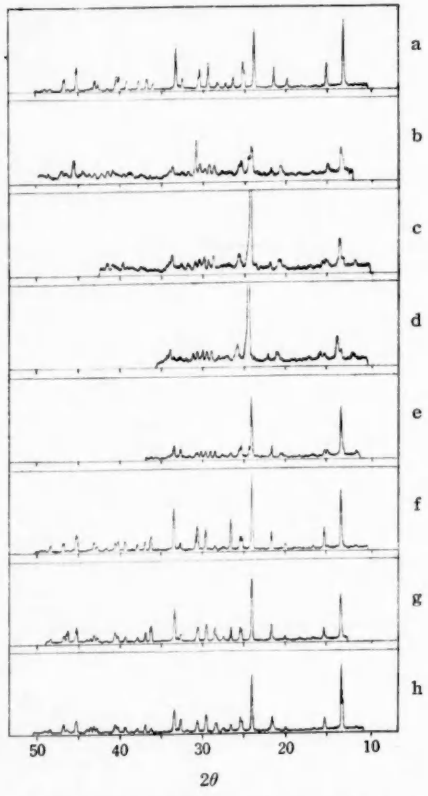

Fig. 6. Change of X-ray diffraction diagrams due to the transition; (a) α-modification of the hydrate, (b) ten minutes after once heating the hydrate to 117°C, (c) 40 min. after b, (d) 60 min. after b, (e) 18 hr. after b, (f) 42 hr. after b, (g) 90 hr. after b, (h) 138 hr. after b.

*** The infrared absorption spectra were recorded with Hilgar Model H800 Spectrophotometer.

TABLE II. POWDER DIFFRACTION LINES IN 2θ VALUES (deg.)

α-Hydrate	β-Hydrate	Anhydrous crystal
13.08 (110)	11.62 (210)	11.25
15.14 (020)	13.16 (021)	11.74
19.9 (002)	13.45 (220)	12.54
21.5 (200)	15.0 (040) (201)	13.14
23.9 (112)	20.7*	13.8
25.1 (022)	21.9 (400)	14.8
25.3 (130)	24.2 (222)	18.2
26.4 (220)	24.5	19.8
27.3 (131)	25.5 (042)	20.2
28.3	25.7 (260)	20.4
29.4 (202)	28.6**	20.6*
30.4 (212)	29.2	21.5
30.6 (040)	29.7* (402)	21.9
32.5 (140)	30.4	23.8
32.9	30.8 (422) (080)	24.1
33.3 (220) (310)	31.8	24.6
36.0 (320)	32.3	25.0
36.1	33.5 (442)	25.4
36.8 (042)	33.6 (620)	27.1
37.7 (240)	34.0	27.4
39.2	36.4 (640)	27.7
40.1 (330)	37.5 (082)	28.3**
40.4 (150) (004) (223)	38.9	28.9
42.6	39.6	29.5
43.0, 43.1 (242)	40.8**	30.0
	41.4	
43.4	42.2	
45.1 (340) (303) (250) (401)	43.0	
	44.4	
46.6 (420)	45.4	
	45.6	

* Diffraction lines due to $HgCl_2$.

** Diffraction lines due to KCl.

patterns of the anhydrous crystal (Fig. 7a) and of the hydrate (Fig. 6a) which is stable at room temperature (α modification) are also given for the sake of reference. The series of patterns shows the change in the crystal structure from the high-temperature modification (β modification) to the low-temperature modification (α modification) slowly occurring at room temperature. Fig. 6b is itself an intermediate or a mixture of the two modifications. Attempts were made to assign the diffraction lines to either α or β modification by comparing the members of the series of the diffraction patterns. The results are summarized in Table II.

Although some of the lines ascribed to the β modification coincide with the lines of the α modification or with the lines of the anhydrous crystal, there exist lines essentially attributable to the β modification. The time change of the intensities also supports this view. The patterns of Fig. 6b and its succeeding changes can not be obtained by a mere superposition of the diffractions from the α-hydrate and those from the β-hydrate. In fact, the intensities of lines belonging to various crystalline forms show intricate changes, for example, (1) 24.1* line first becomes stronger with time, (2) 13.4 and 15.4 are both characteristic to the α-hydrate but their recovery in the intensity is not proportional with each other; the recovery is first more rapid in 15.4 line than 13.4 line, and then the recovery of 13.4 line predominates again, and (3) five lines between 28 and 31 do not change their intensities in a regular, simple way.

It was first supposed that the sample chilled from above the transition temperature might be a mixture of the α and the β modifications, and that the transition might be observed as the decrease in intensity of the characteristic lines of the β form accompanied with the increase in the intensities of lines of the α form by equal fractions. If so, it should be possible to determine the rate of transformation at a supercooled condition which is itself a rare experimental information. Instead, it has become very plausible that the transition is essentially of gradual nature: a structure does not abruptly transform itself into another but there is a continuous series of structures between the β and the α modifications.

This is an analogous situation to the order-disorder transitions in such respect that there are an infinite number of phases between two extreme phases**. But a difference from the order-disorder transition is that nothing like the order parameter may be introduced and that every step of the transition probably corresponds to an ordered state because no regular, proportional change in the diffraction intensities with time was observed in contrast to the case of order-disorder transitions, in which it is possible to calculate the order parameters from the monotonous change of a superstructure-line intensity with temperature[8]. In the case of order-disorder transitions, a unit cell within a crystal has only statistical significance in the sense that a particular unit cell has not necessarily the structure identical with the neighboring unit cell. In the present case of the transition in $K_2HgCl_4 \cdot H_2O$, every unit cell is considered to have the identical structure which gradually changes with time. This type of transition may be termed a slow "Martensite transition" which does not accompany nucleation-and-growth[9].

The determination of the precise structure of the β modification*** seems to be very difficult because the unit cell is relatively large, being

$$a = 16.51\text{Å},\ b = 23.26\text{Å},\ \text{and}\ c = 8.89\text{Å}$$

and containing 16 formula units of $K_2HgCl_4 \cdot H_2O$. This cell is four times as large as the unit cell in the α modification[4] owing to the appearance of the line ($2\theta = 11.75°$) which may be indexed as inhibited ($1\,{}^1/_2\,0$) on the basis of the structure of the α form.

Rehydration of Anhydrous Crystals

$K_2HgCl_4 \cdot H_2O$ was dehydrated in the apparatus of the differential thermal

* 2θ value (twice the diffraction angle).

** It may not be immediately evident that the transition at 114°C from the α to the β form is of the same nature as that from the β to the α form occuring at room temperature. But there is no reason, at present, to believe otherwise.

8) Y. Saito, *X-sen*, **7**, 9 (1952); Z. W. Wilchinsky, *J. Appl. Phys.*, **15**, 806 (1944).

9) M. Cohen, "Phase Transformations in Solids", John Wiley & Sons, Inc., New York (1958), p. 588.

*** Kiriyama and Ibamoto[10] reported the structure of the high-temperature form of $K_2HgCl_4 \cdot H_2O$ by use of a high-temperature camera after prolonged heat-treatment at high temperature. Their experimental condition was very different from the present one. There are some discrepancies between their results and the results of the current investigation; for instance, the 11.75 line is missing from their X-ray photographs and therefore the unit cell dimentions are also different from those described here.

10) R. Kiriyama and H. Ibamoto, This Bulletin, **27**, 317 (1954).

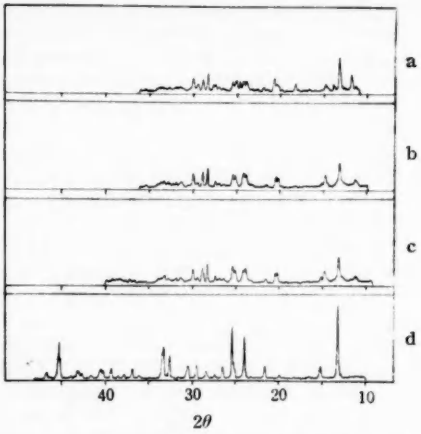

Fig. 7. Change of X-ray diffraction patterns due to rehydration of anhydrous crystal at room temperature; (a) Anhydrous phase, (b) after standing for 60 min. in the open air, (c) after 140 min. (d) after 30 hr. (α-modification of the hydrate).

analysis and it was immediately transferred to the goniometer of the Norelco X-ray diffractometer. It was observed that rehydration occurred in the open air at room temperature, at a measurable rate. This series of diffraction patterns, which is a cinematogram of the rehydration reaction, is reproduced in Fig. 7. It took about 30 hr. at about 30°C for the complete rehydration. This is a comparatively rapid rate of rehydration and therefore it is confirmed that the measurements of the dehydration pressures of the crystalline hydrate correspond to the equilibrium property of the system.

Summary

The dehydration pressures of the crystalline $K_2HgCl_4 \cdot H_2O$ are measured and given by $\log P = 8.538 - (2161/T)$ with P expressed in mmHg. No thermal hysteresis effect was observed. Production and some experiments for partly amorphous hydrate are briefly discussed. A consideration of the entropy of dehydration led to the conclusion that the dehydration is zeolitic. The differential thermal analysis revealed that there is a non-dehydrating transition at 114°C and that the dehydration occurs at 123°C. Infrared spectra of the solids showed that the 6-micron band of water persisted between 114 and 123°C. The X-ray study of the transition at the supercooled condition showed that this is a transition quite different in nature from those of ordinary nucleation-and-growth mechanism. The rehydration of dehydrated crystals was followed by the X-ray diffraction method and found to be relatively rapid at room temperature.

The authors wish to express their sincere thanks to Professor I. Nitta for his interest in the present investigation and to Assistant Professor K. Sakurai and Dr. K. Osaki for their discussions on the X-ray data. The cost of the research was partly defrayed by the financial support of the Ministry of Education to which the authors' appreciation is due.

Department of Chemistry
Faculty of Science
Osaka University
Nakanoshima, Osaka

Studies on Crystal Hydrates. V. Zeolitic Dehydration of DL-Tris-ethylenediamine-cobalt(III) Chloride Hydrate, DL-[Co en$_3$]Cl$_3$·nH$_2$O. Sorption and Desorption of Water Vapor. A Preliminary Study of the Dielectric Properties*

By Hideaki CHIHARA and Kazumi NAKATSU

(Received February 13, 1959)

Crystal hydrates may be classified into two extremes from the standpoint of the dehydration isotherm[1]:

i) crystals which are dehydrated in a stepwise manner (Fig. 1a); $CuSO_4 \cdot 5H_2O$ belongs to this class of hydrates,

ii) crystals which are dehydrated continuously (Fig. 1b); zeolite minerals belong to this class.

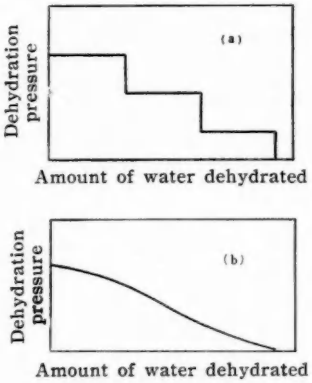

Fig. 1. Two extreme types of dehydration isotherm. (a) the stepwise dehydration, (b) the continuous dehydration.

Zeolites, chabazite, for instance, generally possess two or more kinds of channels of different diameter and each channel crosses with others at cage-like rooms[2]. Analcite has spiral channels which are relatively independent of each other but their diameter is not uniform throughout a channel[3]. We have long been looking for a type of crystal which belongs to the class ii and has only one kind of channel in which positions of water molecules can be located exactly by the method of X-ray analysis. If we can obtain such a crystal, it will provide us with an ideal model substance for examining the role of water in the stabilization of crystal lattice, the capillary condensation theory generally adopted in the adsorption research ane the state of aggregation of water molecules in the channels.

The crystal structure of DL-[Co en$_3$]Cl$_3$·nH$_2$O (n=3) has recently been determined[4] and this was found to be a substance that nearly meets our requirements.

The present paper deals with the experiments aiming at establishing the zeolitic nature of the dehydration of this crystal and with some results obtained in regard to the thermodynamic quantities of dehydration. A preliminary measurement of the dielectric absorption will also be briefly reported.

Experimental

Material.—The preparation of DL-tris-ethylenediamine-cobalt(III) chloride has already been described[4]. Crystals were purified by repeating recrystallization from aqueous solution (Found: C, 20.77; H, 7.01; N, 24.73; Cl, 29.83% on the basis of the anhydrous crystal. From the residue the Co purity was found to be 99.601% by the α-nitroso-β-naphthol method**). The measurements of the dehydration pressure were conducted with powdered crystals unless otherwise stated. Dielectric measurements were made with single crystals grown from the aqueous solutions.

Differential Thermal Analysis.—The differential thermal analysis (Fig. 2) shows that the dehydration takes place over the temperature region between 70 and 170°C. Such gradual

* Report IV may be found in This Bulletin, **32**, 897 (1959).

1) R. Büll, *Angew. Chem.*, **49**, 145 (1936).

2) G. L. Kington and W. Laing, *Trans. Faraday Soc.*, **51**, 287 (1955).

3) E. Schiebold, "Kristallstruktur der Silikate" in Ergebnisse der exakten Naturwissenschaften Bd. 12, Verlag von Julius Springer, Berlin (1933).

4) K. Nakatsu, Y. Saito and H. Kuroya, This Bulletin, **29**, 428 (1956).

** The analysis of Co was kindly carried out by Dr. T. Fujino of the Institute of Science and Industry, Osaka University, Sakai, Osaka, to whom the authors are very grateful.

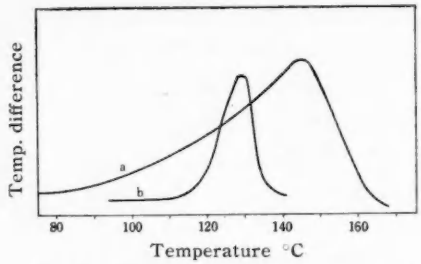

Fig. 2. The differential thermal analysis of (a) DL-$[Co\,en_3]Cl_3$ hydrate and (b) $NiSO_4 \cdot 6H_2O$.

dehydration stands in contrast with the case of nickel sulfate hydrate, for example, and suggests the zeolitic nature of dehydration.

Dehydration Pressures. — The dehydration pressures of the hydrate were measured between 19 and 45°C at various water contents by using the apparatus already described in the preceding paper. The results are summarized in Table I and Fig. 3. The approach to the equilibrium was very rapid, not later than ten minutes after the water bath was thermostated. The pressure values were read by use of a traveling microscope to 0.01 mm. Corrections in the value of the water content for the amount of water present in the vapor phase were not made, since a rough estimate based on the dimensions of the manometer and the sample container showed that it was well within the experimental error. No hysteresis effect was observed: the pressures in the heating and in the cooling directions coincided with each other.

The experiments of dehydration and rehydration (desorption and sorption) of a single crystal was undertaken in order to compare it with the powder data. A single crystal (about 325.6 mg.) placed in a glass vessel (144.9 mg.) was hung under a quartz helical balance, the sensitivity of which was 0.2711 mm./mg. The water vapor pressure in the apparatus was kept constant by use of 72% sulfuric acid solution covering the water vapor pressures up to 13 mmHg. The results are plotted in Fig. 7. No hysteresis was observed between the dehydration and rehydrotion branches.

The differential molar heats and entropies of dehydration were computed from the pressure equations given in Table I. Table II lists these results and Fig. 6 indicates that there is a maximum both in the heat and in the entropy at a certain water content (approximately at $n=2.7$ mol. of water per formula weight of the hydrate).

TABLE I. DEHYDRATION PRESSURES. n IS THE NUMBER OF MOLES OF WATER PER FORMULA WEIGHT OF $[Co\,en_3]Cl_3$

n	Pressure equation (in mmHg)
3.35	$\log P = 9.0406 - (2334.0/T)$
3.11	$\log P = 10.003 - (2693.1/T)$
2.96	$\log P = 10.577 - (2910.0/T)$
2.63	$\log P = 10.734 - (3035.9/T)$
2.47	$\log P = 10.699 - (3045.6/T)$
2.02	$\log P = 9.7583 - (2773.2/T)$
1.18	$\log P = 9.7791 - (2782.0/T)$
0.82	$\log P = 9.3500 - (2649.8/T)$
0.39	$\log P = 9.7320 - (2770.1/T)$
0.23	$\log P = 10.119 - (2889.5/T)$
0.02_5	$\log P = 7.5790 - (2206.9/T)$

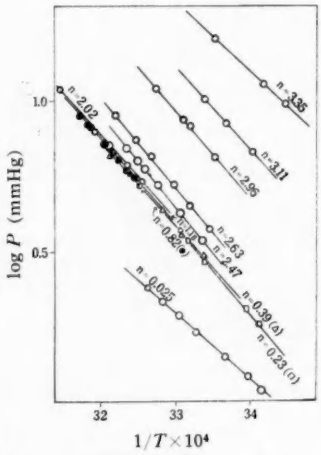

Fig. 3. Dehydration pressure of DL-$[Co\,en_3]Cl_3 \cdot nH_2O$ at different water contents n.

TABLE II. DIFFERENTIAL MOLAR HEAT AND ENTROPY OF DEHYDRATION AS A FUNCTION OF WATER CONTENT

n	ΔH (kcal./mol.)	ΔS (e.u.)	n	ΔH (kcal./mol.)	ΔS (e.u.)
3.35	10.7	28.2	1.18	12.7	31.6
3.11	12.3	32.6	0.82	12.1	29.6
2.96	13.3	35.2	0.39	12.7	31.2
2.63	13.9	35.9	0.23	13.2	33.1
2.47	13.9	35.8	0.02_5	10.1	21.5
2.02	12.7	31.5			

Description of Crystal Structure

The crystal structure may be briefly outlined here with particular attention to the arrangement of the water molecules. The structure projected on the (0001) plane is represented in Fig. 4. A channel of hexagon cross-section filled with water molecules runs through the origin in the direction of the c-axis. The way in which the water molecules are arranged is schematically shown in Fig. 5 and the crystal data together with the atomic coordinates are reproduced in Table III.

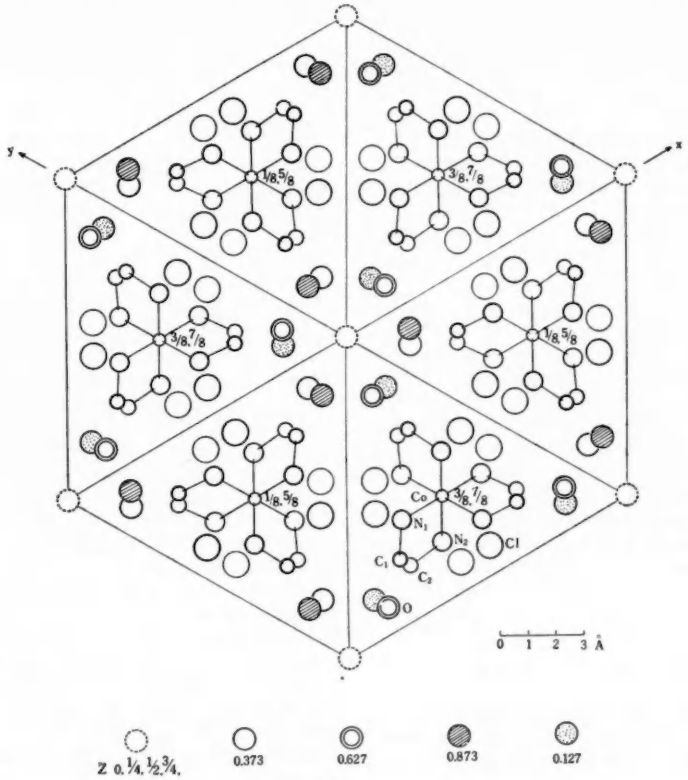

Fig. 4.

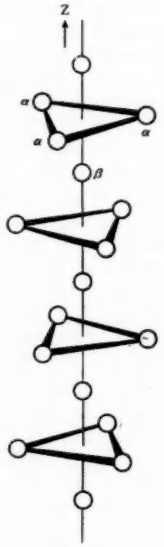

Fig. 5.

TABLE III. CRYSTALLOGRAPHIC DATA

$a=11.50\pm0.02$ Å, $c=15.52\pm0.04$ Å,
Density 1.504 (17°C), $Z=4$,
Space Group $P\bar{3}c1$–D_{3d}^4

Fractional atomic coordinate

Atom	No. of positions & Wyckoff notation	x	y	z
C_0	4d	1/3	2/3	0.125
Cl	12g	0.097	0.493	0.372
O_1	12g	0.087	0.225	0.873
O_2	2a	0	0	1/4
O_3	2b	0	0	0
C_1	12g	0.180	0.397	0.077
C_2	12g	0.215	0.397	0.173
N_1	12g	0.192	0.525	0.050
N_2	12g	0.333	0.535	0.200

TABLE IV. SOME INTERATOMIC DISTANCES

$O_\alpha\cdots Cl$	3.34 Å
$O_\alpha\cdots C_1$	3.36, 3.61 Å
$O_\alpha\cdots C_2$	3.12, 3.55 Å
$O_\alpha\cdots O_\alpha$	3.90, 4.19, 4.54 Å

Water molecules which occupy the 12g positions amount to three moles per formula weight of the hydrate ($n=3$). These positions will be referred to as the α-sites. In view of the long O···O distances listed in Table IV, if water molecules are to occupy only α-sites, and of the improvement of the reliability index by about 2%, it was concluded that water molecules are distributed also on the 2a and 2b special positions (referred to as the β-sites). The fact that the peak at the origin in the electron-density projection on the (0001) plane was not eliminated even at the final stage of the refinement of the structure analysis also led to this conclusion. This addition of water is also consistent with the chemical analysis that the water content of a freshly prepared crystal is $n=3.6$. The $O_\alpha \cdots O_\beta$ distances will then be 2.96 and 3.00 Å corresponding to weak hydrogen bonding.

A single-crystal oscillation photograph was obtained after the crystal was almost dehydrated and its unit cell dimensions were the same as those of the hydrate crystal.

Results and Discussion

The dehydration isotherm derived from the data of Table I by inter- or extrapolating them to 25°C is shown in Fig. 7

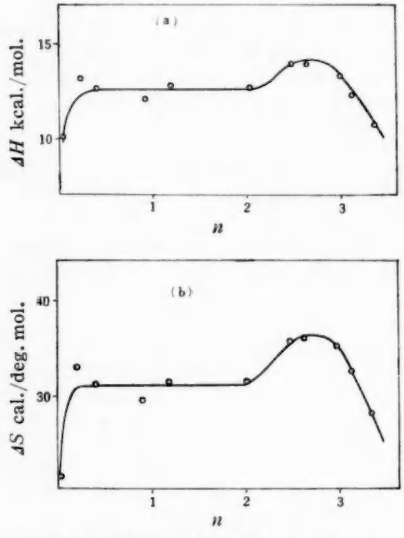

Fig. 6. Differential molar heat (a) and entropy (b) of dehydration as functions of water content n.

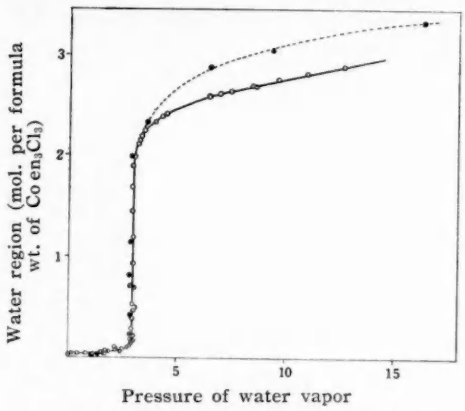

Fig. 7. Dehydration isotherm at 25°C derived from the powder data (solid circle) and determined directly for a single crystal (open circle).

by solid circles. The pressure at 25°C remains almost constant (2.85 mmHg) between the water contents $n=0.2$ and 2.5. Another independent direct measurement of the isotherm at 25°C for a single crystal (denoted by open circles in Fig. 7) gave nearly the same result as that derived from the powder data***. Important conclusions may be drawn from these experimental data.

(a) The fact that the powder and the single-crystal data give the same results clearly shows that the isotherm obtained for the single crystal is not due to adsorption of water vapor on the outer surface of the solid but to the sorption and desorption into and from the interior of the crystal lattice.

(b) That the pressure is constant over a wide range of n reminds us of the character of the destructive dehydration (class i). A close examination, however, shows that the boundary values of n (0.2 and 2.5) do not correspond to any single crystalline phases. In fact there is no set of equivalent positions in the space group $P\bar{3}cl$ that can accommodate the states $n=0.2$ or $n=2.5$. Therefore, it must be emphasized that an appearance of the stepwise dehydration does not always correspond to the destructive dehydration. This conclusion argues against the widely accepted criterion for zeolitic dehydration[1,5-7]. X-ray examination would be necessary for the decision as to whether

*** The small discrepancy at higher pressures is probably due to the larger adsorption of water on the outer surface of powdered crystals.

or not the dehydration is zeolitic.

(c) From the standpoint of the sorption-desorption system, the isotherm of Fig. 7 corresponds to the type V isotherm of the Brunauer-Emmett-Teller classification[8]. It is evident that the horizontal portion of the isotherm corresponds to the capillary condensation into pores of uniform size. Analogous transitions in adsorbed monolayer have been reported and interpreted by many investigators since Harkins and his collaborators observed the first-order phase transition of *n*-heptane on the surface of silver[9], although its reality was open to some discussion[10]. Recent investigations[11] show that such transitions are due to a kind of cooperative phenomena occurring in the assembly of adsorbed vapors. The transitions are sharp on a homogenous surface but they are diffuse on a heterogeneous surface. Capillary condensation phenomena that have been observed at any time are diffuse, because the experiments were carried out on gels which are inevitably inhomogeneous. The transition phenomenon observed in the present study is unique because it occurs in the true equilibrium system (the water regain of the solid did not change during 24 hr. after dosage of vapor; cf. E. V. Ballou, Ref. 10) and also because it is the capillary condensation entirely equivalent, in principle, to the transition on a uniform outer surface of a single crystal.

(d) The maxima in the differential molar heat and entropy in Fig. 6 will be accounted for by the theory of cooperative phenomena. Analogous results were reported by Rhodin[12] for nitrogen adsorbed on single crystals of copper, by Young[13] for argon absorbed on octahedral potassium chloride and by Hayakawa[14]. In all the adsorption systems ever examined, the maximum of the differential heat of adsorption appears when the amount of the gas adsorbed nearly suffices to cover the surface with a monolayer. This is also to be expected theoretically[15]. In the present case the maximum is also near the monolayer coverage of the inner surface of pores ($n=2.7$). The number of pairs of water molecules in a channel interacting with each other increases more rapidly than linearly as the coverage increases, even after the monolayer has been completed. The differential heat thus increases with the coverage on the assumption that the pair interaction energy is constant. On the other hand, the water molecules in the second layer (β-sites) interact with the lattice much more weakly than do the molecules in the first layer (α-sites). Those two counteracting effects give rise to the maximum of the heat of sorption branch.

(e) The differential heat and entropy are very small at very low n values. This is an extraordinary fact as many sorption systems exhibit a great increase in ΔH towards the lower surface coverage. On the surface of a single crystal, the differential heat is constant down to very low pressures[12]. The experimental error involved in the present determination of ΔH does not exceed 0.7 kcal./mol. and, therefore, the small value of ΔH and ΔS may possibly be due to a slight rearrangement of atoms in the completely dehydrated crystal lattice.

The Preliminary Results of Dielectric Measurements.—The dielectric power loss was measured of single crystals ($n=3.6$) between −180°C and room temperature in the frequency range of 300 c/sec. to 10 Mc/sec. The dielectric absorption was found with the electric field in the *c*-axis direction and perpendicular to the *a*-plane of the hexagonal crystal. The activation energies for the relaxation process were 7.7 and 6.3 kcal./mol., respectively. By extrapolation to room temperature, the relaxation times ($\log \tau = (1379/T) - 14.72$ for the *c*-plane) nearly agree with the relaxation time in liquid water and it was inferred that the absorption is due to the hindered rotation of water molecules. In the experiment with the electric field parallel to the *c*-axis, an additional absorption increasing progressively towards lower frequencies was observed. Further precise study of the dielectric properties and the d. c. conduction is going on and will be reported later.

5) W. Eitel, "Physikalische Chemie der Silikate", Johann Ambrosius Barth, Leipzig (1941).
6) O. Glemser, *Z. Elektrochem.* **45**, 820 (1939).
7) G. Tammann, *Z. physik. Chem.* **27**, 323 (1893).
8) S. Brunauer, "Adsorption of Gases and Vapors", Vol. I, Princeton University Press, N. J. (1945), p. 150.
9) G. Jura, E. H. Loser, P. R. Basford and W. D. Harkins, *J. Chem. Phys.* **13**, 535 (1949).
10) R. J. Tykodi, *J. Chem. Phys.*, **22**, 1647 (1954); *J. Phys. Chem.*, **59**, 383 (1955); E. V. Ballou, *J. Am. Chem. Soc.*, **76**, 1199 (1954).
11) B. B. Fisher and W. G. McMillan, *J. Chem. Phys.*, **28**, 549 (1958).
12) T. N. Rhodin, Jr., *J. Am. Chem. Soc.*, **72**, 5691 (1950).
13) D. M. Young, *Trans. Faraday Soc.*, **48**. 548 (1952).
14) J. Hayakawa, This Bulletin, **30**, 124, 236, 243, 332, 337, 343 (1957).
15) W. J. C. Orr, *Trans. Faraday Soc.*, **35**, 1247 (1939).

Summary

The dehydration pressures of DL-$[Co\,en_3]Cl_3 \cdot nH_2O$ ($n \leqq 4$), were measured between 19 and 45°C at various water contents. The dehydration isotherm derived from the data is of type V of the BET classification with a constant pressure (2.85 mmHg at 25°C) region between $n=2.5$ and $n=0.2$, corresponding to the case of capillary condensation into pores of uniform size. The crystal lattice is stable after dehydration, showing the zeolitic nature of dehydration. The usual criterion of stepwise dehydration for the lattice-destructive dehydration does not apply to this type of crystal. The differential molar heat and entropy of dehydration have maximum values around $n=2.7$; this can be accounted for by the theory of co-operative phenomena. At very low water content, there is a possibility of rearrangement of atoms in the crystal as inferred by the entropy consideration. A preliminary study of the dielectric properties showed that the relaxation absorption occurs between −180°C and room temperature in the megacycle region with the activation energy for the relaxation about 7 kcal./mol. The dielectric loss due probably to the d.c. conduction was observed in the *c*-axis direction.

The authors with to thank Professor I. Nitta and Assistant Professor S. Seki of Osaka University and Professor Y. Saito of Osaka City University for their valuable discussions. The present study was partly supported by the financial aid of the Ministry of Education, to which the authors' thanks are also due.

Department of Chemistry
Faculty of Science
Osaka University
Nakanoshima, Osaka (*H. C.*)

Institute of Polytechnics
Osaka City University
Kita-ku, Osaka (*K. N.*)

Studies on Crystal Hydrates. VI[1]*. Thermodynamics of Dehydration of Crystal Hydrates. A New Criterion for the Continuous Zeolitic Dehydration. Capillary Condensation of Water Vapor into Exactly Uniform Pores and an Experimental Test of the Kelvin Equation. Case of* DL-*Tris-ethylenediamine-cobalt(III) Chloride Hydrate*

By Hideaki CHIHARA

(Received February 13, 1959)

A criterion has generally been adopted as to the manner of dehydration of a crystal hydrate, which makes use of the dehydration isotherm[1]. The experimental determination of a complete dehydration isotherm, however, is sometimes quite an elaborate matter owing to difficulty in obtaining the true equilibrium of dehydration[2]. It was found that a new criterion, which is equivalent to the "isotherm criterion", can be obtained by the measurement of dehydration pressures at different temperatures for a fixed content of water in the solid phase; the water content needs not be accurately known. This may be termed "entropy criterion" as it is based on the value of the entropy of dehydration.

Although the entropy criterion is exactly as useful as the isotherm criterion, both were found to fail to apply to a particular case of DL-tris-ethylenediamine-cobalt(III) chloride hydrate, in which only one kind of channel filled with water molecules runs parallel to the direction of the *c*-axis[1]. This cobalt complex presents a remarkable model substance as a crystal

1) Report V: H. Chihara and K. Nakatsu, This Bulletin, 32, 903 (1959).
2) Report IV: H. Chihara and S. Seki, ibid., 32, 897 (1959).

hydrate of zeolite type, as a porous adsorbent having exactly uniform capillaries, as a host-lattice of an *Einchluss-verbindung* like a urea adduct, and as an isothermal order-disorder assembly of water molecules.

Thermodynamics of Dehydration

For a dehydration equilibrium

$$A\cdot nH_2O \rightleftarrows A\cdot(n-1)H_2O + H_2O(g)$$

the change in the standard entropy ΔS is given by

$$S_H - S_A = S_W - \Delta S$$

where S_H, S_A and S_W are the standard entropies of the hydrate, the lower hydrate (or the anhydrous crystal) and the water vapor (45.1 cal./deg. mol.), respectively. $S_H - S_A$ can be obtained from the measurements of the heat capacities and ΔS from the tensiometric measurements. Table I lists these values for a few hydrate systems. It is seen in Table I that $S_H - S_A$ is nearly constant being around 10 e. u., which is also nearly equal to the entropy of ice at the standard state. This shows that an additivity rule holds for these crystalline solids. The values of $S_W - \Delta S$, on the other hand, scatter far and wide, being as large as 21.6 e. u. and as small as -2.5 e. u. One of possible reasons for the discrepancies between $S_H - S_A$ and $S_W - \Delta S$ would be that the stable equilibrium may not have been attained in the tensiometric measurements. This may undoubtedly cause a serious discrepancy. However, it is readily shown that a discrepancy can naturally occur even if the equilibrium was obtained in both thermal and tensiometric measurements.

TABLE I ENTROPY PER MOLE OF WATER IN CRYSTALLINE HYDRATES

Hydrate	$S_H - S_A$[3]	$S_W - \Delta S$
$MgCl_2\cdot 2H_2O$	10.2	10.8[4]
$MgCl_2\cdot 4H_2O$	10.1	10.4[4]
$MgCl_2\cdot 6H_2O$	12.2	13.9[5]
$CaSO_4\cdot \frac{1}{2}H_2O$	11.4	-2.5[6]
$ZnBr_2\cdot 2H_2O$	11.7	21.6[7]
$ZnSO_4\cdot 2H_2O$	10.4	8.5[8]
$ZnSO_4\cdot 7H_2O$	5.6	2.9[8]
$CdBr_2\cdot 4H_2O$	10.7	9.9[9]
$CdSO_4\cdot \frac{8}{3}H_2O$	10.1	12.6[10]
$CuSO_4\cdot H_2O$	8.7	7.9[11]
$CuSO_4\cdot 3H_2O$	9.0	11.6[10]
$CuSO_4\cdot 5H_2O$	9.6	8.0[10]
$NiCl_2\cdot 6H_2O$	8.3	13.2[4]
$BaCl_2\cdot 2H_2O$	8.5	6.8[12]

3) F. D. Rossini et al., "Selected Values of Chemical Thermodynamic Properties", NBS Circular 500, National Bureau of Standards, U. S. Department of Commerce, U. S. Government Printing Office, Washington (1952).
4) I. Sano, *J. Chem. Soc. Japan* (*Nippon Kwagaku Kwaishi*) **59**, 1145 (1938).
5) J. H. Derby and V. Yngve, *J. Am. Chem. Soc.*, **38**, 1439 (1916).
6) H. Lescoeur, *Ann. chim. Soc.*, **21**, 511 (1890).
7) Y. P. Baxter and R. D. Warren, *J. Am. Chem. Soc.*, **33**, 340 (1911).
8) P. C. F. Frowein, *Z. physik. Chem.*, **1**, 1 (1887).
9) F. Ishikawa and Y. Ueda, *Sci. Rept. Tohoku Univ.*, **22**, 275 (1935).
10) C. D. Carpenter and E. R. Jette, *J. Am. Chem. Soc.*, **45**, 583 (1923).
11) A. Siggel, *Z. Elektrochem.*, **19**, 349 (1913).
12) G. F. Hüttig and Ch. Slonim, *Z. anorg. Chem.*, **181**, 65 (1929).

Let us consider a system consisting of a hydrate phase (denoted by the subscript 1), the anhydrous phase (subscript 2) and the water vapor phase (subscript 3) in equilibrium. The molar Gibbs free energy of the whole system is given by

$$G_m = (1-\theta)\mu_1 + \theta\mu_2 + c\theta\mu_3 \qquad (1)$$

in terms of the chemical potentials μ_i where θ corresponds to the degree of dehydration or the mole fraction of the anhydrous phase in the solid components. One mole of the hydrate is assumed to produce c moles of water vapor. The conditions for the stable equilibrium are

$$\frac{dG_m}{d\theta} = 0 \qquad \frac{d^2G_m}{d\theta^2} > 0 \qquad (2)$$

Case A.—The simplest case in which

$$\left(\frac{\partial\mu_1}{\partial\theta}\right)_{P,T} = \left(\frac{\partial\mu_2}{\partial\theta}\right)_{P,T} = 0 \qquad (3)$$

leads to the ordinary condition of equilibrium

$$\mu_1 = \mu_2 + c\mu_3 \qquad (4)$$

By defining the absolute activity λ_i by

$$\mu_i = kT\log\lambda_i \qquad (5)$$

the equilibrium constant K is then obtained as

$$K \equiv \frac{\lambda_1}{\lambda_2\cdot(\lambda_3^+)^c} = \left(\frac{p}{P^+}\right)^c \qquad (6)$$

where λ^+ and P^+ are the standard-state quantities. The pressure equation will then be

$$\log p - \log P^+ = \frac{1}{c}(\log\lambda_1 - \log\lambda_2 - c\log\lambda_3)$$

$$= -\frac{\Delta h}{kT} + \frac{\Delta s}{k} \qquad (7)$$

where

and
$$\left.\begin{aligned}\Delta h&=(h_2+ch_3-h_1)/c\\ \Delta s&=(s_2+cs_3-s_1)/c\end{aligned}\right\} \quad (8)$$

Eq. 7 is the integrated form of the Clapeyron-Clausius equation. The second condition (Eq. 2) gives

$$\frac{\mathrm{d}\log p}{\mathrm{d}\theta}=\frac{\mathrm{d}}{\mathrm{d}\theta}\left\{-\frac{1}{kT}(\mu_1-\mu_2-c\mu_3{}^+)\right\}=0 \quad (9)$$

showing that the dehydration pressure should be constant over the range of the θ values or, in other words, the dehydration should be stepwise as is the case for $CuSO_4\cdot5H_2O$ and its lower hydrates. Eqs. 7 and 8 then indicate that the Clapeyron-type equation gives the integral heat and entropy of dehydration when the condition (3) is satisfied. The heat and entropy thus obtained should be comparable with the third-law values S_H-S_A. It is inferred that the condition (3) holds in hydrates for which one sees approximate agreement between S_H-S_A and $S_W-\Delta S$ in Table I.

Case B.—In a general case where the condition (3) is not satisfied,

$$\left(\frac{\partial\mu_1}{\partial\theta}\right)_{P,T}\neq0 \qquad \left(\frac{\partial\mu_2}{\partial\theta}\right)_{P,T}\neq0 \quad (10)$$

the condition for the equilibrium gives

$$-\log\lambda_1+\log\lambda_2+c\log\lambda_3+(1-\theta)\left(\frac{\partial\log\lambda_1}{\partial\theta}\right)_{P,T}+\theta\left(\frac{\partial\log\lambda_2}{\partial\theta}\right)_{P,T}=0 \quad (11)$$

which then leads to the pressure equation

$$c\log(p/P^+)=\frac{1}{kT}\{h_1-\bar{h}_2-ch_3{}^+-T(\bar{s}_1-\bar{s}_2-cs_3{}^+)\} \quad (12)$$

where h and $\bar{s}$ are the differential molar heat and entropy. The shape of the dehydration isotherm must satisfy the second condition for the equilibrium:

$$\frac{\mathrm{d}^2G_m}{\mathrm{d}\theta^2}=\frac{\mathrm{d}}{\mathrm{d}\theta}\left\{-\mu_1+\mu_2+c\mu_3+(1-\theta)\left(\frac{\partial\mu_1}{\partial\theta}\right)_{P,T}+\theta\left(\frac{\partial\mu_2}{\partial\theta}\right)_{P,T}\right\}>0 \quad (13)$$

which then leads to

$$\frac{\mathrm{d}}{\mathrm{d}\theta}(\bar{\mu}_2+c\mu_3{}^+-\bar{\mu}_1)=\frac{\mathrm{d}}{\mathrm{d}\theta}(\bar{\mu}_2-\bar{\mu}_1)>0 \quad (14)$$

Differentiating Eq. 12 with respect to θ gives

$$ckT\frac{\mathrm{d}\log(p/P^+)}{\mathrm{d}\theta}=\frac{\mathrm{d}}{\mathrm{d}\theta}(\bar{\mu}_1-\bar{\mu}_2-c\mu_3{}^+)$$
$$=\frac{\mathrm{d}}{\mathrm{d}\theta}(\bar{\mu}_1-\bar{\mu}_2) \quad (15)$$

Therefore we have

$$\frac{\mathrm{d}\log p}{\mathrm{d}\theta}<0 \quad (16)$$

This shows that the dehydration pressure decreases constantly with increasing θ, or it corresponds to the zeolitic dehydration. The Clapeyron-Clausius equation gives differential molar heat and entropy in this case.

S_H-S_A as obtained from the calorimetric results corresponds to the difference in the integral entropies s_1-s_2 which is related to ΔS by Eq. 8.

Now, it will be evident that the discrepancies between S_H-S_A and $S_W-\Delta S$ may naturally occur if the dehydration proceeds zeolitically as the differential and the integral entropies of dehydration do not usually coincide with each other*, except for accidental coincidence.

In view of the fast that the integral entropy assigned to water molecules within a hyrate lattice is nearly constant being approximately 10 e. u., ΔS values obtained by the tensiometric measurements can be used to determine whether or not the dehydration is zeolitic even if the corresponding calorimetric data are unavailable. In Table I, the discrepancy is appreciable in $CaSO_4\cdot\frac{1}{2}H_2O$, $ZnBr_2\cdot2H_2O$ and $ZnSO_4\cdot7H_2O$. The hemihydrate of $CaSO_4$ undergoes zeolitic dehydration as shown by the isotherm reported by Gregg and Willing[13]. The cases of $ZnBr_2$ and $ZnSO_4$ hydrates have not been examined in detail and it is not clear if these are really zeolitic cases.

TABLE II. COMPARISON OF THE ISOTHERM AND ENTROPY CRITERIONS FOR THE TWO TYPES OF DEHYDRATION

	For dehydration by which crystal lattice collapses	For dehydration by which lattice does not collapse
S_H-S_A	about 10 e. u.	about 10 e. u.
$S_W-\Delta S$	equal to S_H-S_A	not equal to S_H-S_A
Clapeyron eq. gives	integral heat and entropy	differential heat and entropy
Pressure vs. deg. of dehydration	constant pressure	monotonous decline

* It is possible to calculate the intergral entropy for zeolitic hrdrates, if complete data of isotherms are available particularly at a very low presure region. See T. L. Hill, P. H. Emmett and L. G. Joyner, *J. Am. Chem. Soc.*, **73**, 5102, 5933 (1951).

13) S. J. Gregg and E. G. G. Willing, *J. Chem. Soc.*, **1951**, 2373, 2916.

Table II summarizes and compares the "isotherm" and "entropy" criterions. The "entropy criterion" is thus entirely equivalent to the "isotherm criterion" which has widely been accepted. The applicability or the inapplicability should be the same for both criterions. The advantage of the "entropy criterion" rests on the fact that the measurements of the dehydration pressure at different water contents are not necessary.

A Notable Case in which the Criterions Fail to Apply

When one correlates a thermodynamic relation to an atomistic interpretation, there is a risk of his over-relying upon empirical rules. Thus the "isotherm criterion" depends on a lot of experimental facts on the isotherm determinations and the structural studies before and after dehydration. This is in a way based on the analogy between zeolitic dehydration and adsorption. The phase rule of course can make judgement if the number of phases is known unambiguously.

The case of DL-$[Co\ en_3]Cl_3 \cdot nH_2O$ ($n \leq 4$), the dehydration of which was reported in the preceding paper[1], provides us with a notable exception to both criterions, which are however mutually consistent. Fig. 1

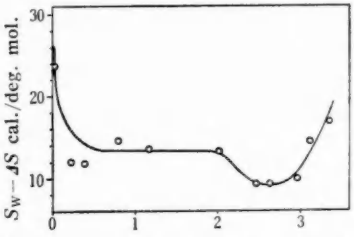

Fig. 1. Change with the water content in the differential molar entropy of water in $[Co\ en_3]Cl_3$ hydrate.

shows the change in $S_W - \Delta S$ as the hydration proceeds. $S_W - \Delta S$ is nearly constant between $n = 0.2$ and 3 except for a minimum occurring around $n = 2.6$[1]. Below and above this range of values of n, $S_W - \Delta S$ tends to increase, deviating from the additivity value of 10 e. u. The entropy criterion tells that the crystal undergoes zeolitic dehydration when $n \leq 0.2$ and when $n \leq 3$ and the lattice-destructive dehydration when n is between 0.2 and 3. This apparent conclusion is consistent with the isotherm criterion as judged from the isotherm given in Fig. 7 of the preceding paper[1], in which the pressure remains constant between $n = 0.2$ and 3. However, as already reported[1], this conclusion is not justified by the crystal structure studies by which we see that the structure is unchanged by dehydration except for the loss of water molecules in the channels. This must evidently correspond to zeolitic dehydration and thus the failure of both criterions is apparent.

The extreme uniformity of the pore structure of this crystal seems to be responsible for the failure. There exists only one kind of pore running parallel in the direction of the c-aixs of the crystal. Such uniformity has never been realized in actual hydrate systems or adsorption systems and has been out of reach of empirical rules mentioned in the first paragraph of the present section. This type of isotherm should lead to a sharp distribution function of pore sizes if we treat it by a standard method utilizing the desorption branch of sorption isotherm[14].

The most reliable criterion would be the structure investigation by the X-rays but in most of zeolite minerals and gels there is a broad distribution of pore size, which necessarily gives rise to the isotherm corresponding to the *Case B*; $[Co\ en_3]Cl_3$ hydrate is one of the rarest exceptions. The "entropy criterion" as well as the "isotherm criterion" is, therefore, considered to be still valid in judging which type of dehydration a particular hydrate would undergo.

Comparison of Capillary Radius as Determined by Dehydration Isotherm and by X-ray Study

It will be interesting to see to what extent the well-known Kelvin equation

$$\log(p_r/p) = -2\sigma M/(\rho r R T) \qquad (17)$$

gives reasonable pore radius when it is applied to the system of pores of molecular dimensions. p is the saturation pressure over a plane surface of the adsorbate liquid (water in the present case) whose surface tension is σ, density is ρ, and molecular weight is M. p_r is the saturation pressure over the surface, its radius of curvature being r. This equation has been known to hold for a macroscopic pore or a macroscopic droplet of liquid but we

14) C. Pierce, *J. Phys. Chem.*, **57**, 149 (1953).

seem to have available no direct experimental test of the equation down to pores of a few Ångstroms in radius.

The horizontal portion of the isotherm given in Fig. 7 of the preceding paper[1] gives $r=5.8$Å if $\rho=0.9971$, $\sigma=71.97$ dyn./cm., $p=23.756$ mmHg and $p_r=2.85$ mmHg are inserted in Eq. 17. It would not be necessary to add to r the thickness of a monolayer or of statistical layers as the capillary condensation begins at $n=0.2$, far below the monolayer capacity $n=3$**. On the other hand, the result of the crystal structure analysis[15] gives the distances from the origin (the center of a pore, see Fig. 3 of the preceding paper), in the plane parallel to the base of the hexagonal cell, 2.9 Å to the periphery of the van der Waals radius of the nearest CH_2 group and 3.4Å to the periphery of the nearest chloride ion (the inner wall of the pore is a little pleated).

We are now led to the conclusion that for water vapor as the adsorbate the Kelvin equation gives only the order of magnitude of the pores radius of micropores. We shall undertake experiments with nitrogen as the adsorbate later. For macropores the discrepancy would be much smaller. In view of the fact that the concept of the surface tension would undoubtedly lose its significance in such systems of water molecules, the Kelvin equation has been applied beyond its reasonable limit of application, although the method has been in extensive use for evaluating the pore size distribution in many adsorbents. The use of the Kelvin equation was partly justified for macropores by the experimental results that it gives the pore sizes in good agreement with those obtained by the mercury porosimeter method[16]. The present result gives some clue to the error caused by the use of the Kelvin equation for micropores.

Summary

A simple theory of the thermodynamics of hydrates is developed, which is able to show that the differential molar entropy of dehydration changes with the water content continuously if the hydrate undergoes zeolitic (continuous) dehydration. In this case the integral molar entropy of dehydration does not agree with the differential entropy. The same is true for the heat contents. For stepwise dehydration, on the other hand, both differential and integral entropies coincide in values. A new criterion, termed "entropy criterion", is presented that if the differential entropy of the water of crystallization, obtained by subtracting the entropy of dehydration (determined by the pressure measurements) from the standard entropy of water vapor 45.1 e. u., differs greatly from 10 e. u., the hydrate should undergo zeolitic dehydration and should have water molecules weakly bonded to the crystal lattice, from which water can be removed without causing collapse of the lattice. This new criterion is equivalent to using the current "isotherm criterion".

DL-$[Co\ en_3]Cl_3 \cdot nH_2O$ ($n \leq 4$) presents a notable exception to both criterions in that the crystal undergoes zeolitic dehydration in spite of its entropy of dehydration and its isotherm indicating the stepwise dehydration. The failure of the criterions in this crystal is due to the extreme uniformity of pore structure of the hydrate. The Kelvin equation for calculating the pore radius (giving 5.8Å) from the dehydration isotherm is tested against the pore radius obtained by the X-ray crystal structure analysis (giving 2.9 to 3.4Å). It may be concluded that the Kelvin equation is considered to give only the order of magnitude for micropore size. This cobalt complex hydrate is one of the rarest examples having exactly uniform pores and the criterion for the type of dehydration here presented is still effective in most cases.

The author wishes to express his sincere thanks to Professor I. Nitta and Assistant Professor S. Seki of the Department of Chemistry, Osaka University for illuminating discussions.

Department of Chemistry
Faculty of Science
Osaka University
Nakanoshima, Osaka

** It is rather surprising to note the capillary condensation is completed just befor the monolayer is filled.

15) K. Nakatsu, Y. Saito and H. Kuroya, This Bulletin, **29**, 428 (1956).

16) E. P. Barrett, L. G. Joyner and P. P. Halenda, *J. Am. Chem. Soc.* **73**, 373 (1951).

Quantum-Mechanical Considerations of Chemical Reaction Rates. II. The Transmission through Curved Reaction Path

By Iwao YASUMORI

(Received February 17, 1959)

Previous quantum-mechanical treatments[1-5] of chemical reaction rates deal principally with the behavior of the wave which represents the reacting system, passing from the region of the reactant to that of the resultant on the potential energy surface of reaction. These treatments also may be classed in two ways according to whether their objects are the transmission of the wave through the potential energy barrier[1-4] or through the curve or bend of the reaction path[5], for both the barrier and the bend are the important characteristics of the reaction path on the potential energy surface. Much knowledge of the microscopic feature of reaction rates, was obtained from these studies, but all these results were derived by the use of highly idealized models of potential, for example, one-dimensional square barrier or a path with a perpendicular turn, etc., to avoid mathematical difficulties.

Therefore, it is necessary to examine which of the conclusions correspond to the real behavior of reaction or are due merely to the used model itself.

For the purpose of considering the problem by the use of the more plausible potential models than those used before, Fueki and the present author have recently treated the transmission through the two-dimensional smooth barrier with a parabolic section and have made clear the properties of the quantum-mechanical correction which is necessary for the ordinary estimation of rate by the absolute reaction rate theory[6].

In this paper, another important problem, the transmission through the smoothly curved path with reasonable vibrational potential section is discussed in general and the extent of reflection and transmission is computed for some reaction examples. Then the inspection stated above is made comparing the present results with that of Hulburt and Hirschfelder's work[5] which was previously the first and only detailed one for the effect of the curved path. Also a consideration is made for their predictions of null transmission for the system with particular values of energy and of the availability of this effect for the isotopic separation.

Theoretical

Now we take, as a typical example of reaction, an elementary displacement reaction between atom A and molecule BC, A+BC→AB+C. The general feature of the potential energy surface for linear configuration is as shown in Fig. 1.

In order to discuss the transmission through the bend, we do not take the potential barrier into consideration and use a simplified surface and coordinate system shown in Fig. 2 hereafter.

We assume, as shown in Fig. 2, that the equi-potential lines are parallel with y and y' axes in regions I and II respectvely and that their radii at the bending part are constant. The dotted line shows the reaction path of radius r_e in region II, which traces minima in the direction of x, r or x' in the respective region.

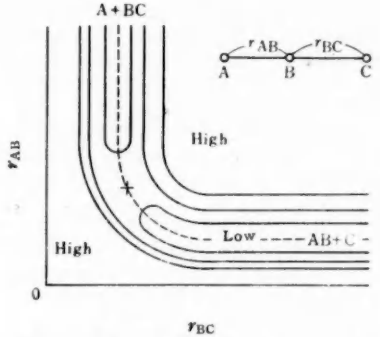

Fig. 1. Potential energy surface of reaction A+BC→AB+C.

1) J. O. Hirschfelder and E. Wigner, *J. Chem. Phys.*, **7**, 616 (1939).
2) E. Wigner, *Z. physik. Chem.*, **B19**, 203 (1932).
3) R. P. Bell, *Proc. Roy. Soc.*, **A139**, 466 (1933).
4) F. A. Matsen, *J. Chem. Phys.*, **22**, 165 (1954).
5) H. M. Hulburt and J. O. Hirschfelder, ibid., **11**, 276 (1943).
6) Paper I of this series: I. Yasumori and K. Fueki, This Bulletin, **29**, 1 (1956).

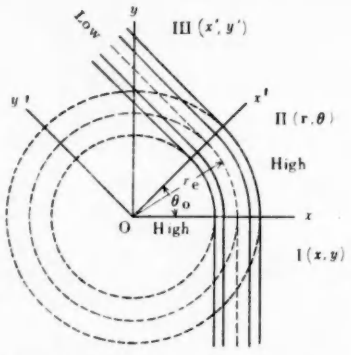

Fig. 2. Coordinate system of curved reaction path.

The wave equation to be satisfied by the system is

$$\nabla^2\Psi+\frac{8\pi^2\mu}{h^2}(E-V)\Psi=0 \qquad (1)$$

where μ is the reduced mass of the system. According to the assumed form of potential V, the wave equation is separable with respect to the variables (x,y), (r,θ) and (x',y') in the regions I, II and III, respectively.

Now let us consider an incident wave of unit amplitude in region I, which expresses the state of reactant and comes from $y<0$ to the boundary $y=0$, being partly reflected at the boundary and partly transmitted through the bend.

Now, the wave functions which express the states of the system in each region are given as follows: In region I,

$$\Psi^{\mathrm{I}}=\phi_\kappa{}^{\mathrm{I}}(x)\cdot\exp\left(\frac{2\pi i}{h}p_\kappa\cdot y\right)+\sum_\lambda B_{\kappa\lambda}\phi_\lambda{}^{\mathrm{I}}(x)\cdot\exp\left(-\frac{2\pi i}{h}p_\lambda\cdot y\right) \qquad (2)$$

where the first term represents the incident wave and the second the reflected waves. $\phi_\kappa{}^{\mathrm{I}}(x)$ is the eigenfunction of vibrational motion of the system in κ-th state and $\exp[(2\pi i/h)\cdot p_\kappa\cdot y]$ represents the eigenfunction of translational motion with the momentum p_κ. The total energy of the system, E, is equal to the sum of those of each motion, E_{vib} and E_{trans}. $B_{\kappa\lambda}$ is the coefficient of reflected wave referring to the transition between states, κ and λ.

In a similar way, the wave functions in regions II and III are expressed as

$$\Psi^{\mathrm{II}}=\sum_k[C_{\kappa k}\cdot\phi_k{}^{\mathrm{II}}(r)\cdot\exp(im_k\theta)+D_{\kappa k}\cdot\phi_k{}^{\mathrm{II}}(r)\cdot\exp(-im_k\theta)] \qquad (3)$$

and

$$\Psi^{\mathrm{III}}=\sum_{\kappa'}F_{\kappa\kappa'}\phi_{\kappa'}{}^{\mathrm{III}}(x')\cdot\exp\left(\frac{2\pi i}{h}p_{\kappa'}\cdot y'\right) \qquad (4)$$

where m_k is a constant and we may define a new constant q_k by the equation

$$m_k=\frac{2\pi}{h}\cdot q_k\cdot r_e \qquad (5)$$

The coefficients of the transmitted waves, $C_{\kappa k}$ or $D_{\kappa k}$, are defined corresponding to the forward or backward translational motion in k-th state of region II and that of the transmitted wave, $F_{\kappa\kappa'}$ referring to κ'-th state in region III. We assume that all the wave functions for the vibrational motion, $\phi_\kappa{}^{\mathrm{I}}(x)$, $\phi_{\kappa'}{}^{\mathrm{III}}(x')$ and $\phi_k{}^{\mathrm{II}}(r)$ are normalized to unity.

Thus the following equations are readily obtained by the usual procedure of substituting the wave functions into the boundary conditions,

$$\Psi^{\mathrm{I}}=\Psi^{\mathrm{II}} \text{ and } \frac{\partial\Psi^{\mathrm{I}}}{\partial y}=\frac{\partial\Psi^{\mathrm{II}}}{\partial y}=\frac{1}{r}\left(\frac{\partial\Psi^{\mathrm{II}}}{\partial\theta}\right)_{\theta=0} \qquad \text{(a), (b)}$$

at $y=0$ and

$$\Psi^{\mathrm{II}}=\Psi^{\mathrm{III}} \text{ and } \frac{\partial\Psi^{\mathrm{III}}}{\partial y'}=\frac{\partial\Psi^{\mathrm{II}}}{\partial y'}=\frac{1}{r}\left(\frac{\partial\Psi^{\mathrm{II}}}{\partial\theta}\right)_{\theta=\theta_0} \qquad \text{(c), (d)}$$

at $y'=0$; we have

$$\delta_{\kappa\lambda}+B_{\kappa\lambda}=\sum_k(C_{\kappa k}+D_{\kappa k})u_{k\lambda} \qquad (6)$$

$$\delta_{\kappa\lambda}p_\kappa-B_{\kappa\lambda}p_\lambda=\sum_k(C_{\kappa k}-D_{\kappa k})\cdot q_k\cdot v_{k\lambda} \qquad (7)$$

$$\sum_k[C_{\kappa k}\cdot\exp(im_k\theta_0)+D_{\kappa k}\times\exp(-im_k\theta_0)]u'_{k\kappa'}=F_{\kappa\kappa'} \qquad (8)$$

and

$$\sum[C_{\kappa k}\cdot\exp(im_k\theta_0)-D_{\kappa k}\times\exp(-im_k\theta_0)]\cdot q_k\cdot v'_{k\kappa'}=F_{\kappa\kappa'}\cdot p'_{\kappa'} \qquad (9)$$

The expansion coefficients $u_{k\lambda}$'s and $v_{k\lambda}$'s are defined by the equations

$$[\phi_k{}^{\mathrm{II}}(r)]_{\theta=0}=\phi_k{}^{\mathrm{II}}(x)=\sum_\lambda u_{k\lambda}\cdot\phi_\lambda{}^{\mathrm{I}}(x) \qquad (10)$$

and

$$\left[\frac{r_e}{r}\cdot\phi_k{}^{\mathrm{II}}(r)\right]_{\theta=0}=\frac{r_e}{x}\cdot\phi_k{}^{\mathrm{II}}(x)=\sum_\lambda v_{\kappa\lambda}\cdot\phi_\lambda{}^{\mathrm{I}}(x) \qquad (11)$$

Similarly the coefficients $u'_{k\lambda'}$'s and $v'_{k\lambda'}$'s are also defined by the equations

$$[\phi_k{}^{\mathrm{II}}(r)]_{\theta=\theta_0}=\phi_k{}^{\mathrm{II}}(x')=\sum_{\lambda'}u'_{k\kappa'}\cdot\phi_{\lambda'}{}^{\mathrm{III}}(x') \qquad (12)$$

and

$$\left[\frac{r_e}{r}\cdot\phi_k{}^{\mathrm{II}}(r)\right]_{\theta=\theta_0}=\frac{r_e}{x'}\cdot\phi_k{}^{\mathrm{II}}(x')$$

$$=\sum_{\lambda'} v'_{k\lambda'} \cdot \phi_{\lambda'}^{\mathrm{III}}(x') \tag{13}$$

Eqs. 6—9 are expressed by the use of the matrix form as

$$1+B=(C+D)u \tag{6'}$$

$$p-Bp=(C-D)qv \tag{7'}$$

$$(CW+DW^*)u'=F \tag{8'}$$

and

$$(CW-DW^*)qv'=Fp' \tag{9'}$$

where W and its complex conjugate W^* are diagonal matrices whose elements are $\exp(im_k\theta_0)$'s and $\exp(-im_k\theta_0)$'s, respectively. Accordingly the coefficient matrix of the reflected waves, B, and that of the transmitted waves, F, are formally derived as follows: We have

$$B=-(NWM'+MW^*N') \times (MWM'+NW^*N')^{-1} \tag{14}$$

and

$$F=1/2\cdot[B(MW+NW^*) +(NW+MW^*)]\cdot u' \tag{15}$$

where

$$M=u^{-1}-pv^{-1}q^{-1} \tag{16}$$

$$N=u^{-1}+pv^{-1}q^{-1} \tag{17}$$

$$M'=u'-qv'p'^{-1} \tag{18}$$

and

$$N'=u'+qv'p'^{-1} \tag{19}$$

By the use of the expressions of B and F, the reflection and transmission coefficients $\rho_{\kappa\lambda}$ and $\kappa_{\kappa\kappa'}$ are given by

$$\rho_{\kappa\lambda}=|B_{\kappa\lambda}|^2\cdot p_\lambda/p_\kappa \tag{20}$$

and

$$\kappa_{\kappa\kappa'}=|F_{\kappa\kappa'}|^2\cdot p_{\kappa'}/p_\kappa \tag{21}$$

Furthermore, the total reflection and transmission coefficients from a definite initial κ-th state, ρ_κ, and κ_κ, are defined as

$$\rho_\kappa=\sum_\lambda \rho_{\kappa\lambda} \text{ and } \kappa_\kappa=\sum_{\kappa'}\kappa_{\kappa\kappa'} \tag{22), (23}$$

κ_κ may be estimated from the value of ρ_κ by the use of the following equation,

$$\kappa_\kappa=1-\rho_\kappa \tag{24}$$

For the simple case with a single boundary $y=0$, taking

$$D_{\kappa k}=0 \text{ and } F_{\kappa\kappa'}=0$$

the equations to be solved become

$$1+B=Cu \text{ and } p-Bp=Cqv. \tag{25), (26}$$

Then the formal solutions of B and C are

$$B=(S-1)\cdot(S+1)^{-1} \tag{27}$$

and

$$C=2S(S+1)^{-1}\cdot u^{-1} \tag{28}$$

where the matrix S has the form of

$$S=pv^{-1}q^{-1}u \tag{29}$$

Therefore, the transmission coefficient, $\kappa_{\kappa k}$ is given by

$$\kappa_{\kappa k}=|C_{\kappa k}|^2\cdot q_k/p_\kappa \tag{30}$$

in this case.

It is very difficult to obtain explicitly the rigorous form of the coefficients $B_{\kappa\lambda}$, $F_{\kappa\kappa'}$ and $C_{\kappa k}$ for general cases. We, therefore, confine ourselves to the simple case where the radius of the path, r_e, is much larger than the classical amplitude of vibration, $\rho_{\max}$,

$$r_e \ll \rho_{\max}$$

The approximate expressions of the coefficients in this case are given in Appendix I.

Vibrational Wave Function and Computation of the Coefficients

Now we treat the case in which the section of the channel is parabolic and the vibrational motion is simple harmonic. When we put, as the explicit form of vibrational potential,

$$V=2\pi^2\mu\nu_0^2x^2 \tag{31}$$

the normalized vibrational eigenfunction with the quantum number κ in region I is

$$\phi_\kappa^{\mathrm{I}}(x)=N_\kappa\cdot\exp\left(-\frac{\alpha}{2}\rho^2\right)H_\kappa(\sqrt{\alpha}\cdot\rho) \tag{32}$$

where

$$\rho=x-r_e \quad \text{and} \quad \alpha=4\pi^2\mu\nu_0/h \tag{33}$$

$N_\kappa=[(\alpha/\pi)^{1/2}/2^\kappa\cdot\kappa!]^{1/2}$ is a normalization factor, $H_\kappa(\sqrt{\alpha}\cdot\rho)$ the κ-th Hermite polynomial and ν_0 the fundamental frequency of vibration. The total energy of the system in region I is

$$E=E_{\mathrm{vib}}+E_{\mathrm{trans}}=h\nu_0(\kappa+1/2)+(1/2\mu)p_\kappa^2 \tag{34}$$

The eigenfunction of κ'-th state in region III is readily obtained by replacing κ and x in the above expressions with κ' and x' respectively.

The radial function $\phi_k^{\mathrm{II}}(r)$ in region II is obtained in the same way as the well-known treatment of the vibrational and rotational motions of diatomic molecule[7], since it is related to the circular potential shown in Fig. 2.

Therefore, under the condition $r_e \gg \rho_{\max}$, an approximate form of $\phi_k^{\mathrm{II}}(r)$ is given by

$$\phi_k^{\mathrm{II}}(r)=\frac{n}{r^{1/2}}\cdot N_k\cdot\exp\left(-\frac{\alpha'}{2}\zeta^2\right)\cdot H_k(\sqrt{\alpha'}\cdot\zeta) \tag{35}$$

where

$$n\simeq[r_e(1+\beta)]^{1/2}\Big/\left[1+\frac{(2k+1)}{2\alpha r_e^2(1+\beta)^2}\right]^{1/2} \tag{36}$$

7) L. Pauling and E. B. Wilson, "Introduction to Quantum Mechanics", McGraw-Hill Book Co., Inc., New York (1935), p. 298.

$$\zeta = \rho - \beta r_e \tag{37}$$

$$\beta = \xi^2/(1+3\xi^2) \tag{38}$$

$$\nu' = \nu_0(1+3\xi^2)^{1/2} \tag{39}$$

$$\xi = q_k/2\pi\mu r_e\nu_0 \tag{40}$$

α' is obtained by replacing ν_0 in α, Eq. 33, with ν' and N_k by replacing κ and α in N_κ with k and α', respectively.

The total energy in this region is described as

$$E \simeq h\nu'(k+1/2) + (1/2\mu)(1-\beta)q_k^2 \tag{41}$$

The matrix elements of u and v are calculated by Eqs. 32 and 35 as shown in Appendix II.

The above consideration is also applicable, in principle, to the potential with Morse function-type section, but the formulation will be quite tedious.

Few potential energy surfaces with considerable accuracy have been constructed except for the ortho-para hydrogen conversion reaction, $H+H_2 \rightarrow H_2+H$[8,9]. Therefore, we performed the computation of the reflection and transmission coefficients for the potential surfaces which have a similar fearture to that of this reaction except that the barrier is neglected.

The constants used in the computation are

$$h\nu_0 = 12.56 \text{ kcal./mol.}$$

$$\mu = (2/3)\cdot m_H = 1.1156\times10^{-24} \text{ g.}$$

$$\theta_0 = 2\pi/3$$

and $r_e = 1.0$ and 0.5 Å

These values of r_e scarcely satisfy the condition $r_e \gg \rho_{max}$, since the classical amplitudes of vibrational motion for the ground and the first excited levels are 0.09 and 0.15Å, respectively. Calculations were performed for the range of the total energy $E < h\nu_0(2+1/2) = 31.4$ kcal./mol. The obtained values of coefficients are shown in Figs. 3 and 4.

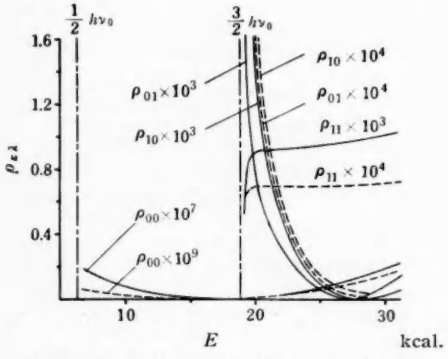

Fig. 3. Reflection coefficients for single boundary.
—— $r_e = 0.5$Å, ---- $r_e = 1.0$Å

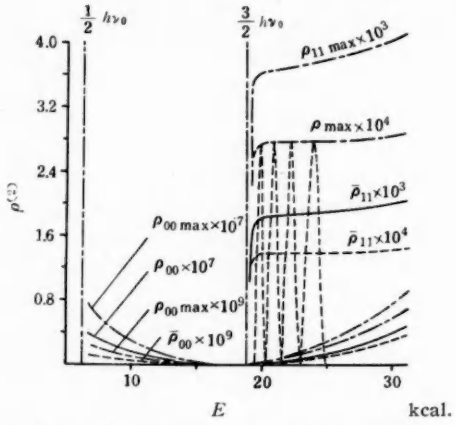

Fig. 4. Reflection coefficients for two boundaries.
—— $r_e = 0.5$Å, ---- $r_e = 1.0$Å, $\theta_0 = 2/3\cdot\pi$

Discussion

The present results agree, in many points, with those of Hulburt and Hirschfelder's in which the potential surface of square-well channel with 90° turn is used, but there are some noticeable differences between them.

That the reflection and transmission coefficients $\rho_{\kappa\lambda}$ and $\kappa_{\kappa\lambda}$ are not zero for $\kappa \neq \lambda$, shows the occurrence of the cross transition between the different vibrational states and also verifies their prediction about this occurrence obtained from the consideration of the classical motion of a particle in smoothly curved channel[10].

Apart from their absolute magnitude, the general properties of the coefficients resemble the results of Hulburt et al. for the case with vibrational transition.

In our case of single boundary with which their results include nothing to be compared, $\rho_{\kappa\kappa}$'s vary slightly with the increase of the translational energy, while $\rho_{\kappa\lambda}$'s, which rise where the translational energy is just equal to $\kappa h\nu_0$ $(\kappa > \lambda)$ or $\lambda h\nu_0$ $(\lambda > \kappa)$, fall rapidly and then increase

8) J. O. Hirschfelder, N. Rosen and H. Eyring, *J. Chem. Phys.*, **4**, 121 (1936).
9) J. O. Hirschfelder, H. Eyring and B. Topley, ibid., **4**, 173 (1936).
10) Ref. 5, p. 280.

gradually as the energy increases. In general, $\rho_{\varepsilon\lambda}$'s are much larger than $\rho_{\varepsilon\varepsilon}$'s in the available range of energy. For the case of two boundaries, the reflection coefficients are oscillating function of energy as shown in Fig. 4. This property is readily seen from the expressions of $B_{\varepsilon\lambda}$'s in Appendix I and those of ρ's, Eq. 20: By the introduction of such approximations as $(v_0^{-1}\cdot u_0)p \simeq q$, etc., the resultant forms are

$$\rho_{\varepsilon\varepsilon} \simeq 4\rho^{(1)}{}_{\varepsilon\varepsilon} \sin^2 m_\varepsilon\theta_0 \qquad (42)$$

and $$\rho_{\varepsilon\lambda} \simeq 4\rho^{(1)}{}_{\varepsilon\lambda} \sin^2\{(m_\varepsilon + m_\lambda)/2\cdot\theta_0\} \qquad (43)$$

where $\rho^{(1)}$'s represent those of single boundary under the same condition. The angle of bending, θ_0, which is related to the masses of component species, m_A, m_B and m_C, by the equation[11]

$$\sin(\theta_0 - \pi/2) = [m_A m_C/(m_A+m_B)(m_B+m_C)]^{1/2}$$

takes value which is between $\pi/2$ and π. A larger value of θ_0 makes the period of oscillation shorter (Fig. 5).

They also found such an oscillating property of coefficient as stated above and regarded it as an essential one for the transmission of waves through a bend. The present author presumes, however, that the property is partly of artificial nature being due to the form of potential models which have two discontinuous boundaries and is partly of real nature relating to the efficiency of energy transfer between the translational and vibrational motions, by the considerations given below.

The reasons why the form of potential model is responsible are as follows:

(a) Whatever the transmission to be estimated is for a bend or a barrier, all the reflection and transmission coefficients obtained change monotonously with energy in the case of smooth potential without any boundary[3,6], or even in those of single boundary[1], while they always oscillate in the cases of two boundaries[1,5].

(b) From the present result with two boundaries as shown in Fig. 4, it is found that the coefficients which are averaged over each period of oscillation[12] are about twice as large as those of a single boundary under the same condition. This property is based, perhaps, on the fact that the coefficients are the functions of amplitude of the standing waves which exist between boundaries and the amplitude of a wave with a definite phase varies periodically with respect to the momentum q and θ_0 at one of the boundaries. Therefore, when we take the average for each period of oscillation, which corresponds to superposition of all waves with any phase, the results seem to give good approximation for the actual behavior[13]. It goes without saying that such a property as stated above can not be expected in a real case, since the potential energy surface of reaction would be continuous everywhere considering the nature of valence force.

In the next place, their result that the oscillating transmission coefficients get zero values when the energy of translation is just equal to several energy units of quantized motion which is perpendicular to the direction of the above motion, is explained as the complete transfer of translational energy to the vibrational one. This property is also seen from the present result that the value of ρ_{01} rises steeply as the translational energy approaches to $h\nu_0$.

It seems that the speciality of the square-well channel with 90° turn used by them comprises incidentally these effects of real and of virtual: The wave functions which express the translational and vibrational motions are of similar form and their eigenvalues in the bending part are identical to each other.

From these considerations, it will be concluded that the total transmission coefficients κ_ε's decrease stepwise with the increase of energy on account of the entry of reflections in which the higher vibrational states are concerned. This tendency also agrees with that which Hulburt et al. pointed out previously.

Subsequently, the effect of the curvature is examined. A larger curvature (smaller radius) brings about the increase of reflection in both the cases with and without the vibrational transition (Figs. 3 and 4). Because of the smallness of net reflection, however, almost all systems pass through the bend, preserving initial vibration quanta. This persistency of vibrational state was also found for the transmission through the barrier which was treated in

11) S. Glasstone, K. J. Laidler and H. Eyring, "The Theory of Rate Processes", McGraw-Hill Book Co., Inc., New York (1941), p. 102.

12) Since $\frac{1}{\pi}\int_0^\pi \sin^2 x dx = 1/2$, the averaged value of $\rho_{\varepsilon\varepsilon}$ in Eq. 43, $\bar{\rho}_{\varepsilon\varepsilon}$, is expressed by $\bar{\rho}_{\varepsilon\varepsilon} \simeq 2\rho_{\varepsilon\varepsilon}{}^{(1)}$, where $\rho_{\varepsilon\varepsilon}{}^{(1)}$ is assumed to be nearly constant in each period. Other coefficients are also treated analogously.

13) A similar situation is held in the case of Ref. 1, p. 621, in which the transmission through an energy barrier was treated.

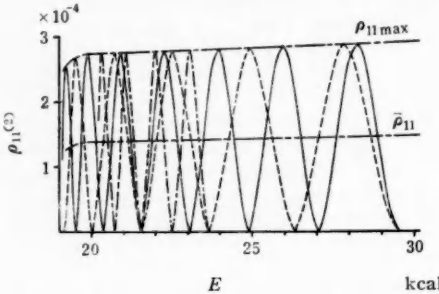

Fig. 5. Variation of $\rho_{11}^{(2)}$ with increase of bending angle θ_0.
r_e=1.0Å,
---- $\theta_0=\pi/2$, —— $\theta_0=2\pi/3$, ------ $\theta_0=\pi$

Paper I of this series[14]. The case of Hulburt and Hirschfelder's, in which rather large decrease of transmission was estimated, corresponds to that of extremely small radius $r_e=\rho_{max}$ in our case.

It is expected that the transmission coefficient becomes different for the system including isotopes, since the resultant μ changes its magnitude for the same value of energy. This effect was also pointed out by them and their result of oscillating coefficient with perfect reflection made them expect its availability for the isotopic separation. Since, however, the difference between reflections for isotopic reactions is also very small, the transmission through the bend seems not to be effective for the process.

As a quantum-mechanical correction necessary for the rate-estimation by the usual method, the overall transmission coefficient κ_{bend} is defined by[6]

$$\kappa_{bend}=\sum_{\varepsilon} e^{-\frac{E_{vib}}{kT}}\cdot\int_0^{\infty}\kappa_{\varepsilon}\cdot e^{-\frac{p_{\varepsilon}^2}{2\mu kT}}\cdot p_{\varepsilon}\,dp_{\varepsilon}\times\left[\sum_{\varepsilon} e^{-\frac{E_{vib}}{kT}}\cdot\int_0^{\infty} e^{-\frac{p_{\varepsilon}^2}{2\mu kT}}\cdot p_{\varepsilon}\,dp\right]^{-1}$$
$$=1-(\mu kT)^{-1}\cdot(1-e^{-\frac{h\nu_0}{kT}})\times\left[\sum_{\varepsilon=0} e^{-\frac{\varepsilon h\nu_0}{kT}}\cdot\int_0^{\infty}\rho_{\varepsilon}e^{-\frac{p_{\varepsilon}^2}{2\mu kT}}\cdot p_{\varepsilon}\,dp_{\varepsilon}\right] \quad (44)$$

Since the individual κ_{ε}'s are nearly equal to unity, the resultant κ_{bend} is also close to unity and gradually decreases as the temperature becomes higher. The values, $1-\kappa_{bend}$, for the hydrogen atom-molecule reaction, for example, are shown in Table I.

TABLE I. VALUES OF $(1-\kappa_{bend})$[15]

Temp. °K	300	500	1000	2000
r_e=0.5 Å	3.0×10^{-8}	1.3×10^{-6}	3.8×10^{-4}	3.4×10^{-3}
r_e=1.0 Å	2.0×10^{-11}	7.3×10^{-7}	2.3×10^{-4}	2.8×10^{-3}

Finally, as concerns the reacting system which includes heavier species than hydrogen, it is very difficult to presume the exact behavior of the transmitting waves, because the factors μ, r, ν_0 and θ_0 change markedly for respective cases. In general, increased μ and lowered ν_0 provide an increase of the reflection which is canceled to some extent by an increased r_e. However, the deviation of the total transmission from unity will be very small after all, since the fact that the de Broglie wavelength corresponding to the translational motion becomes shorter than that of hydrogen atom-molecule reaction (1.8Å at 300°K) makes the classical consideration of motion more valid.

The author wishes to thank Professor S. Shida for his kind advice and encouragement. The author is also much indebted to Professor J. Horiuti and Dr. T. Toya of Hokkaido University and Dr. K. Fueki of Osaka University for their valuable discussion and suggestions.

Laboratory of Physical Chemistry
Tokyo Institute of Technology
Meguro-ku, Tokyo

Appendix I. Approximate Formulae of the Coefficients $B_{\varepsilon\lambda}$, $C_{\varepsilon k}$ and $F_{\varepsilon\varepsilon'}$

Under the condition $r_e \gg \rho_{max}$, it is expected that the vibrational eigenfunction in region II, $\phi_k^{II}(r)$ becomes close to the function $\phi_{\varepsilon}^{I}(x)$ with $\kappa=k$ in its form at the boundary between regions I and II and that the matrix v is nearly equal to u. Accordingly, when we divide u into the two parts, u_0, the diagonal part of u, and u_1, the offdiagonal part,

$$u=u_0+u_1 \quad (A1)$$

and also
$$v=v_0+v_1 \quad (A2)$$

in a similar manner, it may be assumed that the elements of u_1 (or v_1) are small compared with those of u_0 (or v_0).

(a) The Case of Single Boundary.—We have the matrix S, Eq. 29, of the following approximate form,

$$S=pv_0^{-1}(1-v_1\cdot v_0^{-1})q^{-1}(u_0+u_1) \quad (A3)$$

or neglecting the term including $u_1\cdot v_1$,

14) This effect means that the perturbation at the bend should be very small compared with the total energy of the system. The present condition, $r_e\gg\rho_{max}$, which is equivalent to that in Ref. 6, p. 2, $a_0\gg aV_r(r)$, satisfies this restriction.

15) In the estimation, the values of ρ_{10} and ρ_{01} at $E=3/2\cdot l\nu_0$ were assumed for convenience to be unity.

$$S=S_0+S_1 \tag{A4}$$

where $S_0=p v_0^{-1} q^{-1} u_0$ (A5)

and $S_1 \simeq p v_0^{-1} q^{-1} u_1 - p v_0^{-1} v_1 v_0^{-1} u_0 q^{-1}$ (A6)

Since the matrix B of Eq. 27 is expressed by the use of the above equations, as

$$B=(S_0-1)(S_0+1)^{-1}+2(S_0+1)^{-1}S_1(S_0+1)^{-1} \tag{A7}$$

we can finally get the expressions of the coefficients of reflected waves $B_{\kappa\lambda}$'s and those of transmitted waves $C_{\kappa k}$'s,

$$B_{\kappa\lambda}=\frac{p_\kappa(v_0^{-1}\cdot u_0)_\kappa - q_\kappa}{p_\kappa(v_0^{-1}\cdot u_0)_\kappa + q_\kappa}\delta_{\kappa\lambda} + \frac{2p_\kappa(v_0^{-1})_\kappa[u_{1,\kappa\lambda}q_\lambda - q_\kappa v_{1,\kappa\lambda}(v_0^{-1}\cdot v_0)_\lambda]}{[p_\kappa(v_0^{-1}\cdot u_0)_\kappa + q_\kappa]\cdot[p_\lambda(v_0^{-1}\cdot u_0)_\lambda + q_\lambda]} \tag{A8}$$

and

$$C_{\kappa k}=\frac{2p_\kappa(v_0^{-1}\cdot u_0)_\kappa u^{-1}{}_{\kappa k}}{p_\kappa(v_0^{-1}\cdot u_0)_\kappa + q_\kappa} + \sum_\lambda \frac{2p_\kappa(v_0^{-1})_\kappa[u_{1,\kappa\lambda}q_\lambda - q_\kappa\cdot v_{1,\kappa\lambda}(v_0^{-1}\cdot u_0)_\lambda]u^{-1}{}_{\lambda\kappa}}{[p_\kappa(v_0^{-1}\cdot u_0)_\kappa + q_\kappa]\cdot[p_\lambda(v_0^{-1}\cdot u_0)_\lambda + q_\lambda]} \tag{A9}$$

(b) The Case of Two Boundaries.—By the introduction of the same approximations for u' and v' as those for u and v, the coefficients $B_{\kappa\lambda}$'s are expressed as follows:

$$B_{\kappa\kappa}=L_\kappa[(v_0^{-1}\cdot u_0)_\kappa p_\kappa{}^2-(u_0^{-1}\cdot v_0)_\kappa q_\kappa{}^2]\cdot(Q_\kappa)^{-1} \tag{A10}$$

and

$$\begin{aligned}B_{\kappa\lambda}=&2p_\kappa(Q_\kappa\cdot Q_\lambda)^{-1}\\ &\times[(4-G_\kappa\cdot G_\lambda)q_\lambda q_\kappa\{(v_0^{-1})_\kappa v_{1,\kappa\lambda}p_\kappa\\ &-(u_0^{-1})_\kappa u_{1,\kappa\lambda}p_\lambda\}\\ &-L_\kappa L_\lambda\{(u_0^{-1})_\kappa v_{1,\kappa\lambda}(v_0^{-1}\cdot u_0)_\lambda p_\lambda q_\kappa{}^2\\ &-(v_0^{-1})_\kappa\cdot u_{1,\kappa\lambda}(u_0^{-1}\cdot v_0)_\lambda\cdot p_\kappa\cdot q_\lambda{}^2\}\\ &+G_\kappa L_\lambda q_\kappa\{(v_0^{-1})_\kappa\cdot v_{1,\kappa\lambda}(v_0^{-1}\cdot u_0)_\lambda p_\kappa p_\lambda\\ &-(u_0^{-1})_\kappa\cdot u_{1,\kappa\lambda}(u_0^{-1}\cdot v_0)_\lambda q_\lambda{}^2\}\\ &+G_\lambda L_\kappa\{(u_0^{-1})_\kappa\cdot v_{1,\kappa\lambda}q_\kappa{}^2\\ &-(v_0^{-1})_\kappa\cdot u_{1,\kappa\lambda}p_\kappa p_\lambda\}]\end{aligned} \tag{A11}$$

where

$$\begin{aligned}Q_\kappa=&L_\kappa\{(v_0^{-1}\cdot u_0)_\kappa\cdot p_\kappa{}^2+(u_0^{-1}\cdot v_0)_\kappa\cdot q_\kappa{}^2\}\\ &-2G_\kappa p_\kappa\cdot q_\kappa\end{aligned} \tag{A12}$$

$$G_\kappa=(W+W^*)_\kappa=2\cos m_\kappa\theta_0 \tag{A13}$$

and $$L_\kappa=(W-W^*)_\kappa=2i\sin m_\kappa\theta_0 \tag{A14}$$

The $F_{\kappa\kappa'}$'s is obtained by substituting the above expressions of $B_{\kappa\lambda}$'s into Eq. 15.

Appendix II. Calculations of $u_{k\lambda}$ and $v_{k\lambda}$

The matrix element $u_{k\lambda}$ is defined by

$$\psi_k^{\mathrm{II}}(x)\sum_\lambda u_{k\lambda}\cdot\psi_\lambda^{\mathrm{I}}(x) \tag{A15}$$

Making use of the property of ψ^{I}, we obtain

$$u_{k\lambda}=\int_{-\infty}^{+\infty}\psi_\lambda{}^{\mathrm{I}*}\cdot\psi_k{}^{\mathrm{II}}\mathrm{d}\rho \tag{A16}$$

where the lower limit of integration with respect to ρ can be practically extended to minus infinity instead of $\rho=-r_e$ because of the rapid diminution of $\psi_\lambda{}^{\mathrm{I}}$ and $\psi_k{}^{\mathrm{II}}$ where ρ is smaller than $-\rho_{\max}$.

From the condition $r_e \gg \rho_{\max}$, $\psi_k{}^{\mathrm{II}}(x)$, Eq. 35, is described approximately by

$$\psi_\kappa{}^{\mathrm{II}}(x)\simeq\frac{n}{r_e{}^{1/2}}\cdot\left(1-\frac{\rho}{2r_e}+\frac{3\rho^2}{8r_e{}^2}\right)\cdot N_k \times\exp\left(-\frac{\alpha'}{2}\zeta^2\right)\cdot H_k(\sqrt{\alpha'}\zeta) \tag{A17}$$

Accordingly, $u_{k\lambda}$ which is given by Eq. A16 consists of the sum of the general term,

$$\text{const.}\times\int_{-\infty}^{+\infty}\rho^n\cdot N_k N_\lambda\cdot\exp\left(-\frac{\alpha'}{2}\zeta^2-\frac{\alpha}{2}\rho^2\right) \times H_k(\sqrt{\alpha'}\cdot\zeta)\cdot H_\lambda(\sqrt{\alpha}\cdot\rho)\,\mathrm{d}\rho$$

which is resolved, furthermore, into the sum of the following integrals with some coefficients[16],

$$I_{\kappa\lambda}=N_k N_\lambda\cdot\int_{-\infty}^{+\infty}\exp\left(-\frac{\alpha'}{2}\zeta^2-\frac{\alpha}{2}\rho^2\right) \times H_k(\sqrt{\alpha'}\cdot\zeta)\cdot H_\lambda(\sqrt{\alpha}\cdot\rho)\cdot\mathrm{d}\rho \tag{A18}$$

Since

$$\alpha'\zeta^2+\alpha\rho^2=(\alpha+\alpha')\left[\rho-\left(\frac{\alpha'}{\alpha+\alpha'}\right)\beta r_e\right]^2=at^2 \tag{A19}$$

where a and t are defined by

$$a=\alpha+\alpha' \quad\text{and}\quad t=\rho-\left(\frac{\alpha'}{\alpha+\alpha'}\right)\beta r_e \tag{A20), (A21}$$

Eq. A18 is also written as

$$I_{k\lambda}=N_k N_\lambda\cdot\exp\left[-\frac{1}{2}\left(\frac{\alpha\alpha'}{\alpha+\alpha'}\right)(\beta r_e)^2\right] \times\int_{-\infty}^{+\infty}\exp\left(-\frac{a}{2}t^2\right)H_k H_\lambda\mathrm{d}\rho \tag{A22}$$

Transforming the variables, $\sqrt{\alpha}\cdot\rho$ in H_λ and $\sqrt{\alpha'}\cdot\zeta$ in H_k, into a new variable,

$$s=\sqrt{a}\cdot t \tag{A23}$$

we can write

$$H_\lambda(\sqrt{\alpha}\cdot\rho)=\sum_l g_{\lambda l}H_l(\sqrt{a}\cdot t) \tag{A24}$$

and $$H_k(\sqrt{\alpha'}\cdot\zeta)=\sum_l h_{kl}H_l(\sqrt{a}\cdot t) \tag{A25}$$

where $g_{\lambda l}$ and h_{kl} are coefficients of expansion.

Substituting Eqs. A24 and A25 into Eq. A22, we can get the final expression of $I_{k\lambda}$,

$$I_{k\lambda}=N_k N_\lambda\cdot\exp\left[-\frac{1}{2}\left(\frac{\alpha\alpha'}{\alpha+\alpha'}\right)(\beta r_e)^2\right] \times\sum_l g_{\lambda l}\cdot h_{kl}(N_l)^{-2} \tag{A26}$$

where N_l is obtained by replacing α and λ in N_λ with a and l respectively. In a similar way, the matrix element $v_{k\lambda}$

$$v_{k\lambda}=\int_{-\infty}^{+\infty}\left(\frac{r_e}{r_e+\rho}\right)\cdot\psi_\lambda{}^{\mathrm{I}*}\cdot\psi_k{}^{\mathrm{II}}\mathrm{d}\rho \tag{A27}$$

is computed, since the function $r_e/(r_e+\rho)\cdot\psi_k{}^{\mathrm{II}}(x)$ has the following approximate form,

16) See, for example, H. Eyring, J. Walter and G. E. Kimball, "Quantum Chemistry", John Wiley & Sons, Inc., New York (1949), p. 60.

$$\left(\frac{r_e}{r_e+\rho}\right)\cdot\phi_k^{II}(x)\simeq\frac{n}{r_e^{1/2}}\cdot\left(1-\frac{3\rho}{2r_e}+\frac{15\rho^2}{8r_e^2}\right)\cdot N_k \times\exp\left(-\frac{\alpha'}{2}\zeta^2\right)\cdot H_k(\sqrt{\alpha'}\cdot\zeta) \quad (A28)$$

and can also be resolved into the sum of $I_{k\lambda}$ with reasonable coefficient as well as in the case of $u_{k\lambda}$.

The obtained expressions of $u_{k\lambda}$ and $v_{k\lambda}$ for $k,\lambda=0,1$ are shown as follows:

$$u_{00}=A_{00}\cdot\left[\left(1-\frac{1}{2}\varepsilon+\frac{3}{8}\varepsilon^2\right)+\frac{3}{8}\eta\right] \quad (A29)$$

$$u_{10}=2A_{10}\sqrt{\alpha' r_e}\cdot\left[\left(1-\frac{1}{2}\varepsilon+\frac{3}{8}\varepsilon^2\right)(\varepsilon-\beta)+\frac{1}{8}\{9\varepsilon-(4+3\beta)\eta\}\right]$$

$$u_{01}=2A_{01}\sqrt{\alpha}\cdot r_e\cdot\left[\left(1-\frac{1}{2}\varepsilon+\frac{3}{8}\varepsilon^2\right)\varepsilon+\frac{1}{8}(9\varepsilon-4)\eta\right]$$

$$u_{11}=4A_{11}\sqrt{\alpha\alpha'}\cdot r_e^2\cdot\left[\left(1-\frac{1}{2}\varepsilon+\frac{3}{8}\varepsilon^2\right)(\varepsilon-\beta)\varepsilon+\frac{3}{8}\eta^2+\left\{\left(1-\frac{1}{2}\varepsilon+\frac{3}{8}\varepsilon^2\right)+\left(\frac{3}{4}\varepsilon-\frac{1}{2}\right)(2\varepsilon-\beta)+\frac{3}{8}(\varepsilon-\beta)\varepsilon\right\}\eta\right]$$

and

$$v_{00}=A_{00}\cdot\left[\left(1-\frac{3}{2}\varepsilon+\frac{15}{8}\varepsilon^2\right)+\frac{15}{8}\eta\right] \quad (A30)$$

$$v_{10}=2A_{10}\sqrt{\alpha' r_e}\cdot\left[\left(1-\frac{3}{2}\varepsilon+\frac{15}{8}\varepsilon^2\right)(\varepsilon-\beta)+\frac{1}{8}\{45\varepsilon-(12+15\beta)\}\eta\right]$$

$$v_{01}=2A_{01}\sqrt{\alpha}\cdot r_e\cdot\left[\left(1-\frac{3}{2}\varepsilon+\frac{15}{8}\varepsilon^2\right)\varepsilon+\frac{1}{8}(45\varepsilon-12)\eta\right]$$

$$v_{11}=4A_{11}\sqrt{\alpha\alpha'}\cdot r_e^2\cdot\left[\left(1-\frac{3}{2}\varepsilon+\frac{15}{8}\varepsilon^2\right)(\varepsilon-\beta)\varepsilon+\frac{15}{8}\eta^2+\left\{\left(1-\frac{3}{2}\varepsilon+\frac{15}{8}\varepsilon^2\right)+\left(\frac{15}{4}\varepsilon-\frac{3}{2}\right)(2\varepsilon-\beta)+\frac{15}{8}(\varepsilon-\beta)\varepsilon\right\}\eta\right]$$

where,

$$A_{k\lambda}=(n_k/r_e^{1/2})\,(N_kN_\lambda/\bar{N}_0^2)\times\exp\left[-\frac{1}{2}\left(\frac{\alpha\alpha'}{\alpha+\alpha'}\right)\cdot(\beta r_e)^2\right] \quad (A31)$$

$$\bar{\alpha}=(\alpha+\alpha')/2 \quad (A32)$$

$$\varepsilon=\{\alpha/(\alpha+\alpha')\}\beta \quad (A33)$$

$$\eta=(2\bar{\alpha}r_e^2)^{-1} \quad (A34)$$

and $\bar{N}_0$ is obtained from the normalization factor N_κ of vibrational eigenfunction by replacing α and κ with $\bar{\alpha}$ and zero.

The expressions of $u'_{k\lambda}$ and $v'_{k\lambda}$ are identical with the above, because the form of the potential channel is symmetrical at the two boundaries.

Hydrazinolysis of Nucleic Acids. I. The Formation of Deoxyribopyrimidinic Acid from Herring Sperm Deoxyribonucleic Acid

By Shosuke TAKEMURA

(Received March 23, 1959)

In spite of our recognition of the biological importance of nucleic acid, there are many points on the structure of nucleic acid still left ambiguous, i. e., the nucleotide sequence, the localization in the molecule of certain nucleotides, the structural differences between nucleic acids of different origin, and so on. Some fruitful information on the general structural features of deoxyribonucleic acid has been obtained by Chargaff et al. from chemical degradative studies of a derivative, named apurinic acid, in which deoxyribonucleic acid has been deprived of the purine constituents[1-4]. Many other chemical degradations of deoxyribonucleic acid by which the nucleotide sequence can be studied have been attempted[5-13]. These

1) C. Tamm, M. E. Hodes and E. Chargaff, *J. Biol. Chem.*, **195**, 49 (1952).
2) C. Tamm, H. S. Shapiro, R. Lipshitz and E. Chargaff, ibid., **203**, 673 (1953).
3) C. Tamm and E. Chargaff, ibid., **203**, 689 (1953).
4) M. E. Hodes and E. Chargaff, *Biochim. et Biophys. Acta*, **22**, 348 (1956).
5) A. S. Jones and D. S. Letham, ibid, **14**, 438 (1954).
6) A. S. Jones and D. S. Letham, *J. Chem. Soc.*, **1956**, 2573.
7) A. S. Jones, D. S. Letham. and M. Stacey, ibid., **1956**, 2579.
8) A. S. Jones, D. S. Letham and M. Stacey, ibid., **1956**, 2584.
9) A. S. Jones, M. Stacey and B. E. Watson, ibid., **1957**, 2454.
10) J. A. Lucy and P. W. Kent, *Research*, **6**, 49s (1953).

studies have more or less utilized the particular instability of the purine deoxyribosidic linkages to even a mild acid hydrolysis. Therefore, the information about the nucleotide sequences has been exclusively limited to the pyrimidines in deoxyribonucleic acid. No information was available about the distribution of purines in deoxyribonucleic acid, or of either purines or pyrimidines in ribonucleic acid.

Attention was paid to the reaction of aqueous hydrazine with uracil[14], pyrimidine ribonucleosides[15,16] and ribomononucleotides[16]. Of the latter, uracil and cytosine residues were decomposed to pyrazolone and 3-aminopyrazole, respectively, and simultaneously, ribose 2- and 3-phosphate were obtained from the nucleotide isomers, a and b, respectively. This reaction of hydrazine was successfully applied to both ribo- and deoxyribonucleic acid from which for the first time nondialyzable derivatives almost free from the pyrimidines were obtained and the name ribo- and deoxyribo-apyrimidinic acid were proposed for the products[17,18]. These compounds, especially deoxyribo-apyrimidinic acid, may be useful for structural studies as well as apurinic acid[2,4] and aldehydoapurinic acid di(carboxymethyl)-dithioacetal[7,9].

Anhydrous hydrazine was used for this work, in order to avoid alkaline hydrolysis of the internucleotide linkage which might be caused by the basicity of hydrazine itself even if only a trace of water remained. Since powdered deoxyribonucleic acid of herring sperm took more than 30 min. for its complete dissolution in five parts of anhydrous hydrazine at 60°C, lyophilized preparations were used to prevent a heterogeneous reaction. Experiments using various reaction conditions were carried out and are summarized in Table I. In the course of dissolution in distilled water of the alcohol precipitates after the hydrazinolysis, the viscosity of the solution rapidly decreased. Hydrazine was expected to remain in the precipitates and to cause alkaline hydrolysis. Therefore, in the preparation of DAPYA V, V′ and V″, the alcohol precipitates were dissolved in 0.2 M phosphate buffer of pH 6 and dialyzed. The products thus obtained proved to have longer mean chain lengths and fewer periodate consumptions than others (Table V).

The hydrazinolysis of the deoxyribonucleic acid afforded products the nitrogen content and the N/P ratio of which were lower than those of the parent materials (Table II). Increased removal of the pyrimidines resulted in higher phosphorus contents (Table II). The color intensities by the reaction with diphenylamine were, on the basis of phosphorus content, much more than those given by the parent nucleic acids, although the color intensities were not always parallel to the degree of detachment of the pyrimidines. The estimation of reducing sugar proved that the products had a considerable amount of reducing power, whereas the nucleic acids had only a little. These results, together with the positive qualitative tests for reducing sugar, show that the bulk of the sugar moieties, which in the intact nucleic acid were pyrimidine nucleotides, are in nonglycosidic forms. During the hydrazinolysis and the subsequent treatment, there may be possibilities of side reactions, e. g., formation of hydrazonium salt, hydrazone and sugar alcohol. However, it can be seen from the ratio of N/P that these side reactions occur only slightly if at all.

As shown in Table III the greater part of the pyrimidines was removed from herring sperm deoxyribonucleic acids without impairment of the original interpurine ratios, but small amounts of thymine remained, even in the product obtained through the reaction by which the removal of the pyrimidines was most effective. As for pyrimidine ribomononucleotides, uracil was far more rapidly decomposed by aqueous hydrazine than was cytosine, which was studied by Baron and Brown[16]. Hence it is concluded that thymine is the most resistant to the hydrazinolysis among the main pyrimidine constituents in nucleic acids. The reaction of hydrazine, in the presence of water, gave directly ribose 3-phosphoric acid from pyrimidine ribonucleotides. In the absence of water, however, ureido-deoxyriboside phosphate residues may be formed from the pyrimidine nucleotide residues in the

11) P. W. Kent, J. A. Lucy and P. F. V. Ward, *Biochem. J.*, **61**, 529 (1955).
12) K. Burton and G. B. Peterson, *Biochim et Biophys. Acta*, **26**, 667 (1957).
13) H. S. Shapiro and E. Chargaff, ibid., **23**, 451(1957).
14) H. R. Fosse, J. Hieulle and L. W. Bass, *Compt. rend.*, **178**, 811 (1955).
15) P. A. Levene L. W. Bass, *J. Biol. Chem.*, **71**, 167 (1926).
16) F. Baron and D. M. Brown, *J. Chem. Soc.*, **1955**, 2855.
17) S. Takemura, *J. Biochem.*, **44**, 321 (1957).
18) S. Takemura, *Biochim. et Biophys. Acta*, **29**, 447 (1958).

TABLE I. REACTION OF HERRING SPERM DEOXYRIBONUCLEIC ACID WITH ANHYDROUS HYDRAZINE

Preparation[a]		Amount of DNA	Anhydrous hydrazine	Reaction temp.	Reaction time	Yield of nondialyzable product	
		mg.	ml.	°C	min.	mg.	%[b]
DAPYA	I	850	3.5	50	30[d]	650	87
DAPYA	II	240	1.0	60	30[d]	170	80
DAPYA	III	120	0.7	60	55	71	72
DAPYA	IV	600	2.8	60	60	389	78
DAPYA	V	248	1.2[c]	37	90	208	95
DAPYA	V'	150	0.7[c]	50	75	113	86
DAPYA	V''	195	1.0[c]	50	150	130	82
APA	II	140	HCl, pH 1.6	37	24 hr.	98	91
APA	IV	250	HCl, pH 1.6	37	26 hr.	183	94
PDRP	ID	150	HCl, pH 1.6	37	26 hr.	39	26
PDRP	IID	70	HCl, pH 1.6	37	26 hr.	17	26
PDRP	IIA	50	0.2	60	60	9.5	17
PDRP	IVD	150	HCl, pH 1.6	37	27 hr.	58	42

a) DAPYA=deoxyribo-apyrimidinic acid; APA=apurinic acid; PDRP=poly-deoxyribose phosphate. DAPYA I and II were obtained from powdered DNA and through acid precipitation; DAPYA III and IV obtained from lyophilized DNA and through acid precipitation; DAPYA V, V' and V'' obtained from lyophilized DNA and through dissolution in phosphate buffer (See *Experimental*).

b) These are per cent of DNA phosphorus recovered in the product

c) Twice dehydrated hydrazine was used.

d) Reaction times after the complete dissolution of DNA.

TABLE II. COMPOSITION OF THE HYDRAZINOLYSIS PRODUCTS OF HERRING SPERM DEOXYRIBONUCLEIC ACID. PART 1

Preparation[a]		N (%)	P (%)	Atomic N/P	Color reaction with diphenylamine[b]	Reducing deoxyribose residues, mol. per 100 g.-atoms of P[c]
DNA	I	13.4	8.0	3.7	100	5
DNA	II	13.6	8.2	3.7	100	4
DNA	III	13.7	8.2	3.7	100	6
DNA	IV	14.2	8.5	3.7	100	5
DNA	V	13.7	8.2	3.7	100	—
DAPYA	I	12.2	9.1	3.0	135	30
DAPYA	II	12.0	9.6	2.8	156	31
DAPYA	III	12.3	10.0	2.7	133	27
DAPYA	IV	12.2	10.2	2.7	131	36
DAPYA	V	12.3	9.2	3.0	—	—
DAPYA	V'	12.0	9.5	2.8	—	—
DAPYA	V''	11.9	10.1	2.6	—	—
APA	II	6.3	10.6	1.3	116	54
APA	IV	6.5	10.9	1.3	99	51
PDRP	ID	7.4	9.2	1.8	87	51
PDRP	IID	4.7	10.3	1.0	107	63
PDRP	IIA	3.6	9.6	0.85	113	—
PDRP	IVD	3.9	11.0	0.79	110	63

a) See Table I.

b) Compared with each DNA on the basis of P content.

c) Compared with deoxyribose as the standard.

TABLE III. COMPOSITION OF THE HYDRAZINOLYSIS PRODUCTS OF HERRING SPERM DEOXYRIBONUCLEIC ACID. PART 2

Preparation[a]		Mol. of bases/100 g.-atoms of phosphorus[b]						Molar ratios of	
		Adenine	Guanine	Cytosine	Thymine	Total purines	Total pyrimidines	A/G	T/C
DNA	I	29	23	21	27	52	48	1.3	1.3
DNA	II	27	24	22	27	51	49	1.1	1.2
DNA	III	29	23	21	27	52	48	1.3	1.3
DNA	IV	29	23	21	27	52	48	1.3	1.3
DNA	V	28	23	22	27	51	49	1.2	1.2
DAPYA	I	29	23	1.2	19	52	20	1.3	
DAPYA	II	27	24	0.7	8.0	51	8.7	1.1	
DAPYA	III	29	23	0.2	5.4	52	5.6	1.3	
DAPYA	IV	29	23	0.3	4.1	52	4.4	1.3	
DAPYA	V	28	23	1.2	16	51	17	1.2	
DAPYA	V′	28	23	1.0	10	51	11	1.2	
DAPYA	V″	27	24	0.5	5.2	51	5.7	1.1	
APA	II	1.6	2.6	22	27	4.2	49		1.2
APA	IV	0.6	1.0	22	26	1.6	48		1.2
PDRP	IID	2.8	4.3	0.7	6.6	7.1	7.3		
PDRP	IVD	1.8	2.4	0.7	8.3	4.2	9.0		

a) See Table I.
b) The values were corrected for a 100% recovery. Actual recoveries of total bases were between 89 and 96%.

TABLE IV. ULTRAVIOLET ABSORPTION SPECTRA OF THF HYDRAZINOLYSIS PRODUCTS OF HERRING SPERM DEOXYRIBONUCLEIC ACID[a]

Preparation[b]		Maximum			Minimum		
		mμ.	E_p*	E_{np}**	mμ.	E_p*	E_{np}**
DNA	I	259	7350		230	3100	
DNA	II	259	7200		230	2950	
DNA	III	258	6850		230	2900	
DNA	IV	258	7700		230	3200	
DAPYA	I	257.5	7200	10000	228	2850	3950
DAPYA	II	256.5	6900	11500	227.5	2800	4650
DAPYA	III	255	6450	11100	227.5	2450	4250
DAPYA	IV	255	6650	11900	227	2600	4650
APA	II	268	4450	8400	238	2700	5100
APA	IV	267.5	4450	8900	237	2650	5300
PDRP	ID	260	5100		232	2500	
PDRP	IID	260	3500		235	2350	
PDRP	IVD	256.5	2400		234	1900	

a) All measurements were carried out in 0.1 M phosphate buffer of pH 7.0.
* The extinction coefficient with respect to one gram-atom of phosphorus per liter.
** The extinction coefficient with respect to one gram-atom of nucleotide phosphorus per liter.
b) See Table I.

deoxyribonucleic acid. The subsequent treatment of the intermediate product may hydrolyze the glycosidic linkage between deoxyribose and urea which seems to be unstable in the presence of water. The deoxyribose phosphate residues thus formed may be present in an equilibrium between the furanose (III) and the free aldehydo-form (II) in the aqueous solution of the deoxyribo-apyrimidinic acid, but are certainly present to a considerable extent in the free aldehydo-form[19-21].

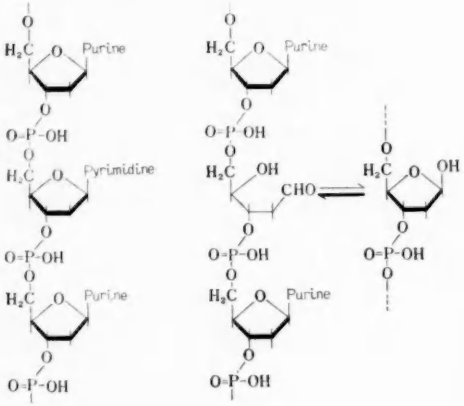

(I) (II) (III)

To remove both the purines and the pyrimidines, the apurinic acid from herring sperm deoxyribonucleic acid was treated with anhydrous hydrazine and the deoxyribo-apyrimidinic acid was treated with dilute acid. These products contained bases to the extent of about 10 to 15 mol. % of total phosphorus. The combination of the mild acid hydrolysis with the hydrazinolysis, however, caused greater degradation of the internucleotide linkages than did the hydrazinolysis alone. Moreover, the color intensities with diphenylamine and the estimations of reducing sugar of the products seem to show that a part of the deoxyribose moieties undergo some unknown decompositions.

The mean chain length of apurinic acid (Table V) corresponds to a mean molecular weight of about 5,000. This value is much lower than that obtained by Tamm et al. (15,000; light scattering method)[1] and that by Miura et al. (17,000;

Table V. Mean chain length and periodate consumption of the hydrazinolysis products of herring sperm deoxyribonucleic acid

Preparation*		Mean chain length	Periodate consumption, mol. per 1 mol. of P
DAPYA	I	7.3	0.24
DAPYA	III	8.4	0.20
DAPYA	IV	7.0	0.34
DAPYA	V	15	0.17
DAPYA	V'	10	0.17
DAPYA	V''	10	0.19
APA	IV	18	0.14
PDRP	IVD	4.8	0.57

* See Table I.

surface membrane method)[22]. This discrepancy may be partly due to the quality of the parent deoxyribonucleic acid and also to the presence of many terminal phosphate groups caused by the inclusion in the apurinic acid of a small amount of oligonucleotides. Consequently, it can be assumed that the deoxyriboapyrimidinic acids contain many fragments of much longer chain length than the mean, although fission of the phsophodiester linkages during the hydrazinolysis and the subsequent treatment may have been considerable. Periodate should be consumed only by the nonglycosidic deoxyribose residues which occupy the chain end of nucleotide and do not bear terminal phosphate groups IV and V. If both ends are occupied by nucleotides or bear the terminal phosphate group VI, periodate

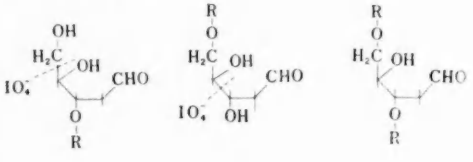

(IV) (V) (VI)

can not be consumed. Therefore, it is impossible to predict the amount of the periodate consumption of the hydrazinolysis products from their mean chain lengths. The ultraviolet absorption coefficient of the purines are, on the molar basis, greater than that of the pyrimidines. Hence, in addition to the hyperchromic effects of degradation, the removal of the

19) S. M. Cantor and Q. P. Peniston, *J. Am. Chem. Soc.*, **62**, 2113 (1940).
20) Chong-Fu Li, W. G. Overend and M. Stacey, *Nature*, **163**, 538 (1949).
21) W. G. Overend, *J. Chem. Soc.*, **1950**, 2769.
22) K. Miura, K. Imahori and I. Watanabe, *J. Chem. Soc. Japan, Pure Chem. Sec.* (*Nippon Kagaku Zasshi*), **78**, 276 (1957).

pyrimidines results necessarily in the higher absorption coefficient with respect to nucleotide phosphorus (E_{np}) than that of the apurinic acid and the deoxyribonucleic acid (Table IV).

Some fission of the internucleotide linkages occurred during the hydrazinolysis and the subsequent treatment, and small amounts of intact thymine were left in the preparations. However, there will be possibilities to improve the preparative method. Since about 80% of the material was nondialyzable and the interpurine ratios were not distorted during the reaction, the deoxyribo-apyrimidinic acid must be useful for the structural studies of deoxyribonucleic acid. The apyrimidinic acids were used for the study of the specificity of pancreatic deoxyribonuclease which are reported in the subsequent paper.

Experimental

Nitrogen was determined by micro-Kjeldahl method and phosphorus by Allen's method[23]. The color reaction of the hydrazinolysis products with diphenylamine[24] was carried out and compared with each parent deoxyribonucleic acid as the standard. The nonglycosidic deoxysugars which were initially bound to the pyrimidines also participate in the color reaction. Reducing deoxysugar was determined by means of Fujita-Iwatake's method[25]. These results are summarized in Table II. The base composition was determined chromatographically after hydrolyzing samples in a scaled tube with 70% perchloric acid at 100°C for 1 hr.[26] (propan-2-ol—hydrochloric acid[27], Toyo Roshi Co. 51a paper, descending). Each value listed in Table III represents the average of at least three individual determinations. The absorption spectra were determined in 0.1 M phosphate buffer of pH 7.0 (Fig. 1 and Table IV). The mean chain length was determined by the ratio of the total phosphorus to the terminal phosphate which was liberated as inorganic phosphorus by prostatic phosphomonoesterase[28] (Table V). The periodate consumption was carried out at pH 4 with sodium metaperiodate, in the dark at 10°C or below, for 60 min.; excess periodate was reduced with sodium arsenite at pH 8 and the excess arsenite was back titrated with standard iodine solution[29] (Table V).

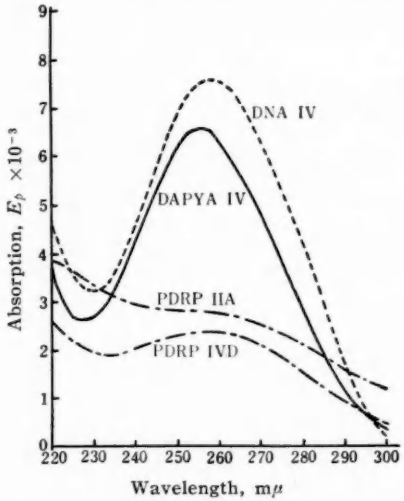

Fig. 1. Ultraviolet absorption curves of the hydrazinolysis products of herring sperm deoxyribonucleic acid in phosphate buffer, pH 7.
E_p=extinction per g.-atom of phosphorus.

Dehydration of Hydrazine.—Eighty per cent hydrazine hydrate was dehydrated with sodium hydroxide pellets at 113°C for 2 hr. and distilled[30]. For more strict dehydration, the distillate was again refluxed with sodium hydroxide pellets at 180°C for 3 hr. and distilled[31].

Deoxyribonucleic Acids.—Five preparations of the sodium deoxyribonucleate of herring sperm, DNA I to V, were used. DNA III was a highly polymerized specimen (MW. ca. 6×10^6)[32]. Before treatment with anhydrous hydrazine, the nucleic acids were dried over concentrated sulfuric acid in vacuo at 60°C for 5 hr. or at 100°C for 3 hr. The compositions of the specimens are summarized in Tables II and III.

Designation of the Reaction Products.—The hydrazinolysis gave products in which the nucleic acid was more or less deprived of the pyrimidines. In order to avoid confusion and to simplify descriprions, the name deoxyribo-apyrimidinic acid (DAPYA) is given to all the hydrazinolysis products and the name polydeoxyribose phosphate (PDRP) to the products obtained either by the hydrazinolysis of the apurinic acid (APA) or by the mild acid hydrolysis, as used for the preparation of apurinic acid, of the hydrazinolysis product. The preparation numbers of the reaction products are the same as those given to the parent deoxyribonucleic acids, i. e., DAPYA II and APA II were obtained from DNA II, PDRP IIA from APA II, and PDRP IID from DAPYA II.

23) F. W. Allen, *Biochem. J.*, **34**, 858 (1940).
24) Z. Dische, *Mikrochem.*, **8**, 4 (1930); F. B. Seibert, *J. Biol. Chem.*, **133**, 593 (1940).
25) A. Fujita and D. Iwatake, *Biochem. Z.*, **242**, 43 (1932).
26) A. Marshak and H. J. Vogel, *J. Biol. Chem.* **189**, 597 (1951).
27) G. R. Wyatt, *Biochem. J.*, **48**, 584 (1951).
28) P. R. Whitfeld and R. Markham, *Nature*, **171**, 1151 (1953).
29) J. R. Dyer, "Methods of Biochem. Anal.", Vol. III, Interscience Publishers, Inc., New York, (1955). p. 111.
30) I. M. Kolthoff, *J. Am. Chem. Soc.*, **46**, 2009 (1924).
31) D. H. R. Barton, D. A. J. Ives and B. R. Thomas, *J. Chem. Soc.*, **1955**, 2056.
32) K. Iso and I. Watanabe, *J. Chem. Soc., Japan, Pure Chem. Sec. (Nippon Kagaku Zasshi)*, **78**, 1268 (1957).

Preparation of the Deoxyribo-apyrimidinic Acids.—The mixture of lyophilized herring sperm deoxyribonucleic acid and anhydrous hydrazine was kept free from moisture under the conditions described in Table I. Within a few minutes, the nucleic acid dissolved in the hydrazine, excepting deoxyribonucleic acid III which took about 10 min. for its complete dissolution. After cooling, absolute alcohol (5 vol.) was added to the highly viscous solution, the fibrous precipitate was made into a powder by scratching, centrifuged, washed with absolute alcohol, with ether, and dried. The dry solid was dissolved with cooling in cold distilled water and the solution dialyzed against running tap water for 20 hr., against frequent changes of distilled water at 4°C for 40 hr. and the inside fluid was freeze-dried. Light yelllow colored products were obtained. The composition of the products thus obtained is listed in Tables II and III.

When the alcohol precipitate was dissolved in 0.2 M phosphate buffer of pH 6 instead of distilled water, the solution was dialyzed against the same buffer at 4°C for 16 hr. against running tap water and finally against distilled water. Faint yellow products were obtained and are described as DAPYA V, V' and V'' in the tables.

Preparation of Poly-deoxyribose Phosphate.—Apurinic acid was prepared from herring sperm deoxyribonucleic acid in the same way as it was prepared by Tamm et al.[1] Apurinic acid II was dried at 60°C for 5 hr. and then treated with anhydrous hydrazine as above. Deoxyribo-apyrimidinic acids I, II and IV were also treated by the same mild acid hydrolysis as used for the preparation of apurinic acid. The nondialyzable products of yellowish brown color were obtained from each treatment and were incompletely soluble in water, although these gave clear solutions before freeze-drying. The composition of these products is given in Tables II and III.

Qualitative Tests for Nonglycosidic Deoxysugar.—In contrast to the deoxyribonucleic acid, the hydrazinolysis products and the apurinic acid reacted with ammoniacal silver solution yielding brown precipitates, reduced Fehling's solution on warming, reacted with benzidine giving a brown color, reduced mercuric chloride solution yielding a white precipitate, and gave pink color with reduced fuchsin solution, but the reaction of the hydrazinolysis products was much slower than that of the apurinic acid. The hydrazinolysis products spotted on filter paper gave a reddish purple color with the aniline hydrogen phthalate reagent used for the development of chromatogram of reducing sugars[33].

The author thanks Professor F. Egami for his close interest and Professor I. Watanabe, the University of Tokyo, for a supply of herring sperm deoxyribonucleic acids. The expense of this study was defrayed in part by a grant from the Ministry of Education.

Department of Chemistry
Faculty of Science
Nagoya University, Nagoya

33) S. M. Partridge, *Nature*, **164**, 443 (1949).

Hydrazinolysis of Nucleic Acids. II. The Formation of Ribo-apyrimidinic Acid from Yeast Ribonucleic Acid

By Shosuke TAKEMURA and Masazumi MIYAZAKI

(Received March 23, 1959)

In the preceding paper[1], one of the authors has dealt with the formation of a new derivative devoid of pyrimidines, named deoxyribo-apyrimidinic acid, by the hydrazinolysis of herring sperm deoxyribonucleic acid, by the hydrozinolysis of herring sperm deoxyribonucleic acid. In connection with studies on the specificity of pancreatic ribonuclease in which this laboratory is engaged[2-6], it was desired to prepare ribonucleic acid derivatives devoid of the pyrimidines. The hydrazinolysis was first investigated using yeast ribonucleic acid and gave, for the first time, a nondialyzable derivative free from the pyrimidines, for which the name ribo-apyrimidinic acid was proposed[7]. Besides

1) S. Takemura, This Bulletin, **32**, 920 (1959).
2) S. Takemura, *J. Chem. Soc. Japan, Pure Chem. Sec.* (*Nippon Kagaku Zasshi*) **72**, 674 (1951).
3) F. Egami, H. Ishihara and M. Shimomura, *Z. physiol. Chem.*, **295**, 349 (1953).
4) F. Egami, *J. Japan. Biochem. Soc.* (*Sei Kagaku*), **27**, 139 (1955).
5) S. Takemura, *Protein, Nucleic Acid and Enzyme*, **2**, 79 (1957).
6) S. Takemura, "Intern. Kongr. Biochem", Zusammenfassung, IV Kongr., Wien (1958), p. 34.
7) S. Takemura, *J. Biochem.* **44**, 321 (1957).

TABLE I. REACTION OF YEAST RIBONUCLEIC ACID WITH ANHYDROUS HYDRAZINE AND COMPOSITION OF THE NITROGENEOUS CONSTITUENTS OF THE PRODUCTS

Preparation*	Condition of reaction		Yield of nondialyzable product	Mol./10 mol. of adenine[b]			
	t°C	min.	(%)**	Adenine	Guanine	Cytidylic acid	Uridylic acid
RNA, commercial	—	—	—	10.0	12.4	9.4	10.3
RNA, purified	—	—	—	10.0	12.6	11.5	10.2
RAPYA I[a]	0	60	93	10.0 (10.0)	12.4 (12.3)	9.7 (9.5)	7.2 (7.0)
RAPYA II	0	180	—	10.0	12.3	6.2	3.7
RAPYA III	30	120	—	10.0	12.7	1.0	1.8
RAPYA IV[a]	50	60	88	10.0 (10.0)	12.6 (12.3)	0.6 (0.6)	0.7 (0.7)
RAPYA V[a]	70	60	77	10.0 (10.0)	12.5 (12.4)	0.7 (0.7)	0.6 (0.6)
RAPYA VI[a]	50	60	73	10.0	12.3	1.2	2.5
RAPYA VII	80	60	50	10.0	12.9	1.0	1.5
RAPYA VIII	60	60	70	10.0	12.5	1.3	2.8
PAPYA IX	65	90	64	10.0	12.8	0.5	0.5

* RNA=ribonucleic acid; RAPYA=ribo-apyrimidinic acid; RAPYA VI, VII and VIII were obtained from commercial powdered RNA, others from purified and lyophilized RNA.

a) Twice dehydrated hydrazine was used.

** These are per cent of RNA phosphorus recovered in the product.

b) The values in parentheses are the composition of the dialyzable materials.

the problem of the specificity of ribonucleases which are reported in subsequent papers, some information about the general structure of ribonucleic acid may be derived from degradative studies of the derivative.

When yeast ribonucleic acid was treated with 80% aqueous hydrazine, a complete hydrolysis of the phosphodiester linkages resulted and only 2′- and 3′-isomers of purine mononucleotides were detected on the paper chromatogram, as the ultraviolet absorbing materials. In the case where anhydrous hydrazine was used, drastic condtions such as reaction at 90°C did not, however, offer any advantages, but indeed resulted in a serious destruction of the phosphodiester linkages and formation of considerable amounts of purine mononucleotide isomers. Experiments using various conditions of time and temperature were carried out and are summarized in Table I. The use of nucleic acid which was not purified and especially not lyophilized resulted in the incomplete removal of the pyrimidines. After treatment with hydrazine and precipitation with alcohol, there were difficulties in obtaining the derivatives without an accompanying serious destruction of the internucleotide linkages. In most cases, the alcohol precipitates were dissolved at 0°C in distilled water and the products precipitated with dilute hydrochloric acid. This procedure was effective for removign hydrazine, which was expected to be included as hydrazonium salt in the alcohol precipitates. However, it was thought that there might be possibilities of the formation of hydrazones or osazones using such acidic conditions. An experiment showed that the use of concentrated phosphate buffer of neutral range converted hydrazonium salts to sodium salts and minimized fissions of the phosphodiester linkages (see Table IV).

The reaction of the lyophilized ribonucleic acid of yeast with anhydrous hydrazine at 50°C for 60 min. was found to be most suitable for the preparation of ribo-apyrimidinic acid. Using these conditions, the product was practically free from pyrimidines and fissions of the phosphodiester linkages were not serious. As attempts to remove the pyrimidines with milder reagents than anhydrous hydrazine, anhydrous methylhydrazine and phenylhydrazine were used. The latter did not react but the former removed considerable amounts of uracil and a little cytosine when the reaction was carried out at 60°C for 90 min. The white product was obtained through acid precipitation and the yield was quantitative. The use of

anhydrous methylhydrazine in a more drastic condition is, therefore, of great promise.

The hydrazinolysis products gave slightly higher values for the atomic N/P ratios than those expected from the base composition of the products. The products, excepting that obtained through the dissolution in the buffer, were slightly yellow. A small part of ribose residues may be present as hydrazone or osazone and also as ureido-ribose formed from the pyrimidine riboside moieties by the hydrazinolysis. From the color intensities in the reaction with orcinol and the estimation of reducing sugar, however, it can be seen that these possibilities occure only slightly, if at all. Direct evidence for the presence of free ribose residues in the hydrazinolysis products was obtained by treating one of the products with Takadiastase, which hydrolyses nucleic acids to nucleosides. Much ribose was liberated, as shown by paper chromatography. Qualitative tests for reducing sugar were also strongly positive.

During the hydrazinolysis and the subsequent treatment, the initial interpurine ratios were not distorted. This was most clearly confirmed by analyzing the dialyzable fragments. The base compositions of the dialyzable fragments were the same as those of the corresponding nondialyzable products. The removal of the pyrimidines from yeast ribonucleic acid was easier than that from herring sperm deoxyribonucleic acid. In the initial stage of the reaction, uracil was decomposed faster than was cytosine, but this was reversed later. Yeast ribonucleic acid is presumed to be hydrazinolyzed in a similar way to that shown in the preceding paper on the hydrazinolysis of herring sperm deoxyribonucleic acid[1]. Thus the ribose phosphate residues in the aqueous solution of the ribo-apyrimidinic acid may be present in the furanose form (II) rather than in the free aldehydoform (III)[8].

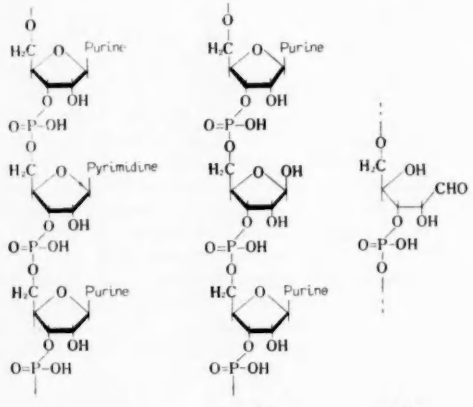

(I) (II) (III)

In alkaline solutions, the hydrazinolysis products were as unstable as ribonucleic acid. The product which is free from the pyrimidines was unstable, even in solutions of neutral pH or below at 37°C for one day, about 10% of its total phosphorus was rendered soluble in acid—uranyl reagent, but this was greatly reduced at 0°C. In spite of this instability, the product obtained using the most suitable conditions showed a fairly high mean chain length. Periodate should be consumed not only by the nonglycosidic ribose residues within VI or at the end of the chains (IV, V), but also by the purine nucleosides which occupy the chain ends and do not bear a terminal 3′-phosphate group (VII). The periodate consumption

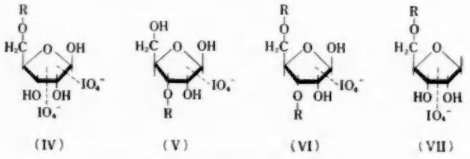

(IV) (V) (VI) (VII)

R = nucleotides or phosphate

of a product obtained through the dissolution in the phosphate buffer was less than that obtained through the acid precipitation. The electrometric titration curve of the product obtained by the reaction at 65°C for 90 min. showed the disappearance of one –NH–CO– dissociation titrating in the range pH 8~12. This can be explained by the removal of uracil. The absence of the amino group of cytosine was, however, not clearly indicated, being obscured by the increased secondary phosphoric acid dissociations which are due to fissions of the phosphodiester linkages.

In the most suitable condition of the hydrazinolysis, about 90% of the material was nondialyzable. Moreover, the interpurine ratio was not distorted during the reaction. Hence, the ribo-apyrimidinic acid must be useful for the structural studies of ribonucleic acid.

8) S. M. Cantor and Q. P. Peniston, *J. Am. Chem. Soc.*, **62**, 2113 (1940).

TABLE II. COMPOSITION OF THE HYDRAZINOLYSIS PRODUCTS OF YEAST RIBONUCLEIC ACID

Preparation*	N (%)	P (%)	Atomic N/P	Color reaction with orcinol[a]	Reducing ribose residues, mol./100 g.-atoms of P[b]
RNA, commercial	14.5	8.4	3.8	100	—
RNA, purified	15.0	8.8	3.8	100	3
RAPYA I	14.7	9.3	3.6	127	32
RAPYA IV	13.4	9.9	3.0	164	53
RAPYA V	12.7	9.2	3.0	183	45
RAPYA VIII	12.4	9.1	3.0	163	43
RAPYA IX	13.4	9.9	3.0	153	48

* See Table I.

a) Compared with RNA on the basis of phosphorus content.

b) Compared with ribose as the standard.

Experimental

Nitrogen, phosphorus, reducing sugar (Table II), the ultraviolet absorption spectra (Table III and Fig. 1), the mean chain length and the periodate consumption (Table IV) were determined by methods described in the preceding paper[1]. The nucleotide composition (Table I) was determined chromatographically after hydrolyzing samples in a sealed tube with 1 N hydrochloric acid[9] at 100°C for 1 hr. (propan-2-ol—

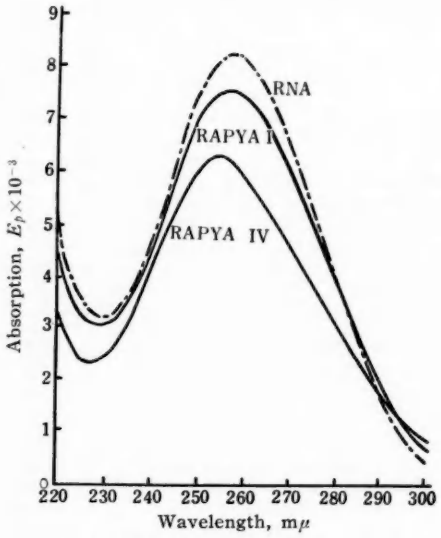

Fig. 1. Ultraviolet absorption curves of the hydrazinolysis products of yeast ribonucleic acid in phosphate buffer, pH 7.
E_p=extinction per g.-atom of phosphorus.

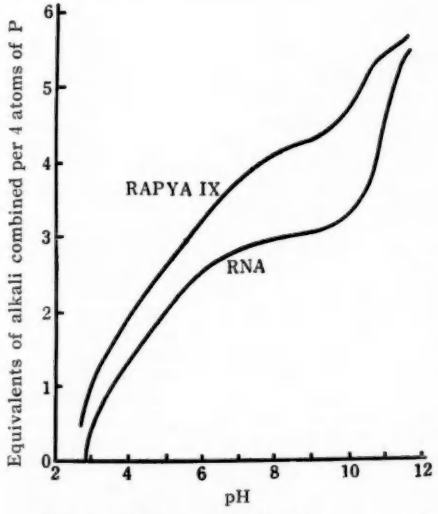

Fig. 2. Electrometric titration curve of the hydrazinolysis product (RAPYA VIII) of yeast ribonucleic acid.

TABLE III. ULTRAVIOLET ABSORPTION SPECTRA OF THE HYDRAZINOLYSIS PRODUCTS OF YEAST RIBONUCLEIC ACID[a]

Preparation*	Maximum		Minimum	
	mμ	E_p[b]	mμ	E_p[b]
RNA, purified	259	8200	230	3200
RAPYA I	259	7600	230	3100
RAPYA IV	255.5	6250	228	2350
RAPYA VIII	255.5	6600	228	2650

a) Measurements were carried out in 0.1 M phosphate buffer of pH 7.

* See Table I.

b) The extinction coefficient with respect to one gram-atom of phosphorus per liter.

9) J. D. Smith and R. Markham. *Biochem. J.*, **46**, 509 (1950).

TABLE IV. MEAN CHAIN LENGTH AND PERIODATE CONSUMPTION OF THE HYDROZINOLYSIS PRODUCTS OF YEAST RIBONUCLEIC ACID

Preparation*	Mean chain length	Periodate consumption, mol. per 1 mol. of P
RNA, purified	21.2	0.05
RAPYA I	19.0	0.46
RAPYA IV	13.5	0.65
RAPYA IV'[a)]	—	1.76
RAPYA IV[a)]''	15.4	0.47
RAPYA V	9.8	0.72

* See Table I.

a) These were obtained by a modified method (see *Experimental*); RAPYA IV'—before treatment with phosphate buffer; RAPYA IV''—after treatment with phosphate buffer.

hydrochloric acid[10], Toyo Roshi Co. No. 51a paper, descending). The color reaction of the hydrazinolysis products with orcinol[11] was compared with the parent ribonucleic acid (Table II). The ribose residues, which in the intact ribonucleic acid were in the pyrimidine nucleotides, also participate in the color reaction. For the electrometric titration of a product (RAPYA IX) a Beckman Type G pH-meter was employed. The measurement was carried out in the absence of carbon dioxide (Fig. 2).

Dehydration of Hydrazines. — Anhydrous hydrazine was prepared as described in the corresponding section of the preceding paper[1]. Fifty per cent aqueous methylhydrazine was dehydrated with sodium hydroxide pellets at 90°C for 12 hr., stood overnight at room temperature and distilled (b. p. 86.6~87.3°C)[12]. Phenylhydrazine was distilled under diminished pressure before use.

Ribonucleic Acid.—A commercial yeast ribonucleic acid, Schwarz Laboratories, Inc., was purified by Sevag's method[13] and freeze-dried. Before treatment with hydrazine, the nucleic acid was dried over concentrated sulfuric acid in vacuo at 60°C for 5 hr. The composition of the nucleic acid is listed in Tables I and II.

Preparation of Ribo-apyrimidinic Acid.—The hydrazinolyses at different conditions gave products in which the ribonucleic acid was more or less deprived of the pyrimidines (Table I). In order to simplify descriptions, the name ribo-apyrimidinic acid (RAPYA) is given to all nondialyzable products obtained by the reaction of the ribonucleic acid with anhydrous hydrazine. A typical preparation was as follows. The mixture of lyophilized and dried yeast ribonucleic acid (1.5 g.) and anhydrous hydrazine (3 ml.) was kept free from moisture at 50°C for 1 hr. Within a few minutes, the nucleic acid dissolved in the hydrazine, making a clear solution, with a slight evolution of heat and foam. After cooling, absolute alcohol (5 vol.) was added to the solution, the white precipitate thus formed washed with absolute alcohol and ether, and dried. The dry solid was then dissolved in cold distilled water at 0°C and the pH adjusted to 1.5 with dilute hydrochloric acid. The slightly yellow precipitate thus formed was washed with absolute alcohol and ether, dried, and then suspended in water and dilute alkali was added carefully until the solid just dissolved. The solution was dialyzed against frequent changes of distilled water at 4°C for 3 days. The nondialyzable fraction was freeze-dried. The light yellow product (RAPYA IV) was obtained in 88% yield with respect to phosphorus recovery. Other reaction products using different conditions were obtained by the same procedure, excepting RAPYA IV' and IV''. For the latter the procedure was modified as mentioned below since yellow materials were obtained at the step where the products were precipitated with acid. This was possibly due to reaction between hydrazine and free ribose residues. After treatment with hydrazine and precipitation with alcohol, the precipitate was dissolved in distilled water at 0°C and the pH was adjusted to 7. This solution was then dialyzed against frequent changes of distilled water and freeze-dried. The white product so obtained still contained hydrazine (RAPYA IV'). This was removed by dissolving the material in ice-cold 0.2 M sodium phosphate buffer (pH 6.2) and dialyzing it against the same buffer at 4°C for 8 hr., then against tap water (24 hr.) and finally against frequent changes of distilled water (48 hr.) and lyophilized (RAPYA IV'').

Reaction of Yeast Ribonucleic Acid with Anhydrous Methylhydrazine. — Lyophilized yeast ribonucleic acid (50 mg.) and anhydrous methylhydrazine (1.5 ml.) were kept free from moisture at 60°C for 90 min., then precipitated with absolute alcohol, dissolved in water, and precipitated with acid. This was again suspended in water and dissolved by the careful addition of dilute alkali and dialyzed. The white product thus obtained, in quantitative yield, contained 10.0 mol. of cytidylic acid and 4.6 mol. of uridylic acid per 10 mol. of adenine. The ratio of guanine to adenine was the same as in the parent nucleic acid.

Reaction of Yeast Ribonucleic Acid with Phenylhydrazine. — Freshly distilled phenylhydrazine (12 g.) and lyophilized yeast ribonucleic acid (0.5 g.) were kept at 150°C for 2 hr. and then treated as mentioned above. The material thus obtained was identical with the parent nucleic acid in the nucleotide composition.

Composition of the Dialyzable Materials. —In the preparation of ribo-apyrimidinc acid I, and also IV and V, the outside fluids of each dialysis were combined, adjusted to pH 7 and freeze-dried. The dialyzable fragments were hydrolyzed with 1 N hydrochloric acid and the products were separated by paper chromatography. The nucleotide compositions are shown

10) G. R. Wyatt, ibid., **48**, 584 (1951).
11) W. Mejbaum, *Z. physiol. Chem.*, **258**, 117 (1939).
12) G. V. Brüning, *Ann.*, **253**, 7 (1889).
13) M. G. Sevag, *Biochem. Z.*, **273**, 419 (1934).

in parentheses in Table I. Practically no differences were shown between the composition of the nondialyzable and the dialyzable materials.

Detection of Ribose and Nucleosides after Enzymic Hydrolysis. — Ribo-apyrimidinic acid IV was dissolved in 0.5 M acetate buffer of pH 5.0 and incubated with dialyzed Takadiastase solution at 37°C for 48 hr. The hydrolyzate was applied on paper and separated with *n*-butanol—ammonia[14]. Ribose was detected by spraying aniline hydrogen phthalate reagent[15]. The ultraviolet photo-print showed only the spots of adenosine and guanosine, whereas yeast ribonucleic acid was completely hydrolyzed to purine and pyrimidine nucleosides by this enzyme.

Qualitative Tests for Nonglycosidic Ribose. —0.2% aqueous solutions of ribo-apyrimidinic acid IV and of yeast ribonucleic acid, and 0.1% ribose solution were used for all tests. Excepting the ribonucleic acid, they reacted with ammoniacal silver solution when heated at 100°C for 15 min., reduced Fehling's solution when heated at 100°C for 5 min., gave a reddish brown color with benzidine in glacial acetic acid at 100°C in a few minutes, and reduced mercuric chloride solution at room temperature. Ribo-apyrimidinic acid IV reacted with phenylhydrazine hydrochloride when heated at 50°C for 15 min. and gave a brownish yellow product. All the hydrazinolysis products spotted on filter paper gave a reddish purple color with aniline hydrogen phthalate reagent used for the development of paper chromatograms of reducing sugars[15].

14) R. Markham and J. D. Smith, *Biochem. J.*, **45**, 294 (1949).
15) S. M. Partridge, *Nature*, **164**, 443 (1949).

The authors thank Professor F. Egami for his close interest. The expense of this study was defrayed in part by a grant from the Ministry of Education.

Department of Chemistry
Faculty of Science
Nagoya University
Nagoya

Amino Acid Synthesis from Nitromalonic Ester. III[1]. *Note on the Synthesis of Glutamic Acid*

By Tôru Okuda

(Received March 25, 1959)

Several amino acids have been prepared by means of the addition reaction of diethyl nitromalonate with α,β-unsaturated compounds such as acrylonitrile[2] and acrolein[1]. If the similar type of reaction could occur between nitromalonic and acrylic esters, an approach to the synthesis of glutamic acid would be possible. Both the esters have been found to react in the presence of a catalytic amount of triethylamine in alcoholic solution to give 2-carbomethoxyethyl-nitromalonic ester in a good yield. Elimination of one α-ester group of the substituted nitromalonic ester and subsequent hydrogenation[3] gave pyrrolidonecarboxylic ester, which was easily converted into DL-glutamic acid monohydrate. The overall yield was about 50%. Direct reduction of 2-carbomethoxyethyl-nitromalonic ester with Raney nickel in alcoholic solution gave 2-carbomethoxyethyl-malonic ester, indicating the hydrogenolysis occurred during the reaction[4].

1) Paper II of this series; T. Okuda, This Bulletin, **30**, 358 (1957).
2) S. Akabori, Y. Izumi and T. Okuda, *J. Chem. Soc. Japan, Pure Chem. Sec.* (*Nippon Kagaku Zasshi*), **77**,490 (1956).
3) D. I. Weisblat and D. A. Lyttle, U. S. Pat., 2,606,921 (1952).

Experimental

Diethyl 2-Carbomethoxyethyl-nitromalonate.—Forty-four grams of diethyl nitromalonate and 22 g. of methyl acrylate in 70 ml. of absolute alcohol were heated under reflux in the presence of 3 ml. of triethylamine for 7 hr. and after the concentration of the reaction mixture the residue was dissolved in 400 ml. of ether. The ether solution was extracted with cold aqueous sodium bicarbonate, washed with water and dried. Evaporation of ether gave 55 g. of crude product. When the crude product was distilled in vacuo, there was obtained 49 g. of the pure material boiling at 120~150°C/2 mmHg.

Anal. Found: C, 45.74; H, 6.07; H, 4.83. Calcd. for $C_{11}H_{17}O_8N$: C, 45.36; H, 5.84; N, 4.81%.

4) D. I. Weisblat and D. A. Lyttle, *J. Am. Chem. Soc.*, **71**, 3079 (1948).

Ethyl 2-Carbomethoxyethyl-nitroacetate[3,5].—A solution of 51 g. of crude diethyl 2-carbomethoxyethyl-nitromalonate in 450 ml. of dry ether was treated with 4.10 g. of sodium dissolved in 100 ml. of absolute alcohol at 0°C as already reported in the preceding papers[1,2]. The resulting slurry was transferred to a separatory funnel, 150 ml. of ether and 70 ml. of cold 10% hydrochloric acid were added and vigorous shaking was applied. The ether layer was separated and the aqueous layer was extracted with ether. The ether solutions were combined, washed with water and dried. Concentration and vacuum-distillation gave 34 g. of the product of b.p. 115~128°C/2 mmHg.

Anal. Found: C, 43.10; H, 5.95; N, 6.18. Calcd. for $C_9H_{13}O_6N$: C, 43.83; H, 5.98; N, 6.39%.

Ethyl Pyrrolidonecarboxylate.—The pressure-hydrogenation of 34 g. of 2-carbomethoxyethyl-nitroacetate was carried out using 150 ml. of ethanol and 4 g. of Raney nickel. The catalyst was filtered off, and the ethanol was evaporated. Crude ethyl pyrrolidonecarboxylate thus obtained weighed 22 g. This can be purified either by recrystallization from ether-petroleum ether or by distilling at 2 mm., m.p. 48~50°C, b.p. 153°C/2 mmHg.

Anal. Found: C, 53.80; H, 7.14; N, 8.99. Calcd. for $C_7H_{11}O_3N$: C, 53.49; H, 7.05; N, 8.91%.

The ester was converted into DL-glutamic acid monohydrate by acid hydrolysis. The overall yield with respect to diethyl nitromalonate was about 50%.

Anal. Found: C, 36.59; H, 6.62; N, 8.92. Calcd. for $C_5H_{11}O_5N$: C, 36.36; H, 6.71; N, 8.48%.

Diethyl 2-Carbomethoxyethylmalonate.—Twelve grams of diethyl 2-carbomethoxyethyl-nitromalonate was reduced in alcohol with 2 g. of Raney nickel. After the removal of the catalyst and the alcohol the residue was distilled. There was obtained 8 g. of diethyl 2-carbomethoxyethylmalonate boiling at 125~130°C/2 mmHg.

Anal. Found: C, 53.23; H, 7.73. Calcd. for $C_{11}H_{19}O_6$: C, 53.66; H, 7.32%.

Institute for Protein Research
Osaka University
Nishi-ku, Osaka

5) N. Kornblum and J. H. Eeicher, ibid. 78, 1499 (1956).

Studies on the Silk-Palladium Catalyst. I. Preparation and Stability

By Yoshiharu IZUMI

(Received March 27, 1959)

A number of methods have so far been attempted in order to increase the active surface of hydrogenation catalysts of metal or metal oxide nature. Thus, for example, a method has been devised to deposit certain metals or metal oxides onto porous carriers such as carbon or Kieselguhr, to disperse them into colloidal states with the aid of various protective colloids, or to remove a constituent metal from an alloy by chemical treatments as in the case of preparation of Raney nickel. The other methods so far attempted are also based on physical or mechanical dispersion of catalyst metals into colloidal solutions or on the surface of porous substances.

A few years ago, Akabori et al.[1-3] for the first time reported an entirely new type of hydrogenation catalyst and showed that it was capable of catalyzing asymmetric reduction of certain unsaturated compounds. This catalyst was prepared by coordinating palladous chloride with silk fibroin fibers and then hydrogenating the resulting silk-$PdCl_2$ complex. Since palladous can form a chelate compound with silk fibroin, it is not unreasonable to assume that the palladium in the catalyst is firmly fixed to the asymmetric structure of the protein fibers in an almost atomic state. The capacity of asymmetric catalysis may be explained on the basis of the asymmetric structure of the carrier fibroin.

Although this catalyst was originally developed for the purpose of asymmetric synthesis, it also has a number of characteristics suitable for use as a general hydrogenation catalyst. Thus, it is quite easy to mix the catalyst with reacting substances because of its unusual low

1) S. Akabori, Y. Izumi, Y. Fujii and S. Sakurai, *Nature*, 178, 323 (1956).
2) S. Akabori, Y. Izumi, Y. Fujii and S. Sakurai, *J. Chem. Soc. Japan, Pure Chem. Sec.* (*Nippon Kagaku Zasshi*), 77, 1374 (1956).
3) S. Akabori, Y. Izumi, Y. Fujii and S. Sakurai, ibid., 78, 168 (1957).

density. The catalyst is also unique in that its carrier is a fibrous protein and therefore it can be spun or woven into sheets, cloth or fluffs. In hydrogenation catalysts hitherto devised, the metal is either bound to the carrier by simple mechanical attraction or finely dispersed as colloidal particles. Therefore, it is sometimes not very easy to separate the catalyst from the reaction mixture due to the detachment of the metal from the carrier or to the colloidal nature of the catalyst. With the silk-palladium catalyst, however, the catalyst can be readily separated from the reactants by simple filtration owing to the fact that the metal, though highly dispersed, is tightly held by the micelle structure of silk-fibroin.

The investigations to be reported in this and the following papers were undertaken with an object of obtaining some basic data concerning the applicability of this hydrogenation catalyst for general practical purposes. Also included in this series of papers are observations on the properties of a Nylon-palladium catalyst in which silk fibroin is replaced by the synthetic fiber, 6-Nylon, as the carrier.

Results and Discussion

Activity and Conditions of Preparation of Catalyst.—For the purpose of obtaining the catalyst of a high activity, optimum conditions were sought for the preparation of the catalyst. Table I records the palladium contents of various preparations prepared under different sets of conditions. As can be seen, the highest content was attained when 350 mg. of silk fibroin was boiled for 8 min. with 100 ml. of 0.1 N acetic acid containing 100 mg. of palladous chloride and the resulting chelate was reduced with hydrogen in an autoclave. These conditions were, therefore, used in preparing the catalysts studied in the following sections.

TABLE I. PALLADIUM CONTENTS OF CATALYSTS

Condition for preparation				Pd content in 50 mg. catalyst* (μg.)
Medium (ml.)		$PdCl_2$ (mg.)	Carrier (mg.)	
Water	100	100	Fibroin 350	2590
N/5 HOAc	50	〃	〃	3950
N/10 〃	100	〃	〃	4600
N/10 〃	100	〃	6-Nylon 350	1165
N/15 〃	50	〃	Fibroin 350	3700
N/30 〃	100	〃	〃	4300

* Pd contents were determinated with *p*-nitrosodimethylaniline.

Prolonged boiling for more than 8 min. resulted in an increased palladium content in the catalyst, but this increase was found to be mainly due to an easily detachable form of palladium and did not contribute to the activity. Although the solubility of palladous chloride could be considerably increased by the addition of sodium chloride or sodium acetate to the aqueous solution, these salts were found to inhibit the chelate formation between palladous chloride and fibroin and consequently lead to less active preparations. When silk fibroin was boild with palladous chloride in distilled water, a preparation containing less palladium was obtained as compared with the preparation which was boiled in dilute acetic acid.

The silk-palladium chelate was usually converted into the active catalyst by reducing it with hydrogen in an autoclave. When this activation was carried out by means of formic acid, the resulting catalyst showed appreciably less activity as shown in Table III.

Capacity of Asymmetric Catalysis.—The asymmetric catalyst reported in previous papers was prepared by boiling silk fibroin with palladous chloride in water. This catalyst, as reported previously, was able to catalyze, for example, the asymmetric hydrogenation of 4-benzylidene-2-methyl-oxazol-5-one(4-benzylidenazlacton) to give optically active products. The catalyst prepared in 0.1 N acetic acid instead of in water, and mainly used in this investigation failed to achieve asymmetric catalysis despite its higher palladium content. The reason for such a peculiar behavior of the silk-palladium catalyst is not yet clear. In any event, it seems that the mechanism responsible for the asymmetric catalysis is of a quite delicate nature and can be profoundly affected by slight alterations of the system.

Stability of Catalyst.—Table II is a summary of an investigation in which the activity of the catalyst and its precursor, silk-palladium chelate, was examined both immediately after preparation and after storage for several days in methanol or under dried condition. The activity of the chelate was of course measured after activation. The activity in the table is expressed in terms of "70% reaction time (t)" and reaction velocity (v) observed in the hydrogenation of nitrobenzene to aniline. The results recorded in Table II clearly show that both the catalyst itself and its precursor chelate are quite stable and can be stored for a long period

TABLE II. STABILITY OF CATALYST AND PRECURSOR CHELATE UNDER VARIOUS CONDITIONS

Sample	Storage condition	Storage time	70% Reaction time (min.)	Reaction velocity	Reaction temp. (°C)
Silk-Pd·Cl_2* 350 mg.	In dry state	0	15.5	6.5	16~17
		12 d.	15.0	6.7	〃
Silk-Pd 350 mg.	In methanol	0	18.5	5.4	12~14
		5 d.	20.5	5.0	13~15
		11 d.	18.5	5.4	〃
	In dry state	0	2.1	47.5	40
			9.0	11.1	20~21
		19 h.	9.5	10.5	20
		14 d.	9.0	11.1	20~21
		30 d.	9.5	10.5	18~20

* The activity was measured after conversion to catalyst by hydrogenation.

without loss of activity. Furthermore, no spontaneous combustion took place even when the catalyst was stored in air dried conditions.

TABLE III. ACTIVITY OF CATALYST ACTIVATED WITH FORMIC ACID

Catalyst (mg.)	70% Reaction time (min.)	Reaction velocity	Reaction temp. (°C)
Silk-Pd (350) Activated with HCOOH	15.0	6.7	20

Activation Energy of Hydrogenation Reaction.—The catalytic hydrogenation of nitrobenzene to aniline in the presence of the silk-palladium catalyst was measured at various temperatures. In Fig. 1 is plotted logarithm of reaction velocity (log v) against reciprocal absolute temperature ($^1/_T$). From this graph the activation energy of the catalyzed reaction was computed to be approximately 14.5 kcal./mol.

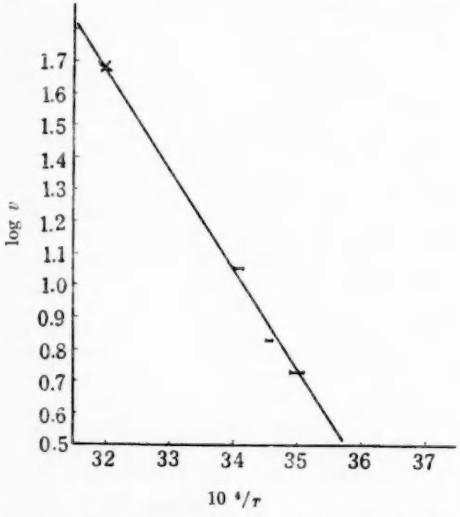

Fig. 1. Dependence of reaction velocity upon temperatures.

Nylon-Palladium Catalyst. — When 6-Nylon (caprolactam polymer) fibers were used as the carrier and treated in the same way as described for silk fibroin fibers, a 6-Nylon-palladium catalyst could be obtained. It was revealed, as shown in Table IV, that the Nylon-palladium catalyst also exhibits a high activity in catalyzing the hydrogenation of nitrobenzene. Nitrobenzene was readily reduced to aniline with hydrogen even at atmospheric pressure in the presence of this catalyst. It was found that the activity was proportional to the palladium content as shown in Table I.

TABLE IV. ACTIVITY OF NYLON-PALLADIUM CATALYST

Catalyst (mg.)	70% Reaction time (min.)	Reaction velocity	Reaction temp. (°C)
Nylon-Pd 350	65	1.5	10
Control (Silk-Pd)		4.9*	10

* Calculated value.

Experimental

I. Preparation of Catalyst. — *1) Palladous Chloridd Solutions.* — *a) Solution in water.*—One hundred milligrams of palladous chloride was added to 100 ml. of cold water and the mixture was stirred for 30 min. in the cold with the aid of a magnetic stirrer.

b) Solution in 0.1'N acetic acid.—One hundred milligrams of palladous chloride were dissolved at 60°C in 10 ml. of 1 N acetic acid and the solution was diluted 10-fold before use.

2) Silk-Palladium Chelate.—Three hundred and fifty milligrams of silk fibroin fibers previously cut into ca. 3 mm. pieces was mixed with 100 ml. of palladous chloride solution (palladous chloride,

100 mg.) and the mixture was boiled for 8 min. The fibers gradually became dense and brownish and finally precipitated as a dark brown mass. After cooling, the precipitated chelate was filtered, washed with water and then methanol, and finally air-dried.

3) Silk-Palladium Catalyst.—The chelate was converted to the active catalyst by the following two methods.

a) The chelate corresponding to 3.5 g. of silk fibroin was suspended in 50 ml. of methanol and reduced with hydrogen (80 kg./cm^2) at 100°C for 1 hr. in a 100 ml. autoclave. (80°C, 2 hr. for the Nylon catalyst).

b) The chelate corresponding to 350 mg. of fibroin was suspended in 30 ml. of 2% formic acid and boiled for 4 min. The chelate became black with vigorous evolution of hydrogen. In both cases, the catalyst, after cooling, was washed with water and methanol and then air-dried.

II. Determination of Palladium.—This was performed by the *p*-nitrosodiethylaniline method of Overholser[4].

III. Reaction Vessel.—A 100 ml. of autoclave was used as the vessel for hydrogenation reactions. The autoclave is illustrated in Fig. 2. The cap A was filled with absorbent cotton in order to prevent the catalyst from invading into the accessory parts of the autoclave. The apparatus was also so designed that the part B could be opened after the reaction. This device rendered it very easy to wash the inside of the tube. Although an aluminum packing was used

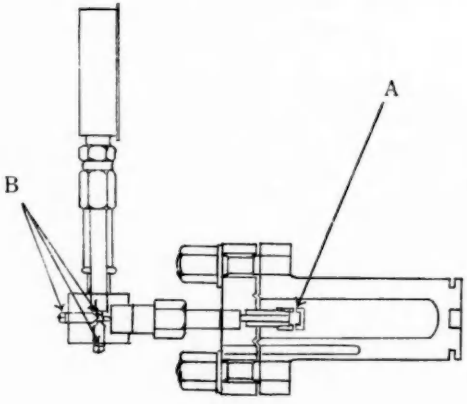

Fig. 2.

at the interface between the lid and the vessel, silver packings were employed in other parts to minimize the unfavorable effects due to metal ions. The autoclave was shaken 100 times per min. with an inclination angle of 15°.

IV. Reaction Velocity Measurement.—*1) Reaction Conditions.*—Four grams of nitrobenzene dissolved in 50 ml. of methanol and the catalyst to be tested were placed in the autoclave and it was filled with hydrogen to 90 kg./cm^2. The initial pressure was read after 15 sec. shaking for equilibriation and the shaking was continued until the theoretical amount of hydrogen was taken up.

2) Calculation of Reaction Velocity.—The reaction velocity (v) was calculated according to the equation,

$$v = \frac{100}{t}$$

where t is the time in minutes required until 70% of the theoretical hydrogen uptake occurred ("70% reaction time").

V. Isolation of Product.—The reaction mixture was filtered and 10 g. of acetic anhydride was added to the filtrate. The mixture was then evaporated to dryness. On cooling the residue after treating with 10 ml. of water, 4.0 g. of crude acetanilide (m. p. 111°C) was obtained. Its melting point was increased to 113°C on recrystallization from water.

VI. Tests of Stability.—*1) Stability Test of Chelate.*—Silk-palladium chelate was dried at 40°C and stored in a stoppered bottle. After 12 days it was activated by hydrogen as described above and its activity for the reduction of nitrobenzene was measured.

2) Stability Tests of Catalyst.—The catalyst preparations prepared by reduction with hydrogen were stored either in methanol or in the dry state (in a stoppered bottle). After suitable periods of storage, their activities were measured as above.

Summary

1. The highest hydrogenation activity was obtained when the silk-palladium catalyst was prepared by boiling the silk fibroin fibers with 0.1% palladous chloride solution in 0.1 N acetic acid for 8 min. and then hydrogenating the resulting chelate.

2. The catalyst prepared as above was, however, devoid of the capacity of asymmetric catalysis, although the same catalyst prepared in distilled water (instead of dilute acetic acid) was able to achieve asymmetric reduction.

3. The catalyst and its precursor chelate could be stored in dry state without any loss of activity.

4. The synthetic fiber, 6-Nylon, could be successfully used as the carrier in place of silk fibroin.

The author wishes to express his sincere thanks to Professor Shiro Akabori for valuable suggestions and encouragement throughout this work. He is also greatly indebted to the Toyo Rayon Co., Ltd. for the supply of 6-Nylon fibers used in this investigation. His thanks are also due to

4) L. G. Overholser and J. H. Yoe, *J. Am. Chem. Soc.*, **63**, 3224 (1941).

Mr. Y. Fujii, for his assistance, and to Dr. R. Sato for his advice on preparing this manuscript.

Division of Organic Chemistry
Institute for Protein Research
Osaka University, Nishi-ku, Osaka

Studies on the Silk-Palladium Catalyst. II. General Properties

By Yoshiharu IZUMI

(Received March 27, 1959)

In the previous paper[1] of this series it was reported that the silk-palladium catalyst possesses a number of excellent characteristics suitable for the purpose of catalytic hydrogenation. In order to obtain further information concerning the fundamental properties of the catalyst and to provide a basis for its practical application, it is intended in the present investigation to study its selectivity, durability and behaviors towards catalytic poisons. The present paper describes the results obtained in these experiments.

Results and Discussion

I. Selectivity of the Catalyst.—The catalytic efficiency of the silk-palladium catalyst was mainly examined in the previous paper[1] on the hydrogenation of nitrobenzene to aniline. In the present study the activity of the catalyst was examined with a variety of unsaturated compounds listed in Table I. The results obtained are also recorded in the same table.

Hydrogenation of C=C Double Bonds.—The C=C double bonds were found to be very easily reduced at low temperatures in the presence of the silk-palladium catalyst. For instance, it was found that mesityl oxide absorbed 70% of the theoretical amount of hydrogen at 30°C for 20 min. if the catalyst (containing ca. 0.08% of palladium metal per substrate) was supplied. This could be compared with the data obtained with 1% (by weight) Raney nickel in the presence of which it took 60 min. at 60°C for mesityl oxide to absorb the same amount of hydrogen. It was further noticed that the catalyst was able to selectively hydrogenate the C=C double bonds in mesityl oxide, crotonaldehyde and acrolein, leaving their carbonyl groups quite unattacked even at higher temperatures.

These results indicate that the silk-palladium catalyst is particularly suitable for the preparation of saturated aliphatic aldehydes and ketones from the corresponding unsaturated compounds. That azlactone and acetaminocinnamic acid are readily hydrogenated by the silk-palladium catalyst was previously reported[2-4]. The catalyst was, however, unable to reduce phenol at all, indicating that the double bonds in benzene rings are inert to the catalytic action.

Hydrogenation of Carbonyl Groups.—As described above, the silk-palladium catalyst was rather inactive in hydrogenating aliphatic carbonyl compounds. This conclusion was further confirmed in an attempt to reduce acetone and methyl ethyl ketone which were not reduced at all. It was, however, found that the hydrogenation of benzaldehyde in the presence of the catalyst readily gave rise to the formation of toluene. It is, therefore, probable that carbonyl groups attached to aromatic rings may be susceptible to the action of the catalyst. The catalyst which was recovered after having been used for the reduction of acetone was found to show no appreciable depression in the activity of hydrogenating nitrobenzene. It therefore seems that the failure in the hydrogenation of acetone (and other aliphatic

1) Y. Izumi, This Bulletin, **32**, 932 (1959).

2) S. Akabori, Y. Izumi, Y. Fujii and S. Sakurai, *Nature*, **178**, 323 (1956).

3) S. Akabori, Y. Izumi, Y. Fujii and S. Sakurai, *J. Chem. Soc. Japan, Pure Chem. Sec.* (*Nippon Kagaku Zasshi*), **77**, 1374 (1956).

4) S. Akabori, Y. Izumi, Y. Fujii and S. Sakurai, ibid., **78**, 168 (1957).

TABLE I. SPECIFICITY OF CATALYST

Substrate (g.)	Product	Yield (%)	Solvent	Catalyst (mg.)	Temp. (°C)	Reaction time (min.) 70%	100%
Mesityl oxide 41	Me-isobutyl ketone	86	—	350	30	21.5	60
Crotonaldehyde 21	Butyraldehyde	70	Ether	100	20	21	102
Acroleine 13	Propionaldehyde	100*	Ether	350	20	4	36
Acrylonitrile 50	Ethyl cyanide	79	—	100	6	47	71
Fumaric acid 12	Succinic acid	88	NaOH	350	53	16	28
Phenol 5	—	—	Methanol	350	170	—	—
Acetone 30	—	—	—	350	120	—	—
Methyl ethyl ketone 30	—	—	—	350	120	—	—
Benzaldehyde 11	Toluene	46	Methanol	350	27	41.3	426
Benzyl cyanide 6	Acetylphenethylamine	79	Ac_2O HOAc	350	75	179	276
Benzaldehyde 10.6	Dibenzylamine	65	Methanol NH_4OH	350	80	145	220
α-Ketoglutaric acid 5	Glutamic acid	50	Methanol NH_4OH	350	60	—	60
Nitrobenzene 4	Aniline	90	Methanol	350	20	9.5	23
MDAN** 12.4	MDAA***	80	Methanol	350	60	38	90
ω-Nitrostyrene 15	Phenylacetoaldoxime	35	Methanol	350	20	9.5	23
Diethyl nitro malonate 6.9	Diethyl aceto-aminomalonate	36	Ac_2O HOAc	350	100	31	90
Azobenzene 5.2	Hydrazobenzene	58	Methanol	100	20	95	185
Azobenzene 10	Aniline	88	Methanol	350	70	20	125
Dimethylglyoxime 3	—	—	Methanol	350	90	—	—
Acetophenonoxime 3	—	—	Methanol	350	70	—	—

* Calculated from dinitrophenylhydrazone.

** $CH_3(CH_3)CH-CH_2-CH((CH_3)_2N)-CH(O-COC_6H_4NO_2)-CH_3 \cdot HCl$

*** $CH_3(CH_3)CH-CH_2-CH((CH_3)_2N)-CH(O-COC_6H_4NH_2)-CH_3 \cdot HCl$

carbonyl groups) is an intrinsic property of the catalyst and not due to the poisoning by these compounds.

Reduction of Nitrile Groups.—It has already been mentioned that the catalyst was inactive in reducing the nitrile group of acrylonitrile, at least at low temperatures. Using acetic anhydride as a solvent, however, benzyl nitrile was converted to *N*-acetyl-phenethylamine in the presence of hydrogen and the silk-palladium catalyst.

Reductive Amination of α-Ketoglutaric Acid and Benzaldehyde.—The silk-palladium catalyst was able to convert α-ketoglutaric acid to glutamic acid in the presence of ammonia and hydrogen. When benzaldehyde was subjected to reductive amination under similar conditions, the main product obtained was identified as dibenzylamine.

Reduction of Nitro Groups.—In the previous paper[1] the reduction of nitrobenzene to aniline was employed as the test system for comparing the catalytic activity. In the present study, it was further found that 5-methyl-3-dimethyl-aminohexan-2-ol-*p*-nitrobenzoate hydrochloride (MDAN) was also readily hydrogenated by this catalyst to form the corresponding amine hydrochloride (MDAA) in as excellent a yield as in the case of the reduction of nitrobenzene. On the contrary, both ω-nitrostyrene and diethyl nitromalonate were reduced very slowly, yielding phenylacetaldoxime and diethyl acetamidomalonate, respectively; their yields also being low. It may be inferred that the catalyst is able effectively to catalyze the hydrogenation of aromatic nitro groups, but relatively weakly that of aliphatic nitro groups.

Reduction of Azobenzene.—Hydrogenation of azobenzene by means of the silk-palladium catalyst at low temperatures resulted in the formation of hydrazobenzene. At higher temperatures, on the other hand, the hydrogenation proceeded in two steps, as shown in Fig. 1, taking up more than one mole of hydrogen and the main product was aniline.

Reduction of Oximino Groups.—It was already reported[2-4] that the silk-palladium catalyst could catalyze the reduction of

TABLE II. DURABILITY TEST OF CATALYST

Substrate	Catalyst sample (Pd mg.)	Reaction temp. (°C)	Reaction velocity	Temp. at which H_2 uptake starts (°C)
Diethyl maleate 50 g.	Original silk-Pd (9.2)	150	9.5	105
	After 1st recovery	〃	22.0	90
	〃 2nd 〃	〃	18.0	70
	〃 3rd 〃	〃	17.0	50
	〃 4th 〃	〃	25.0	60
〃	Original carbon-Pd (10)	〃	30.0	50
	After 1st recovery	〃	7.4	60
	〃 2nd 〃	〃	9.1	70

benzyldioxime, α-acetoximino-phenylpropionic ethyl ester and glutaric diethyl ester to the corresponding amines. It was, however, found in the present study that both dimethylglyoxime and acetophenone oxime could not be reduced at all.

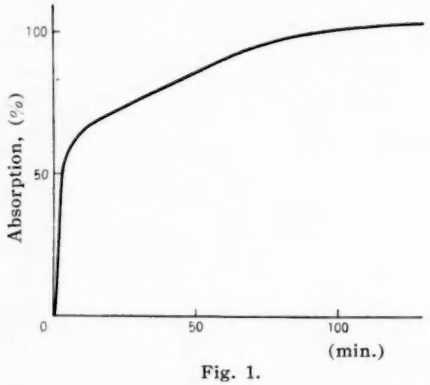

Fig. 1.

II. Durability of Catalyst.—The hydrogenation of diethyl maleate to diethyl succinate was selected as the test system to study the durability of the silk-palladium catalyst. The durability test was conducted in comparison to the carbon-palladium catalyst[5] commonly used as a hydrogenation catalyst.

The results of the test are summarized in Table II. As can be seen from Table II, a very interesting phenomenon was observed concerning the durability of silk-palladium catalyst. When freshly prepared silk-palladium catalyst was used, the temperature at which hydrogen absorption starts was relatively high (105°C) and the reaction proceeded rather slowly. In the hydrogenation using the catalyst recovered from the first run, however, the temperature of initial hydrogen uptake was not only considerably lowered (90°C), but also the reaction itself was accelerated. This elevated activity of pre-used catalyst persisted at least after the fifth run. Such a phenomenon was not observed with the carbon-palladium catalyst which showed the highest activity in the first run and lost it thereafter. It does not seem unreasonable to suppose that such an excellent durability of the silk-palladium catalyst is due to the possibility that the palladium attached to the carrier protein may be sterically rearranged after the first run in favor of the catalytic activity.

In connection with the durability, it might be pointed out that the relatively high ignition point (as compared to the carbon-palladium catalyst) and bulkiness of the fibrous silk-palladium catalyst were very convenient for its handling and recovery.

III. Poisoning of Catalyst.—The silk-palladium catalyst was found to be sensitive to poisonous substances or to various chemical treatments. In Table III are summarized the results of such inhibition studies. In examining the toxic effects, the hydrogenation of either nitrobenzene or diethyl maleate was adopted as the test system and the velocity of hydrogen uptake was calculated and compared as previously described. The carbon-palladium catalyst was also tested as a reference.

Inhibition by Mercaptan.—As can be seen from Table III, the addition of or treatment with ethyl mercaptan markedly decreased the catalytic activity of silk-palladium to hydrogenate both nitrobenzene and diethyl maleate. This poison, which is a well-known inhibitor of palladium catalysts, was also deleterious to the carbon-palladium catalyst. The silk catalyst was, however, much more

5) R. Mozingo, "Organic Syntheses", Vol. 26, John Wiley & Sons., Inc., New York (1947), p. 77, (Procedure D).

TABLE III. EFFECT OF VARIOUS TREATMENTS AND ADDITIONS ON THE ACTIVITY OF SILK AND CARBON-PALLADIUM CATALYSTS

Substrate	Catalyst (Pd mg.)	Addition (mg.)	Reaction temp. (°C)	Reaction velocity
Nitrobenzene 4 g. in 50 ml. MeOH	Silk-Pd (18.4)*	None	50	84
	Carbon-Pd (20)	〃	21	100
	Silk-Pd (18.4)** treated with EtSH	〃	50	22
	Carbon-Pd (20)** treated with EtSH	〃	〃	100
	Silk-Pd (18.4)	EtSH	〃	16.6
	Carbon-Pd (20)	〃	〃	16.6
	Silk-Pd (18.4) acetylated	None	19	1.75
Diethyl maleate 50 ml.	Silk-Pd (18.4)	〃	150	22
	The same after recovery	〃	〃	50
	Silk-Pd (18.4)	EtSH	〃	1.1
	Carbon-Pd (20)	〃	〃	6.25
	Silk-Pd (18.4)	$Fe(NO_3)_3 \cdot 12H_2O$ (40)	〃	1.7
	The same after 1st recovery	〃	〃	22.5
	The same after 2nd recovery	〃	〃	7.4
	The same after 3rd recovery reactivated with EDTA	None	〃	125
	Silk-Pd (18.4)	$Cu(NO_3)_3 \cdot 3H_2O$ (25)	〃	5.3
	The same after 1st recovery	〃	〃	2.7
	The same after 2nd recovery reactivated with EDTA	None	〃	45.0

* Calculated from the activity at 20°C.

** The catalyst was brought in contact with 15 ml. of 0.02% EtSH methanol.

seriously poisoned by the mercaptan than the carbon catalyst. It was, however, noted that no palladium was extracted from the silk catalyst in the presence of ethyl mercaptan, in contrast to the considerable extraction observed in the case of the carbon catalyst. It appears probable that the mercaptan inhibits the catalysts by directly blocking the active palladium.

Inhibition by Metal Ions.—Unlike the carbon palladium and other palladium catalysts, the activity of the silk-palladium catalyst was greatly lowered in the presence of ferric and cupric ions as supplied in the form of nitrates. Cupric ion was somewhat more toxic than ferric ion. It is more likely that these metal ions form chelate linkages with the carrier protein, sometimes three-dimentionally, and thus prevent the reactant from approaching the active palladium atoms which are distributed inside the fibroin micelles.

Reactivation by Ethylenediamine Tetraacetic Acid.—The catalyst poisoned by ferric or cupric ion could be reactivated by treating it with ethylenediamine tetraacetic acid (EDTA). As a matter of especial interest it was revealed that the catalyst thus reactivated exerts very powerful catalytic activity. In fact, EDTA treatments of ferric ion- and cupric ion-poisoned catalysts produced preparations 2.5 and 3 times, respectively, as active as the control catalyst (pre-used once under normal conditions, see above). This peculiar phenomenon suggests that the internal structure of the carrier protein was altered on removal of the metal ions by EDTA to favor the catalytic activity.

Effect of Acetylation.—As previously reported[4], an acetylated silk-palladium catalyst prepared from pre-acetylated silk fibroin and palladous chloride in the usual manner is more active than the unacetylated silk-palladium catalyst in hydrogenating azlactone. Quite unexpectedly, however, it was found in the present investigation that acetylation with acetic anhydride of the pre-formed silk-palladium catalyst greatly depressed the activity. It may be inferred that acetylation of the carrier protein of silk-palladium catalyst blocks the

openings of the fibroin micelles in which the active palladium atoms reside and thus makes it difficult for the substrate to reach the active centers.

In short, there are two types of inhibition; the first, including ethyl mercaptan, inhibits the catalyst by directly combining with palladium atoms and the second, such as ferric ion, cupric ion, and acetylation, by modifying the structure of carrier fibroin. The latter type of inhibition is unique to the silk-palladium catalyst and has special bearings to the structural interpretation of the catalytic activity.

Experimental

I. Preparation of the Catalyst. — The catalyst was prepared by the method of previous papers.

II. Selectivity of the Catalyst.—*1) Reduction of C=C Double Bonds.—a) Reduction of fumaric acid.*—Seventy milliliters of aqueous solution containing 12 g. of fumaric acid adjusted to pH 7.0 with 20% sodium hydroxide and 100 mg. of the catalyst were shaken in 90 kg./cm^2 of hydrogen at 53°C. The reduction was complete after 28 min. The reaction mixture was filtered and the filtrate evaporated to 60 ml. which was then acidified with 20 ml. of concentrated hydrochloric acid. After standing overnight, 9.5 g. succinic acid (m.p. 184°C) was obtained. It was confirmed that the product is devoid of unsaturated bond by infrared spectroscopy.

b) Reduction of mesityl oxide.—Forty-one grams of mesityl oxide was reduced, using 350 mg. of the catalyst with 90 kg./cm^2 hydrogen at 30°C. The reduction was complete after an hour and 1 mol. of hydrogen was absorbed per 1 mol. of mesityl oxide. 36 g. of methyl isobutyl ketone (b. p. 113~115°/760 mm Hg) was obtained from the reaction mixture. Infrared spectroscopy showed a disappearance of unsaturated bond.

c) Preparation of Raney-nickel catalyst.—0.5 g. of Raney-nickel-alloy was added to 6 ml. of 25% sodium hydroxide solution in small portions during 5 min. and then heated for an hour on a water bath. The catalyst sludge was washed three times with each 30 ml. of water and washed with methanol decantation.

d) Reduction of crotonaldehyde. — Twenty-one grams of crotonaldehyde dissolved in 30 ml. of ether was reduced at 20°C with 85 kg./cm^2 hydrogen using 100 mg. of the catalyst. The reduction was continued for 102 min. The reaction mixture was distilled in a 30 cm. dephlegmator. Fifteen grams of butyraldehyde (b. p. 75°C) was obtained and this sample contained no C=C double bonds as examined by infrared spectroscopy.

Analysis of the dinitrophenylhydrazone of this compound showed the following results.

Anal. Found: N, 22.6. Calcd. for $C_{10}H_{12}O_4N_4$: N, 22.2%.

The aldehyde group of crotonaldehyde was never reduced even at higher temperature (130°C).

e) Reduction of acrolein.—When 13 g. acrolein in 20 ml. ether was reduced at 20°C with 85 kg./cm^2 hydrogen using 350 mg. of the catalyst, hydrogen was readily absorbed and the absorption ceased in 36 min.

On adding 2,4-dinitrophenylhydrazone to 1/100 portion of the reaction mixture, there was obtained 550 mg. propionaldehyde-2,4-dinitrophenylhydrazone with m.p. 126°C, indicating a yield of 100% in the reduction.

Anal. Found: N, 23.7. Calcd. for $C_9H_{10}O_4N_4$: N, 23.5%.

By distillation of the residue through 15 cm. Widmer column 2 g. of the distillate of b.p. 49°C was obtained. It was proved infrared spectroscopically that this material has no C=C double bond.

This catalyst did not catalyze the reduction of the aldehyde group of this product even when the reduction was carried out at 120°C.

f) Reduction of acrylonitrile. — Fifty grams of acrylonitrile was reduced at 6°C, 100 atm. with 100 mg. of this catalyst and spontaneously the reaction temperature rose to 24°C. The reaction was concluded for 71 min. By fractional distillation, 41 g. of ethyl cyanide (b. p. 96~98°C) was obtained. The product was identified by infrared spectroscopically and gas-chromatographically.

g) Reduction of phenol.—Phenol was not hydrogenated in methanol at 170°C with 80 atm./cm^2 hydrogen by 350 mg. of this catalyst.

2) Reduction of Carbonyl Compounds.—a) Reduction of acetone and methyl ethyl ketone.—Thirty grams of acetone (or methyl ethyl ketone) was not reduced with 90 kg./cm^2 hydrogen at 120°C in the presence of 350 mg. of the catalyst. (Activity of recovered catalyst was tested by the method of previous report[1]). It was clear that the activity of this catalyst was maintained through this condition).

b) Reduction of benzaldehyde.—Eleven grams of benzaldehyde dissolved in 40 ml. of methanol was reduced with 90 kg./cm^2 hydrogen at 27°C using 350 mg. of catalyst. The reduction was continued for 426 min. absorbing of hydrogen per mol. of the aldehyde. 4.3 g. of toluene was obtained from the reaction product, and identified by infrared spectrum.

3) Reduction of Cyanides.—Reduction of benzyl cyanide.—Using 350 mg. of the catalyst 6.0 g. of benzylcyanide was reduced with 100 kg./cm^2 hydrogen at 75°C in a mixture of 15 g. acetic anhydride and 30 g. of acetic acid. The reduction was completed in 276 min. Six grams of acetylphenethylamine (b. p. 145°C/5 mm Hg) was obtained by fractional distillation reaction mixture under reduced pressure.

Anal. Found: N, 8.35. Calcd. for $C_{10}H_{13}ON$: N, 8.58%.

4) Reductive Aminations of Carbonyl Compounds.—a) Reductive amination of benzaldehyde.—Using 350 mg. of the catalyst 10.6 g. of benzaldehyde was reduced in the presence of 6.7 ml. of aqueous ammonia and 25 ml. of methanol with 94 kg./cm^2 hydrogen at 80°C. The reduction was completed in 220 min. By fractional distillation, 6.4 g. of

dibenzylamine (b. p. 156°C/11mmHg) was obtained. The results of analysis were as follows:

Dibenzylamine. *Anal.* Found: N, 6.74. Calcd. for $C_{14}H_{15}N$: N, 7.07%.

Dibenzylamine hydrochloride. *Anal.* Found: N, 5.76. Calcd. for $C_{14}H_{16}NCl$: N, 6.00%.

b) Reductive amination of α-ketoglutaric acid.—Five grams of α-ketoglutaric acid, 14 ml. of 28% ammonia and 36 ml. of methanol were placed in the autoclave. Hydrogenation was carried out at 60°C, 90 kg./cm² for 1 hr. After the reaction mixture was filtered, the filtrate was evaporated in vacuo, dissolved in 5 ml. of water and adjusted to pH 3.2 with hydrochloric acid, then 2.5 g. of glutamic acid was obtained. This product was identified paper-chromatographically and was optically inactive.

5) Reductions of Nitro Compounds.—a) Reduction of nitrobenzene.—This was hydrogenated in the same way as previously reported[1].

b) Reduction of 5-methyl-3-dimethylaminohexyl-(2) p-nitrobenzoate hydrochloride (MDAN).—12.4 g. of MDAN in 40 ml. methanol was reduced at 60°C, 80 atm. for 90 min. with the 350 mg. catalyst. The reaction mixture was concentrated to a volume of 20 ml. and kept at 0°C overnight. There was obtained 8 g. of 5-methyl-3-dimethylaminohexyl-(2) *p*-aminobenzoate hydrochloride (MDAA) with m. p. of 217°C. The mixed melting point with an authentic sample showed no depression.

c) Reduction of ω-nitrostyrene.—When 15 g. of ω-nitrostyrene was hydrogenated at 20°C, 97 atm. in the presence of 350 mg. of the catalyst, the absorption of hydrogen came to an end in 23 min. Filtration, concentration and vacuum-distillation gave 6 g. of the product boiling at 96~108°C/2 mmHg, which crystallized on standing. 4.8 g. of the crystal (m. p. 102°C) obtained. The material was identified as phenylaldoxime.

Anal. Found: N, 10.0. Calcd. for C_8H_9ON: N, 10.4%.

d) Reduction of diethylnitromalonate.—Using 350 mg. of the catalyst 6.9 g. of diethylnitromalonate was reduced in a mixture of 16 ml. of acetic anhydride and 27 ml. of acetic acid with 100 kg./cm² hydrogen at 100°C for 90 min. Two grams of diethyl acetoaminomalonate (m. p. 89°C) was obtained from the reaction mixture after evaporation, addition of 5 ml. of ethyl acetate and overnight standing.

Anal. Found: C, 50.11; H, 7.13; N, 6.52. Calcd. for $C_9H_{15}O_5N$: C, 49.76; H, 6.96; N, 6.45%.

6) Reduction of Azobenzene.—a) Reduction to hydrazobenzene.—5.2 g. of azobenzene was reduced in 50 ml. of ethanol with 94 kg./cm² hydrogen at 20°C. The reduction was concluded for 185 min. absorbing 1 mol. of H_2 per mol. of azobenzene. The reaction mixture was evaporated and the residue was dissolved in 10 ml. of hot methanol. After cooling, 3.0 g. of hydrazobenzene (m. p. 288°C) was obtained as orange crystals. The crystals identified with infrared spectroscopy.

b) Reduction to aniline.—Ten grams of azobenzene was reduced with the 350 mg. catalyst under the same conditions as above except that the reaction temperature was elevated to 70°C. The reduction was concluded for 125 min. Thirteen grams of acetanilide (m. p. 112°C) was obtained from the reaction mixture by the following method. The filtered reaction mixture was evaporated in the presence of 10 g. of acetic anhydride and the residue dissolved in 10 ml. of water and cooled.

III. Durability of Catalyst.—*1) Preparation of the Carbon-Palladium Catalyst.*—The catalyst was prepared by the method of R. Mozingo[5] and stored in wetness.

2) General Procedures.—Hydrogenation experiments were carried out using an autoclave as already reported[1] and the reaction velocity of the hydrogenation of diethyl maleate was calculated according to the equation:

Reaction velocity = 100/reaction time (in min.)

where the reaction time is the time required from 30 to 70% of the hydrogen uptake proceeds.

IV. Poisoning of Catalyst. — *1) General Procedures.* — Hydrogenation velocity of diethyl maleate was measured by the III—*2* method and the reaction velocity of the hydrogenation of nitrobenzene was calculated by the method of the previous paper[1].

2) Inhibition of Mercaptan.—a) Preparation of inhibited catalyst. — Two hundred and fifty milligrams of the silk-palladium or carbon-palladium containing 20 mg. of palladium (In the following experiments, this amount of catalyst was used as a unit.) was mixed with 50 ml. of 0.02% ethyl mercaptan methanol solution, stirred for 15 min. at 20°C, filtered and washed with water and methanol.

b) Poisoning test by substrate containing mercaptan.—b-1) Reduction of nitrobenzene.—The reaction velocity was measured in relation to the reduction system containing 1 mg. of ethylmercaptan, 4 g. of nitrobenzene, 50 ml. of methanol and 1 unit of each catalyst.

b-2) Reduction of dietyl maleate (DEM).—The reaction velocity was measured in relation to 50 g. of DEM containing 4 mg. of ethyl mercaptan.

3) Inhibition by Metal Ions (Metal Ion Effect to the Reduction System of DEM).—Forty milligrams of $Fe(NO_3)_3 \cdot 12H_2O$ or 25 mg. of $Cu(NO_3)_2 \cdot 3H_2O$ was added to the reaction system containing 50 g. of DEM and 1 unit of each catalyst, and the reaction velocity was measured.

4) Reactivation by Ethylenediamine Tetraacetic Acid (EDTA). — Recovered catalysts of experiment (IV-*3*) were boiled with 0.5% EDTA for 5 min., filtered and washed with water and methanol. (Filtered solution was apparently colored with Cu^{2+} or Fe^{3+} EDTA complex.) Using this catalyst, 50 g. of DEM was reduced with hydrogen at 150°C.

5) Effect of Acetylation.—Acetylation of silk-palladium.—Three hundred and fifty milligrams of silk-palladium catalyst was boiled with 50 ml. of an acetic acid anhydride for 2 hr. filtered and washed with water and methanol.

Summary

1. The silk-palladium catalyst was found to catalyze the hydrogenation of

aliphatic C=C double bonds, aldehyde, nitriles and nitro groups directly attached to aromatic rings, azobenzene, and some oximino groups, but relatively weakly that of aliphatic nitro groups. The catalyst was completely inactive to aromatic C=C double bonds, aliphatic carbonyl (with the exception of α-ketoglutarate which was reduced to glutamate in the presence of ammonia), nitriles, and several oximes.

2. The catalyst, when used once, considerably increased its catalytic activity and this elevated activity persisted after several repeated uses.

3. Ethyl mercaptan was poisonous to the catalyst probably due to its combination with the active palladium atoms. Ferric and cupric ions inhibited the catalyst by forming chelate linkages with the carrier protein. The inhibition by these metal ions could be restored by ethylenediamine tetraacetic acid. Acetylation of the catalyst with acetic anhydride markedly reduced the activity, although the treatment of silk fibroin with acetic anhydride prior to the preparation of the catalyst gave a strongly active catalyst.

The author wishes to express his hearty gratitude to Professor Shiro Akabori for encouragement and valuable discussion. He is also indebted to Mr. Yasuo Fujii for cooperation in some phases of this work, to Dr. S. Sakurai and to the Ajinomoto Co., Inc. for the gift of diethyl maleate, and to Dr. R. Sato for his advice on preparing this manuscript.

Division of Organic Chemistry
Institute for Protein Research
Osaka University, Nishi-ku, Osaka

Studies on the Silk-Palladium Catalyst. III. Physicochemical Characterization

By Yoshiharu IZUMI

(Received March 27, 1959)

In the preceding papers of this series[1,2], it was reported that silk and 6-Nylon-palladium catalysts are in a number of respects superior as hydrogenation catalysts to carbon-palladium and other palladium catalysts hitherto described. It was also suggested that these catalysts resemble enzymes in that their activity is considerably affected by metal ions and other agents and some of them are endowed with an ability to catalyze asymmetric hydrogenation reactions[3-5].

It, therefore, seemed of special interest to study their structure and the process of their activation from physicochemical points of view. It was also hoped that such studies would shed some light on the mechanism by which some of these catalysts achieve the asymmetric reactions.

The present paper describes X-ray diffraction, infrared spectrophotometric experiments on silk fibroin, its palladous chloride chelate compound, and silk-palladium catalyst (samples of silk series) and on the corresponding samples of 6-Nylon* (samples of Nylon series). The behaviors of these samples towards *p*-nitrosodiethylaniline (PNDA), a specific reagent for palladium[6], were also included in this paper.

Results and Discussion

X-Ray Diffraction Studies. — X-ray diffraction pictures of fibrous preparations of the silk series and the Nylon series are shown in Figs. 1 and 2, respectively. X-ray diffraction measurements were also made on powdered samples of the silk series using a Norelco X-ray instrument and the charts obtained are reproduced in Fig. 3.

1) Y. Izumi, This Bulletin, **32**, 932 (1959).
2) Y. Izumi, ibid., **32**, 936 (1959).
3) S. Akabori, S. Sakurai, Y. Izumi and Y. Fujii, *Nature*, **178**, 323 (1956).
4) S. Akabori, Y. Izumi, Y. Fujii and S. Sakurai, *J. Chem. Soc. Japan, Pure Chem. Sec.* (*Nippon Kagaku Zasshi*), **77**, 1374 (1956).
5) S. Akabori, Y. Izumi and Y. Fujii, ibid., **78**, 886 (1957).
* Polycaprolactum.
6) L. G. Overholser and J. H. Yoe, *J. Am. Chem. Soc.*, **63**, 3224 (1941).

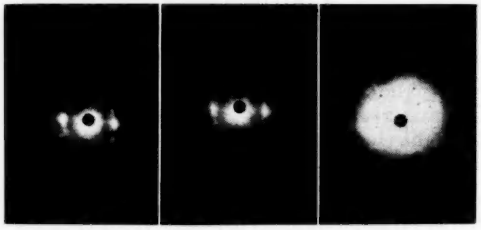

a b c

Fig. 1. X-ray diffraction pictures of silk series.

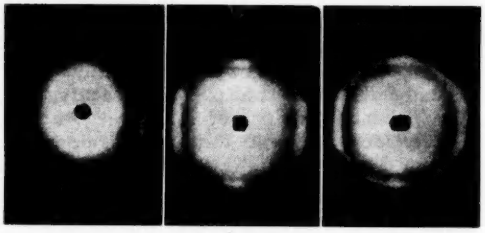

a b c

Fig. 2. X-ray diffraction pictures of Nylon series.

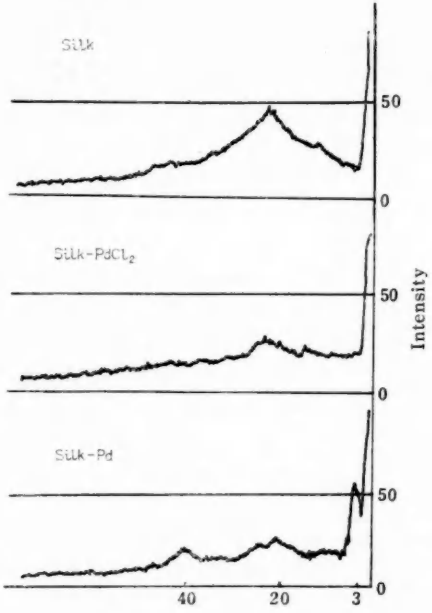

Diffraction angle (2θ)

Fig. 3. X-ray diffraction patterns of powdered silk series.

As has been known for some time, Figs. 1a and 2a clearly indicate that both silk fibroin and 6-Nylon fibers contain crystalline parts in their structures. The X-ray fiber diagrams of palladous chloride chelates of silk fibroin and 6-Nylon are essentially the same with those of silk fibroin and 6-Nylon, respectively, suggesting that the chelate formation with palladous chloride does not significantly alter the arrangement of these fibers. Conversion of these chelate compounds to catalytic active forms by hydrogenation, however, seems to cause some changes as can be judged from the distinct patterns due to palladium atoms seen in the diagrams of the catalysts.

The Norelco patterns of powdered samples of the silk series are in good agreement with the fiber diagrams of the corresponding preparations. It is noted that the pattern for the powdered silk-palladium catalyst shows in the low-angle region (ca. 3.5°), a peak of which may be due to a ca. 25 Å regular arrangement of the structure.

In summary, it may be concluded that a part of the palladium atoms in the silk-palladium catalysts are assembled in fine crystalline particles and the other part of the palladium probably becomes regularly arranged in the micelle structures of the fibers. However, the possibility that certain regular structures have emerged in the silk protein itself can not be excluded.

Infrared Absorption Measurements. — For the infrared absorption studies powdered samples of the silk series and thin sheet forms of the Nylon series were employed. The spectra of these samples are shown in Fig. 4. As a reference substance carbobenzoxy triglycylleucine and its palladous chloride complex were chosen, the spectra of which are shown in Fig. 4.

Generally speaking, the infrared absorption spectra of the samples of the silk series did not show any remarkable differences, probably due to the high polymeric nature of silk fibroin. Especially, the spectra of the Nylon samples were quite similar to each other, because of the fact that the measurements were made on thin sheet samples, and they contained only a small amount of palladium. However, it can be pointed out, on close examination of the spectra, that the powdered silk-palladium catalyst is similar to the silk fibroin powder rather than to the chelate preparation. A comparison of the infrared absorption spectra of carbobenzoxy triglycylleucine (Cbz. Trigly-Leu) and its palladous chloride complex on one hand and silk fibroin and its palladous chelate on the other hand reveals that an absorption at 3000 cm^{-1} region, which is due

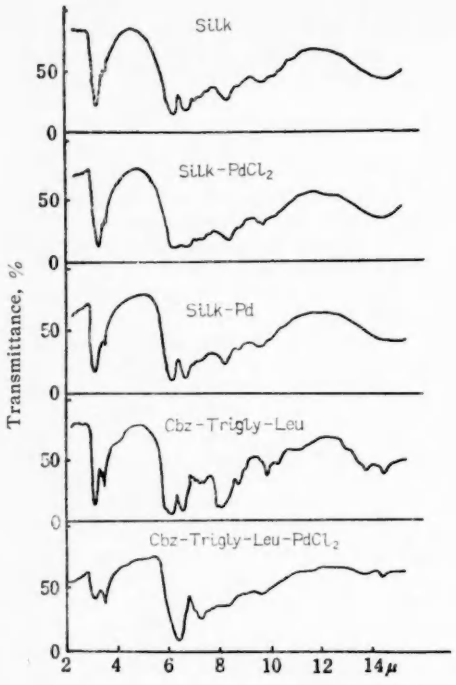

Fig. 4. IR-spectra of silk, silk-$PdCl_2$, silk-Pd, Cbz-Trigly-Leu and Cbz-Grigly-Leu-$PdCl_2$.

to NH groups (probably also OH groups) decreases on the formation of chelates. This suggests that the NH groups (probably also OH groups) of both silk fibroin and the carbobenzoxy tetrapeptide are involved in the chelation with palladous chloride. It may also be noticed that in the spectra of chelate compounds, absorptions at 1640 and 1530 cm^{-1} are diminished and that at 1590 cm^{-1} is increased as compared with the spectra of unchelated forms. The absorptions at 1640 and 1530 cm^{-1} are usually interpreted as caused by CO in COOH and CONH groups, and the absorption at 1590 cm^{-1} as caused by COO^- groups, and Gierer[7] has reported that the complex formation of an amide results in a shift of the absorptions due to CONH to longer wave-lengths. It is therefore probable that the observed changes in the region of 1530 to 1640 cm^{-1} are due to a complicated effect of chelate bond formation between palladous chloride and COOH and/or CONH groups.

It may be concluded that palladous chloride forms chelate linkages with NH_2 (-OH), CONH and COOH groups of fibroin and the dipeptide. These linkages appear to be broken on hydrogenation of the chelate. In the activated chelate, therefore, the palladium seems to be in an almost atomic state.

Behaviors towards *p*-Nitrosodiethylaniline (pNDA). — When silk fibroin and Nylon-$PdCl_2$ chelate compounds were treated with pNDA, a specific reagent for palladium, parts of palladous chloride were released. However, the rest of palladous chloride remained in fibers, although the fibers were strongly colored like pNDA-$PdCl_2$ complex. Furthermore, Fujii[8] observed that silk fibroin-$PdCl_2$ chelate treated with pNDA is more active than silk fibroin-$PdCl_2$ itself and pNDA in catalyzing the decarboxylation of oxalacetic acid. These facts suggest that a considerable part of the palladium is firmly kept in the fiber structure and that on treatment with pNDA the reagent becomes combined with silk fibroin through the mediation of palladium atom or pNDA-$PdCl_2$ complex becomes wrapped into the fiber micelles.

In summary, it can be inferred that palladous chloride is first dispersed in the fiber structures because of the chelate formation. On reduction, palladous chloride in the chelate is converted into an atomic state leaving the carrier protein.

Experimental

I. Preparation of Powdered Silk Fibroin Preparations. — One gram of silk fibroin was dissolved in a modified Schweizer reagent made from 1.6 g. of ethylenediamine and 1.2 g. of $Cu(OH)_2$, and the solution was neutralized with acetic acid and dialyzed. Five milliliters of 1% ethylene diamine tetraacetate solution and 0.1 g. of celite were added to the dialyzed solution and the mixture was filtered under suction. To the filtrate were gradually added 3 volumes of acetone and the precipitate formed was collected by centrifugation. The precipitate was dried at 50°C after washing 4 times with acetone and then once with ethyl ether. The dried silk fibroin was ground in a mortar and passed through a 200 mesh sieve. 0.5 g. of finely powdered silk fibroin was obtained.

This powdered fibroin was converted to palladous chloride chelate and catalyst forms according to the standard methods described in Part I. The chelate was brown in color, and the catalyst resembled active carbon in its appearance.

II. Preparation of 6-Nylon Catalyst Samples for X-ray Measurements. — In order to prevent the tangling of the chelate fibers during the reduction, they were fixed to a holder of the X-ray apparatus. After measurement of the

7) A. Gierer, *Z. Naturforsch.* **8b**, 654 (1953).

8) Y. Fujii, *J. Biochem.*, in preparation.

X-ray diffraction, the holder with the chelate fibers in it was wrapped in gauze and then reduced in the autoclave.

III. 6-Nylon-$PdCl_2$ Complex.—The complex was prepared analogously to the silk fibroin-$PdCl_2$ complex.

IV. Triglycyl-carbobenzoxyleucine-$PdCl_2$ Complex. — Forty-four milligrams of triglycyl-carbobenzoxyleucine was boiled for 4 min. with 140 ml. 0.1 N acetic acid containing 140 mg. palladous chloride and the resulting peptide-$PdCl_2$ complex was isolated centrifugally and washed completely with water and then with methanol and dried.

V. X-ray Diffraction Measurements. — X-ray fiber photographs were taken with K_α line of copper filtered through a nickel filter. For powdered samples a Norelco X-ray instrument was used.

VI. Infrared Absorption Measurements. —A Perkin-Elmer apparatus was used. The measurements were made by the KBr tablet method.

Summary

1. From the infrared absorption measurements of silk fibroin, silk fibroin-$PdCl_2$ complex, and silk-palladium catalyst, it was concluded that the NH, OH, COOH and CONH groups of the fibroin participate in the chelate formation with palladous chloride. On reduction of the chelate with hydrogen, the chelate bonds are broken and the fibroin restores its original form.

2. X-ray diffraction pictures of the above-mentioned samples and of the corresponding preparations of the 6-Nylon series suggest that a part of the palladium atoms in the silk-palladium catalyst is assembled in fine crystaline particles and the other part of the palladium probably becomes regularly arranged in the micelle structures of the fibers. However, the possibility that certain regular structures have emerged in the carrier protein itself can not be excluded.

3. Part of the palladium in silk fibroin-$PdCl_2$ complex can be readily released with *p*-nitrosodimethylaniline, while the rest appears to be strongly kept in the fiber structure.

The author wishes to express his sincere thanks to Professor Shiro Akabori for encouragement and valuable advice. He is also indebted to Mr. Yasuo Fujii for skilful collaboration, to Dr. K. Ogawa for measurement of X-ray pictures, to Dr. H. Tadokoro and Mr. T. Inui for infrared measurements, to Mr. F. Sakiyama for the gift of tetrapeptide, to the Toyo Rayon Co. for the gift of 6-Nylon fibers, and to Dr. R. Sato for his advice on preparing this manuscript.

Division of Organic Chemistry
Institute for Protein Research
Osaka University
Nishi-ku, Osaka

*The Reaction of the Aquopentamminechromium(III) Complex Ion in Aqueous Solution. I. Substitution Reaction of a Coordinated Water with a Chloride Ion**

By Shinpei HASHIMOTO

(Received January 6, 1959)

Garrick[1] and Adell[2] have investigated a substitution reaction of aquopentamminecobalt(III) ion in which a coordinated water molecule of the complex ion is replaced by a chloride ion[3]. They have reported that the reaction is of first order with respect to the complex ion and the chloride ion respectively, and that the reaction rate decreases markedly as ionic strength increases.

A similar substitution reaction occurs in the case of aquopentamminechromium (III) ion as well. On addition of hydrochloric acid to the aqueous solution of an aquopentamminechromium (III) complex salt, red crystals precipitate slowly. The

* Presented at the Symposium on Coordination Compounds, held at Nagoya, November, 1957.

1) F. J. Garrick, *Trans. Faraday Soc.*, **33**, 486 (1937).

2) B. Adell, *Z. anorg. u. allgem. Chem.*, **246**, 303 (1941).

3) In Ref. 6b, the reaction of this type was called "anation reaction". This word will be used in this paper for convenience.

absorption spectrum of a solution of the crystallines is identical with that of chloropentamminechromium(III) complex ion. The fact shows that the following substitution reaction occurs in the solution containing aquopentamminechromium(III) complex ion and chloride ion.

$$[Cr(NH_3)_5OH_2]^{3+} + Cl^- \rightarrow [Cr(NH_3)_5Cl]^{2+} + H_2O \quad (1)$$

Since aquopentamminechromium (III) complex ion is very similar to that of cobalt(III) in steric configuration, ionic size and charge, but different only in electronic configuration of the central metal ion, it is interesting to investigate whether this difference in electronic configuration may appear in the reactions of these two metal-ammine-complexes.

This paper presents a study of the substitution reaction in which a coordinated water molecule of aquopentamminechromium(III) complex ion is replaced by a chloride ion in aqueous solution. Furthermore, the influence of ionic strength on the aquation of chloropentamminechromium(III) complex ion is also reported.

Experimental

Materials. — Aquopentamminechromium (III) perchlorate was prepared by the method of Linhard et al.[4] and was purified by recrystallization from perchloric acid solution twice and then from warm water once.

Chloropentamminechromium(III) chloride was prepared according to the direction of Biltz[5]. The chloride was converted by treatment with perchloric acid into perchlorate, and the latter was purified twice by reprecipitation from cold perchloric acid solution.

Sodium chloride of reagent grade was used without further purification. Sodium perchlorate was prepared by neutralizing sodium hydroxide with perchloric acid both of which were of reagent grade. Absorbancies for solutions of sodium chloride and sodium perchlorate were both so small that they could be neglected practically. Their magnitudes for the solutions of unit molarity at 44000 cm^{-1}, where all rate measurements were carried out, were 0.015 and 0.020, respectively against water.

Measurements.—Experimental solutions were prepared as follows. The solution of aquo-complex salt (10^{-3}~10^{-2} M) which was acidified with perchloric acid was placed in a stoppered and brown-colored flask. The solution of sodium chloride (10^{-2}~1 M) whose ionic strength was adjusted with sodium perchlorate was prepared. These two solutions were kept at a constant temperature in a thermostat, and were mixed together quickly; then at intervals of a few minutes, the amount of chloropentamminechromium(III) ion formed was determined spectrophotometrically.

The measurement of absorbancy was made with a Beckman Model DU photoelectric spectrophotometer using stoppered 10 mm. quartz cells. The temperature of the cell compartment was kept constant within ±0.1°C by circulating thermostated water.

The aqueous solution of aquopentamminechromium(III) perchlorate which was acidified with perchloric acid did not change so fast as its neutral solution. When the pH of the solution was lower than approximately 4, no changes in absorbancy nor pH were observed during the course of measurements.

The aquation rate of chloropentamminechromium(III) ion was followed also spectrophotometrically. After dissolving chloropentamminechromium(III) perchlorate in a solution containing appropriate amounts of perchloric acid and sodium perchlorate at an experimental temperature, the change in absorbancy at 44000 cm^{-1} was followed with a thermostated spectrophotometer.

Results

Apparent Molar Extinction Coefficients of Complex Cations. — In order to determine the rate of the formation of chloropentamminechromium(III) complex ion by the measurements of a change in ultraviolet absorption, the correct molar extinction coefficients of complex ions under the reacting condition must be known. Table I shows the temperature dependence of molar extinction coefficients of chloro and aquopentamminechromium (III) ions at 44000 cm^{-1} in aqueous solution containing no chloride ion. These molar extinction coefficients were more or less greater when chloride ion was added.

Fig. 1 shows the variations of molar extinction coefficients of chloro and aquopentamminechromium(III) ions with respect to chloride ion concentration. This increase in extinction coefficients caused with chloride ion may be attributed

TABLE I. MOLAR EXTINCTION COEFFICIENTS OF COMPLEX IONS $\tilde{\nu}$ = 44000 cm^{-1}

Temp., °C	$[Cr(NH_3)_5OH_2]^{3+}$	$[Cr(NH_3)_5Cl]^{2+}$
26		1213
30	21.3	
35	22.2	1236
40	23.3	
45	25.1	1281
50	27.6	
53		1314

4) M. Linhard and W. Berthold, *Z. anorg. u. allgem. Chem.*, **276**, 173 (1955).

5) H. Biltz and W. Biltz, "Laboratory Methods of Inorganic Chemistry", translated by W. T. Hall et al., 2nd Ed., John Wiley & Sons, Inc, New York (1928), p. 185.

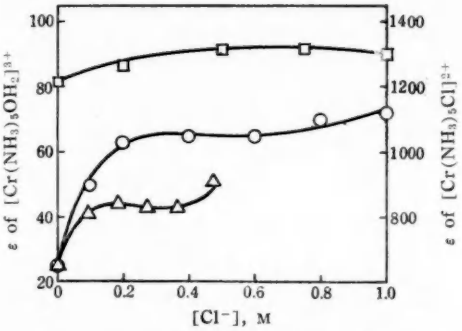

Fig. 1. The change in molar extinction coefficients of complex ions at 44000 cm^{-1} with the chloride ion concentration:
□, $[Cr(NH_3)_5Cl]^{2+}$ (20~23°C);
○, $[Cr(NH_3)_5OH_2]^{3+}$ (45°C);
△, $[Cr(NH_3)_5OH_2]^{3+}$ (45°C, at constant ionic strength).

to the formation of outer sphere association complexes[6] between complex cations and chloride ion. Furthermore, since the formation of the association complex generally depends on the ionic strength of solution[7], the apparent extinction coefficient of a complex ion varies on addition of sodium perchlorate[8] to the solution containing chloride and complex ions. Extinction coefficients of complex ions under various conditions were obtained by extrapolating the absorbancies with regard to the time zero. On the estimation of the molar extinction coefficient of chloropentamminechromium(III) ion under reacting conditions, the small effect of ionic strength mentioned above was neglected. The magnitudes were determined from the data of Table I and Fig. 1, assuming that the temperature dependence of extinction coefficient of outer sphere association complex was similar to that of free complex ion.

The solution of chloropentamminechromium(III) ion obeys the Beer's law strictly where no chloride ion exists, and also satisfies it fairly well even in chloride solution.

6) a. M. Linhard, *Z. Elektrochem.*, **50**, 224 (1944).
b. Many other works are summarized and surveyed in the following book: F. Basolo and R. G. Pearson, "Mechanisms of Inorganic Reactions", John Wiley & Sons, Inc., New York (1958), p. 376.
7) a. F. A. Posey and H. Taube, *J. Am. Chem. Soc.*, **78**, 15 (1956).
b. T. Kubota, *J. Chem. Soc. Japan, Pure Chem. Sec. (Nippon Kagaku Zasshi)*, **75**, 552 (1954).
8) Perchlorate ion itself is considered to have hardly any ability of association.

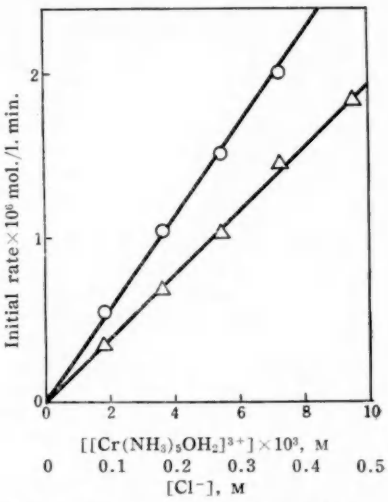

Fig. 2. The first order tests with each of two reactants at 45°C:
○, $[Cr(NH_3)_5OH_2]^{3+}$; △, Cl^-.

The Rate of Formation of Chloropentamminechromium(III) Ion. — It is shown in Fig. 2 that the initial rates of the formation of chloropentamminechromium(III) ion in the solution of the constant ionic strength are proportional to the concentrations of aquo-complex cation and chloride ion, respectively. Accordingly the rate constants of the anation reaction 1 were calculated by the usual method based on Eq. 2, being regarded as a second order reaction. To obtain more correct values of the anation rate, a reverse reaction, that is, an aquation of chloropentammine-complex ion, was taken into account according to the method of Garrick[1].

$$\frac{d[[Cr(NH_3)_5Cl]^{2+}]}{dt} = \vec{k}_2[[Cr(NH_3)_5OH_2]^{3+}][Cl^-] \qquad (2)$$

As is shown in Table II, the reaction

TABLE II. TEST FOR THE EFFECT OF HYDROGENE ION ON THE RATE OF ANATION REACTION OF $[Cr(NH_3)_5OH_2]^{3+}$ WITH Cl^- AT 45°C

$[HClO_4]$, mol./l.	Ionic strength, ω	$\vec{k}_2\times10^3$, l./mol. min.
0	0.510	1.55
0.49*	0.500	1.48
0.095	0.625	1.27
0.009	0.630	1.26
0.001	0.631	1.31

* HCl was used.

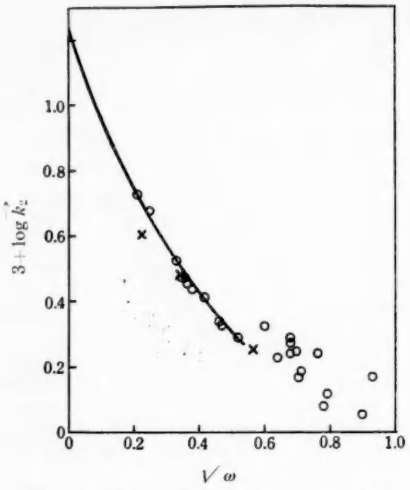

Fig. 3. Influence of ionic strength on the rate of anation:
○, $[Cr(NH_3)_5OH_2]^{3+}$—Cl^- at 45°C;
×, $[Co(NH_3)_5OH_2]^{3+}$—Cl^- [1] at 25°C,
rate scale is for $4+\log \vec{k}_2$. The curve represents Eq. 3.

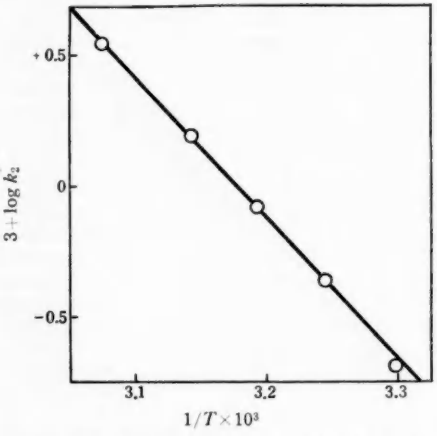

Fig. 4. Arrhenius plot of the anation reaction of $[Cr(NH_3)_5OH_2]^{3+}$ with Cl^- ($\omega=0.52\pm0.01$).

rates are independent of hydrogen ion concentrations so far as the solutions are acidic.

The reaction rate decreases remarkably with increasing ionic strength of solution. The influence is particularly significant in the lower ionic strength region. In Fig. 3, logarithms of rate constants measured at 45°C are plotted against the square root of the ionic strengths in molarity scale, which are calculated from the initial composition of solutions. Observed rates fluctuate markedly in a higher ionic strength region, whereas below a $\sqrt{\omega}$ of about 0.4, experimental results show a good regularity that can be reproduced by Eq. 3. The rate constant at infinite

$$\log \vec{k}_2 = -1.77 - \frac{3.09\sqrt{\omega}}{1+1.36\sqrt{\omega}} \qquad (3)$$

dilution at 45°C was evaluated to be 1.7×10^{-2} l. mol^{-1} min^{-1}.

The results obtained at 30, 35, 40, 45 and 52°C ($\omega=0.52\pm0.01$) give a good Arrhenius plot (see Fig. 4), leading to the value of 24.6 kcal. mol^{-1} for the experimental activation energy, and 1.2×10^{14} l. mol^{-1} min^{-1} for the frequency factor.

Aquation of Chloropentamminechromium (III) Ion.—In order to obtain more correct rate constants of anation reaction 1 it is necessary to take the rate of the aquation[9] into account. Accordingly we were obliged to determine the rate of aquation of chloropentamminechromium(III) ion under various conditions. The results obtained are summarized in Table III.

The influence of ionic strength on the aquation is quite different from that on the anation reaction. In lower ionic strength region, the reaction rate rather increases with increasing ionic strength; then the rate decreases gradually and the gradient of the relation is steepest about $\omega=0.4$, and after that the decrease in rate becomes gradual again. It was observed that the aquation rate was independent of perchloric acid concentration from

TABLE III. RATE CONSTANTS OF AQUATION REACTION OF $[Cr(NH_3)_5Cl]^{2+}$

Temp., °C	$[HClO_4]$, mol./l.	Ionic strength, ω	$\overleftarrow{k}_A\times10^3$, min^{-1}
25			0.58*
26.2	0.00086	0.002	0.589
26.2	0.086	0.087	0.598
35	0.00086	0.002	1.91
35	0.0086	0.009	1.94
35			1.9*
45	0.00086	0.002	5.41
45	0.00082	0.089	5.45
45	0.001	0.263	5.32
45	0.001	0.502	4.67
45	0.00086	0.912	4.31
53.2	0.001	0.002	14.3

* Taken from Ref. 9.

9) Freundlich et al. had studied this aquation, but their data were not sufficient to use for this purpose; H. Freundlich and H. Pape, *Z. physik. Chem.*, **86**, 458 (1914).

10^{-4} M to 10^{-1} M. The experimental activation energy and the frequency factor calculated from the temperature dependence of aquation rate were 22.8 kcal. mol^{-1} and 2.6×10^{13} min^{-1}, respectively. When the transmission coefficient is assumed to be unity, the activation entropy is calculated as -7 e. u.

Discussion

It is shown in Fig. 1 that the absorbancy of aquopentamminechromium(III) ion changes markedly with the concentration of chloride ion. The formation of outer sphere association complex, $[Cr(NH_3)_5\cdot OH_2]^{3+}\cdot Cl^-$, ought to be thought for the reason of this absorbancy change, as was indicated by Linhard[6] in the case of hexamminechromium(III) ion and chloride ion.

The anation reaction 1 is experimentally shown to be of second order and the rate constant varies with the ionic strength of solution as is reproduced by the Brönsted-Bjerrum-Christiansen type Eq. 3[6b], which is the kinetic equivalent of the Debye-Hückel equation. The slope of the line in Fig. 3 is -3.09 at infinite dilution. This value is in good agreement with what is expected from a term $2Az_+z_-$[10] in the Debye-Hückel equation. But it can not be concluded that the anation is a bimolecular reaction. Because these results may also be explained by the following unimolecular path through the outer sphere association complex.

$$[Cr(NH_3)_5OH_2]^{3+}+Cl^- \rightarrow [Cr(NH_3)_5OH_2]^{3+}\cdot Cl^- \quad \text{(fast)}$$

$$[Cr(NH_3)_5OH_2]^{3+}\cdot Cl^- \rightarrow [Cr(NH_3)_5Cl]^{2+}+H_2O \quad \text{(slow)}$$

The formation constant of the outer sphere association complex is about 10^2 under these experimental conditions[11], therefore, a considerable amount of association complex exists in solution. If the reaction proceeds through such an outer sphere association complex, the rate-determining step is not the process of bimolecular association, but the following unimolecular process in which central chromium(III) ion releases a coordinated water molecule.

It is noteworthy that the reaction rate varies regularly according to the Debye-Hückel equation in spite of the considerable formation of the association complex. Moreover, its formation is also found to vary roughly according to the Debye-Hückel equation[11]. These facts indicate that the path through a simple five coordinated intermediate is less probable. In other words, the outer sphere association complex releases its coordinated water molecule more easily than the free complex ion. In the water exchange of hexaquochromium(III) complex ion, Plane et al.[12] have found that various anions speed up the reaction. The fact is also explicable by assuming a higher lability of outer sphere association complex. On the other hand, the results of anation reaction for cobalt(III) complex ion obtained by Garrick[1] seem rather extraordinary from the viewpoint of a gradual slope as is shown in Fig. 3, which is about -1. This gradualness may be explained by assuming an inert association complex and the contribution of another path which has a simple five coordinated intermediate[13] in this case.

The effect of ionic environment on the aquation of chloropentamminechromium (III) ion is quite different from that on the anation reaction. The Brönsted-Bjerrum equation predicts a linear dependence of $\log \overleftarrow{k}_A$ ($\overleftarrow{k}_A$ is the rate constant of aquation) upon ionic strength ω[14] when the Hückel's empirical term is taken into account in the expression of activity coefficients. Though only sodium perchlorate and perchloric acid were used to adjust ionic strength, the dependence was not linear even in the lower ionic strength region. It seems that perchlorate ion may also have some specific effects on the aquation.

Summary

The substitution reaction of aquopentamminechromium(III) ion in which a coordinated water molecule is replaced by a chloride ion was investigated spec-

10) A denotes $0.4343\ e^3(2\pi N)^{1/2}/(10\varepsilon kT)^{3/2}$, and approximately equals 0.53 for aqueous solution at 45°C, z_+ and z_- are the ionic charges of reactants.

11) Result presented by the present author at the Symposium on Coordination Compounds, held in Tokyo, November, 1958. The details will appear elsewhere.

12) R. A. Plane and H. Taube, *J. Phys. Chem.*, **56**, 33 (1952); J. P. Hunt and R. A. Plane, *J. Am. Chem. Soc.*, **76**, 5960 (1954).

13) F. Basolo, *Chem. Revs.*, **52**, 459 (1953).

14) S. Glasstone, K. J. Laidler and H. Eyring, "The Theory of Rate Processes", McGraw-Hill Book Co., New York (1941), p. 441.

trophotometrically. The reaction proceeds according to the second order rate law, $d[[Cr(NH_3)_5Cl]^{2+}]/dt = \vec{k}_2[[Cr(NH_3)_5OH_2]^{3+}][Cl^-]$, and the rate constant varies regularly with the ionic strength of solution according to the Debye-Hückel type equation. The formation of outer sphere association complex in the solution was detected from the change in ultraviolet absorption. From these results the rate-determining process of this reaction was inferred to be a unimolecular process through the outer sphere association complex. The experimental activation energy and the frequency factor of this reaction were determined to be 24.6 kcal. mol^{-1} and 1.2×10^{14} l. mol^{-1} min^{-1} ($\omega\sim0.52$), respectively.

The aquation of chloropentamminechromium(III) ion was also studied in the solutions of various ionic strengths and the reaction rate was found to vary to some extent with ionic environment.

The author wishes to thank Professor Y. Inamura for his guidance and encouragement throughout this work. Thanks are also due to Professor I. Tanaka for his kind and helpful advice and to Mr. H. Kobayashi and Mr. Y. Mori for many valuable discussions.

Laboratory of Inorganic Chemistry
Tokyo Institute of Technology
Meguro-ku, Tokyo

Intramolecular Interaction between Hydroxyl Group and π-Electrons. IV[1]. *Rotational Isomers of Alcohols and Shift of ν_{O-H} Absorptions in Phenyl Substituted Alcohols*

By Michinori ŌKI and Hiizu IWAMURA

(Received February 16, 1959)

The authors have found[2] an unsymmetric ν_{O-H} absorption band for 10-undecen-1-ol in the course of the investigation of the intramolecular interaction between the hydroxyl group and π-electrons of an isolated double bond. But the origin of the second minor band, obtained by dividing the band on the assumption that the unsymmetric band is an overlap of two symmetric bands which can be expressed by the Lorentz function, has been unknown. The present author expected that saturated aliphatic alcohols, such as ethanol, may also possess two ν_{O-H} absorptions as 10-undecen-1-ol does in spite of the improbable internal interaction. This has been found to be true.

Experimental

Measurement and Calculation.—They were carried out similarly as described previously[2].

Materials.—The materials, all being known compounds, were purified as stated in the literature. Their physical constants agreed with those reported.

Results aud Discussion

The apparent curves for methanol, ethanol, isopropyl alcohol and *tert*-butyl alcohol are given in Fig. 1. The ν_{O-H} absorption is one of the best explored and

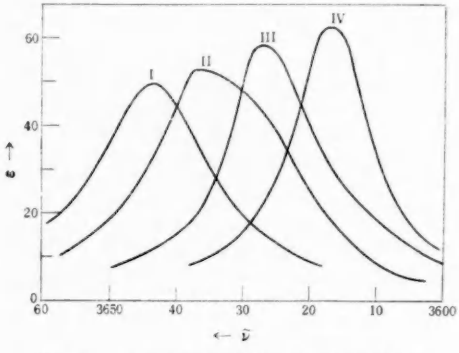

Fig. 1. ν_{O-H} Absorptions of methanol(I), ethanol(II), isopropyl alcohol(III) and *tert*-butyl alcohol(IV).

1) Part III of this series: M. Ōki and H. Iwamura, This Bulletin, **32**, 306 (1959).
2) M. Ōki and H. Iwamura, ibid., **32**, 567 (1959).

it is accepted that the wave number where the absorption maximum appears shifts to the lower side as the alcohol varies from primary to secondary and then to tertiary. The results obtained agree with the above rule, except that ethanol and isopropyl alcohol possess unsymmetric bands which were found with high resolvability of the grating spectrophotometer. The unsymmetric band is divided into two symmetric bands, on the assumption that the unsymmetric curve is an overlap of the two symmetric ones which obey the Lorentz function. The results are given in Table I with those of other aliphatic alcohols.

TABLE I. ν_{O-H} ABSORPTION OF ALIPHATIC ALCOHOLS

R	Band	ν_{max} (cm^{-1})	$\Delta\nu^{e}_{1/2}$ (cm^{-1})	$A\times10^{-3}$ ($mol^{-1}\cdot l.\cdot cm^{-1}$)	A_I/A_{II}
Primary alcohols (RCH_2OH)					
H		3643.8	22.2	3.99	—
CH_3	I	3637.3	18.2	2.80	1.8
	II	3627	19	1.6	
C_2H_5	I	3639.7	19.5	3.36	2.6
	II	3626	18	1.3	
$C_2H_5CH_2$	I	3639.3	17.6	2.81	2.2
	II	3627	20	1.3	
$(CH_3)_2CH$	I	3641.5	17.9	3.61	2.0
	II	3628	22	1.8	
$(CH_3)_3C$	I	3642.0	20.7	4.83	6.0
	II	3632	18	0.8	
Secondary alcohols (RCH_3CHOH)					
CH_3	I	3627.1	13.8	2.42	1.7
	II	3617	26	1.4	
C_2H_5	I	3628.8	20.0	3.35	3.3
	II	3615	27	1.0	
$(CH_3)_2CH$	I	3631.6	21.0	3.55	2.2
	II	3618	33	1.6	
$(CH_3)_3C$	I	3635.6	17.4	3.42	2.5
	II	3621	23	1.4	
Tertiary alcohols [$R(CH_3)_2COH$]					
CH_3		3616.9	15.2	3.46	—
C_2H_5		3617.3	20.0	3.46	—

The origin of the second minor peak can not be the formation of the dimer, because Liddel and Becker[3] reported that they observed no dimer band at the concentration of 0.001~0.003 mol./l. at which the present measurement was carried out. Neither can be the origin the hydrogen bonding between the solute and the chlorine atom of carbon tetrachloride, since methanol, tertiary alcohols and phenols always show symmetric bands. Therefore it should be sought elsewhere.

Richards[4], Barrow[5] and Flett[6] tried to explain the shift of the ν_{O-H} absorption maxima, as the alcohol varies from primary to secondary and then to tertiary, on the basis of the mesomeric or inductive effect of the substituent. That is to say, the contribution of the resonance structure $H^-CH_2=O^+-H$ or $H^+CH_2=O^--H$ will increase as the result of stabilization due to the presence of the alkyl groups on the carbon atom to which the hydroxyl group is attached, and the resulting weaker force constants cause the ν_{O-H} absorption to appear at a lower wave number. However, this explanation is not convincing, since it does not explain the presence of the two bands for O-H stretching.

Badger and Bauer[7] found two ν_{O-H} absorptions for the primary alcohols and tried without success to assign them to the rotational isomers, because they failed to observe a doublet for the secondary alcohols. However, the idea of the rotational isomerism is attractive to the present authors, since this is a promising explanation for the existence of the two ν_{O-H} absorptions. Though the energy barrier for the rotational isomers around the O-C axis of the alcohols is estimated to be even lower than that of the rotation around the C-C axis of ethane derivatives, a 0.8 or 0.9 kcal./mol. energy barrier would suffice for the presence of the isomers at room temperature. Barrow[8] estimated the energy barrier 0.8 kcal./mol. for ethanol and Weltner and Pitzer[9] estimated 0.9 kcal./mol. for methanol around the O-C axis by comparison of the values obtained by computation and by observation of heat capacities and entropies. The energy barrier is also estimated by the microwave method as 1 kcal./mol.[10]

Now, let us consider the rotational isomers of aliphatic alcohols in respect of the O-C axis. In Fig. 2, the isomers are projected through the O-C axis and the oxygen atom is on the upper side. The circle indicates a carbon atom to which the hydroxyl group is attached.

In type I, the hydrogen atom of the hydroxyl group is situated between the two hydrogen atoms which are attached

3) U. Liddel and E. D. Becker, *Spectrochim. Acta*, **10**, 70 (1957).

4) R. E. Richards, *Trans. Faraday Soc.*, **44**, 40 (1948).
5) G. M. Barrow, *J. Phys. Chem.*, **59**, 1129 (1955).
6) M. St. C. Flett, *Spectrochim. Acta*, **10**, 21 (1957).
7) R. M. Badger and S. H. Bauer, *J. Chem. Phys.*, **4**, 711 (1936).
8) G. N. Barrow, ibid., **20**, 1739 (1952).
9) W. Weltner and K. S. Pitzer, *J. Am. Chem. Soc.*, **73**, 2606 (1951).
10) E. V. Ivash and D. M. Dennison, *J. Chem. Phys.*, **21**, 1804 (1953).

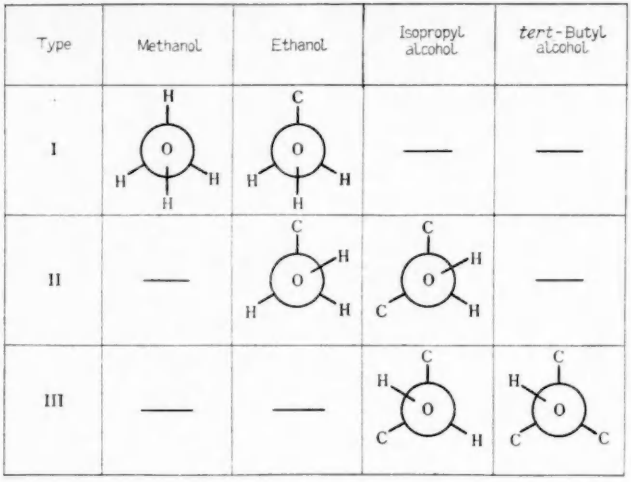

Fig. 2.

to the next carbon atom; in type II, between carbon and hydrogen atoms; and in type III, between two carbon atoms. Then, it is quite understandable that methanol and *tert*-butyl alcohol have single symmetric bands because they have only one rotational isomer and that also ethanol, higher primary alcohols and secondary alcohols have two bands which form an apparently unsymmetric band because they have two rotational isomers.

It is also expected from the above models that the force field will be almost the same in type I, irrespective of the other part of the molecules, and the same situation is also expected for type II or III. Therefore, the type of the rotational isomers of the alcohols determines the wave number where the ν_{O-H} band appears. This turned out to be really the case. The ν_{O-H} absorption of type I appears at about 3640 cm^{-1}, that of type II at about 3626 cm^{-1} and that of type III at about 3617 cm^{-1} irrespective of the nature of the alcohols. The main peak for the primary alcohols comes from type I and that for the secondary alcohols comes from type II.

The reason for such assignment is as follows. When Table I is examined, it is obvious that primary alcohols possess the property of methanol to some extent, because they show one of the ν_{O-H} bands at about 3640 cm^{-1}. Thus the absorption at ca. 3640 cm^{-1} is assigned to type I. Comparison of the absorptions of secondary alcohols with those of tertiary alcohols in a similar way indicates that the band at about 3617 cm^{-1} must be assigned to type III. The remaining band at about 3626 cm^{-1} is assigned to type II.

The probability of type I for primary alcohols is considered one third and that of type II two thirds. Although such expectation does not agree with the results obtained with the primary alcohols, it does agree with those for the secondary alcohols. One of the possibilities which may explain this phenomenon is repulsion between the hydrogen atom of the hydroxyl group and the alkyl group attached to the alpha carbon. In order to clarify this point, a bulky substituent, such as isopropyl or *tert*-butyl group, is introduced to the primary or secondary alcohols. As to the integrated intensities, the steric effect of the substituent is clearly observed in the primary alcohols but not in the secondary alcohols; since the integrated intensity the ν_{O-H} band, affected by the steric environment, is the minor one in the former, while, in the latter both types are affected as far as the present compounds are concerned. The error included in dividing the unsymmetric band may not allow the drawing of a clear-cut conclusion, but it is still clear that the most stable point for the hydrogen atom of the hydroxyl group is pushed toward the hydrogen rather than the bulky group because of the steric effect and consequently the wave number at which ν_{O-H} absorption appears is heightened. Thus the main peak for *tert*-butylmethylcarbinol

appears very close to the main peak of the primary alcohols (type I). The same phenomenon is also observed in the primary alcohols, but in this case the more outstanding feature is the increase of the ratio of the integrated intensity of type I to that of type II. In other words, in neopentyl alcohol, A_I/A_{II} increased to 6.0 from about 2.0 for the other primary alcohols and the increase in the integrated intensity of type I must be attributed to the greater number of the molecules due to the steric requirement.

Thus, it is now evident that the second minor peaks of ν_{O-H} absorption found in 4-penten-1-ol, 5-hexen-1-ol and 10-undecen-1-ol[2] do not represent the intramolecular interaction between the hydroxyl group and the π-electrons of the double bond, but are attributable to the existence of the two rotational isomers which can be represented by types I and II.

It is expected from the above results that the idea of rotational isomerism will be applicable to the phenyl substituted alcohols and therefore the authors have extended their work to benzyl alcohol and its derivatives. The results are shown in Table II.

TABLE II. ν_{O-H} ABSORPTION OF PHENYLCARBINOLS

Compounds	Band	ν_{max} (cm^{-1})	$\Delta\nu^{\circ}_{1/2}$ (cm^{-1})	$A\times10^{-3}$ ($mol^{-1}\cdot l.\cdot cm^{-2}$)
$C_6H_5CH_2OH$	I	3636.3	24.0	2.52
	II	3617.1	17.0	4.26
$C_6H_5CH(CH_3)OH$	I	3627.0	21.0	1.15
	II	3616.0	16.3	4.32
$C_6H_5C(CH_3)_2OH$	I	3620.6	15.4	1.61
	II	3607.1	15.0	3.43
$C_6H_5C(C_2H_5)_2OH$	I	3618.2	17.8	3.49
	II	3608.2	19.0	1.38
$(C_6H_5)_2CHOH$	I	3619.0	15.6	4.92
	II	3609.8	21.4	2.40
$(C_6H_5)_2C(CH_3)OH$	I	3613.0	14.8	4.26
	II	3608.0	20.0	1.85
$(C_6H_5)_2C[CH(CH_3)_2]OH$	I	3617.3	13.2	4.39
	II	3609.7	13.0	0.89
$(C_6H_5)_3COH$		3610.7	15.6	5.95

Ethylmethylphenylcarbinol and ethyldiphenylcarbinol are not included in Table II, because they show a nearly symmetric band which may be an overlap of two similar symmetric bands and can not be divided by the present technique.

It has long been in question why benzyl alcohol and allyl alcohol show an absorption band at about 3620 cm^{-1} in spite of the fact that they are primary alcohols, the only observation of the two bands for benzyl alcohol having been made by Fox and Martin[11]. Quite recently Schleyer, Trifan and Bacskai[12] also reported the existence of the two bands for the O–H stretching absorption of allyl and benzyl alcohols, their results being in good agreement with the present ones. Although the present authors as well as Schleyer et al. attributed the band at 3619 cm^{-1} to the intramolecular interaction between the hydroxyl group and π-electrons, it now seems probably correct to introduce the concept of rotational isomers involving the interaction mentioned above for the explanation of the phenomenon, because type IV shows the absorption band at 3636 cm^{-1} where the normal primary alcohols do, type V at 3618 cm^{-1} and type VI at 3610 cm^{-1}.

The fairly large shifts (7~8 cm^{-1}) between types II and V and between types III and IV are most conveniently explained by introducing the concept of neutralization or the intramolecular interaction between the hydroxyl group and the π-electrons. That is, when a π-electron exists at the β-carbon atom of the alcohol, the interaction takes place and the extension of the O–H bond length occures. Thus the force constant is weakened and the weaker force constant gives rise to the shift of the absorption maximum toward the lower wave number.

Then the rotational isomers represented in Fig. 3 must be somewhat different from those in Fig. 2. In benzyl alcohol it is understood that the hydrogen atom of the hydroxyl group is not in the midst of the two atoms attached to the α-carbon, different from the cases of aliphatic alcohols, but is located closely to the carbon atom which possesses a π-electron. But the O–H bond can not be *cis* in respect of the C_{Ph}–C_α bond; since, if it were, there should not be any difference between types V and VI or between benzhydrol and triphenylcarbinol. The intramolecular interaction in allyl alcohol may be of this type, because its interacted form shows an absorption band at 3619.4 cm^{-1}.

It is also noticed that the band intensity of type V is greater than that of type IV in benzyl alcohol in contrast with the reverse in the primary aliphatic alcohols. This fact can be attributed to greater stabilization of type V in benzyl alcohol

11) J. J. Fox and A. E. Martin, *Trans. Faraday Soc.*, **36**, 897 (1940).
12) P. von R. Schleyer, D. S. Trifan and R. Bacskai, *J. Am. Chem. Soc.*, **80**, 6691 (1958).

Type	Benzyl alcohol	Benzhyolrol	Triphenylcarbinol
IV	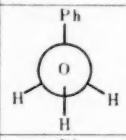	—	—
V	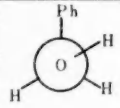	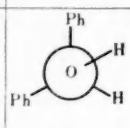	—
VI	—	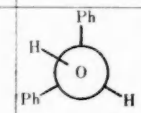	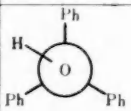

Fig. 3.

than of type IV in aliphatic alcohols because of the intermolecular interaction.

The only unknown ν_{O-H} absorption for the rotational isomers in the alcohols now is the one which should be assigned to the type in which the hydrogen atom of the hydroxyl group is situated between the aromatic carbon and the aliphatic carbon (type VII). The example is provided by alkyldiphenylcarbinols. The absorption at 3617 cm^{-1} is assigned to this, since the other absorption at 3609 cm^{-1} has been assigned to type VI.

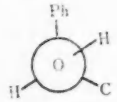

Fig. 4.

Theoretically, it is expected that alkylphenylcarbinols exhibit three ν_{O-H} absorptions, because they have the possibility of taking three types represented by II, V and VII. However, the ν_{O-H} absorptions of the types V and VII are so closely located that it is impossible to resolve them and consequently only two bands are observed for type II and for a mixture of types V and VII with methylphenylcarbinol.

There are some exceptions which are represented by dialkylphenylcarbinols. In these cases, the absorptions occur at 3620 cm^{-1} and at 3607 cm^{-1}, the latter being in the same position as type VI. However, the steric interference between the two alkyl groups and the ortho hydrogen atoms of the benzene nucleus causes the different situation from the others and the case is more complicated. The authors tentatively attribute this abnormality to the internal rotation around the C_{Ph}–C_{α} axis which is forced by the environment. Although the shift in wave number may be too great to assign the bands in an analogous way, it may still be valid that type VII of dialkylphenylcarbinol shows an absorption band at a lower wave number than type III because of the lowered force constant. Thus, the band at 3608 cm^{-1} is tentatively assigned to type VII and that at 3620 cm^{-1} to type III.

Summary

The authors observed symmetric ν_{O-H} absorptions for methanol and tertiary alcohols and unsymmetric bands for primary and secondary alcohols. The unsymmetric band was divided into two bands, assuming that the band is an overlap of the two symmetric bands. The idea of the rotational isomerism was successfully introduced for assigning the band and the following points were concluded.

1) Types I and IV show absorption bands at 3644~3636 cm^{-1}, type II at 3626~3629 cm^{-1}, type III at 3615~3618 cm^{-1}, type V at 3616~3619 cm^{-1}, type VI at 3608~3611 cm^{-1}, and type VII at 3613~3617 cm^{-1}.

2) The exception is dialkylphenylcarbinols which show the ν_{O-H} absorptions at about 3620 cm^{-1} and 3608 cm^{-1}, the former being assigned to type III and the latter to type VII. This ruling-out may be

attributed to the steric effect and the rotation around the C_{Ph}–C_{α} axis.

The steric effect on the integrated intensities and on the wave number where ν_{O-H} absorption falls is also discussed. The differences between types II and IV and between types III and VI were attributed to the existence of the intramolecular interaction between the hydroxyl group and π-electrons of the benzene nucleus. The same reason may cause allyl alcohol to show its main ν_{O-H} absorption at about 3620 cm^{-1}.

The authors are indebted to Professor Y. Urushibara and Professor T. Shimanouchi for their valuable suggestions and discussions. The authors also wish to express their hearty thanks to the Ministry of Education for the Grant in Aid for Fundamental Scientific Research.

Department of Chemistry
Faculty of Science
The University of Tokyo
Hongo, Tokyo

Intramolecular Interaction between Hydroxyl Group and π-Eelctrons. V[1]. *Electronic Effect in Arylcarbinols and a Preliminary Note on the Interaction in Benzylaniline Derivatives*

By Michinori Ōki and Hiizu Iwamura

(Received March 17, 1959)

It has long been in question why absorption due to the O–H stretching vibration of benzyl alcohol or allyl alcohol appears at about 3620 cm^{-1}. However, from the standpoint of the rotational isomerism, the interaction between the hydroxyl group and the π-electrons will be a valuable explanation for the phenomenon, as suggested in the previous paper[1]. If the interaction is the real cause of the shift of the ν_{O-H} absorption, it is expected that the electron density of the carbon atom (C_1) to which the hydroxymethyl group is attached or the next (C_2) to it should have profound effect on the ν_{O-H} absorptions of arylcarbinols. Hence, fourteen meta- and para-substituted benzyl alcohols were prepared and their ν_{O-H} absorptions were determined with a grating spectrophotometer. Ortho-substituted benzyl alcohols are excluded because formation of the internal hydrogen bonding can not be avoided when an atom with a lone pair of electrons is involved.

Experimental

Measurement and Calculation.—They were carried out similarly as reported previously[2].

Materials.—The materials used for the measurement are known compounds, unless otherwise stated. Their physical constants agreed with those in the literature.

m-Cyanobenzyl alcohol.—It was prepared according to the procedure reported by Langguth[3]. Although he reported the compound as an oil, it boiled at 127~127.5°C/3 mm. and solidified to form colorless needles on standing. The melting point is 28~29°C.

m-Phenylbenzyl alcohol.—It was prepared by the lithium aluminum hydride reduction of *m*-phenylbenzoic acid. Although this compound has been reported[4] as syrup, it formed colorless needles, m. p. 55~55.5°C, on recrystallization from carbon tetrachloride—petroleum ether.

Anal. Found: C, 84.70; H, 6.59. Calcd. for $C_{13}H_{12}O$: C, 84.75; H, 6.57%.

m-Benzyloxybenzaldehyde.—To a sodium ethoxide solution prepared from 5.5 g. (0.24 atom) of sodium and 150 ml. of alcohol was added 24.4 g. (0.2 mol.) of *m*-hydroxybenzaldehyde followed by 27.8 g. (0.22 mol.) of benzyl chloride. The mixture was heated under reflux for five hours, cooled and filtered to remove insoluble materials. Evaporation of the solvent gave crystals which were recrystallized to colorless small plates, m. p. 52~53°C, from petroleum ether. Yield, 32.5 g. (82%).

Anal. Found: C, 79.29; H, 5.81. Calcd. for $C_{14}H_{12}O_2$: C, 79.22; H, 5.70%.

m-Benzyloxybenzyl alcohol.—To a slurry prepared from 1.5 g. (0.04 mol.) of lithium aluminum

1) Part IV: M. Ōki and H. Iwamura, This Bulletin, **32**, 950 (1959).
2) M. Ōki and H. Iwamura, ibid., **32**, 567 (1959).
3) St. Langguth, *Ber.*, **38**, 2062 (1905).
4) M. P. Adam, *Ann. Chim. Phys.*, **15**, 245 (1888).

hydride and 50 ml. of ether was gradually added 19.6 g. (0.1 mol.) of *m*-benzyloxybenzaldehyde in 50 ml. of ether and the mixture was stirred at room temperature for two hours. The excessive lithium aluminum hydride was decomposed by adding ethyl acetate in ether and finally the mixture was treated with dilute sulfuric acid. The aqueous layer was extracted with ether and the ethereal extract was washed with aqueous sodium hydroxide and dried over potassium carbonate. Fractional distillation furnished a colorless oil boiling at 160°C/3 mm. which solidified. Recrystallization from benzene-petroleum ether (3 : 7) gave the substance in colorless needles, m. p. 44.5~45°C. Yield, 16.0 g. (81%).

Anal. Found: C, 78.54; H, 6.70. Calcd. for $C_{14}H_{14}O_2$: C, 78.48; H, 6.59%.

N-(p-Methoxybenzyl)-p-anisidine. — A mixture of 3.0 g. of *N*-(*p*-methoxybenzylidene)-*p*-anisidine, 1 g. of Raney nickel T-4 catalyst[5] and 100 ml. of alcohol was stirred in an autoclave at 80~100°C with 100 kg./cm² initial pressure. The heating was discontinued after two hours and, after cooling, the catalyst was removed by filtration. Evaporation of the solvent afforded a crystalline residue which was recrystallized from petroleum ether. Colorless plates, m. p. 94.5~95.5°C, were obtained in 1.5 g. (50%) yield. The rather low yield must be attributed to the hydrogenolysis of the *p*-methoxybenzyl group, since the oder of *p*-cresol methyl ether was distinct in the hydrogenation product.

Anal. Found: C, 74.22; H, 7.23. Calcd. for $C_{15}H_{17}NO_2$: C, 74.05; H, 7.04%.

N-p-Methoxybenzylaniline.—It was prepared in an analogous way. Though the melting point of this material was reported as 64.5°C[6], it melted at 46~47°C (colorless plates from petroleum ether). Since the micro-analyses agreed with the calculated values, it seems that this is one of the polymorphs.

Anal. Found: C, 78.99; H, 7.18. Calcd. for $C_{14}H_{15}NO$: C, 78.84; H, 7.09%.

Results and Discussion

The apparent ν_{O-H} absorption curves of *p*-nitrobenzyl alcohol, *m*-cyanobenzyl alcohol, benzyl alcohol and *p*-benzyloxybenzyl alcohol are shown in Fig. 1. The selection was made because the para-nitro group is the most electron-attracting and the para-benzyloxyl group is the most electron-releasing group in respect of Hammett's σ values[7] among the compounds used in the present work and benzyl alcohol is an intermediate. *m*-Cyanobenzyl alcohol is also included because it gives two apparent maxima.

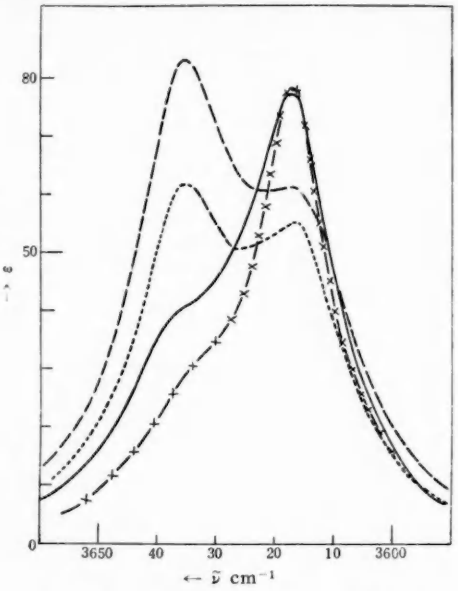

Fig. 1. ν_{O-H} absorption of *p*-nitrobenzyl alcohol (– – –), *m*-cyanobenzyl alcohol (·····), benzyl alcohol ( ) and *p*-benzyloxybenzyl alcohol (—×—).

Introduction of an electron-releasing group such as a benzyloxyl group in the para position in respect of the hydroxymethyl group enhances the intensity of the band at 3617 cm^{-1} and an electron-attracting group such as nitro group in the para position enhances the band at 3636 cm^{-1}. Thus the main peak for the ν_{O-H} absorption of *p*-nitrobenzyl alcohol lies at ca. 3636 cm^{-1}. Splitting of the two bands into the two apparent maxima in *m*-cyanobenzyl alcohol will be a firm proof for the presence of the two ν_{O-H} absorption bands in benzyl alcohol derivatives. The results suggest that the number of molecules which possess internal interaction is greater in the benzyl alcohol with an electron-releasing group and this kind of electronic effect must be caused by the presence of the interaction between the hydroxyl group and the π-electrons, since such enhancement in the band intensities is naturally expected from the assignment suggested in the previous paper[1].

Now, when the internal interaction is taken into account, there are four possibilities in structure as shown in Fig. 2. The figures are presented both as sketches

5) S. Nishimura. This Bulletin, **32**, 61 (1959). The authors are indebted to Dr. Nishimura for preparation of this catalyst.

6) O. F. Steinhart, *Ann.*, **241**, 332 (1887).

7) L. P. Hammentt, "Physical Organic Chemistry", McGraw-Hill Book Co., New York (1940), p. 184. Also see: H. H. Jaffé, *Chem. Revs.*, **53**, 191 (1953).

8) D. S. Trifan, J. L. Weinmann and L. P. Kuhn, *J. Am. Chem. Soc.*, **79**, 6566 (1957).

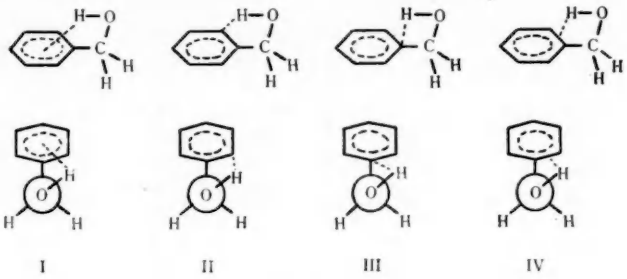

Fig. 2.

and as projections through the O–C axis. The first (I) is the interaction between the hydroxyl group and the aromatic nucleus as a whole and this type of interaction was empirically quoted by Trifan and his co-workers[8] for α-hydroxyethylferrocene. In the second case (II), the direction of the hydrogen atom of the hydroxyl group points to the carbon atom (C_2) or the π-electron on C_2. This type of interaction has not been suggested, but the suggestion by Lüttke and Mecke[9] for 2-hydroxybiphenyl may fall into this category. In the third (III), the hydrogen atom of the hydroxyl group points to C_1 of the benzene nucleus or the π-electron on C_1. This type of interaction was implied by Goldman and Crisler[10] for phenethyl alcohol derivatives. The fourth case (IV) is the interaction in which the hydrogen atom turns toward the midst of C_1 and C_2, and the overlapping π-electrons on C_1 and C_2, take part in the interaction. The last case was suggested by Baker and Shulgin[11] for *o*-allylphenol and *o*-propenylphenol. Structures I and IV are considered as sorts of π-complexes and structures II and III σ-complexes.

Since the above assignments of the structures are all empirical, it is necessary to assign the structure on the basis of the experimental results. Now it can be hoped that the nature of the interaction may be clarified by changing the substituent on the benzene nucleus, because it is known, as mentioned above, that the interaction is markedly affected by the introduction of certain kinds of substituents. The same substituent was introduced into meta and para positions in respect of the hydroxymethyl group, because electron density on C_2 caused by a substituent in the para position should be roughly reproduced[12] on C_2 by introducing the same substituent into the meta position to the hydroxymethyl group.

If the π-complex (I or IV) is the real case, there should not be much difference between the two arylcarbinols which possess the same substituent, since the electron density of the aromatic ring as a whole must be the same and that in the middle of the two carbon atoms (C_1 and C_2) is considered to be nearly the same, although the effect of the substituent may be seen because of the different electron densities. If II is the case and an electron-releasing group is introduced, the meta-substituted benzyl alcohol would have a stronger absorption band at 3617 cm^{-1} than the para-substituted isomer, because the electron density on C_2 is higher in the meta-substituted compound than in the para-substituted one. And if III is the case, the situation must be opposite to that stated in case II and a compound with an electron-releasing group in the para-position to the hydroxymethyl group must have stronger absorption at 3617 cm^{-1} than the meta-substituted one.

The actual absorption curves are divided into two, assuming that the curves are the overlap of two symmetric bands which are expressed by the Lorentz function and the half widths and the integrated intensities are shown together with absorption maxima in Table I.

As is seen from Table I, an electron-releasing group in the para-position to the

9) W. Lüttke and R. Mecke, *Z. Elektrochem.*, **53**, 241 (1949); *Z. physik. Chem.*, **196**, 56 (1950).
10) I. M. Goldman and R. O. Crisler, *J. Org. Chem.*, **23**, 751 (1958).
11) A. W. Baker and A. T. Shulgin, *J. Am. Chem. Soc.*, **80**, 5358 (1958).
12) In addition to the effect given by σ_p, we must consider σ_o because the ortho positions to the hydroxymethyl group correspond to ortho and para positions to a new substituent for meta-substituted benzyl alcohol. Therefore, the electron density on C_1 or C_2 is different, even if the effect of the hydroxymethyl group is neglected.

TABLE I. ν_{O-H} ABSORPTION OF ARYLCARBINOLS (x-$RC_6H_4CH_2OH$)

R	x	OH	ν_{max} (cm^{-1})	$\Delta\nu_{max}$ (cm^{-1})	$\Delta\nu^a_{1/2}$ (cm^{-1})	$A\times10^{-3}$ ($mol^{-1}\cdot l.\cdot cm^{-2}$)	A_i/A_f
NO_2	m	i *	3616.3	18.9	20.4	3.70	0.84
		f **	3635.2		18.8	4.41	
	p	i	3616.0	19.5	23.6	3.98	0.77
		f	3635.5		20.0	5.15	
CN	m	i	3616.2	19.2	19.0	2.98	0.75
		f	3635.4		20.8	3.98	
	p	i	3616.4	19.0	19.8	3.49	0.71
		f	3635.4		20.8	4.93	
Cl	m	i	3617.0	19.4	18.6	3.74	1.30
		f	3636.4		21.4	2.88	
	p	i	3617.1	18.2	17.6	3.56	1.38
		f	3635.3		21.2	2.58	
C_6H_5	m	i	3616.6	19.6	16.6	4.17	1.92
		f	3636.2		21.6	2.18	
	p	i	3617.0	19.4	15.4	3.92	1.88
		f	3636.4		20.4	2.08	
H***		i	3617.1	19.2	17.0	4.26	1.69
		f	3636.3		24.0	2.59	
CH_3	m	i	3616.7	20.1	16.6	4.18	1.85
		f	3636.8		22.6	2.26	
	p	i	3617.4	18.4	15.6	3.67	2.02
		f	3635.8		24.2	1.82	
CH_3O	m	i	3616.9	19.3	16.6	4.04	1.69
		f	3636.2		25.6	2.40	
	p	i	3617.1	18.9	16.4	4.33	2.48
		f	3636.0		27.8	1.75	
$C_6H_5CH_2O$	m	i	3616.1	20.4	16.6	4.32	2.11
		f	3636.5		20.0	2.05	
	p	i	3617.0	18.2	15.0	3.89	2.70
		f	3635.2		20.0	1.44	

* i: denotes interacted form of the hydroxyl group.
** f: denotes free form of the hydroxyl group.
*** Taken from reference 1.

hydroxymethyl group enhances the intensity of the band at 3617 cm^{-1} more than one in the meta position and the tendency is opposite when an electron-attracting group is introduced. This fact excludes the possibility of structure I, II or IV. Hence it is concluded that the interaction between the hydroxyl group and the π-electrons of the aromatic nucleus in benzyl alcohol is of the type expressed by structure III.

The consistency of the wave number (3615.9~3617.4 cm^{-1} and 3635.2~3636.8 cm^{-1}) at which two absorption maxima exist is another proof that the origin of the bands is the rotational isomers, because in phenethyl alcohol derivatives the shift of the wave number, where an absorption of the interacted form appears, is observed[13].

The sum of the integrated intensities of the two bands is not always constant and there is a tendency that a more electron-attracting group gives rise to greater integrated intensity, as has been observed in substituted phenols[14]. However, when $\log \frac{A_i/A_f}{(A_i/A_f)_0}$, where A_i is the integrated intensity of the absorption band due to the interacted form, A_f that of free form and $(A_i/A_f)_0$ is the ratio given by benzyl alcohol, is taken into consideration, this value would represent the equilibrium constant and is in linear relation with

13) See the following paper.
14) P. J. Stone and H. W. Thompson, *Spectrochim. Acta*, **10**, 17 (1957).

TABLE II. ν_{N-H} ABSORPTION OF *N*-ARYLMETHYLARYLAMINES (p-$XC_6H_4CH_2NHC_6H_4$-Y-p)

X	Y	N-H	ν_{max} (cm^{-1})	$\Delta\nu^{e}_{1/2}$ (cm^{-1})	$A\times10^{-3}$ ($mol^{-1}\cdot l.\cdot cm^{-2}$)	$\Delta\nu_{max}$ (cm^{-1})
H	H	I	3417.4	28.0	2.24	32.8
		II	3450.2	25.6	2.11	
CH_3O	H	I	3418.0	26.8	2.63	32.1
		II	3450.1	23.7	1.73	
H	CH_3O	I	3405.6	35.8	1.93	37.1
		II	3442.7	30.2	1.74	
CH_3O	CH_3O	I	3406.6	35.3	2.03	36.2
		II	3442.8	29.6	1.30	

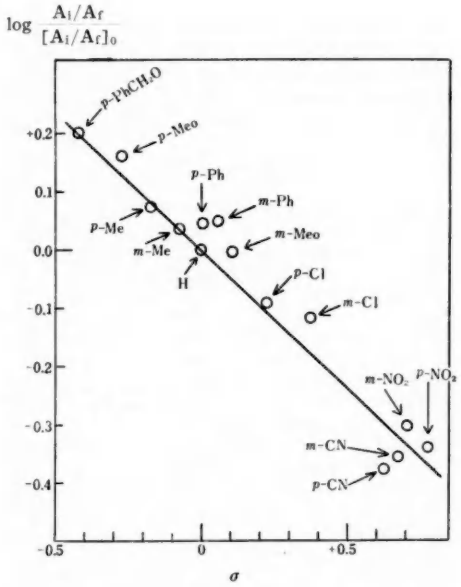

Fig. 3.

Hammett's σ values (Fig. 3). This linear relationship result is again a strong support to the idea of the existence of structure III. Although σ value for the *m*-benzyloxyl group has been unknown, it is now estimated from Fig. 2, by pointing 2.11 on the straight line and projecting to the σ axis, as -0.204.

A similar situation is expected for benzylaniline derivatives, which showed two distinct maxima for N-H stretching 30~40 cm^{-1} apart. The data are given in Table II.

It is understood from Table II, 1) that higher electron density on the benzene nucleus enhances the N-H stretching band at lower wave number, 2) that ν_{N-H} absorption shifts to lower wave number as Colichman & Liu[15] and also Krueger & Thompson[16] have pointed out for the arylamines, and 3) that $\Delta\nu_{max}$ is greater when the basicity of the arylamine increases. The full discussion will be presented in the near future.

Summary

Absorption due to the O-H stretching vibration in the fundamental region was measured with fourteen benzyl alcohol derivatives to see the electronic effect of the substituent on the interaction between the hydroxyl group and the π-electrons and the following conclusions are deduced.

1) The nature of the interaction or the structure of the molecule which gives rise to the ν_{O-H} absorption at 3617 cm^{-1} is discussed and the interaction between the hydroxyl group and the π-electron on the carbon atom to which hydroxymethyl group is attached (structure III) is favored.

2) The consistency of the wave numbers at which two ν_{O-H} absorptions appear, gives further support to the idea that these absorptions originate in the existence of the two rotational isomers.

3) $\mathrm{Log}\dfrac{A_i/A_f}{(A_i/A_f)_0}$ is in linear relation with Hammett's σ values and the σ value of the *m*-benzyloxyl group is estimated as -0.204.

A similar phenomenon is also observed in the substituted benzylanilines.

The authors are indebted to Professor Y. Urushibara and Professor T. Shimanouchi for their valuable advice and encouragement throughout this work, and their thanks are also due to the Ministry of Education for a Grant in Aid for the Fundamental Scientific Research.

Department of Chemistry
Faculty of Science
The University of Tokyo
Hongo, Tokyo

15) E. L. Colichman and S. K. Liu, *J. Am. Chem. Soc.*, **76**, 913 (1954).

16) P. J. Krueger and H. W. Thompson, *Proc. Roy. Soc.*, **A243**, 143 (1957).

Resonance Effect in Hammett Relationship. I. The Substituent Effect in the Acid Catalyzed Decompositions of ω-Diazoacetophenones in Acetic Acid

By Yuho TSUNO, Toshikazu IBATA and Yasuhide YUKAWA

(Received January 28, 1959)

As reported in a previous paper, the Curtius rearrangement of substituted benzazides in toluene did not give a linear Hammett relationship[1], whereas, the decomposition catalyzed by sulfuric acid[2] showed an approximately linear one, which had the negative ρ value. In such an electrophilic reaction, as has been pointed out frequently[3-7], electron releasing para substituents would favor the rate to a greater extent than would be expected from the normal Hammett constants. The same may be anticipated in this reaction. *p*-Hydroxyl and *p*-methoxyl groups indicated the tendency of some higher acceleration, but the scatters of the other groups, especially *p*-nitro group, made it impossible to ascertain this trend. The detailed re-examination as never improved the result. The acid catalyzed solvolytic decomposition of ω-diazoacetophenones is an electrophilic reaction of similar type. Hence, one might anticipate that para substituted derivatives probably show a similar behavior to what is seen in other electrophilic reactions. Furthermore, the rate changes of this reaction might suggest the contribution of substituents at least in such a reaction of which the substituent effects are transmitted through a carbonyl group to an electron deficient reaction center. Lane and coworkers[8], in their study of the substituent effect of this reaction, reported that the rate fitted the Hammett equation, whereas the effect of strongly electron releasing groups has not been reported. Therefore, kinetic study of decomposition of various substituted ω-diazoacetophenones was carried out in acetic acid, and the results are discussed on the basis of the Hammett relationship.

1) Y. Yukawa and Y. Tsuno, *J. Am. Chem. Soc.*, **79**, 5530 (1957).
2) Y. Yukawa and Y. Tsuno, ibid., **81**, 2007 (1959).
3) C. G. Swain and W. P. Langsdorf, Jr., ibid., **73**, 2813 (1951).
4) J. K. Kochi and G. S. Hammond, ibid., **75**, 3445 (1953).
5) (a) N. C. Deno and A. Schriesheim, ibid., **77**, 3051 (1955); (b) N. C. Deno and W. L. Evans, ibid., **79**, 5804 (1957).
6) H. C. Brown and Y. Okamoto, ibid., **79**, 1913 (1957); Y. Okamoto and H. C. Brown, *J. Org. Chem.*, **22**, 485 (1957).
7) J. Miller, *Australian J. Chem.*, **9**, 61 (1956).
8) J. F. Lane and R. L. Feller, *J. Am. Chem. Soc.*, **73**, 4230 (1951).

Experimental

Materials. — Substituted and unsubstituted diazoacetophenones used in this investigation were prepared by the usual procedure[8,9]; all benzoyl chlorides reacted satisfactorily with an excess of diazomethane in ethereal solution with cooling. After this solution was allowed to stand overnight at room temperature, the solvent was removed in vacuo and the residue was collected. Several recrystallizations from ligroin or benzene solution gave pale yellow crystals. The melting points of the diazoketones thus obtained are listed in Table I, together with the boiling points of the starting benzoyl chlorides.

Solvent. — Acetic acid was purified by the same method as that described in a previous paper[2]; b. p. 117.5~118.0°C.

Kinetic Experiments.—The rates of decompositions were determined in 75 ml. of anhydrous acetic acid at 40.00±0.01°C, by collecting the evolved nitrogen by an azotometer. The procedure and the apparatus were the same as those described in several recent papers[1,2,8]. The solution was not stirred but powdered glass was added to the solution in order to prevent the supersaturation of nitrogen gas evolved. In each run, the initial concentration of diazoketone was about 1/200 mol. Volume readings were taken covering the extent of 75% completion of reaction. The infinity reading was determined at the time after a period of 9—10 times as much as the half life of the reaction. The measurements were repeated at least three times for respective diazoketones in order to minimize the experimental error. The total volume of nitrogen collected was close to the theoretical amount. The change in the initial concentration did not show any effect on the rate.

Reaction Product. — The reaction solution was allowed to remain at 40.00°C in a bath until no further evolution of nitrogen occurred, and then the solvent was removed in vacuo. The

9) W. E. Bachmann and W. S. Struve, "Organic Reactions", Vol. 1, John Wiley & Sons, Inc., New York (1942), p. 38.

TABLE I. ω-DIAZOACETOPHENONES, BENZOYL CHLORIDES AND THE DECOMPOSITION PRODUCTS

Subst.	Melting point and boiling point[a] (°C)		
	XC_6H_4COCl	$XC_6H_4COCHN_2$	$XC_6H_4COCH_2Ac$
H	(192~192.7)	47.2~ 48.0[b]	48
p-CH_3O	(152~155/20 mm.)	87.5~ 88.5[c]	57.5~ 58.5
p-C_2H_5O	(161/27 mm.)	80.0~ 80.5[d]	86.0~ 86.8
p-*t*-C_4H_9	(149.9~150.5/14 mm.)	83.5~ 84.0[e]	60.5~ 61.3
p-CH_3	(122/33 mm.)	52.0~ 52.8[b]	84.0~ 85.0
p-C_6H_5	112.5~113.0	119.0~119.5[f]	112.0~112.8
p-Cl	(120~121/28 mm.)	114.0~115.0[b]	68.5~ 69.0
p-Br	(139.0~139.5/33 mm.)	126.0~126.5[b]	85.8~ 86.5
p-NO_2	72.7~73.3	118.0~119.0[b]	122 ~123.5
m-CH_3	(116~117/30 mm.)	64.2~ 64.8[g]	liquid
m-Br	(138.5~139.5/38 mm.)	73.5~ 75.0[h]	liquid
m-NO_2	(169.0/20 mm.)	139.5~140.0[i](decomp.)	48.5~49.0

a) All melting points are corrected. Boiling points which are given in brackets are uncorrected.
b) J. F. Lane et al., Ref. 8.
c) M. S. Newman and P. Beal, III, *J. Am. Chem. Soc.*, **71**, 1506 (1949).
d) *Anal.* Found: C, 63.56; H, 5.35; N, 14.84%.
Calcd. for $C_{10}H_{10}O_2N_2$: C, 63.16; H, 5.31; N, 14.74%.
e) *Anal.* Found: C, 71.33; H, 6.53; N, 14.17%.
Calcd. for $C_{12}H_{14}ON_2$: C, 71.26; H, 6.98; N, 13.85%.
f) C. E. Blades and A. L. Wilds, *J. Org. Chem.*, **21**, 1013 (1956).
g) *Anal.* Found: C, 67.11; H, 5.21; N, 16.21%.
Calcd. for $C_9H_8ON_2$: C, 67.48; H, 5.03; N, 17.49%.
h) *Anal.* Found: C, 43.01; H, 2.34; N, 12.32%.
Calcd. for $C_8H_5ON_2Br$: C, 42.66; H, 2.22; N, 12.44%.
i) *Anal.* Found: C, 51.02; H, 2.84; N, 20.60%.
Calcd. for $C_8H_5O_3N_3$: C, 50.26; H, 2.62; N, 21.99%.

residues were recrystallized several times from ligroin or ethanol solutions. The corresponding phenacyl acetates having sharp melting points were obtained in quantitative yield (Table I). In the case of *m*-CH_3 and *m*-Br derivatives, the residues were not solidified.

Results and Discussion

The evolution of nitrogen followed strictly the first order equation

$$0.4343 \times kt = \log V_\infty - \log(V_\infty - V)$$

where V_∞ is the volume reading at the infinite time and V the readings at time t. Typical runs of the evolution of nitrogen are given graphically in Fig. 1. The rate constants obtained at 40.00°C are listed in Table II. The average deviations less than 0.7% are obtained in respective runs and the reproducibility of the results is estimated to be about 1%. Some of the rate constants obtained in the present study are slightly lower than those obtained by Lane et al.[8] This appears to be attributable to the difference of acetic acid used as solvent or that of the methods evaluating rate constants.

The mechanism of this reaction proposed is possibly represented as follows:

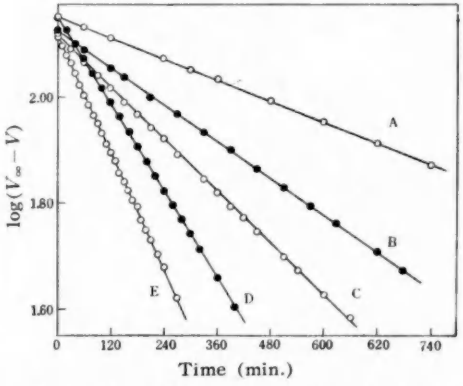

Fig. 1. Typical first order plots for the decomposition of substituted ω-diazoacetophenones in acetic acid at 40.00°C.
A, *m*-NO_2; B, *m*-Br; C, *p*-Cl; D, *m*-CH_3; E, *p*-CH_3.

TABLE II. THE RATE CONSTANTS OF THE DECOMPOSITION OF SUBSTITUTED ω-DIAZOACETOPHENONES IN ACETIC ACID AT 40.00°C

Subst.	$10^3 \times k_1$ a)	Subst.	$10^3 \times k_1$ a)
p-CH_3O	7.76±0.06	*p*-Br	1.91 ±0.02
p-C_2H_5O	7.37±0.07	None	2.74 ±0.02 c)
p-CH_3	4.33±0.04 b)	*m*-CH_3	3.14 ±0.04
p-*t*-C_4H_9	4.12±0.04	*m*-Br	1.32 ±0.02
p-C_6H_5	3.37±0.02	*m*-NO_2	0.744±0.007
p-Cl	1.98±0.01	*p*-NO_2	0.600±0.006

a) Rate in reciprocal minute.
b) Reported 4.88×10^{-3} at 40.05°C by Lane et al., Ref. 8.
c) Reported 2.94×10^{-3}, Ref. 8.

$$C_6H_5COCHN_2 \xrightarrow{H^+} C_6H_5COCH_2N_2^+$$
$$C_6H_5COCH_2N_2^+ + CH_3CO_2^- \rightarrow C_6H_5COCH_2\text{-}OCOCH_3 + N_2$$

the first step is the protonation (presumably reversible process) of diazoketone and the second is the rate determining decomposition of the protonated ketodiazonium ion to the acetate. With regard to the second step, two types of mechanism are possible; one is the unimolecular loss of nitrogen followed by the reaction with solvent of the carbonium ion so produced, another is the bimolecular reaction with solvent or acetate ion. Lane et al. suggested the latter one[8].

It will be of interest to discuss the substituent effects on the basis of the Hammett equation[10]. As is shown clearly in Fig. 2, the plot of $\log k$ against the corresponding Hammett σ-constants fails to give a linear relationship but concaves upward, in contrast to the result by Lane et al.[8] Only with respect to meta substituents and the *p*-nitro group, the linear correlation is obtained. The slope of this correlation line, the ρ_m value, is evaluated using the method of least squares[11] to be −0.830, the probable error of the fit 0.010 in $\log k$ and the correlation coefficient 0.999. On the other hand, the plots of $\log k$ vs. σ for para groups lie substantially above the meta line. The deviations appear to be entirely significant in view of the experimental uncertainty.

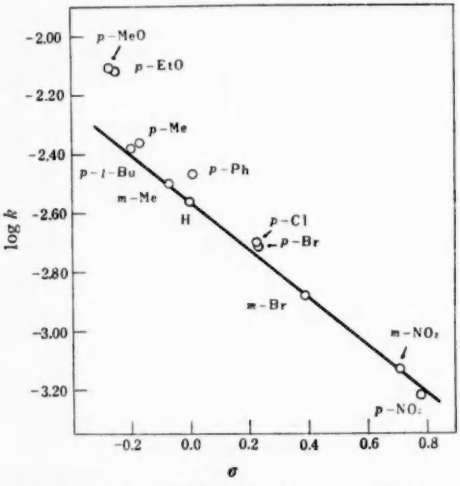

Fig. 2. The Hammett equation applied to the decomposition of ω-diazoacetophenones in acetic acid at 40.00°C.

The above results are not unusual but may be reasonable at least in qualitative consideration. Although the Hammett equation correlates the rates or equilibria of an enormous number of reactions[10,11], some limitations have been noted. One of the limitations is the electrophilic reactions providing the deviations of the plots for electron releasing para substituents such as methoxy, methyl, phenyl and halo groups. In general, these groups show greater electron-release than described by the normal σ-constants in an electrophilic reaction[3-7]. The upward curvature of the plots for these groups is reasonably attributed to differing capacities of the substituents for resonance stabilization of a positively charged transition state. The same considerations as noted above might be employed in the case of the present reaction. If the upward deviations are referred to the resonance capacities, the transition state of this reaction must have a positively charged reaction center, and the charge must be, if possible, delocalized through resonance interaction. This appears to suggest that the driving force of the present reaction may be the elimination of the nitrogen molecule, followed by the attack of acetate ion upon the carbonium ion so produced.

$$C_6H_5\text{-}CO\text{-}CH_2N_2^+ \rightarrow C_6H_5CO\text{-}CH_2^+ + N_2$$
$$\xrightarrow{OAc^-} C_6H_5COCH_2OAc$$

Although this is somewhat inconsistent with Lane's conclusion, this consideration might be reasonable because the decomposition of the diazonium ion into nitrogen and carbonium ion undoubtedly does not

10) L. P. Hammett, *J. Am. Chem. Soc.*, **59**, 96 (1937); "Physical Organic Chemistry", McGraw-Hill Book Co., Inc., New York (1940), p. 194.
11) H. H. Jaffé, *Chem. Revs.*, **53**, 191 (1953).

have high energy requirements[12]. At least the pull factor of the leaving nitrogen may predominate over the push of the attacking species, because of the high stability of the nitrogen molecule. The positive charge so produced at the reaction center would be delocalized through the resonance with powerfully electron releasing aryl groups;

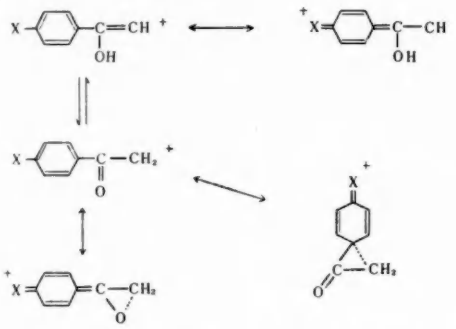

These are consistent with the present data qualitatively. Then, it will be of further interest to treat the deviations in quantitative manner.

The Quantitative Treatment. — The recent advance in this field has prompted us to some attempts to correlate electrophilic reactions with an alternative set of substituent constants. These new substituent constants are denoted by σ^+[13]. Although a number of tentative sets of σ^+ have been proposed by various authors, it is Brown and Okamoto's set[6] that is apparently the most decisive one of general applicability. In Fig. 3 is demonstrated the correlation of present data with Brown and Okamoto's set of σ^+. Least squares treatment[11] indicates that the ρ^+ value, the slope of the regression line, is equal to -0.736 ± 0.0246, the correlation coefficient being 0.994. Brown and Okamoto's set of σ^+ correlates the present data more appropriately than does the normal Hammett constant, whereas it is worthy of remark that all the points for para substituents fall below the ρ_m line to a considerable extent. The ρ^+ value is clearly lower than ρ_m value. This would indicate that the σ^+ values employed for para substituents somewhat overcorrect the present situation. Furthermore, it might possibly be attributed to less availability of the *transition state resonance* of the present reaction than that described on the basis of σ^+. However, this is not surprising, because the contribution of resonance would not always be constant but would vary from reaction to reaction. Such failure of the linear relationship using the set of σ^+ is frequently observed. Some of the examples are provided by the solvolysis of neophyl brosylates[14] in which the resonance effect is less effective than described by Brown and Okamoto's σ^+ values, and the brominolysis of benzeneboronic acids[15] in which the contribution of *transition state resonance* appears greater

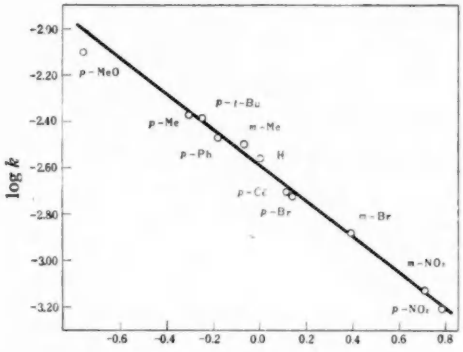

Fig. 3. Plot of decomposition rates of ω-diazoacetophenones against Brown and Okamoto's σ^+.

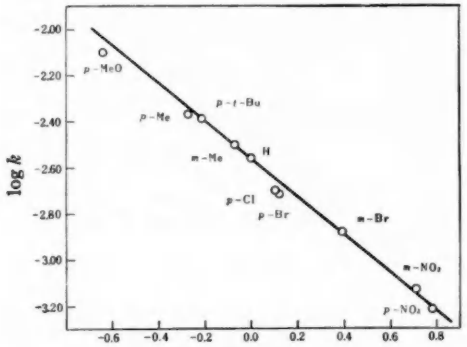

Fig. 4. Correlation of rates of the decomposition of ω-diazoacetophenones with Deno's σ^+.

12) A. Streitwieser, Jr. and W. D. Schaeffer, *J. Am. Chem. Soc.*, **79**, 2888 (1957); A. Streitwieser, Jr., *J. Org. Chem.*, **22**, 861 (1957).

13) See *reference* (*22*) in Y. Okamoto and H. C. Browm, *J. Org. Chem.*, **22**, 485 (1957).

14) R. Heck and S. Winstein, *J. Am. Chem. Soc.*, **79**, 3432 (1957).

15) H. G. Kuivila and A. R. Hendrickson, ibid., **74**, 5069 (1952); H. G. Kuivila and L. E. Benjamin, ibid., **77**, 4834 (1955).

than the estimated. Hence, it is the exsistence of a unique set of σ^+ that would be rather surprising in itself.

On the other hand, through Deno's set of σ^+ [5] the present data can be correlated more successfully than through Brown and Okamoto's, as shown in Fig. 4. The ρ^+ value of this correlation is equal to -0.789 ± 0.024, the correlation coefficient being 0.996. It is evident that the points for para substituents come closer to fitting on the ρ_m line, while the ρ^+ value is not strictly equal to the ρ_m value. The set defined by Pearson from the Beckmann rearrangement[16] also gives a rather more satisfactory result for the present reaction than does Brown and Okamoto's set, although this has not been reported to show any applicability. These facts appear to indicate that the respective sets of σ^+ may be applicable only to respective limited regions of electrophilic reaction series. Then, it would be by no means meaningless to set up tentative σ^+ values from the present reaction. This is encouraged by the success of linear free energy relationship between present data

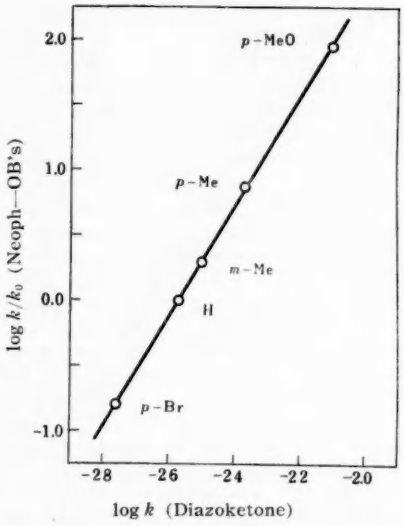

Fig. 5. Correlation of rates of acetolysis of neophyl brosylates and decomposition of ω-diazoacetophenones.

TABLE III. SUBSTITUENT CONSTANTS USED FOR CORRELATING RATES OF DECOMPOSITION OF THE ω-DIAZOACETOPHENONES

Substituent	Hammett[a]	Brown[b]	Deno[c]	σ^+[d]
p-CH_3O	−0.268	−0.764	−0.64	−0.537
p-C_2H_5O	−0.250			−0.512
p-*t*-C_4H_9	−0.197	−0.250	−0.21[f]	−0.209
p-CH_3	−0.170	−0.306	−0.27	−0.234
p-C_6H_5	+0.009	−0.179		−0.103
None	0.000	0.000	0.00	0.000
p-Cl	+0.227	+0.112	+0.11[g]	+0.175
p-Br	+0.232	+0.148		+0.202

a) Taken from the compilation by Jaffé (Ref. 11).
b) Brown and Okamoto's set of σ^+ (Ref. 6).
c) Deno's set of σ^+ (Ref. 5a).
d) The σ^+ values obtained from the present data. These were calculated from the Hammett equation using $\rho = \rho_m = -0.830$ and $\log k_0 = -2.558$.
e) H. C. Brown and Y. Okamoto, *J. Am. Chem. Soc.*, **80**, 4979 (1958).
f) The value derived from the dissociation of benzhydrols (Ref. 5b).
g) The value taken from Ref. 5b. In the original paper (Ref. 5a) +0.08 was given, while the quoted value, +0.11, appears to be more suitable.

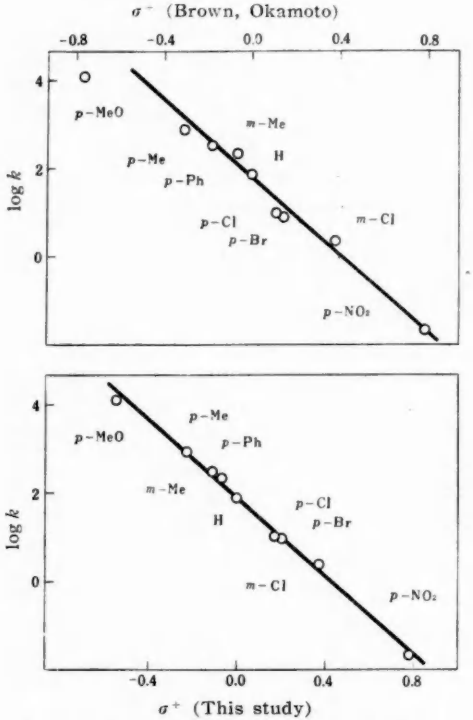

Fig. 6. Correlations of the Beckmann rearrangement of acetophenonoxime picrylethers with Brown and Okamoto's and our σ^+ values.

16) D. E. Pearson, J. F. Baxter and J. C. Martin, *J. Org. Chem.*, **17**, 1511 (1952); D. E. Pearson and J. D. Burton, ibid., **19**, 957 (1954).

and the solvolysis rates of neophyl brosylates[14], as shown in Fig. 5. The new set of σ^+ is given in Table III, along with the values of other sets of substituent constants. The present set does not appear to be applicable to a great many reactions. In some cases, however, it does describe a better correlation than does Brown and Okamoto's. Fig. 6 exhibits the correlations of the Beckmann rearrangement of acetophenone oxime picryl ethers[17] with the present set and with Brown and Okamoto's σ^+. Some other reactions which are satisfactorily correlated by the present set are as follows: the acetolysis of neophyl brosylates[14], the Beckmann rearrangement of acetophenonoximes[16], Diels-Alder reaction of 1-phenyl-1, 3-butadienes with maleic anhydride[18] and acid catalyzed rearrangement of phenylpropenylcarbinols[19].

A particular interest is seen in Table III. For each substituent, σ^+ values become more negative in the following order; the present set $<$ Deno's $<$ Brown and Okamoto's. The correction relative to the normal substituent constant is great in magnitude in Brown and Okamoto's, small in Deno's and smaller in the present set of σ^+. This parallels presumably the degree of resonance stabilization of electron deficient transition states in respective reference reactions, if the other factors remain constant throughout respective substituted derivatives. Thus, the resonance contribution of substituents would be more important in Brown and Okamoto's reference reaction than in Deno's and of even greater importance than in the present reaction. This is consistent with the facts that in Deno's reference reaction, the dissociation of triphenylcarbinols, the charge delocalization is shared separately by three aryl groups and in the present reaction the resonance contribution of a substituent group is reduced through the carbonyl group.

All one can say is that the σ^+ is not essentially constant but variable with respect to the change in reaction. *Rho—Sigma*$^+$ equation should be applied to the limited reaction series in which the availability of *transition state resonance* is equivalent to that in respective reference reactions. Now, it is highly desirable to correlate these sets of σ^+ with a simple relationship, which will be described in Part II.

The authors are indebted to Mr. T. Shishido for performing microanalysis.

Institute of Scientific and Industrial Research
Osaka University
Sakai, Osaka

17) R. Huisgen, J. Witte, H. Walz and W. Jira, *Ann.*, **604**, 191 (1957).
18) E. J. Dewitt, C. T. Lester and G. A. Ropp, *J. Am. Chem. Soc.*, **78**, 2101 (1956).
19) E. A. Braude and E. S. Stern, *J. Chem. Soc.*, **1947**, 1096.

Resonance Effect in Hammett Relationship. II. Sigma Constants in Electrophilic Reactions and their Intercorrelation

By Yasuhide YUKAWA and Yuho TSUNO

(Received January 28, 1959)

Recently, Brown and Okamoto have demonstrated a practical success in correlating various electrophilic reactions by a single set of σ^+ [1,2], obtained from the substituent effects in solvolysis of phenyldimethylcarbinyl chlorides. Their treatment should involve the assumption that the substituent effects in electrophilic reactions remain constant relative to marked variation in the ρ value. This is inconsistent with our view[3] that the reasonance interactions by a para substituent would depend greatly on the nature of the reactions, so that the effects

1) H. C. Brown and Y. Okamoto, *J. Am. Chem. Soc.*, **79**, 1913 (1957); Y. Okamoto and H. C. Brown, *J. Org. Chem.*, **22**, 485 (1957).
2) H. C. Brown and Y. Okamoto, *J. Am. Chem. Soc.*, **80**, 4979 (1958).
3) Y. Tsuno, T. Ibata and Y. Yukawa, This Bulletin, **32**, 960 (1959).

in electrophilic reactions could not possibly be correlated with a unique set of σ^+. The present view may be reasonable and perhaps the general one[4,5]. Brown and Okamoto's view could be confirmed by the identity of σ^+ values independently derived from other reactions. However, the various sets of σ^+ are varied significantly with respect to changes in the reference reaction[3,6-11]. The reported fact that the σ^+ constant derived from the decomposition of ω-diazoacetophenones differed from the corresponding Brown and Okamoto's[3] constant may afford evidence in favor of the present view.

The variations of σ^+ value for a given para substituent are generally referred to different availabilities of the resonance in various reference reactions, if other factors are maintained constant. On the other hand, failure of the linear $\rho\sigma^+$ relationship could be attributable also to the change in mechanism in a reaction series[12]. Brown has quoted[1], as an example, the solvolysis of benzyl tosylates[5,7], in which the change from S_N1 to S_N2 mechanisms occurred through changes of substituent. In the decomposition of diazoacetophenones, it may be possible to consider that the dissociation of nitrogen molecule competes with the attack of acetate ion in the driving force of the reaction[3]. If this was true, both mechanisms should indicate different responses to the ionizing power of the medium possibly because the stabilization of the carbonium ion produced will be important only in the former mechanism. Therefore, the substituent effects may be sensitive to the changes of solvent. Accordingly, kinetic study of the decomposition of diazoacetophenones was carried out in 75% aqueous acetic acid solution at 25.20°C, in order to confirm the reliability of our σ^+ values.

To the completion of this study, the foregoing view has been concreted and our attention has been directed to correlate empirically these independent sets of σ^+ according to a simple but reasonable relationship. In this paper, the results of the kinetics and of an approach to the correlation of σ^+ are presented.

Experimental

All diazoacetophenones were prepared by the procedure described in the preceding paper[3]. The stock solvent was made up by mixing 75 parts by volume of acetic acid with 25 parts by volume of distilled water. Acetic acid was purified by the usual method[13] and carefully fractionated, b. p. 117.5~118.0°C.

Rate Measurements. — The rates of the decomposition were determined by following the rate of evolution of nitrogen. The apparatus and the procedures were similar to those described in previous papers[3,14]. The temperature of the reaction bath was controlled to 25.20°C within an accuracy of ±0.01°C. Measurements were carried out in 75 ml. of aqueous acetic acid. The quantitative amount of nitrogen was obtained by the decomposition of respective derivatives of diazoacetophenone in aqueous acetic acid at 25.20°C. The rate of evolution of nitrogen followed strictly the first order kinetic law. Individual runs showed average deviations of far less than 1%, and duplicate runs gave rate constants agreeing within 2% or better. *p*-Phenyl-, *p*-bromo- and *m*- and *p*-nitro derivatives are soluble with greater difficulty in this solvent at this reaction temperature than in anhydrous acetic acid. Nitro derivatives were warmed with vigorous shaking at about 40°C to complete dissolution, prior to measurement. But this could not be applied to other derivatives, because of their high reactivities. *p*-Phenyl derivative is far less soluble in this solvent and deviation from the first order kinetic law was observed. The calculated rate constant increased gradually as the reaction proceeded and reached a constant value at 60% completion of the reaction. The rate constants obtained are summarized in Table I.

TABLE I. RATES OF THE DECOMPOSITION OF ω-DIAZOACETOPHENONES IN 75% AQUEOUS ACETIC ACID AT 25.20°C

Subst.	$k_1\times10^3$ a)	Subst.	$k_1\times10^3$ a)
p-CH_3O	28.3 ±0.2	H	5.86 ±0.04
p-C_2H_5O	26.9 ±0.3	*p*-Cl	3.71 ±0.03
p-CH_3	12.07±0.08	*p*-Br	2.94 ±0.07
p-*t*-C_4H_9	10.6 ±0.1	*m*-NO_2	0.816±0.005
m-CH_3	7.43±0.06	*p*-NO_2	0.638±0.004
p-C_6H_5	6.97±0.15		

a) The average rate constant in reciprocal min. and the average deviation.

4) P. B. D. de la Mare, *J. Chem. Soc.*, **1954**, 4450.
5) F. T. Fang, J. K. Kochi and G. S. Hammond, *J. Am. Chem. Soc.*, **80**, 563 (1958); G. S. Hammond, C. E. Reeder, F. T. Fang and J. K. Kochi, ibid., **80**, 568 (1958); G. S. Hammond and C. E. Reeder, ibid., **80**, 573 (1958).
6) D. E. Pearson, J. F. Baxter and J. C. Martin, *J. Org. Chem.*, **17**, 1511 (1952); D. E. Pearson and J. D. Burton, ibid., **19**, 957 (1954).
7) J. K. Kochi and G. S. Hammond, *J. Am. Chem. Soc.*, **75**, 3445 (1953).
8) N. C. Deno and A. Schriesheim, ibid., **77**, 3051 (1955).
9) N. C. Deno and W. L. Evans, ibid., **79**, 5804 (1957).
10) J. Miller, *Australian J. Chem.*, **9**, 61 (1956).
11) J. Packer, J. Vaughan and A. F. Wilson, *J. Org. Chem.*, **23**, 1215 (1958).
12) C. G. Swain and W. P. Langsdorf, *J. Am. Chem. Soc.*, **73**, 2813 (1951).
13) A. Weissberger, "Technique of Organic Chemistry", Vol. VII: "Organic Solvents", 2nd Ed., Interscience Publishers, Inc., New York (1955).
14) Y. Yukawa and Y. Tsuno, *J. Am. Chem. Soc.*, **79**, 5530 (1957); J. F. Lane and R. L. Feller, ibid., **73**, 4230 (1951).

Results

As listed in Table I, rates of the decomposition of diazoacetophenones are significantly increased in aqueous acetic acid relative to those in anhydrous acetic acid. Parallel to this, the sensitivity of the reaction to substituent effects appears to be considerably increased. Whereas the failure of the linear Hammett relationship is also observed in the aqueous medium just as in the case of an anhydrous medium[3]. Electron releasing para substituents supply higher acceleration than would be anticipated by the normal Hammett relationship (Fig. 1). Such a result has been discussed by us[3] and a number of other authors[1,2,4-12] and needs no further elucidation.

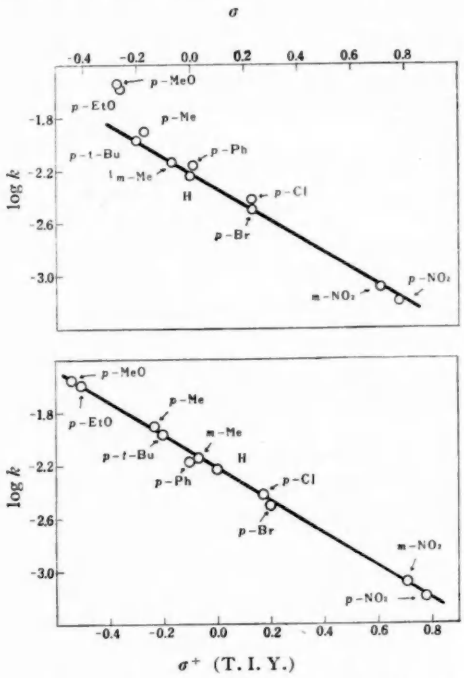

Fig. 1. Plot of the present data against the ordinary σ and our σ^+ constants.

In both reactions, the substituent effects would presumably be invariant, if the transition state remains approximately constant through changes of solvent. An evidence for the identity of substituent effects would generally be provided by a linear relationship between the corresponding $\log k/k_0$ of the two reactions. In fact, all the experimental points of $\log k/k_0$ in aqueous acetic acid fall just on the line expected from the $\log k/k_0$ in anhydrous medium. The correlation is given by an equation

$$\log (k/k_0)_{aq} = 1.510 \log (k/k_0)_{anhyd}$$

This indicates that the changes of medium reflect only ρ value and the substituent effect is not varied in either medium. The above correlation can of course be rewritten in terms of our σ^+ values[3] (Fig. 1). Statistical treatment[15] gives a correlation 1,

$$\log (k/k_0) = (-1.253 \pm 0.020)\sigma^+ \qquad (1)$$

The standard deviation of experimental $\log k$ from the best line is 0.027 and the correlation coefficient is 0.999. The ρ^+ value is closely equal to the ρ_{meta} value, 1.237 ± 0.018, which was obtained from points for *m*-CH_3, *m*-nitro, *p*-nitro and unsubstituted derivatives. On the basis of this ρ^+ value (1), a new set of σ^+ values can be derived from the rates in aqueous acetic acid. They are given in Table II. The present values agree with the previous one. *p*-Phenyl and *p*-bromo groups differ considerably in magnitude from the foregoing ones[3]. These are of no doubt attributable to the lower solubilities in aqueous acetic acid (see, *Experimental*). The discrepancies of others are substantially contained within experimental uncertainty. As a result, it may be conclusively suggested that the σ^+ derived from the previous result describes the best situation of the substituent effect in this reaction. Then, it appears to be evidently confirmed that the changes in mechanism as suggested by Brown and Okamoto might not occur through substituent changes in this reaction, and also that the rise in reactivities

Table II. σ^+ Constants

Subst.	σ^+_{aq} [a]	σ^+_{anhyd} [b]	$\sigma^+_{B.O.}$ [c]
p-CH_3O	−0.537	−0.537	−0.764
p-C_2H_5O	−0.519	−0.512	
p-CH_3	−0.241	−0.234	−0.306
p-*t*-C_4H_9	−0.196	−0.209	−0.250
p-C_6H_5	(−0.051)	−0.103	−0.179[d]
p-Cl	+0.168	+0.175	+0.112
p-Br	(+0.249)	+0.202	+0.148

a) The present study.
b) The set derived from the decomposition in anhydrous acetic acid (Ref. 3).
c) Brown and Okamoto's set of σ^+, taken from Ref. 1.
d) The value quoted from Ref. 2.

15) H. H. Jaffé, *Chem. Revs.*, **53**, 191 (1953).

of electron releasing para substituents could be attributable entirely to the increase of the resonance contribution.

These facts appear evidently to support the present view in preference to Brown and Okamoto's[1,2].

The linear free energy relationship would essentially hold in more or less limited reaction series in which the substituent effects are close to each other[3]. With the above considerations in mind, a given electrophilic reaction should be correlated with one of these sets of σ^+ most suitable to the resonance effects of substituents in it. However, it appears to be inconvenient practically. Therefore, it is necessary and desirable to correlate these independent sets of σ^+ with a relationship of practical use.

Discussion

The substituent effect can generally be treated as the sum of independent contributions of inductive and resonance components[16]. The former contribution refers to the electron distribution through the *sigma* bonds of a benzene nucleus and the latter to the electron delocalization through the resonance interaction of a substituent with the benzene *pi* electron system. An ordinary Hammett σ constant could be represented according to Eq. 2,

$$\sigma = \sigma_I + \sigma_R \tag{2}$$

where σ_I is an inductive effect and σ_R is a so-called *resonance polar effect*[16]; σ_R represents the substituent contribution through resonance with the benzene *pi* bonds to the electron density on the nuclear carbon atom at which the functional group is attached.

The substituent effect should be essentially independent of the reaction, whereas it is not always invariant, causing failure of the Hammett linear free energy relationship. The variation of substituent effect would be attributed only to the changes in contribution of the resonance component. The inductive component, the electron distribution through *sigma* bond, should essentially remain constant. The *resonance polar effect* may also be independent of the nature of reactions. However, the resonance component will no longer remain constant in the case of electrophilic reactions. The large electron demand produced at the reaction center of transition state must be delocalized[1-3]. This could be dissipated by the aid of the resonance interactions with electron releasing para substiuents through benzene *pi* orbitals. Then, the resonance effect becomes far greater than the ordinary *resonance polar effect*, σ_R, and σ^+ values result from this reason.

Brown and Okamoto's set of σ^+ may be represented[1]

$$\sigma^+ = \sigma_I + \sigma_R^+ \tag{3}$$

where σ_R^+ is a resonance effect in the Brown and Okamoto's reference reaction[1,2]. Other authors' sets of σ^+ are also treated in the same manner, although the σ_R^+ are by no means invariant of reactions. In general, the quantity σ_R^+ should be a variable and a function of the resonating capacity of substituent with the electron deficient reaction center through the benzene *pi* electron system. Since σ_I may undoubtedly remain constant through the changes of reaction type[16], the attention could be centered on the changes of σ_R^+. Inductive effect can be eliminated, combining Eqs. 2 and 3

$$\sigma^+ - \sigma = \sigma_R^+ - \sigma_R \equiv G(R) \tag{4}$$

Here, the quantity $\sigma^+ - \sigma$ should be a function of the resonance effect only, and this quantity just describes the magnitude of respective deviations of para substituents from the meta correlation line. Consequently, it may be anticipated that the analysis of the function $G(R)$ could provide a key to correlate the various sets of σ^+. The formulation of $G(R)$ will be realized practically by tracing changes of the quantity $\sigma^+ - \sigma$.

In actual practice, Brown and Okamoto's and Miller's quantities are plotted linearly against the corresponding quantities of the decomposition of diazoacetophenones, as illustrated in Figs. 2 and 3. These correlations are given by the following equations:

$$(\sigma^+ - \sigma)_{\text{Brown, Okamoto}} = 1.847(\sigma^+ - \sigma)$$

and

$$(\sigma^+ - \sigma)_{\text{Miller}} = 3.185(\sigma^+ - \sigma)$$

The standard deviations of the fits are ± 0.015 and ± 0.007, respectively. Then, the substituent effects in the decomposition of diazoacetophenones can be reproduced

16) R. W. Taft, Jr., in Newman's "Steric Effect in Organic Chemistry", Chapt. 13, John Wiley & Sons, Inc., New York (1956). R. W. Taft, Jr., *J. Am. Chem. Soc.*, **74**, 2729 (1952); ibid., **74**, 3120 (1952); ibid., **75**, 4231 (1953); ibid., **79**, 1045 (1957); R. W. Taft, Jr. and I. C. Lewis, ibid., **80**, 2436 (1958). Y. Yukawa and Y. Tsuno, "Yuki Hannokiko no Shimpo (Recent Advances in the Mechanism of Organic Reactions)", Vol. I, Maki Publishers, Inc., Tokyo (1958), p. 1.

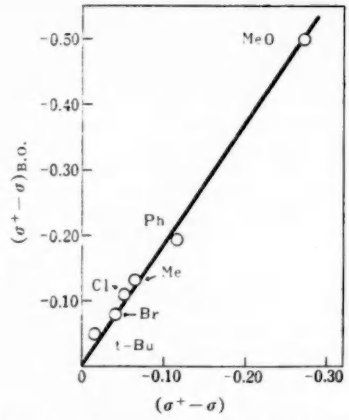

Fig. 2. Plot of Brown and Okamoto's quantity, $\sigma^+-\sigma$, against our quantity.

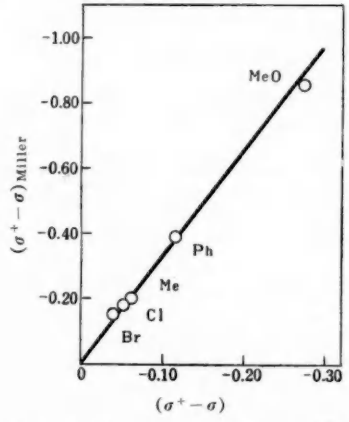

Fig. 3. The correlation between Miller's and our quantities, $\sigma^+-\sigma$.

precisely from various sets of σ^+. This may afford an indirect bit of evidence of our previous discussion of this reaction[3].

Furthermore, strictly linear correlations are observed in respective pairs of other sets of σ^+, as shown clearly in Figs. 4 and 5. These are represented as follows:

$$(\sigma^+-\sigma)_{\text{Brown, Okamoto}}=0.576(\sigma^+-\sigma)_{\text{Miller}}$$

$$(\sigma^+-\sigma)_{\text{Brown, Okamoto}}=1.347(\sigma^+-\sigma)_{\text{Deno}}$$

and

$$(\sigma^+-\sigma)_{\text{Deno}}=0.456(\sigma^+-\sigma)_{\text{Miller}}$$

The standard deviations are 0.015, 0.002 and 0.025, respectively. Then, these correlations can be held covering a wide range of substituent changes, especially, the last one covers the range from *p*-alkyl to *p*-dimethylamino groups. The same is

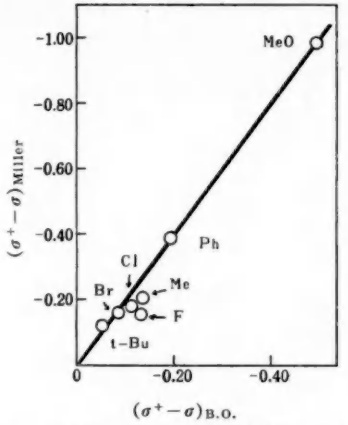

Fig. 4. Correlation of Miller's quantity, $\sigma^+-\sigma$, with Brown and Okamoto's one.

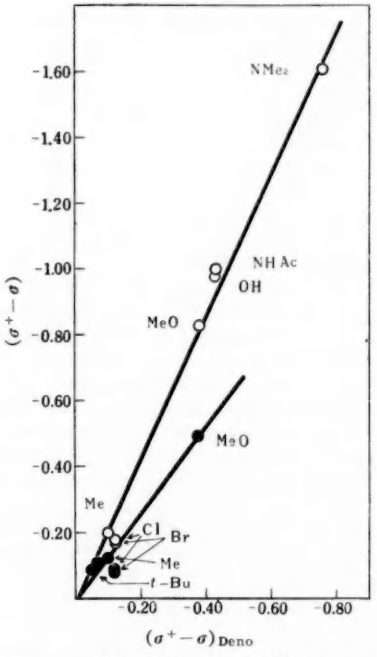

Fig. 5. Correlations of Miller's and Brown and Okamoto's quantities, $\sigma^+-\sigma$, with Deno's one: Open circles, Miller's and closed, Brown and Okamoto's.

true in the case of other sets, such as Packer's[11] and Pearson's[6].

As a conclusion, the function $G(R)$ can be regarded, to a first approximation, as a linear function of the quantity, $\sigma^+-\sigma$. Consequently, the general relationship 5 may be established empirically

TABLE III. CALCULATED VALUE OF BROWN AND OKAMOTO'S σ^+

p-Subst.	Calculated σ^+ value					Exptl.[f] value	Average value	$\sigma^+-\sigma$[h]
	A[a] 1.847[g]	B[b] 0.576[g]	C[c] 1.347[g]	D[d] 0.820[g]	E[e] 0.838[g]	(1.000)		
NMe_2		−1.53	−1.62				−1.60	−1.00
NH_2			−1.40				−1.40	−0.74
NHAc		−0.61	−0.59				−0.60	−0.58
OH		−0.92	−0.91				−0.92	−0.56
CH_3O	−0.765	−0.754	−0.766		−0.729	−0.764	−0.756±0.014[l]	−0.496
C_2H_5O	−0.744						−0.744	−0.494
C_6H_5O		−0.528			−0.559		−0.543	−0.51
CH_3	−0.301[i]	−0.288	−0.305	−0.299	−0.306	−0.306	−0.301±0.006[l]	−0.131
C_2H_5				−0.293	(−0.315)[k]	−0.291	−0.292	−0.141
i-C_3H_7				−0.282		−0.276	−0.279	−0.125
t-C_4H_9	(−0.217)[j]	−0.267	−0.251			−0.250	−0.256±0.010[l]	−0.053
C_6H_5	−0.200	−0.219		−0.177	(−0.240)[k]	−0.179	−0.194±0.020[l]	−0.200
F						−0.071	−0.071	−0.130
Cl	+0.118[i]	+0.122			+0.130	+0.112	+0.121±0.007[l]	−0.106
Br	+0.162	+0.138			+0.154	+0.148	+0.151±0.010[l]	−0.081
I						+0.132	+0.132	−0.144

a) The value calculated on the basis of our σ^+ value (Ref. 3).
b) Calculated from Miller's set of σ^+ (Ref. 10).
c) The value obtained from Deno's set of σ^+ (Refs. 7 and 8).
d) The value on the basis of σ^+ given by Packer et al. (Ref. 11) from the ethanolysis rates of benzhydryl chlorides (E. D. Hughes, C. K. Ingold and N. A. Taher, *J. Chem. Soc.*, **1940**, 949).
e) Calculated from Norris and coworkers' data on the solvolysis of benzhydryl chlorides in absolute ethanol (J. F. Norris and C. Benta, *J. Am. Chem. Soc.*, **50**, 1804 (1928); J. F. Norris and J. T. Blake, ibid., **50**, 1808 (1928): see, the forthcoming paper, (Y. Yukawa and Y. Tsuno, This Bulletin, **32**, 971 (1959).).
f) Brown and Okamoto's σ^+ value (Ref. 1).
g) The r value in the relationship 5; the proportionality constant of the quantity, $\sigma^+-\sigma$, to the corresponding one of Brown and Okamoto.
h) This value should essentially be equal to the difference of Brown and Okamoto's σ^+ from the ordinary Hammett σ constant. This could be regarded as a measure of the resonating power of respective substituents. This has been utilized successfully in regard to the resonance substituent constant, $\Delta\sigma_R^+$, and will be reported in a subsequent paper.
i) The value based on σ^+ obtained in the present study.
j) This group showed deviation from the correlation 5 setting r=1.847, and was omitted from the calculation. Such a deviation was observed in the Pearson's correlation of σ^+ (Ref. 6).
k) This group deviates seriously and was not included in the calculation.
l) Standard deviation.

$$(\sigma^+_A-\sigma)=r(\sigma^+_B-\sigma) \qquad (5)$$

where r is a parameter which remains constant in a reaction series but is a variable of reactions. This parameter may arise without doubt from differing contributions of the resonance effect in reference reactions.

The reliability of the approximation can be substantiated by the close agreement of calculated values on the basis of this relationship with an experimental one. This is clearly exhibited in the comparison of calculated with the experimental values of Brown and Okamoto's σ^+, as shown in Table III. Computed values for respective substituents are in accord with the experimental one, without serious exceptions. The averaged standard deviations of calculated values are estimated to be ±0.009. This is excellent as compared with the agreement of the comparision given by Deno[9], and by Brown and Okamoto[2]. Then, the results in Table III will possibly extend the utility of Brown and Okamoto's set to the substituents having no experimental σ^+ value in their scale.

Through these results, the particular

features of interest have arisen. As mentioned in the above discussion, the quantities $\sigma^+ - \sigma$ may be regarded as a function of the resonance capacity of substituents. Therefore, the relationship 5 is in itself a linear resonance energy relationship. The σ^+ values, in turn, could be represented by the following relationship, using a proper set of the quantities $\sigma^+ - \sigma$ in a single scale

$$\sigma^+ = \sigma + r(\bar{\sigma}^+ - \sigma) = \sigma + r\Delta\sigma_R^+$$

where $\bar{\sigma}^+$ is a correct set of σ^+ and $\Delta\sigma_R^+$ represents the standard set of the quantities $\sigma^+ - \sigma$. Consequently, electrophilic reactions in general will possibly be correlated by a modified Hammett equation,

$$\log (k/k_0) = \rho(\sigma + r\Delta\sigma_R^+)$$

This has been realized by using the numerical values of $\Delta\sigma_R^+$ in Brown and Okamoto's scale. The utility of this relationship will be described in Part III.

The authors gratefully acknowledge the help of Mr. T. Ibata in the preparation of samples.

Institute of Scientific and Industrial Research
Osaka University
Sakai, Osaka

Resonance Effect in Hammett Relationship. III. The Modified Hammett Relationship for Electrophilic Reactions

By Yasuhide YUKAWA and Yuho TSUNO

(Received January 28, 1959)

As shown in Part II[1] of this series, the substituent constants in Brown and Okamoto's scale were derived for a number of electron releasing para substituents by correlating various sets of σ^+ [2-8]. These values will possibly extend the utility of the Brown and Okamoto's equation[2,10] over a wider range of substituent changes[1,5,10,11]. However, it is clear that the unique set of σ^+ does not always describe the best situation of substituent contributions in various reactions, even though Brown and Okamoto's σ^+ may have an apparent generality. It would be attributed to the changes in availability of the *transition state resonance* in various reactions. The resonance contribution of respective para substituents as well as the magnitude of σ^+ would not be maintained constant but varied from reaction to reaction[1]. Then, the Brown and Okamoto's and also other authors' sets of σ^+ [3-9] should be utilized respectively in the limited extent of reaction series[1,3].

Our success in correlating various sets of σ^+ by Eq. 1[1] appears to imply some suggestions in regard to the Hammett type treatment[12] of electrophilic reactions.

$$(\sigma^+{}_A - \sigma) = r(\sigma^+{}_B - \sigma) \qquad (1)$$

Here r is a proportionality constant, and $\sigma^+{}_A$ represents one of various sets of σ^+ and $\sigma^+{}_B$ another set of σ^+. In a given para substituent, the increments of various σ^+ values relative to the usual σ constant[12]

1) Y. Yukawa and Y. Tsuno, This Bulletin, **32**, 965 (1959).
2) H. C. Brown and Y. Okamoto, *J. Am. Chem. Soc.*, **79**, 1913 (1957); Y. Okamoto and H. C. Brown, *J. Org. Chem.*, **22**, 485 (1957).
3) Y. Tsuno, T. Ibata and Y. Yukawa, This Bulletin, **32**, 960 (1959).
4) N. C. Deno and A. Schriesheim, *J. Am. Chem. Soc.*, **77**, 3051 (1955).
5) N. C. Deno and W. L. Evans, ibid., **79**, 5804 (1957).
6) D. E. Pearson, J. F. Baxter and J. C. Martin, *J. Org. Chem.*, **17**, 1511 (1952); D. E. Pearson and J. D. Burton, ibid., **19**, 957 (1954).
7) J. Miller, *Australian J. Chem.*, **9**, 61 (1956).
8) J. K. Kochi and G. S. Hammond, *J. Am. Chem. Soc.*, **75**, 3445 (1953); G. S. Hammond et al., ibid., **80**, 653, 568, 573 (1958).
9) J. Packer, J. Vaughan and A. F. Wilson, *J. Org. Chem.*, **23**, 1215 (1958).
10) H. C. Brown and Y. Okamoto, *J. Am. Chem. Soc.*, **80**, 4979 (1958).
11) Brown has derived recently the averaged σ^+ values for *p*-NHe_2, *p*-NH_2 and *p*-OH, etc., from σ^+ values of other electrophilic reactions, while the agreement is by no means within satisfactory precision (Ref. 10). Deno's expansion of σ^+ in Brown and Okamoto's scale appears also to be unsuccessful (Ref. 5).
12) L. P. Hammett, *J. Am. Chem. Soc.*, **59**, 96 (1937); "Physical Organic Chemistry", McGraw-Hill Book Co., New York (1940), p. 194; H. H. Jaffé, *Chem. Revs.*, **53**, 191 (1953).

are possibly considered to be a function of its resonance ability. Then, the equation may be a linear resonance energy relationship. Therefore, it appears logical to extend this relationship to general electrophilic reactions combining with Hammett equation[12]. If the above relationship would hold in a variety of electrophilic reactions, the Hammett relationship for electrophilic reactions may be represented empirically according to Eq. 2,

$$\log k/k_0 = \rho(\sigma + r\Delta\sigma_R^+) \qquad (2)$$

where r is a reaction constant describing the degree of the transition state resonance or measuring the magnitude of positive charge to be necessarily stabilized at the transition state, and $\Delta\sigma_R^+$ which corresponds to a proper set of $\sigma^+ - \sigma$ is a substituent constant suggesting the resonating capacity of substituent. From the foregoing point of view, we are free to take one of various sets of the quantities $\sigma^+ - \sigma$ as a proper set of the $\Delta\sigma_R^+$.

The *resonance substituent constant*, $\Delta\sigma_R^+$, is now defined conveniently using the set of quantities $\sigma^+ - \sigma$ in Brown and Okamoto's scale[13]; i.e., the r is taken as unity in Brown and Okamoto's reference reaction, the solvolysis of aryldimethylcarbinyl chlorides in 90% aqueous acetone at 25°C,

$$\Delta\sigma_R^+ \equiv \sigma^+_{\text{Brown and Okamoto}} - \sigma \qquad (3)$$

Eq. 2 is undoubtedly to be satisfied by the reactions to which the Brown and Okamoto's equation was applicable, because the latter equation corresponds to the present Eq. 2 when r is equal to unity. The same is also certain in the electrophilic reactions which are correlated linearly with other sets of σ^+. The second term of Eq. 2 would vanish in the correlation of meta substituents, evidently because the Hammett relationship would hold in general electrophilic reactions as far as the mata substituents are concerned. Accordingly, ρ in Eq. 2 can be replaced by the ρ_{meta} value and the equation may be usually solved on the basis of ρ_{meta} value[14].

An empirical relationship should be required to examine critically the general applicability. Fortunately, in an enormous number of electrophilic reactions, satisfactory results have been realized in terms of this relationship. In the present paper, then, the results of application and generality of this relationship are described.

Correlation of Reactivities

In view of the origin of this relationship, it is a matter of course that the relationship should describe satisfactorily the substituent effect in the respective reference reactions, from which various sets of σ^+ were derived. These are clear in Figs. 1 and 2. The rates of decomposition of ω-diazoacetophenones both in acetic acid at 40.00°C[3] and in 75% aqueous acetic acid at 25.20°C[1] are reproduced strictly in terms of Eq. 2, setting r to be 0.556 and nearly the same value 0.60, respectively.

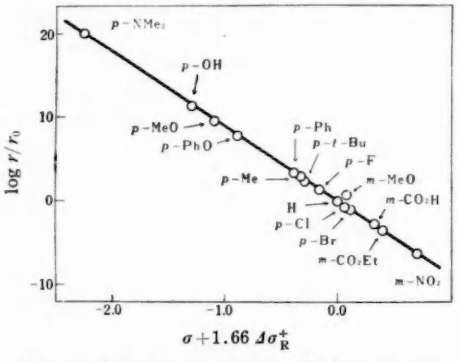

Fig. 1. Relative reactivities in halogenation of monosubstituted benzenes at 25°C (*3*).

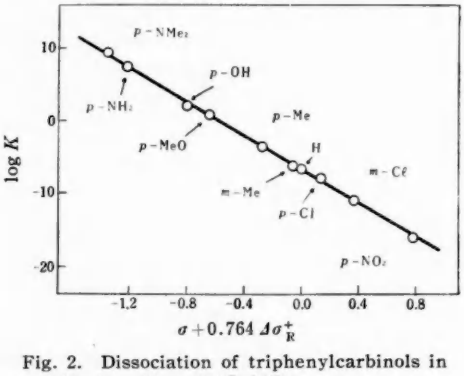

Fig. 2. Dissociation of triphenylcarbinols in sulfuric acid at 25°C (*22*).

13) A tentative set of $\Delta\sigma_R^+$ has been derived on the basis of Deno's reference reaction and applied preliminarily for several electrophilic reactions. [Y. Yukawa and Y. Tsuno, "Yūki Hannōkikō no Shimpo—Recent Advances in the Mechanism of Organic Reactions", (in Japanese) Vol. I. (1958), p. 1.]. However, the present definition of $\Delta\sigma_R^+$ in Brown and Okamoto's scale appears to be more available, in view of its frequent employment encountered in recent literatures.

14) Although various values of σ_{meta}^+ have been given by Brown and others (Refs. 2 and 10), the differences between σ^+_{meta} and σ_{meta} are of magnitude comparable to experimental error. Even if they were significant, the situation of the relationship is unaltered but ρ value must be calculated by solving the regression Eq. 4.

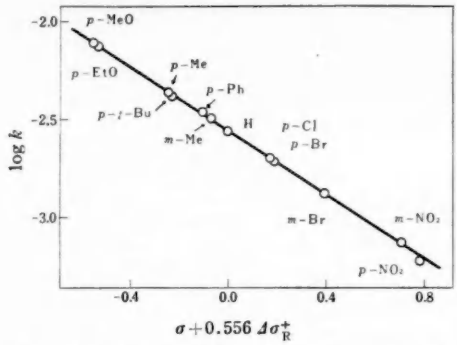

Fig. 3. Decomposition of ω-diazoacetophenones in acetic acid at 40.00°C (*25*).

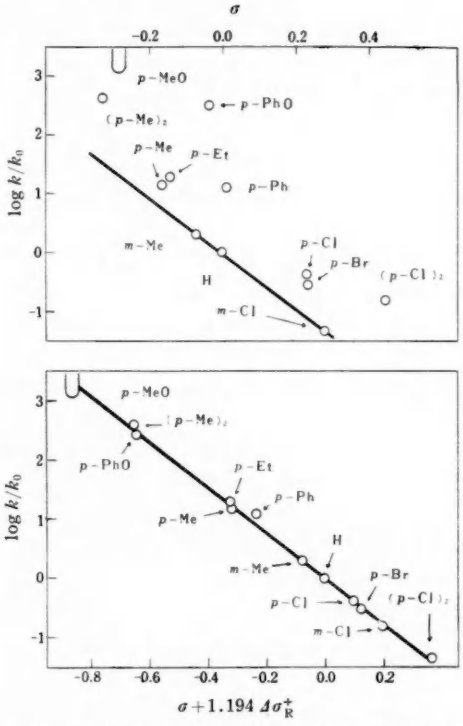

Fig. 4. Ethanolysis of benzhydryl chlorides at 25°C (*10*).

The Pearson's rate data of the Beckmann rearrangement[6] are also correlated in terms of $r=0.434$. The numerical values of $\Delta\sigma_R^+$ used are the one given in Table III of the foregoing paper.

A typical example of electrophilic reactions is the solvolysis of arylalkyl halides. Norris and coworkers[15] reported the ethanolysis rates of benzhydryl chlorides. The Hammett plots of para electron releasing substituents deviate markedly in the upper side of the meta correlation line. With regard to meta substituents, a linear Hammett relationship is obtained, and the slope, ρ_{meta}, is -3.72.

$$\log(k/k_0)_m = -3.72\,\sigma_{meta}$$

Using this ρ value, r is calculated to be 1.194. Then, the rates of the ethanolysis can be expressed by an equation

$$\log k/k_0 = -3.72(\sigma + 1.194\,\Delta\sigma_R^+)$$

In Fig. 4 is demonstrated the fine correlation of $\log k/k_0$ vs. $\sigma+1.194\,\Delta\sigma_R^+$. In the same manner, the rates of ionization of triarylcarbinyl chlorides to form the ion pairs

$$(C_6H_5)_3C\text{-}Cl \rightarrow (C_6H_5)_3C^+ // Cl^-$$

in liquid sulfur dioxide[16] are correlated linearly. As is clear in Fig. 5, the correla-

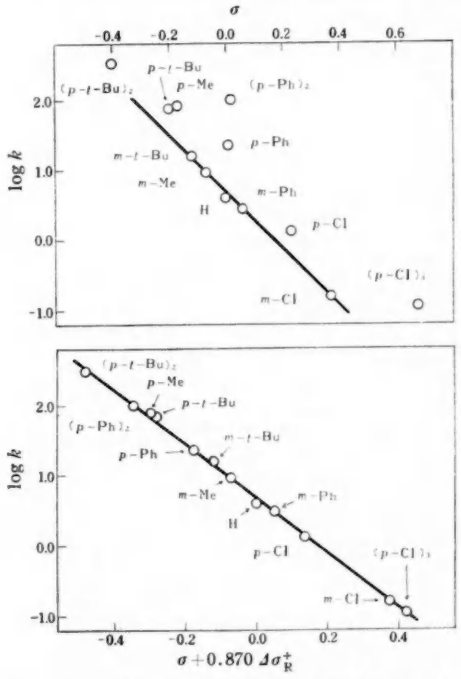

Fig. 5. Dissociations of triphenylcarbinyl chlorides in liquid sulfur dioxide at 0°C (*20*).

15) J. F. Norris and C. Benta, *J. Am. Chem. Soc.*, **50**, 1804 (1928); J. F. Norris and J. T. Blake, ibid., **50**, 1808 (1928).

16) N. N. Lichtin and M. J. Vignale, ibid., **79**, 579 (1957); N. N. Lichtin and P. D. Bartlett, ibid., **73**, 5530 (1951); N. N. Lichtin and H. Glazer, ibid., **73**, 5537 (1951); N. N. Lichtin and H. P. Leftin, *J. Phys. Chem.*, **60**, 164 (1956).

tion is fully satisfactory; $\rho=-4.046$ and $r=0.870$.

At the theoretical ground, the standard of correlation should be based on the meta correlation line, while there are relatively few adequate data which involve the rates of many meta derivatives. For the data involving a few rates of meta derivatives, the correlation is realized by solving the Eq. 4 for a and b on the basis of the method of least squares[17],

$$\log k = a\sigma + b\Delta\sigma_R^+ + \log k_0 \qquad (4)$$

where a and b correspond to ρ and $r\rho$, respectively. In this manner, the solvolysis rates of benzhydryl chlorides in methanol and in isopropanol[18] provide excellent correlations giving $r=1.234$ and 1.350, respectively. Similarly, the dissociation of identically substituted benzhydrols in sulfuric acid at 25°C[5] is correlated linearly in terms of $\rho=-9.112$ and $r=1.175$.

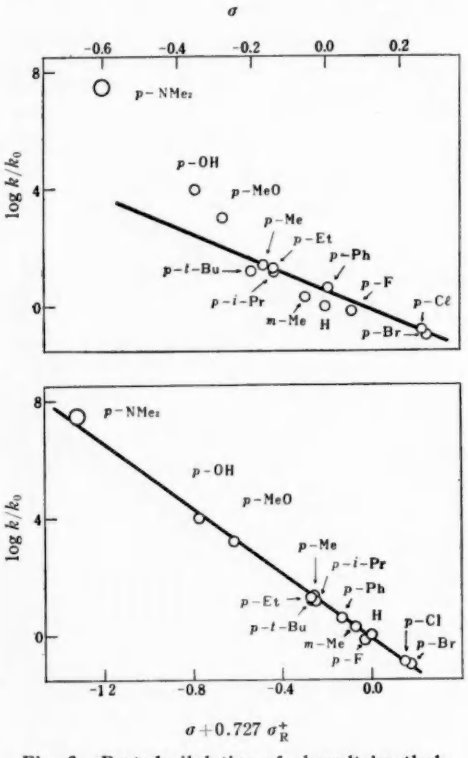

Fig. 6. Protodesilylation of phenyltrimethylsilanes (*23*).

The present treatment is successful not only in the solvolysis but in other types of electrophilic reactions, such as aromatic electrophilic substitutions. Recent data of the nitration[19] and the halogenation[6,20] of substituted benzenes, and protonolysis

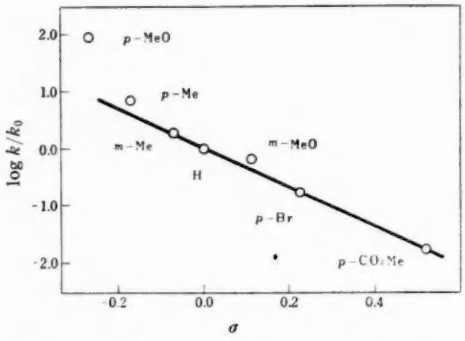

Fig. 7—a. Acetolysis of neophyl brosylates at 70°C (*27*).

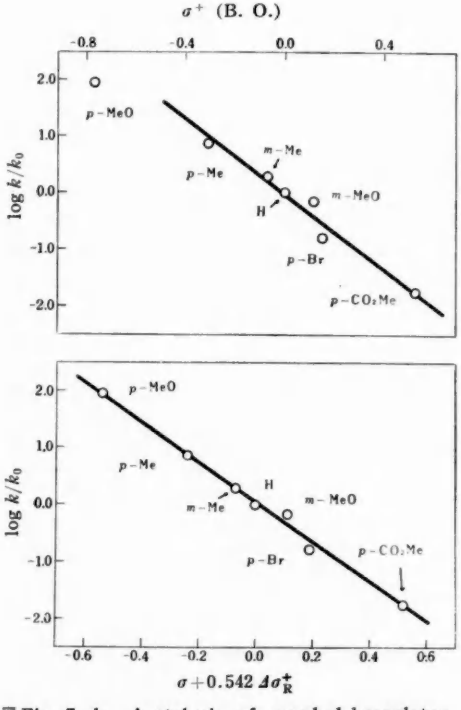

Fig. 7—b. Acetolysis of neophyl brosylates at 70°C (*27*).

17) C. A. Bennett and N. L. Franklin, "Statistical Analysis in Chemistry and the Chemical Industry", John Wiley & Sons, Inc., New York (1954), p. 245.
18) S. Altscher, R. Baltzly and S. W. Blackman, *J. Am. Chem. Soc.*, **74**, 3649 (1952).
19) J. D. Roberts et al., ibid., **76**, 4525 (1954).
20) a) P. B. D. de la Mare, *J. Chem. Soc.*, **1954**, 4450; b) P. B. D. de la Mare and J. T. Harvey, ibid., **1956**, 36; ibid., **1957**, 131; P. B. D. de la Mare and M. Hassan, ibid., **1957**, 3004.

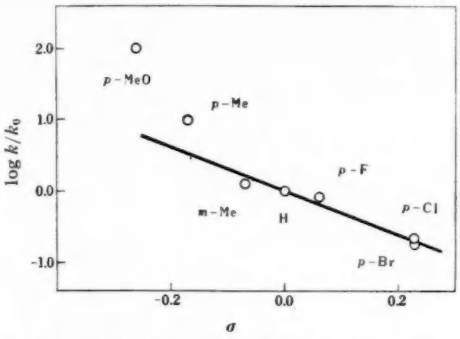

Fig. 8—a. Rearrangement of phenylpropenylcarbinols (*32*).

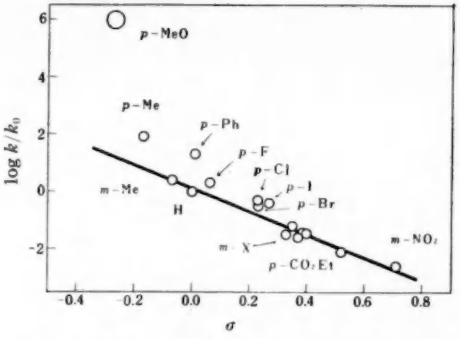

Fig. 9—a. Brominolysis of benzeneboronic acids (*2*).

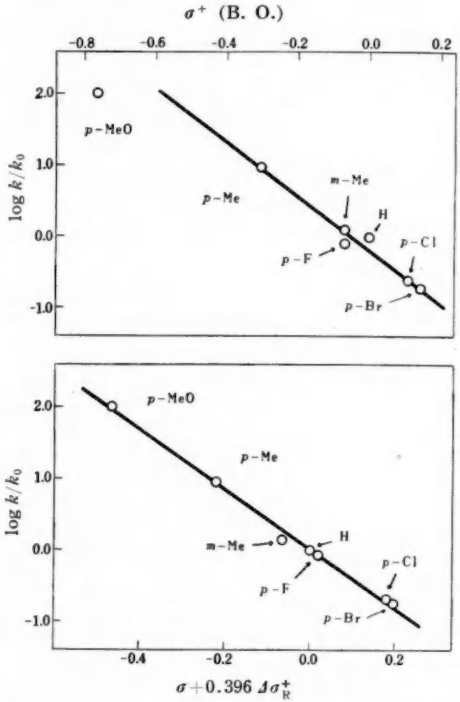

Fig. 8—b. Rearrangement of phenylpropenylcarbinols (*32*).

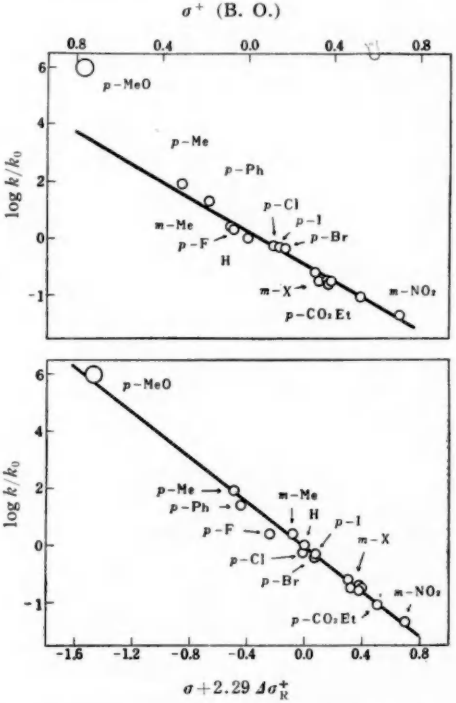

Fig. 9—b. Brominolysis of benzeneboronic acids (*2*).

of phenyltrimethylsilanes[21] (Fig. 6) are described satisfactorily. In the reactions quoted above, the Brown and Okamoto's relationship also results apparently but not strictly linear figures. This may be in accord with the fact that the r factors of these are considerably close to unity (see, Table I).

Recently, Winstein and coworkers[22] reported that the rates of acetolysis of neophyl brosylates failed to give a good result by the Hammett treatment, and also that the correlation was slightly improved by the Brown and Okamoto's. According to the latter treatment, para electron releasing groups fall below the meta line, contrary to the results of the

21) C. Eaborn, ibid., **1956**, 4858.

22) R. Heck and S. Winstein, *J. Am. Chem. Soc.*, **79**, 3432 (1957).

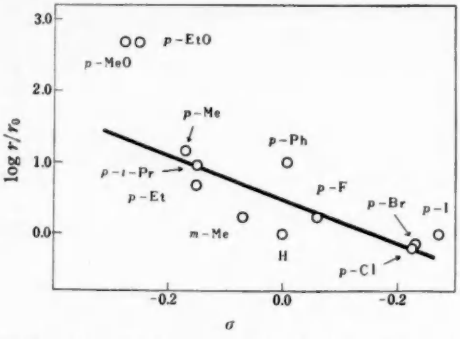

Fig. 10—a, Migratory aptitudes in the pinacol rearrangement (*4*).

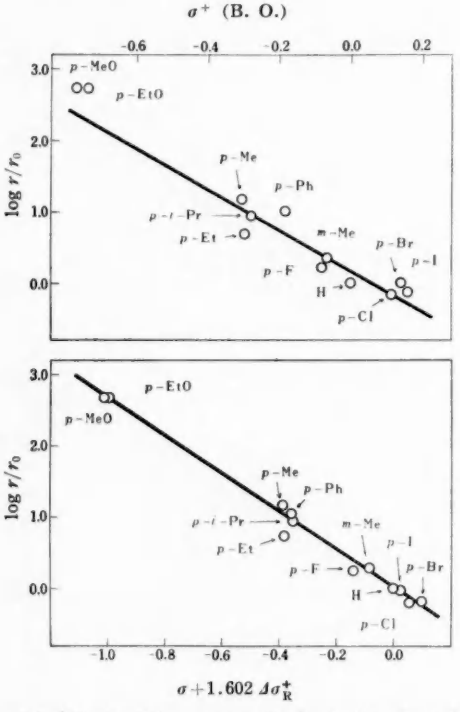

Fig. 10—b. Migratory aptitudes in the pinacol rearrangement (*4*).

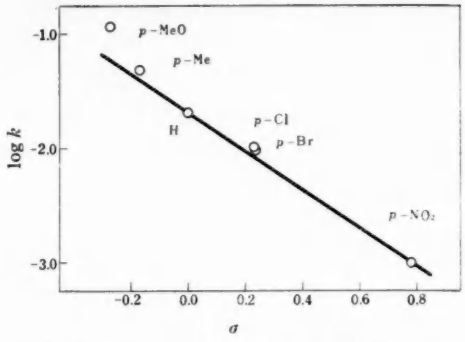

Fig. 11—a. Epoxidation of *cis*-dimethylstilbenes at 30°C (*33*).

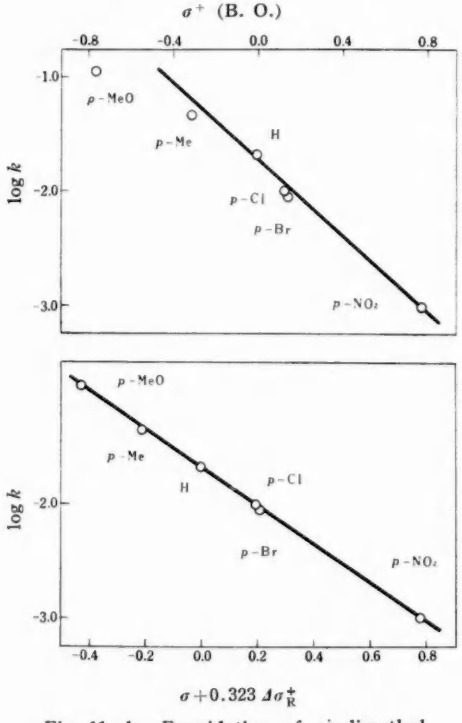

Fig. 11—b. Epoxidation of *cis*-dimethylstilbenes at 30°C (*33*).

Hammett one. However, the present treatment produces a successful figure (Fig. 7) of this reaction, in terms of $r=0.542$. The Beckmann rearrangement of acetophenonoxime picrylethers[23] is correlated with Eq. 2, giving r to be 0.469, although the plot against Brown and Okamoto's σ^+ concaves downward. The rates of the rearrangement of phenylpropenylcarbinols[24] are of the same kind ($r=0.396$), as seen in Fig. 8. The resonance contribution of substituents in these reactions is estimated to be only a half of that in Brown and Okamoto's reference reaction. Therefore, it is natural that Brown and Okamoto's treatment overestimates the

23) R. Huisgen, J. Witte, H. Walz and W. Jira, *Ann.*, **604**, 191 (1957).

24) E. A. Braude and E. S. Stern, *J. Chem. Soc.*, **1947**, 1096.

TABLE I. RESULTS OF APPLICATION OF THE PRESENT RELATIONSHIP

No.	Reaction	ρ	r	s[a)]	n[b)]	Reference
1	Solvolysis of phenyldimethylcarbinyl chlorides in 90% aqueous acetone at 25°C	−4.518	1.000	0.093	21	2, *d*, *e*
2	Brominolysis of the benzeneboronic acids in 20% acetic acid and 0.40 M sodium bromide at 25°C	−3.84	2.29	0.313	16	25, *c*, *f*
3	Halogenation of substituted benzenes at 25°C	−8.82	1.660	0.414	15	7, *c*
4	Migratory aptitudes in the pinacol rearrangement of symmetrically substituted tetraarylpinacols	−2.523	1.602	0.120	12	26, *d*, *g*
5	Dissociation of monosubstituted benzhydrols in sulfuric acid at 25°C	−5.236	1.492	0.023	7	4, 5, *d*
6	Epoxidation of stilbenes with phthaloyl peroxide in tetrachloromethane at 80°C	−1.630	1.388	0.034	7	27, *c*, *h*
7	Solvolysis of benzhydryl chlorides in isopropyl alcohol at 25°C	−4.004	1.350	0.070	6	18, *d*
8	Solvolysis of benzhydryl chlorides in methanol at 25°C	−4.022	1.234	0.110	6	18, *d*
9	Solvolysis of benzhydryl chlorides in ethanol at 25°C	−4.140	1.198	0.095	10	9, 30, *c*, *j*
10	Solvolysis of benzhydryl chlorides in ethanol at 25°C	−3.721	1.194	0.087	12	15, *c*, *i*
11	Dissociation of identically disubstituted benzhydrols in sulfuric acid at 25°C	−9.112	1.175	0.335	8	4, 5, *d*, *k*
12	Rearrangement of α-phenylethyl chlorocarbonates in dioxane at 70°C	−3.060	1.166	0.048	5	31, *d*
13	Bromination of benzenes by hypobromous acid and perchloric acid in 50% aqueous dioxane at 25°C	−5.276	1.145	0.080	7	20b, *d*, *l*
14	Rearrangement of α-phenylethyl chlorocarbonates in toluene at 80°C	−2.808	1.138	0.117	5	31, *d*
15	Chlorination of benzalacetophenones	−3.413	1.128	0.033	4	32, *c*
16	Solvolysis of monohalobenzhydryl chlorides in 70% aqueous acetone at 25°C	−4.118	1.007	0.023	5	33, *d*
17	Migratory aptitudes in the Schmidt rearrangement of diphenylethylenes	−2.77	0.90	0.10	6	34, *c*
18	Reactivities of substituted benzenes toward nitration in nitromethane or acetic acid at 25°C	−6.377	0.897	0.327	12	19, *c*, *m*
19	Solvolysis of triphenylcarbinyl chlorides in 40% ethanol/60% ethyl ether at 0°C	−2.52	0.88	0.132	8	35, *c*, *n*
20	Dissociation of triphenylcarbinyl chlorides in liquid sulfur dioxide at 0°C	−4.046	0.870	0.101	12	15, *c*, *o*
21	Basicities of monosubstituted azobenzenes	−2.293	0.853	0.100	11	36, *c*
22	Equilibrium constants for carbonium ions from triphenylcarbinols in sulfuric acid at 25°C	−11.73	0.764	0.335	10	4, 5, *d*
23	Phenyltrimethylsilanes with perchloric acid in 72% aqueous methanol at 50°C	−5.597	0.727	0.125	13	21, *d*, *p*
24	Epoxidation of *trans*-stilbenes by perbenzoic acid at 30°C	−1.055	0.713	0.029	9	28, *c*
25	Acid catalyzed decomposition of ω-diazoacetophenones in acetic acid at 40°C	−0.823	0.556	0.008	12	1, 3, *d*, *q*
26	Acid catalyzed decomposition of ω-diazoacetophenones in 75% aqueous acetic acid at 25.20°C	−1.222	0.603	0.025	10	1, *d*, *r*
27	Acetolysis of neophyl brosylates at 70°C	−3.384	0.542	0.077	7	22, *c*
28	Diels-Alder reactions of phenylbutadienes with maleic anhydride in dioxane at 45°C	−0.711	0.475	0.038	5	37, *c*
29	The Beckmann rearrangement of acetophenone oxime picrylethers in dichlorbutane at 70°C	−4.243	0.464	0.233	12	1, 23, *d*
30	The Beckmann rearrangement of acetophenone oximes in 94.5% sulfuric acid at 50.9°C	−1.983	0.434	0.044	9	6, *c*
31	Decomposition of diphenylmethylcarbinyl azides in acetic acid/sulfuric acid at 25°C	−2.092	0.436	0.072	7	38, *d*
32	Rearrangement of phenylpropenylcarbinols in 60% aqueous dioxane at 30°C	−4.056	0.396	0.080	7	24, *d*
33	Epoxidation of *cis*-dimethylstilbenes in benzene at 30°C	−1.692	0.323	0.020	6	29, *c*

34	Epoxidation of *trans*-dimethylstilbenes in benzene at 30°C	−1.554	0.249	0.035	6	29, *c*
35	Diphenyldiazomethanes with benzoic acid in toluene at 25°C	−1.570	0.190	0.036	12	39, *c*

a) The standard deviation of experimental points from the regression line.
b) The number of points involved in the calculation.
c) The correlation obtained on the basis of ρ_{meta} value which were derived from the rates for meta substituted and nonconjugating para substituted derivatives.
d) The correlation obtained in aid of Eq. 4.
e) The correlation obtained by setting a priori $r=1.000$.
f) The correlation of $r=2.05$ and $\rho=-4.31$ was resulted on the basis of Eq. 4.
g) *m*-Methoxy group was omitted from the correlation.
h) The point of *p*-carbethoxy group deviates considerably from meta line and was not included in the calculation of ρ_{meta} value.
i) The point for *p*-*t*-butyl group deviates seriously and was omitted from the calculation of *r* value.
j) *p*-Phenyl group supplies a greater driving force than that expected from this correlation.
k) *p*-Dimethylamino and *p*-phenyl groups were not included in the calculation.
l) *m*-*t*-Butyl group was not included in the calculation and experimental value of −0.078 was resulted for σ_{meta} of this group.
m) Points for meta derivatives deviate from the ρ_{meta} line.
n) *p*-Fluoro group deviates significantly.
o) σ value of +0.06 was employed for *m*-phenyl group. Trisubstituted derivatives were omitted from the calculation, since the cross conjugation effect appeared to be possibly involved.
p) Excepting *p*-dimethylamino and *p*-hydroxy groups, was obtained the partial correlation; $r=0.622$, $\rho=-5.535$ and $s=\pm0.026$. $\Delta\sigma_R^+$ values for these groups were calculated on the basis of this correlation; −1.20 for *p*-dimethylamino and −0.60 for *p*-hydroxy groups.
q) On the basis of ρ_{meta} value of −0.830, *r* value of 0.539 was obtained.
r) *p*-Phenyl group was not included in the calculation.

situation in these reactions. The same is true in the case of the decomposition of diazoacetophenones, as mentioned in the foregoing papers[1,3].

Conversely, the plots against Brown and Okamoto's σ^+ remain to be concaved upward in the brominolysis rates of benzeneboronic acids[25] and the migratory aptitudes of tetraphenyl pinacols[26], to the contrary, the present treatment exhibits fine correlations, whose *r* values are 2.29 and 1.60, respectively. These are the reverse of that mentioned above.

The curved correlation with Brown and Okamoto's σ^+ is fairly often observed in other reaction series, in accordance with the view that the availability of resonance contribution of para substituents is varied to a considerable extent by the changes of reaction series. Recently, Greene pointed out[27] that the rates of epoxidation of *trans*-stilbenes with phthaloyl peroxide satisfied the Brown and Okamoto's relationship. According to the present treatment, this reaction provides a fine figure of $r=1.388$. Similarly, the oxidation with perbenzoic acid is successful in terms of $r=0.713$[28]. Furthermore, the perbenzoic acid oxidation of *cis*- and *trans*-dimethylstilbenes[29] exhibits excellent correlations giving *r* of only 0.2∼0.3, in contrast with the failure of the Brown and Okamoto's. Fig. 11 demonstrates the correlation of

25) H. G. Kuivila and A. R. Hendrikson, *J. Am. Chem. Soc.*, **74**, 5068 (1952); H. G. Kuivila and C. E. Benjamin, ibid., **77**, 4834 (1955).
26) W. E. Bachmann and F. H. Mosher, ibid., **54**, 1124 (1932); W. E. Bachmann and J. W. Ferguson, ibid., **56**, 2081 (1934).
27) F. D. Greene and W. W. Rees, ibid., **80**, 3432 (1958).
28) B. M. Lynch and K. H. Pausacker, *J. Chem. Soc.*, **1955**, 1525.
29) O. Simamura, Private communication. The authors are indebted to Professor O. Simamura who kindly made his data available to us prior to publication.
30) E. D. Hughes, C. K. Ingold and N. A. Taher, *J. Chem. Soc.*, **1940**, 949.
31) K. B. Wiberg and T. M. Skryne, *J. Am. Chem. Soc.*, **77**, 2774 (1955).
32) H. P. Rothbaum, I. Ting and P. W. Robertson, *J. Chem. Soc.*, **1948**, 980.
33) C. K. Ingold, "Structure and Mechanism in Organic Chemistry", Cornell University Press, Ithaca, N. Y. (1953), p. 332.
34) S. N. Ege and K. W. Sherk, *J. Am. Chem. Soc.*, **75**, 354 (1953).
35) A. C. Nixon and G. E. K. Branch, ibid., **58**, 492 (1936).
36) H. H. Jaffé and R. W. Gardner, ibid., **80**, 319 (1958).
37) E. J. DeWitt, C. T. Lester and G. A. Ropp, ibid., **78**, 2101 (1956).
38) C. H. Gudmunsen and W. E. McEwen, ibid., **79**, 329 (1957).
39) C. K. Hancook, R. F. Gilby, Jr. and J. S. Westmoreland, ibid., **79**, 1917 (1957).

oxidation of the *cis*-dimethylstilbenes in benzene at 30°C, with Brown's and the present equations.

Discussion

As measured by the standard deviations, the fit is as excellent as that seen in the representative Hammett correlation[12]. It is also clear that the present relationship describes rather precisely or is applicable to a greater extent of electrophilic reactions than the Brown and Okamoto's.

According to the results, r varies over a wide range from 0.2 to 2.3 with respect to the change in reaction, and ρ also from -12 to -0.6. Furthermore, it is significant that the magnitudes of $\Delta\sigma_R^+$ are maintained precisely constant with large variation of ρ and r values. The r and ρ values obtained through Eq. 4 are usually equal within experimental uncertainty to those obtained on the basis of meta correlation line.

In comparison with Brown and Okamoto's results[2,10], the following facts may be pointed out. Brown and Okamoto's ρ^+ values appear to be somewhat more negative than ρ of the present paper, in the reactions giving r values greater than unity. Conversely, they are less negative than the present one when $r<1$. Considering that the present ρ values are identified with the corresponding ρ_{meta} values, it is clear that Brown and Okamoto's equation over- or under-corrects the validity of resonance contribution in these reactions. Only in the reactions having r within 0.7~1.3, the Brown and Okamoto's equation would be apparently successful. This indicates the limitation of the application of Brown and Okamoto's relationship[40]. The application for the reactions far out of the limitation would involve the possibility to lead to some erroneous conclusion. However, a relatively large number of reaction series in the literature appears to be involved in the region of r within 0.7~1.3. Then, the Brown and Okamoto's relationship would be applicable to a considerable extent of reaction series at the practical ground[2,10].

The modified Hammett relationship proposed in this paper involves an additional parameter and variable. The former is defined as a resonance parameter for a given substituent, but the latter is merely a proportionality constant in view of the origin of this equation. Accordingly, it is of interest and necessary to know the character of the latter quantity. Although both ρ and r are varied significantly with respect to the change in reaction series, the variation of r value does not appear to be dependent upon the change in ρ value. In the Beckmann rearrangement of acetophenonoximes in sulfuric acid (*30*)[6] and that of oxime picrylethers in dichlorobutane (*29*)[23], ρ differs greatly but r exhibits an identical value. The identical r value may give a good account of the close similarity of both transition states regardless of the different leaving groups and reaction conditions, while, little is described on the transition state model by the different ρ values. In the solvolysis of aryldimethylcarbinyl chlorides[2] and neophyl brosylates[22], the change in r is significant relative to the change in ρ. This may interpret plausibly the different modes of the resonance stabilizations of both transition states.

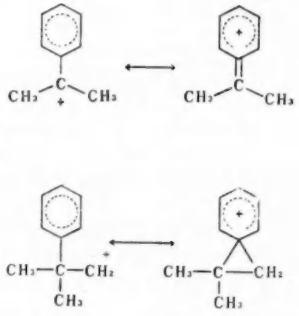

Therefore, it might be acceptable to say that the r would be a parameter characteristic of the structure of the possible transition state model as well as a parameter measuring the availability of the transition state resonance. As seen in Table I, approximately constant r of 1.2 is given for the reaction series to produce benzhydryl carbonium ions, and r of about 0.8 for those to produce trityl carbonium ions. The relatively small fluctuation would be presumably within experimental uncertainty. Unfortunately, few data are available in the literature to examine this concept more precisely.

40) The reactions quoted by Brown and Okamoto contains the reactions giving r less than 0.6 or more than 1.5. The standard deviations of these are slightly large, but the significant trend of curvature would not always parallel the standard deviation. It is evidently suggested by the difference between ρ^+ resulted and ρ_{meta} values.

The remaining subject of interest will be the theoretical consideration of the present relationship 2, and then the resonance substituent constant, $\Delta\sigma_R^+$.

The substituent effect would be considered to consist of inductive and resonance components[41,42], and the σ constant defined by Hammett is usually expressed by Eq. 5[2,41,42],

$$\sigma = \sigma_I + \sigma_R \qquad (5)$$

where σ_I is the inductive effect and σ_R is the resonance polar effect[42] of the substituent. Recently, Taft has evaluated the σ_I values by modifying his σ^* values for aliphatic series[42,43] on the basis of the Roberts' σ' scale[44], and the σ_R values by subtracting the σ_I values from the corresponding Hammett σ constants. It is well known that the substituent constant would not always be independent of the reaction nature. This would be referred to differing contributions of the resonance component of substituent effect[41], independently of the inductive component.

Furthermore, Taft has suggested that the linear free energy relationship would hold as far as the inductive component of reactivity is concernced[45].

Consequently, the Hammett equation may be expressed by Eq. 6,

$$\log k/k_0 = \rho_I\sigma_I + \boldsymbol{R} \qquad (6)$$

In theory, the linear free energy relationship should suffice for the respective one of several components of substituent contribution[46]. If the residual $\boldsymbol{R}$, $\log k/k_0 - \rho_I\sigma_I$, consists of only the resonance contribution, the linear resonance energy relationship may be predictable in regard to the quantity, $\log k/k_0 - \rho_I\sigma_I$.

$$\log k/k_0 - \rho_I\sigma_I = \boldsymbol{R} = \rho_R\bar{\sigma}_R \qquad (7)$$

where ρ_R is a reaction constant and $\bar{\sigma}_R$ is a proper parameter representing the resonating capacity of the substituent. Eq. 7 can be rewritten as Eq. 8,

$$\log k/k_0 = \rho(\sigma_I + q\bar{\sigma}_R) \qquad (8)$$

where $\rho = \rho_I$ and $q = \rho_R/\rho_I$.

Here, $\bar{\sigma}_R$ should be essentially identical with σ_R in Eq. 5 since the $\bar{\sigma}_R$ corresponds to σ_R in the representative Hammett correlations. This relationship may be reasonably adopted also to electrophilic reactions.

On the other hand, the present equation can be formulated as Eq. 9,

$$\log k/k_0 = \rho(\sigma_I + \sigma_R + r\Delta\sigma_R^+) \qquad (9)$$

Combining Eqs. 8 and 9, Eq. 10 is derived.

$$q\bar{\sigma}_R = \sigma_R + r\Delta\sigma_R^+ \qquad (10)$$

Then, the linear relationship 11 must be derived, considering $\bar{\sigma}_R$ is identical with σ_R in Eq. 5,

$$\Delta\sigma_R^+ = q'\sigma_R \qquad (11)$$

where q' is equal to $(q-1)/r$

The exact value of σ_R is difficult to evaluate, but it is logical to replace conveniently the theoretical values by the corresponding Taft's one. In practice, using the Taft's values instead of the σ_R, an apparently linear plot of $\Delta\sigma_R^+$ is provided, as shown in Fig. 12; given q' is equal to 0.962, the standard deviation of the fit being 0.121. If the Taft's σ_R value could describe suitably the σ_R component, it might be possible to realize generally the linear resonance energy relationship

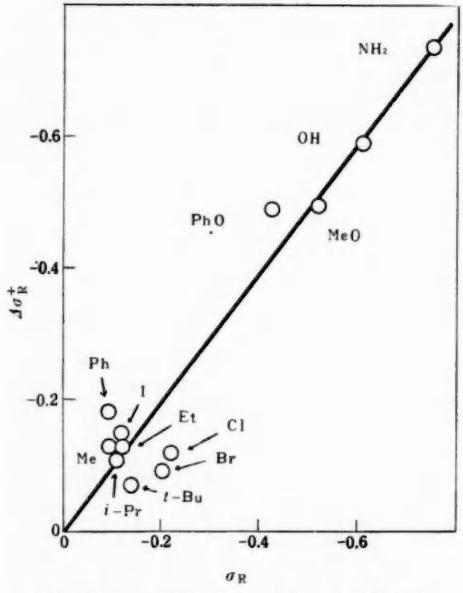

Fig. 12. Correlation of $\Delta\sigma_R^+$ with Taft's σ_R values.

41) The contributions of other specific effects such as solvation and bond energy effects are also involved but they are usually small relative to the above components.

42) R. W. Taft, Jr., in Newman's "Steric Effect in Organic Chemistry", Chapt. 13, John Wiley & Sons, Inc., New York (1956).

43) R. W. Taft, Jr., *J. Am. Chem. Soc.*, **74**, 2729 (1952); ibid., **74**, 3120 (1952); ibid., **74**, 4231 (1953).

44) J. D. Roberts and W. T. Moreland, Jr., ibid., **75**, 2167 (1953).

45) R. W. Taft, Jr., ibid., **80**, 2436 (1958).

46) Y. Yukawa and Y. Tsuno, see the *refrence* under Ref. 13; G. E. K. Branch and M. Calvin, "Theory of Organic Chemistry", Prentice-Hall, Inc., New York (1941), p. 192.

7, therefore, the general Hammett relationship 8. Then, it might be also possible to derive the unique set of σ_R and σ_I on the basis of the present results. However, Taft's σ_R value is by no means excluded from discussion, even though it may be acceptable from a theoretical standpoint. It is a question, at first, whether the Roberts' σ' scale may correspond strictly to that of the inductive effect in benzene system or not. The uncertainty of σ^* increasingly remains in his σ_I value, and must be accumulated in his σ_R value. Furthermore, the actual correlation of electrophilic reactions with his parameters is of considerably poorer precision[47]. On the other hand, $\Delta\sigma_R^+$ stands on a reasonable assumption that the increment of σ^+ relative to σ constant is attributed only to the resonance contribution. The uncertainty derived into this parameter may be entirely referred to only the experimental error of Brown and Okamoto's σ^+.

From these viewpoints, the general Hammett relationship with the parameters derived from $\Delta\sigma_R^+$, if possible, appears to be far more reliable than that with Taft's σ_I and σ_R values. However, it is the generality of Eq. 2, then the $\Delta\sigma_R^+$, that must be settled first. Unfortunately, further examination of the generality is limited by the lack of adequate data in literatures. The adequate literature data which contain rates of many meta derivatives constitute only one third of the data quoted in Table I. Without these reactions, the correlation obtained on the basis of Eq. 4 can not be referred to any standard of correlation such as meta line, although these are believed to be the best descriptions of their respective situations. Moreover, the utilities of $\Delta\sigma_R^+$ values for substituents more negative than *p*-methoxyl group have been scarcely examined at all. Then, the adequate data are highly desirable.

However, the excellent fit of the present relationship for 35 reaction series may be taken to be sufficient support for regarding this as a general relationship. Further investigations now in progress will be reported in forthcoming papers.

Institute of Scientific and Industrial Research
Osaka University
Sakai, Osaka

47) This conclusion is independent of Taft's results (Ref. 45). According to his result in the latest paper on the correlation of Brown and Okamoto's reference reaction, remarkable deviations are observed for *p*-CH_3O and *p*-F derivatives. Full discussion will be made in a proceeding paper, although his treatment disagrees with our concept.

Investigation on Mixed Complexes. II[1]. *Cyano Complexes of Copper and Nickel*

By Sigeo KIDA

(Received October 13, 1958)

A number of studies[2] have been made on the successive formation constants (k_1, k_2, k_3,.....) in a solution of metallic complexes, and it was found[3] that in any complex the ratio of the formation constants ($k_1 : k_2 : k_3$.....) is not far different from the statistically expected one, except in some special cases. Furthermore, recent studies of Watters et al.[4], Marcus[5], Yamatera[6] and the present author[1] have shown that the mixed complexes are formed generally in the statistical way.

These facts seem to imply that in a metallic complex the strength of a co-ordination bond is not seriously influenced

1) Part I of this series: S. Kida, This Bulletin, **29**, 809 (1956).
2) For instance, J. Bjerrum, "Metal Ammine Formation in Aqueous Solution", P. Haase and Son, Copenhagen (1941).
3) J. Bjerrum, *Chem. Revs.*, **46**, 381 (1950).
4) J. I. Watters, A. Aaron, and J. Mason, *J. Am. Chem. Soc.*, **75**, 5212 (1953); R. DeWitt and J. Watters, ibid., **76**, 3810 (1954).
5) Y. Marcus, *Acta Chem. Scand.*, **11**, 339, 599, 610, 811 (1957).
6) H. Yamatera and K. Ohashi, Presented at the Symposium on the Co-ordination Compounds, Nagoya, Japan (1957).

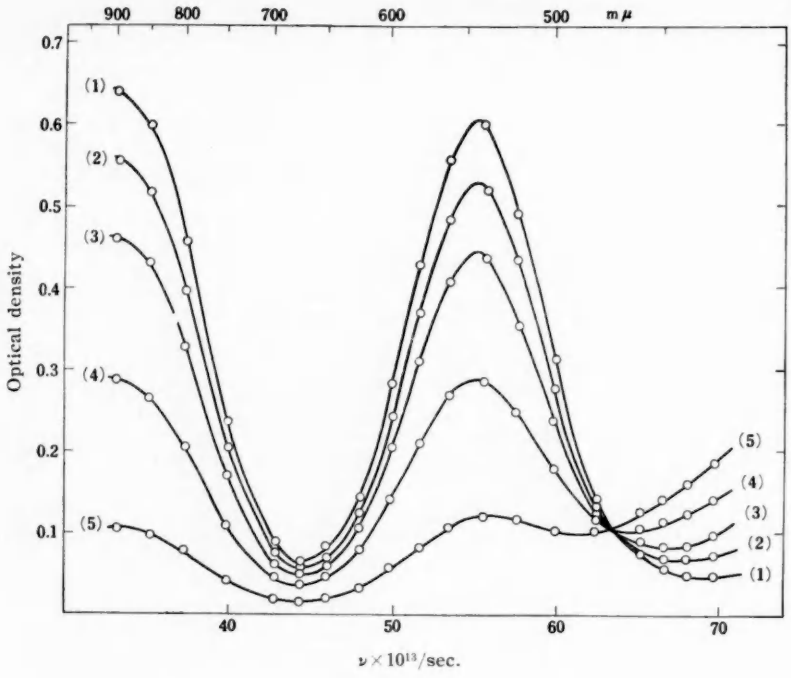

Fig. 1.

by the neighboring ligand; e.g., the strength of the Cu–N bonds are nearly constant in the two complexes, $[Cu\,en_2]^{2+}$ and $[Cu\,en\,C_2O_4]$.

However, it also should be noted that there are many cases in which the formations of the mixed complexes seem not to obey the above-mentioned statistical rule. For instance, the mixed cyano complexes known hitherto are few[7], and difficult to be prepared; this fact would be regarded as suggesting that at least in some cases mixed cyano complexes are not able to be formed or, if it is possibe, they have a strong tendency to be transformed into a complex having only the cyanide ions as ligands. Unfortunately, there is no satisfactory explanation for this phenomenon, since no systematic investigation has ever been made on the conditions leading to the formation of mixed cyano complexes.

This paper will give a report of the investigation which was made for the purpose of getting a clue to this problem.

Results and Discussion

$[Ni\,en_2]^{2+}+CN^-$.—It is well known that the tris-ethylenediamine nickel(II) ion has octahedral configuration, while the tetracyano nickelate(II) ion the planar one. However, it is quite uncertain whether mixed complexes, $[Ni\,en_2(CN)_2]$ and $[Ni\,en(CN)_2]$, which should be closely related to the above-mentioned, can be formed, or not. At first, an attempt, therefore, has been undertaken to clarify this question*.

A sodium cyanide solution was added to a solution of tris-ethylenediamine nickel(II) perchlorate in the ratio as indicated

TABLE I. THE COMPOSITION OF SOLUTIONS

Solution number	(1) cc.	(2) cc.	(3) cc.	(4) cc.	(5) cc.	(6) cc.
0.2 F $[Ni\,en_3](ClO_4)_2$ and 0.1 M en	10	10	10	10	10	10
1.096 F NaCN	0	1	2	4	6	8
Water	10	9	8	6	4	2

7) J. C. Bailar, "The Chemistry of the Coordination Compounds", p. 87; "General Survey", Reinhold Publ. Co., New York (1956).

* Ammine-cyano-nickel(II) compounds, such as $Ni(CN)_2NH_3$, $Ni(CN)_2NH_3H_2O$ and $Ni(CN)_2NH_3C_6H_6$, have been known. [E. E. Aynsley and W. A. Campbell, *J. Chem. Soc.*, **1958**, 1723; K. A. Hofmann and F. Hochtler, *Ber.*, **36**, 1149 (1903)]. However, they are not touched on in this article, since they have complicated structures quite different from that of the mixed complexes in which we are interested here (J. H. Rayner and H. M. Powell, *J. Chem. Soc.*, **1952**, 319).

TABLE II

	(1)	(2)	(3)	(4)	(5)	(6)
([Ni]−1/4[CN])/[Ni]	1.00	0.863	0.726	0.452	0.178	0
D/D_1 for 900 mμ	1.00	0.867	0·719	0.450	0.163	0
for 580 mμ	1.00	0.859	0.714	0.459	0.162	0
for 560 mμ	1.00	0.862	0.718	0.453	0.160	0
1/4[CN]/[Ni]			0.274	0.548	0.822	1.00
D/D_6 for 310 mμ			0.275	0.550	0.841	1.00
for 330 mμ			0.280	0.556	0.816	1.00

Numbers in the first row denote solution numbers in Table I.

in Table I, and extinction measurements were carried out on each of the mixed solutions thus prepared. The results obtained are shown in Fig. 1.

The extinction curves in Fig. 1 tell us that only the tetracyano nickelate(II) and tris-ethylenediamine nickel(II) ions are present, no mixed cyano-amine complex being formed; if any of the mixed complexes were formed, the absorption curve would be more or less subject to deformation, or some new absorption maximum would appear correspondingly.

If we assume all of the added cyanide ion is consumed to form the tetracyano nickelate ion, the calculated values of ([Ni]−1/4[CN])/[Ni] and 1/4[CN]/[Ni] must accord with the experimentally obtainable values, D/D_1 and D/D_6, respectively, where [Ni] and [CN] denote the total concentration of all nickel species and the total concentration of cyanide ion in the solution and D_n is the optical density of the solution, n, shown in Table I and Fig. 1**. Actually, the satisfactory agreement between them can be found as is seen from Table II.

$[Cu\,en_2]^{2+}+CN^-$. — The experiment has been carried out to verify whether the mixed complex such as $[Cu\,en(CN)_2]$ can be formed, or not, when a sodium cyanide solution is added to a solution of bis-ethylenediamine copper(II) perchlorate. Extinction mesurements were made on each of the mixed solutions shown in Table III. The results are shown in Fig. 2.

TABLE III. THE COMPOSITION OF SOLUTIONS

Solution number	(7) cc.	(8) cc.	(9) cc.	(10) cc.	(11) cc.	(12) cc.
0.02 F $[Cu\,en_2](ClO_4)_2$ and 0.01 F NaOH	10	10	10	10	10	10
0.1096 F NaCN	0	1	2	4	6	8
Water	10	9	8	6	4	2

The extinction curves in Fig. 2 indicate that none of the mixed complexes such as $[Cu\,en(CN)_2]$ is existent in the solutions, because the absorption band (due to $[Cu\,en_2]^{2+}$) does not shift at all, being fixed at 500mμ, and yet none of the new absorption bands appears in the shorter wavelength region.

If we assume that four cyanide ions are consumed to convert a copper amine complex into a cyano complex, the calculated value, ([Cu]−1/4[CN])/[Cu], must accord with the experimentally obtainable value, D/D_7, as in the case of nickel. Actually the accordance can be found in Table IV, though it is not so satisfactory as in the case of nickel. Since cyanide complexes of divalent copper can not exist, the following reaction would have possibly occurred:

$$[Cu(en)_2]^{2+}+4CN^- \rightarrow [Cu(CN)_3]^{2-}{}^{***}+1/2(CN)_2+2\,en$$

Stability constants of copper(I) cyanide complexes were determined by Penneman and Jones[8].

$$k_1k_2=[Cu(CN)_2^-]/[Cu^+][CN^-]^2=1\times10^{24}$$

$$k_3=[Cu(CN)_3^{2-}]/[Cu(CN)_2^-][CN^-]=3.8\times10^4$$

$$k_4=[Cu(CN)_4^{3-}]/[Cu(CN)_3^{2-}][CN^-]=50$$

From these data, it seems quite natural that tricyano copper(I) complex is mainly formed.

It must be noted that the possibility of

** If the reaction, $[Ni\,en_3]^{2+}+4\,CN^-\rightarrow[Ni(CN)_4]^{2-}+3\,en$, takes place quantitatively, optical densities of the mixed solutions can be given as follows:

$$D=\varepsilon_1([Ni]-1/4\,[CN])+\varepsilon_2(1/4[CN]),$$

while, for the solutions (1) and (6), $D_1=\varepsilon_1[Ni]$, and $D_6=\varepsilon_2[Ni]$, where ε_1 and ε_2 are extinction coefficients of $[Ni\,en_3]^{2+}$ and $[Ni\,(CN)_4]^{2-}$, respectively. However, the ratios D/D_1 and D/D_6 may be reduced for some wavelength region: for the region of 900~560 mμ, $D/D_1=[(Ni]-1/4[CN])/[Ni]$ with $\varepsilon_2=0$, and for the region of 400~220 mμ, $D/D_6=1/4[CN]/[Ni]$ since ε_1 is quite small as compared with ε_2.

*** For this complex the 4-coordinated configuration such as $[Cu(CN)_2OH_2]^{2-}$ or $[Cu(CN)_2\,en]^{2-}$, may be also considered. However, this is represented tentatively as $[Cu(CN)_3]^{2-}$, and the discussion of this complex will be done in the next section.

8) R. A. Penneman and L. H. Jones, *J. Chem. Phys.*, **24**, 293 (1956).

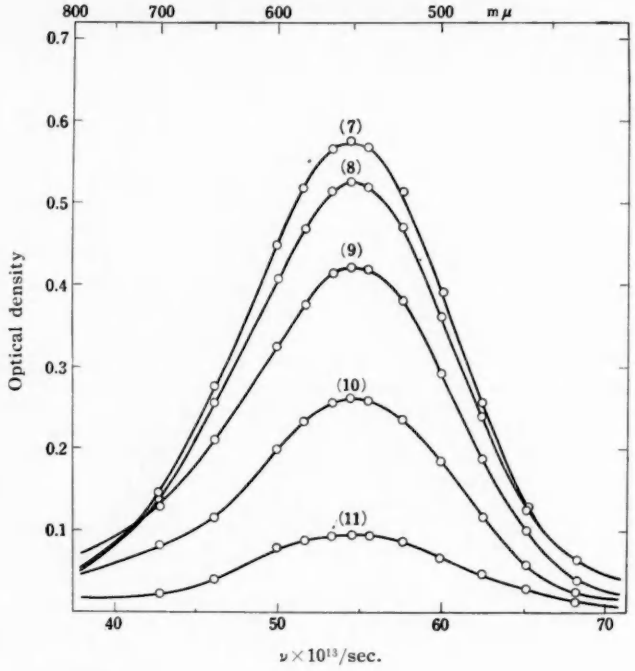

Fig. 2.

TABLE IV

	(7)	(8)	(9)	(10)	(11)	(12)
([Cu]−1/4[CN])/[Cu]	1.00	0.863	0.726	0.452	0.178	0
D/D_7 for 600 mμ	1.00	0.916	0.728	0.450	0.176	0
for 550 mμ	1.00	0.918	0.734	0.458	0.166	0
for 520 mμ	1.00	0.913	0.738	0.456	0.165	0

Numbers in the first row denote solution numbers in Fig. 2.
[Cu] is the total concentration of all copper species in solution.

the existence of a complex of coordination number 5 such as $[Cu\,en_2\,CN]^+$ can not be denied; the formation of this complex might be the cause of the unsatisfactory accordance of the calculated value with the experimental one unlike the case of nickel.

$[Cu(CN)_3]^{2-}$ + en.—Absorption spectra of the tricyano copper(I) complex were measured both with and without excess of ethylenediamine, and it was found that both absorption curves completely coincide within the limit of the experimental error. This fact suggests that the tricyano copper(I) complex does not take an ethylenediamine molecule in the solution to form the mixed complex such as $[Cu(CN)_3\,en]^{2-}$, and that the coordination number of the tricyano copper(I) complex may be 3 (perhaps sp^2 hybridization); if the coordintaion number were 4, the tricyanocopper(I) complex would have the configuration such as $[Cu(CN)_3\,OH_2]^{2-}$, and it would become the mixed complex, $[Cu(CN)_3\,en]^{2-}$, when the ethylenediamine is added to the solution.

$[Cu(CN)_2]^-$ + en.—When ethylenediamine is added to a solution of the dicyano copper(I) complex, the solution becomes turbid and light blue, and then slowly changes into a transparent purple blue solution. The absorption spectrum of this solution completely coincides with that of the bis-ethylenediamine copper(II) complex in the visible region.

From the above results, we can easily understand the fact that neither dicyano nor tetracyano copper(I) complex is formed, but tricyano copper(I) complex, when the cyanide solution is added to the

bis-ethylenediamine copper(II) complex solution.

Experimental

Extinction measurements were made by means of the Beckman D. U. spectrophotometer using 1 cm. quartz cells at room temperature.

In the case of $[Cu\,en_2]^{2+}+CN^-$, each of the solutions prepared as shown in Table III was heated just to boiling, and then cooled to the room temperature before extinction measurements were made; without this treatment, extinction data obtained are not reproducible.

$[Ni\,en_3](ClO_4)_2$ and $[Cu\,en_2](ClO_4)_2$. — The metal quantity of the former was analyzed with dimethylglyoxime, and that of the latter was determined by iodometry.

$[Cu(CN)_2]^-$ and $[Cu(CN)_3]^{2-}$ (in solution). —The copper(I) cyanide was dissolved in the potassium cyanide solution at the ratio of 1 : 1 and 1 : 2 to form these complexes, respectively.

Summary

1. Mixed amino-cyano nickel(II) complexes, such as $[Ni\,en_2(CN)_2]$, $[Ni\,en\cdot(CN_4)_4]^{2-}$ and $[Ni\,en(CN)_2]$ in the solution containing the divalent nickel ion, ethylenediamine and cyanide ion, are not formed.

2. In the solution containing the divalent or the monovalent copper ion, ethylenediamine and the cyanide ion, no mixed amine-cyano copper(I) and copper(II) complexes are formed, except the copper-(II) complex of coordination number 5.

3. Among cyano copper(I) complexes, tricyano copper(I) ion is the most stable, and its coordination number may be 3.

The author wishes to express his sincere thanks to Professor R. Tsuchida of Osaka University for his kind advice and encouragement during this work. The author's appreciation is also expressed to Dr. H. Yoneda for his helpful discussion.

Department of Chemistry
Wakayama University
Masago-cho, Wakayama

---

*Stereoisomers of 2,3-Camphane Diols**

By Tsuneichi TAKESHITA and Masayoshi KITAJIMA

(Received November 21, 1958)

There should exist four possible diastereoisomeric camphane-2,3-diols, which in spite of having been prepared by several authors[1], were mostly obtained as mixtures of isomers, with its single epimer believed to have been isolated in fairly pure state by Rupe and Thommen[2]. Therefore, conformation of each epimer has not been established at all. Only Kwart and Gatos[3,4] recently assigned the structure to the one isomer of the Rupe and Thommen diol with positive evidence of infrared spectra and complex formation. It became then the purpose in these studies to isolate all theoretically possible diols and assign conformation; and, if possible, to correlate the isomeric composition of the diols prepared by various methods with the mode of reaction. Several facts which have been clarified are presented in this report. As the authors have hitherto studied *endo-* and *exo-* isomers of borneols and their epimerization[5,6], the hydrogenation of camphorquinone was similarly followed.

Synthesis of Four Stereoisomers.—Four epimers, namely *exo-exo-* (I), *endo-endo-* (II), *endo-exo-* (III), and *exo-endo-* (IV) may possibly result by reduction of camphorquinone. Effective isolation of pure

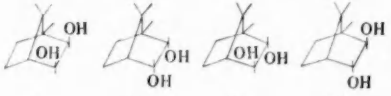

I II III IV

Fig. 1. Stereoisomers of 2,3-camphane diols.

* Partly presented at the Symposium on Terpenes, Kinki Univ., Nov. 30, 1957.

1) O. Mannase, *Ber.*, **30**, 659 (1897); ibid., **35**, 3811 (1902).

2) H. Rupe and W. Thommen, *Hev. Chim. Acta*, **30**, 933 (1947).

3) H. Kwart and G. C. Gatos, *J. Am. Chem. Soc.*, **80**, 881 (1958). The present author is indebted to Dr. H. Kwart for his kind advice and suggestion, and to Dr. S. J. Angyal for his unpublished reslut.

4) S. J. Angyal recently isolated four diols in fairly pure state. (A. C. S. Meeting, Sept., 1957, New York).

5) T. Takeshita and M. Kitajima, *J. Chem. Soc. Japan, Pure Chem. Sec.* (*Nippon Kagaku Zasshi*), **78**, 994 (1957).

6) T. Takeshita and M. Kitajima, ibid., **79**, 1468 (1958).

TABLE I. INFRARED SPECTA OF *cis*-DIOLS

	Free	Int.	Intra	Int.	Inter	Int.	$\Delta\nu$	OH-O[3]	Ratio (%)	Assignment
I	3630	0.151	3540	0.270	3380	0.440	90	1.5 Å	291.4	*exo-exo-*
II	3630	0.127	3535	0.300	3385	0.529	95	1.5 Å	416.5	*endo-endo-*

Concn. 20.0 mg./ml. CS_2; Cell length 0.5 mm. Free Int., Intra Int. and Inter Int. are peak intensity at free, intra-molecular and inter-molecular O–H stretching.
Ratio Inter, Int./Free, Int.

isomers can be achieved by selecting the procedure yielding the least number of components, and this would be possible by avoiding the method of reduction which may cause isomerization of the hydroxyl group which was entered. As proved in the epimerization of borneol by the authors, such reducing agents as copper chromite, sodium or aluminum isopropylate are effective catalysts of epimerization[6]. Therefore, these were not used for the present purpose. Reduction with lithium aluminum hydride and Raney nickel were the methods mostly utilized for this purpose.

When camphorquinone absorbs 1 molar hydrogen, it leads to hydroxy-ketone and giving a diol on further reduction. As an analogous mode of reduction of camphor, Raney nickel or lithium aluminum hydride should give *exo-* and *endo-* isomer with a preponderance of the former. Hydroxy-ketone obtained by these methods can now be assumed to be isomeric with "α-hydroxycamphor" (V) and "β-hydroxycamphor" (VI) by zinc- acetic acid reduction. $LiAlH_4$ reduction of camphorquinone is expected to yield one *cis-* and two *trans-*isomers. On the other hand, however, further reduction of V or VI, separated from each other, should lead to one *cis-*, one *trans-*, respectively. A *cis*-diol can thus be easily purified in $LiAlH_4$ reduction, but it must be somewhat hard in the case of *trans*-diol to purify one from another.

cis-Diol I.—Camphorquinone in ether was reduced with lithium aluminum hydride after Trevoy and Brown's method[7] at dry-ice temperature. Crude *cis*-diol was converted to acetonide, rectified over a sodium ribbon till no more O–H absorption is detected in the 3500 cm^{-1} region of infrared spectra**. After regeneration of the diol, it was recrystallized from ligroin and repeatedly sublimed in vacuo.

cis-Diol II.—"β-Hydroxycamphor" VI purified through its dimolecular methyl ether[8] was hydrogenated over Raney nickel at room temperature, a *cis*-diol was separated from one *trans*-isomer and purified similarly as in the case of I.

trans-Diol III.—The *trans*-diol separated from II in the foregoing reduction product was repeatedly treated with acetone to remove any trace of remaining *cis*-diol.

trans-Diol IV.—The *trans*-diol isolated from Raney nickelhydrogenated diols of "α-hydroxycamphor" V was further purified like III.

Assignment of Conformation.—Tentative assignment of *cis*-I, II and *trans*-III, IV were separately performed by comparison with I.R. spectra at O–H region.

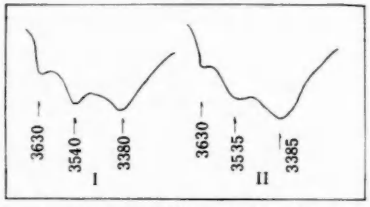

Fig. 2. O–H stretching region (*cis*-diols) CS_2 soln.

The bands at 3540 are intra-molecular O–H; and difference from free O–H, $\Delta\nu = 90$, in case of I and 195 in case of II, corresponds to 1.5Å for O–H distance. Concerning the inter-molecular band, intensity of associated O–H/free O–H is a measure of the ease with which solute associates. Thus, as proved in case of borneol[5], the degree of association is far less in *exo-* than that in *endo-*, owing to *gem-* dimethyl hindrance. Of the two *cis*-diols investigated, I can not associate so much as II since the ratio obtained is 291.0 and 416.0%, respectively. Therefore, so far as two *cis*-epimers are concerned, I can be assigned as *exo-*, and II, in turn, as *endo-*. These assigned stuctures of I and II are satisfied with some difference of chemical property,

TABLE II. SAPONIFICATION OF *cis*-DIOL DIACETATES

Isomer	0.1 N KOH, hr.	% Sap'd 25±1°C
I	3	62.9
II	3	69.1

7) L. W. Trevoy and W. G. Brown, *J. Am. Chem. Soc.*, **71**, 1675 (1949).
** No isomerization of acetonide occurs by distillation over sodium (by I. R.).
8) J. Bredt, *J. prakt. Chem.*, **121**, 153 (1929).

TABLE III. INFRARED SPECTRA OF *trans*-DIOLS

	Free	Int.	Inter	Int.	Ratio	Concn.	Assignment
III	3625	0.232	3450	0.064	27.6%	100.0 mg./10 ml.	*endo-exo-*
IV	3620	0.234	3440	0.057	24.4	〃	*exo-endo-*
III	3620	0.280	3440	0.099	35.4	120.0	*endo-exo-*
IV	3620	0.282	3440	0.085	30.1	〃	*exo-endo-*

Cell length 0.5 mm.

that is, the difference of saponification velocity of corresponding diacetate, as shown in Table II.

The slower saponification rate of I coincides well with the assignment by I. R. And as will be reported in a later paper[9], epimerization of I resulted in a great preponderance of II over I. This corresponds with the known stability of *endo*-isomer in case of borneol.

trans-Diols, III and IV, were similarly compared on the infrared spectra. Although associated OH can best be compared in CCl_4 or CS_2 because a solvent molecule such as $CHCl_3$ is known to prevent intermolecular association of solute***, spectra were taken in $CHCl_3$ solution on account of sparing solubility of *trans*-diol in CS_2****. Therefore, the difference of ratio of polymeric OH/free OH between III and IV was not one-sided as in the case of *cis*-diols. Table III shows comparison of spectra.

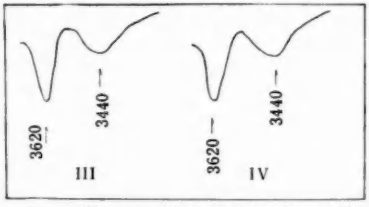

Fig. 3. O-H stretching region (*trans*-diols) $CHCl_3$ soln.

Steric hindrance of *gem*-dimethyl is usually more profound at C_2 than at C_3 because of proximity of adjacent quaternary methyl. That the steric effect of *gem*-dimethyl observed for C_3-OH is not significant has been reported on epi-borneol by Lipp et al.[10] Therefore, an isomer with more bonded OH is suggested to be *2-endo-3-exo-*. This tentative assignment is also supported by the fact that the di-acetate of III is saponified faster than that of IV, as shown in Table IV.

TABLE IV. SAPONIFICATION OF *trans*-DIOL DIACETATES (25±1°C)

Isomer	0.1 N KOH hr.	% Sap'd
III	2	73.1
IV	2	61.3

The properties of four diasteroisomeric diols isolated are summarized in Table V.

TABLE V. PROPERTIES OF DIOLS

Isomer	m. p.(°C)	$[\alpha]_D$	O-H dist.	Conformation
I	262~263	−19.3	1.5 Å	*2-exo-3-exo-*
II	224~225	+30.8	1.5	*2-endo-3-endo-*
III	253~254	+15.0	(3.3)	*2-endo-3-exo-*
IV	251~252	+ 7.7	(3.3)	*2-exo-3-endo-*

Isomeric Composion of Diols by Various Methods of Syntheses.—Diols prepared by direct reduction of camphorquinone and by further reduction of hydroxyketone obtained by zinc-acetic acid reduction of camphorquinone were studied then by infrared spectra. The result of one-step hydrogenation is given in Table VI.

Catalytic hydrogenation affords mainly *cis*-I with some II, *trans*-diols increase with rise of reaction temperature. Therefore, reduction at room temperature easily gives *cis*-diols (I+II) in over 90% yield, though *cis*-I is not easy to purify.

$LiAlH_4$ reduction was much influenced by temperature on the reaction product, *cis*-diol obtained at −70°C being exclusively *exo-*, while that of 0°C was contaminated with *endo-*. Thus, the reduction at dry ice temperature is the procedure employed in this paper for the preparation of uncontaminated *cis-exo*-diol. The Meerwein-Pondorff-Verley type reduction of camphorquinone yielded a characteristic product that consisted of *cis*-diols solely, with very few *trans* isomers. And moreover, II increased considerably, compared with other procedures.

Diols Prepared by Hydrogenation of Hydroxy-camphor. — Camphorquinone

9) T. Takeshita, Presented at the Symposium on Terpenes, held at Hiroshima University, Oct. 10, 1958.

*** The association of ROH in $CHCl_3$ is known to be less than in CS_2. The effect of $CHCl_3$ must be the hydrogen bonding power of CH besides the polarity or molecular size of solvent. (Cf. L. J. Bellamy, "The Infra-Red Spectra of Complex Molecules", Methuen and Co, London (1958), p. 100.

**** Limited solubilty of III in $CHCl_3$, less than 130.0 mg./10 ml., makes possible only narrow concentration range for the present purpose, though IV is more soluble.

10) P. Lipp et al., *Ber.*, **68**, 249 (1935).

TABLE VI. REDUCTION PRODUCT OF CAMPHORQUINONE

Expt.	Reducing agent	I	II	III	IV	Remarks	
1	Raney Ni	88	5	1	6	14~20°C	8 hr.
2	〃	75	7	1	17	90~100	9
3	Copper chromite	54	6	9	31	120~150	3
4	Al-(O-*i*Pr)$_3$	60	39	—	1	88	10
5	$LiAlH_4$	89	4	4	3	0	20
6	〃	94	—	3	3	−70	20

TABLE VII. REDUCTION PRODUCT OF HYDROXYCAMPHOR

Expt.	Starting epimer	Reducing agent	I	II	III	IV	Remarks	
7	β-	Raney nickel	—	48	52	—	20~27°C	10 hr.
8	β-	〃	—	41	59	—	29~34	8
9	α-	〃	14	41	—	45	17~18	12
10	α-	〃	12	34	—	54	32~40	6
11	β-	$LiAlH_4$	—	85	15	—	0	20
12	α-	〃	19	69	—	12	0	20
13	β-	Na-EtOH	—	19	16	65	80~90	5
14	α-	〃	—	22	12	66	80~90	5

yields hydroxy-ketone on zinc-acetic acid reduction, which has been reported to consist of α-hydroxycamphor and β-hydroxycamphor[11]. The configuration of this hydroxycamphor is not clear, but must be *endo*-configuration since β-isomer which was regenerated from sparingly soluble dimolecular methyl ether afforded *cis-endo*-diol. The result of reduction of this hydroxyketone also supports this idea as indicated in Table V.

A point to be noticed is that *cis*-diol obtained from β-hydroxycamphor catalytically or with $LiAlH_4$ was *cis-endo*, while that from α-isomer afforded *endo*- mixed with about one third the amount of *exo*-isomer. This shows the homogenity of β-isomer, *endo*- whereas α-isomer was a mixture of *endo*- and *exo*-, in ratio of 3 to 1. The catalytic hydrogenation of hydroxycamphor presents an interesting problem, since predominant *exo*-addition observed in case of camphor[4] was cut to about half to give *trans*-diol. This indicates steric hindrance in opposing direction by *gem*-dimethyl group to that of *endo*-hydroxyl group. Thus, $LiAlH_4$ reduction gives only 15% of *exo*-reduced product because lithium aluminum salt formed with *endo*-hydroxyl group becomes overwhelmingly bulkier than the *gem*-dimethyl, *exo*-directing radical. Sodium with alcohol gave mostly *trans*-diol as the usual mode of *trans*-addition. Similarity of the reduction product is considered to be isomerization of β-hydroxycamphor to α-isomer as seen in Experiments 13 and 14.

11) β-Hydroxycamphor, so designated, is actually α-hydroxy-epicamphor.

Experimental[12]

I. *exo-exo*-2, 3-Camphane-diol.—A solution of camphorquinone (10 g.) in ether was added dropwise at −60°C to −70°C to an ether solution of $LiAlH_4$ (c=1.6 mol./l.) immersed in a methanol-dry ice bath and kept for 20 hr.[6] After decomposition of excess of reagent with water, the whole was washed with dilute sulfuric acid, saturated sodium chloride solution, dried with anhydrous sodium sulfate and the solvent was evaporated to give the *cis*-diol (9.5 g.). Seven grams of crude product was treated with acetone by the procedure of Rupe et al.[2] to give acetonide (8.4 g.), and vacuum distillation afforded some *trans*-isomer (0.43 g.). Acetonide was purified by rectifying over sodium till it showed no more hydroxyl absorption in 3500 region of its infrared spectra, 4 g. of pure acetonide was saponified to regenerate *cis*-diol (2.7 g.), recrystallized from ligroine, and sublimed in vacuo, m. p. 262~263°C, $[\alpha]_D$−19.3 (c=0.50000 g./5 ml.).

II. *endo-endo*-2, 3-Camphane-diol.—"β-Hydroxy-camphor" (27.7 g., m. p. 204~205°C), purified through dimolecular methyl ether (m. p. 147~148°C)[8,13] was hydrogenated in alcohol over Raney nickel at 14~20°C to yield *cis*-diol (28.0 g.) mixed with *trans*-isomer. To isolate *cis*-diol, 20 g. of diol was treated as I with acetone. The solid product (21.0 g.), wet with *cis-endo*-acetonide was extracted with boiling hexane to free it from *trans*-diol. Evaporation of hexane afforded acetonide contaminated with some *trans*-isomer; this was further treated over sodium as I, saponified, recrystallized, and vacuum sublimed.

12) All melting points are uncorrected. All rotations were measured in 1 dm. tube as an alcoholic solution. Infrared spectra were taken with a Perkin Elmer Model 21 Infrared Spectrophotometer equipped with sodium chloride prism.

13) J. L. Simonsen mis-stated the m. p. of the compoud as 37~38°C in "Therpenes", Vol. II, Cambridge University Press, Cambrige (1949), p. 428.

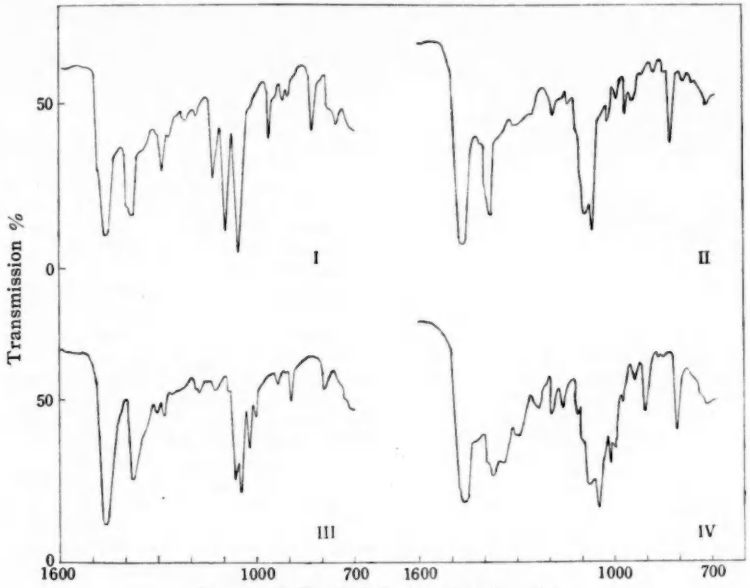

Fig. 4. I. R. of diols (as Nujol mulls)

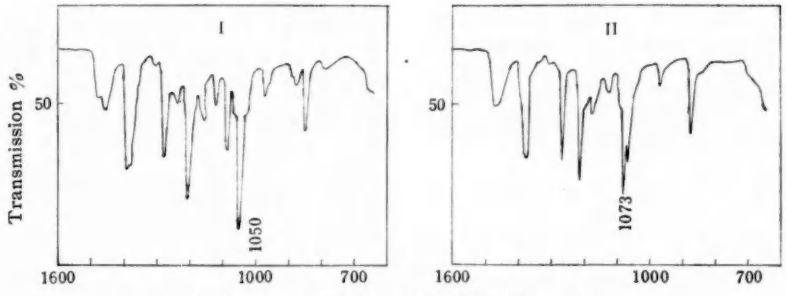

Fig. 5. I. R. of *cis*-acetonide (1600～1650 cm^{-1}) cap.

Yield, 3.6 g., m. p. 224～225°C, $[\alpha]_D$ +30.8 (c= 0.50000 g./5 ml.).

III. *endo-exo*-2,3-Camphane-diol. — The *trans*-diol separated (9.2 g.) in isolation of II was further treated with acetone to remove any trace of *cis*-diol present and recrystallized several times from ligroine and sublimed in vacuo. Yield, 7.5 g., m. p. 253～254°C, $[\alpha]_D$+15.0 (c=0.50000 g. /5 ml.).

IV. *exo-endo*-2,3-Camphane-diol.—Similarly as in the case of III, *trans*-isomer separated from hydrogenation of 8.5 g. of "α-hydroxycamphor" was further treated with acetone, to remove *cis*-isomer, recrystallized sublimed in vacuo, m. p. 251～252°C, $[\alpha]_D$ +7.7 (c=0.50000 g./5 ml.).

Infrared Measurement — All the spectra were taken by Perkin Elmer Model 21 with NaCl Optics. The infrared determination of the isomeric composition of diols which resulted as reduction product was developed as follows.

As stereoisomeric cyclic alcohol usually has a characteristic band around the 1000～1100 region like those of *endo*- and *exo*- borneols[5], the spectra of four isomers are distinguishable (Fig. 4) in this region. These are, however, only effective for qualitative analysis because of the overlapping of bands not at the peaks but at the side of absorption maxima. As shown in the preceding discussion, in dilute solution, *cis*-diols absorb both at 3620 and 3520, while *trans*-isomer does so at only 3620 owing to absence of intra-molecular band of 3520. Thus, *cis-trans* composition can be determined by O—H stretching bands. Individual epimers are then determined by C—O stretching region.

1) Intensity of 3620 and 3520 bands measured.

Diols		3620	Average	3520	Average
cis-	I	0.223	0.217	0.166	0.166
	II	0.211		0.165	
trans-	III	0.351	0.354	0.048	0.046
	IV	0.356		0.044	

Concn. 60.0 mg./10 ml. $CHCl_3$
Cell length 1.2 mm. Room temp. 25±2°C

At the concentration indicated, there was not much variation in optical density between isomers within the same geometrical group (*cis*- or *trans*-), and this presents a rapid method of determination of *cis*- and *trans*-isomers. Trial analysis of some synthetic mixtures of known concentration was found to be accomplished with 2% error, this accuracy being sufficient for the present study.

	cis	*trans*	*cis*	*trans*
Synthetic	II 66.5	IV 33.5	II 33.2	III 66.8
Found	67.2	32.8	34.9	65.1
Synthetic	I 83.2	IV 16.8	III 83.2	III 16.8
Found	85.0	15.0	85.8	14.2

On finding *cis-trans* ratio, determination of each isomer is performed by C—O stretching region.

2) Intensity of C—O stretching region.

Diols	1089	1074	1060
I	0.312	0.095	—
II	0.203	0.282	0.368
III	0.068	0.271	0.168
IV	0.067	0.098	0.401

Concn. 60.0 mg./10 ml. $CHCl_3$
Cell length 0.5 mm.

Fortunately, the 1089 intensity of III and IV does not differ much. *Trans*-contribution at this wave number can be treated as equal in evaluation of *trans* isomers of diols. Compositions III and IV are finally determined after *cis*-diols were removed with acetone as acetonide. Trial analysis was performed with 2% error as follows:

Synthetic	II 66.5	IV 33.5	II 33.2	III 66.8
Found	65.0	35.0	31.0	69.0
Synthetic	I 83.2	IV 16.8	IV 66.5	III 33.5
Found	84.9	15.1	68.3	31.7
Synthetic	III 35.0	IV 65.0		
Found	36.6	64.3		

Thus the ratio of epimers was found to be analyzed on a 2-component system using C—O stretching region with 2% error. However, overall error of analysis amounts to less than 4%, with assay of *cis-trans* ratio combined in analysis of diols. As to *cis*-isomers I and II, characteristic *cis*-acetonide was compared with them. (Fig. 5)

Saponification of Diol Diacetate.—Acetylation of diol was as follows: Each of the diols (3 mmol., 510 mg.) was gently boiled with acetic anhydride (Purity 94.2%, 2.1 g.) and anhydrous sodium acetate (0.4 g.) for 1 hr., settled overnight, the excess of reagent decomposed with 10 ml. of hot water during 2 hr., extracted with ether. After being washed with aqueous solution of sodium chloride, and then sodium bicarbonate, the solution was dried over anhydrous sodium sulfate. Removal of solvent in vacuo, finally by warming at 110°C/7 mmHg afforded slightly colored diacetate oil, in yield ranging from 600 to 700 mg. Purity found. (Theor. Value, Ester Value 441.0 as $(CH_3COO)_2 \cdot C_{10}H_{16}$) Diacetate of I E. V. 427.3, II E. V. 434.5, III E. V. 435.1, IV E. V. 428.1

The diacetate thus prepared was saponified by the usual procedure: Weighed sample, equivalent to 10 ml. of 0.1 N alcoholic KOH, in bottle was immersed in a water bath kept at 25±1°C. To this was added 10 ml. of 0.1 N alcoholic KOH at 25±1°C and maintained at this temperature. Back titration with 0.1 N H_2SO_4 against phenolphthalein gave the amount saponified. (Cf. Table II and IV).

Preparation of Diols by Various Methods.

Expt.	Camphorquinone (g.)	Catalyst		Solvent (ml.)		Temp. (°C)	Time (hr.)	Yield (g.)	m.p. (°C)	$[\alpha]_D$
1	25	Raney Ni	6 g.	EtOH	30	14～ 20	8	25	253～255	−13.9
2	33.2	〃	6 g.	〃	30	90～100	9	33.3	250～252	− 9.6
3	8.3	Copper chromite	3 g.	Benzene	10	120～150	3	7.8	245～249	− 4.6
4	8.3	Aluminum isopropylate	20 g.	IsoprOH	200	85～ 88		4.7	241～242	+ 1.9
5	6.6	$LiAlH_4$	0.04mol.	Ether	30	0	20	6.2	256～257	−16.5
6	10.0	〃	0.06mol.	〃	200	−70	〃	9.5	255～257	−15.7
7	β- 27.7	Raney Ni	6 g.	EtOH	20	20～ 27	10	25.3	232～234	+20.0
8	β- 7	〃	3 g.	〃	15	29～ 34	8	6.2	232～235	+22.6
9	α- 8.5	〃	3 g.	〃	15	17～ 18	12	8.2	235～238	+11.2
10	α- 7	〃	3 g.	〃	15	32～ 40	6	6.8	238～241	+ 8.3
11	α- 4.2	$LiAlH_4$	0.013mol.	Ether	20	0	20	4.0	226～228	+28.7
12	β- 4.2	〃	〃	〃	〃	〃	〃	3.6	229～231	+15.6
13	β- 6.7	Na	9.2 g.	EtOH	150	80～ 90	5	4.8	229～231	—
14	α- 4.0	〃	6 g.	〃	90	〃	〃	3.2	233～234	+11.9

Expts. 1—3) *Reduction of camphorquinone.*—Camphorquinone was hydrogenated in 100 ml. stainless steel autoclave equipped with magnetic stirring-valve. Initial press., 70～120 kg./cm².

Expt. 4) The Meerwein-Pondorff-Verley reduction of camphorquinone was carried out by the usual method, maintaining the inner temperature below 89°C.

Expts. 5 and 6) Lithium aluminum reduction followed after the procedure of Trevoy and Brown[6]. $LiAlH_4$, ether solution (1.6 M).

Expts. 7—10) *Reduction of hydroxycamphor.*—The hydroxycamphor used in the experiment was synthesized after Bredt's method[5]. Catalytic hydrogenation of α- and β-hydroxycamphor were carried out, using Raney nickel.

Expts. 11 and 12) Lithium aluminum hydride reduction is analogous to that of the foregoing.

Expts. 13 and 14) Reduction of hydroxycamphor with sodium in alcohol was by the usual procedure.

Central Research Institute
Japan Monopoly Corporation
Yutaka-machi, Shinagawa-ku
Tokyo

Decomposition Temperature of Urea Adducts

By Naoki YATA

(Received December 16, 1958)

Decomposition temperatures for urea adducts of *n*-hexadecane, *n*-nonadecane, and *n*-paraffins from C_{19}-C_{20} fraction of mineral oil were determined. The results were compared with the data by Redlich et al.[1] and decomposition temperature of *n*-hexadecane by the author was found to be lower than that of Redlich's.

Addition of benzene to the system (adducts and water) results in the lowering of decomposition temperature. This effect becomes remarkable with a decreasing amount of water.

Experimental

Reagents.—Urea (m. p. 132.6°C) was recrystallized from aqueous solution saturated at 30°C. Methanol (b. p. 64~65°C), benzene (b. p. 80~80.5°C) and petroleum ether (b. p. 40~60°C) were redistilled from the commercial product.

n-Hexadecane (commercial) was treated with activated alumina followed by sulfuric acid and sulfur trioxide treatment, m. p. 16.2°C, $n_D^{20}=1.4251$.

n-Nonadecane and *n*-heneicosane were separated from lubricating oil fraction of Yabase crude (b.p. 104~226°C at 3 mmHg) by urea adduction and chemical treatment as mentioned above. Physical constants of these hydrocarbons were compared with the literature values[2,3] and shown in Table I.

Preparation of Adducts.—Adducts from mineral oil (Yabase lubricating oil fraction as described above) were prepared by adding 120 g of urea and 1 cc. of methanol to 150 g. of oil. After the mixed solution being stirred for 50 min., the adduct produced was filtered off and washed with 1500 cc. of benzene. Yield, 150 g. of adducts. Adducts of *n*-paraffins were made from the petroleum ether solution of them. This solution was treated with 3 times of urea to *n*-paraffins, and 0.3 times of methanol, and was stirred for 50 min. The adducts produced were filtered by suction and washed with 30 times the quantity of benzene.

All of these adducts were dried in vacuo until solvent odor was diminished. Analytical data are shown in Table II. Mole ratios in this table were determined by Schiessler's method[4]. Dissociation temperatures were measured by the method of Knight et al.[5]; according to the present author's experiment, dissociation temperatures of *n*-paraffins are quite similar to that of methyl ester which has been measured by Knight et al.

TABLE I. PHYSICAL CONSTANTS OF *n*-NONADECANE AND *n*-HENEICOSANE

Hydrocarbons	Refractive index (n_D^{60})		Melting point (°C)	
	Found	Lit.	Found	Lit.
n-Nonadecane	1.4268	1.4255	31.0	32.0
n-Heneicosane	1.4300	1.4290	40.5	40.5

Procedure.—A small test tube of 2.5 cm. diameter was connected in a large test tube of 4.5 cm. diameter with a rubber stopper. Two

1) O. Redlich, et al., *J. Am. Chem. Soc.*, **72**, 4153 (1950).
2) C. Kroeger and F. Hallfeld, *Erdöl u. Kohle*, **7**, 811 (1954).
3) M. F. Sawer et al., *J. Inst. Petrol.*, **27**, 1 (1941).
4) R. W. Schiessler and D. J. Flitter., *J. Am. Chem. Soc.*, **74**, 1720 (1952).
5) H. B. Knight et al., *Anal. Chem.*, **24**, 1331 (1951).

TABLE II. COMPOSITIONS AND DISSOCIATION TEMPERATURES OF ADDUCTS

Hydrocarbons in adducts	Urea/*n*-paraffin Wt. ratio	Urea/*n*-paraffin Mol. ratio	Dissociation temp. (°C)
Lub. oil paraffin	3.5	—	125
n-Hexadecane	3.1	11.7(12)[6]	112
n-Nonadecane	3.2	14.1(13.9)	129
n-Heneicosane	3.1	14.6(14.6)	129

grams of adduct samples and water were put into the small test tube with a thermometer and a stirrer made of iron wire.

The large test tube was placed in a 500 cc. beaker where warm water was filled in, and heated. Constant hand stirring was continued with temperature rise of about 5°C/min. until a paraffin portion was separated on the upper layer, and this point was considered as the decomposition temperature.

Results and Discussion

Decomposition Temperature.—Table III shows the decomposition temperature, the average value taken from the two measurements. Decomposition curve was made according to the method of Redlich et al., as shown in Fig. 1. These curves were extrapolated and the intersection with the saturation curve (dotted line) of urea in water were considered as the decomposition point.

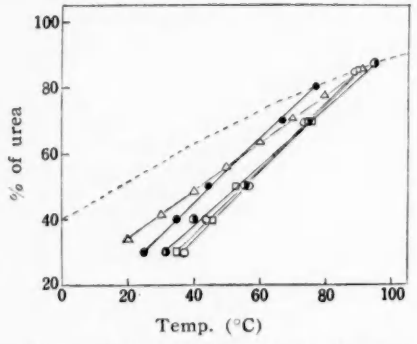

Fig. 1. Decomposition curve of urea adducts.
Dotted line: Urea saturation curve
◑: Mineral oil paraffin adducts
●: *n*-Hexadecane adducts
○: *n*-Nonadecane adducts
□: *n*-Heneicosane adducts
△: *n*-Hexadecane adducts by Redlich

As is shown in Table III, the decomposition point of *n*-hexadecane adduct is 78°C and is lowerthan Redlich's value, 90°C. Schlenk[7] showed that 97.5% of 1 mol. *n*-hexadecane adduct (12 mol. of urea and 1 mol. of *n*-hexadecane) was decomposed in 72 mol. of water at 31°C.

TABLE III. DECOMPOSITION TEMPERATURE OF UREA ADDUCTS

Hydrocarbons in adducts	Decomp. point (°C)	Urea[8] concn. (%)	Decomp. temp. (°C)
Lubricating oil paraffin	95	30	32.0
		40	39.5
		50	55.2
		70	75.0
n-Hexadecane	78	30	24.8
		40	35.0
		50	45.7
		70	67.0
n-Nonadecane	90	30	36.0
		40	43.5
		50	55.2
		70	74.5
n-Heneicosane	90	30	34.5
		40	44.0
		50	53.5
		70	75.0

This result means that 0.975 mol. of *n*-hexadecane adduct is decomposed 72 mol. of water at 31°C and 35.2% aqueous solution of urea is separated. According to the author's result, at the decomposition point of 31°C about 36% aqueous solution of urea is separated, and by Redlich et al. it corresponds to 41%. This deviation of the present result from the data of Redlich et al. was thought to be due to the difference of the determination method.

As *n*-nonadecane and *n*-heneicosane were separated from the same lubricating oil fraction, the decomposition points of these are nearly the same. *n*-Nonadecane sample used in this study is not so pure as is clearly seen from the comparison with the physical properties which have been cited in literature (cf. Table I), but in any case difference of the decomposition point between the carbon number ranges of 1 and 2 seemed to be comparatively small.

Effect of Benzene Addition.—The decomposition of adduct occurs when a sufficient amount of benzene or other hydrocarbon solvents were used at high temperatures. As might be expected, addition of benzene to the system which is composed of adduct and water, lowers the decomposition temperature. Fig. 2 shows the decomposition temperature of adducts containing

6) The values in the brackets were calculated by Redlich's equation[1], $m=0.653n+1.51$, where m is the mole ratio of urea to *n*-paraffin and n is the carbon number.

7) W. Schlenk. Jr., *Ann.*, **565**, 204 (1949).

8) Urea concentration means per cent of urea (in adducts) in the urea-water mixture.

43~233% (for urea in adducts) of water and 0~200% (for adducts) of benzene.

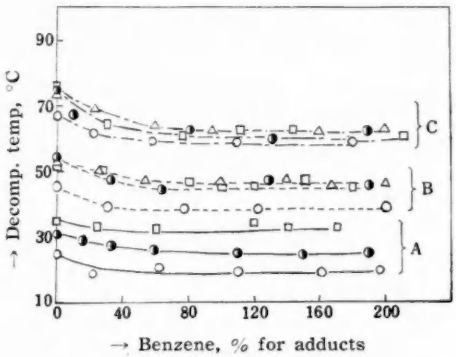

Fig. 2. Effect of benzene addition.
A: 233% water for urea in adducts,
B: 100%, C: 43%
◑: Mineral oil paraffin adducts
○: *n*-Hexadecane adducts
△: *n*-Nonadecane adducts
□: *n*-Heneicosane adducts

When the amount of benzene is increased, the decomposition temperature lowers; but the more the amount of water, the smaller the effect of benzene. The effect of benzene addition of 40~200% for adducts shows almost constant change of decomposition temperature: i.e., on addition of 233% water, temperature change is about 3~5°C, 100% water, 5~8°C, and 43% water, 10~12°C. This unchangeability of the decomposition temperature by the benzene addition may be caused by the limitation of decomposition by benzene itself. Hence, it can be seen that water has greater decomposition velocity than benzene has, and temperature dependence of the benzene decomposition is greater than that of water (Table IV).

Table IV shows the decomposition temperature of *n*-hexadecane adduct by benzene, and complete decomposition is obtained only when the boiling benzene (80°C) is used as 200% for adducts and five hours heating[9].

TABLE IV. DECOMPOSITION OF *n*-HEXADECANE ADDUCT BY BENZENE

Temp. (°C)	Heating time (hr.)	Benzene (% for adduct)	*n*-Hexadecane decomposed (%)
30	4	150	5
50	3	150	19
70	3	150	84
70	6	150	90
80	4	150	93
80	5	150	97.2
30	5	200	7
70	3	200	96
70	5	200	98.7
80	4	200	95
80	5	200	100

Decomposition temperatures of adducts of lower carbon paraffins are lower than those of higher ones, as might be expected from Fig. 2, yet this effect is less striking than water decomposition (Fig. 1).

Thanks are due to Mr. Katsuhiko Ide of this laboratory for many helpful experiments in the course of this work.

Nippon Mining Co.
Funakawa Oil Refinery
Oga-shi, Akita

9) This decomposition is carried out without stirring.

Studies on the Vibrated Dropping Mercury Electrode. I. The Theory of the Limiting Current and its Application to the Electrocapillarity

By Hideo IMAI, Senkichi INOUYE and Shōkichi CHAKI

(Received January 8, 1959)

When the dropping mercury electrode is vibrated by the application of an a. c. electric field, the limiting current of a depolarizer is augmented, the convection current being super-induced on the diffusion-controlled one. We called this new technique for improving the sensitivity of polarographic determinations the "VDME" method, and it was briefly reported in the previous communication[1]. Since the increment of the limiting current beyond the diffusion-controlled one depends upon the electric charge of the mercury-solution interface, this technique has a potentiality for the investigation of the electrocapillarity, especially for the determination of the zero-charge potential, i. e., the Lippmann-potential.

In this report, the theory of the limiting current and an accurate method for determining the Lippmann-potential are presented.

The Theory of the Limiting Current

The a. c. electric field exerts a moment of force as great as $q \cdot E \sin(\omega t) \cdot r \cdot \cos\theta$* on the center of the DME, and causes the forced vibration of the DME about the orifice of the capillary electrode (cf. Fig. 1). Counteracting this vibration, there exists the resistance due to the viscosity of the solution and the restoration of the displacement owing to gravity. Supposing that the former obeys Stokes's law, the moment of force is evaluated as great as $6\pi\eta r \cdot r \cdot r\,\mathrm{d}\theta/\mathrm{d}t$. The latter moment of force is equal to $Mg \cdot r \cdot \sin\theta$. Hence, one obtains the following equation of the vibration.

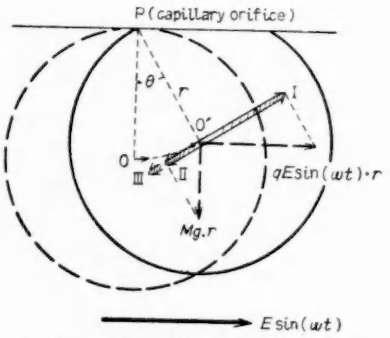

Fig. 1. The schematic representation of the forced vibration of the VDME: The moment of inertia, i, is equal to $q \cdot E \sin(\omega t) \cdot r \cos\theta$, ii is equal to $Mgr \cdot \sin\theta$ and iii is equal to $6\pi\eta r \cdot r \cdot r\,\mathrm{d}\theta/\mathrm{d}t$.

$$I\,\mathrm{d}^2\theta/\mathrm{d}t^2 = q \cdot E \sin(\omega t) \cdot r \cdot \cos\theta - Mg \cdot r \cdot \sin\theta - 6\pi\eta r \cdot r \cdot r\,\mathrm{d}\theta/\mathrm{d}t \qquad (1)$$

where the moment of inertia, I, is nearly equal to $2\pi r^2/5$. In Eq. 1, $\cos\theta$ and $\sin\theta$ can be exchanged for one and θ, respectively, provided the amplitude of the vibration is small. It is noteworthy that Eq. 1 holds only in approximation; the reason is that the sphere of the DME may be deformed by the vibration.

The solution of Eq. 1 is given in the following, the term of damped vibration being neglected.

$$\theta = \alpha\{(\beta-\omega^2)\sin\omega t - \gamma\omega\cos\omega t\}/\{(\beta-\omega^2)^2+\gamma^2\omega^2\} \qquad (2)$$

where $\alpha = qEr/I$, $\beta = Mgr/I$

and $\gamma = 6\pi\eta r^3/I$ (3)

Hence, the center of the DME moves at the velocity of

$$r\,\mathrm{d}\theta/\mathrm{d}t = \alpha r\{(\beta-\omega^2)\omega\cos\omega t + \gamma\omega^2\sin\omega t\}/\{(\beta-\omega^2)^2+\gamma^2\omega^2\} \qquad (4)$$

The mean velocity acquired during the motion from the site right under the capillary orifice to the site of the maximum

1) H. Imai, S. Inouye and S. Chaki, This Bulletin, 31, 767 (1958).

* The symbols used in this paper are listed below.
q=the surface charge of the DME.
E=the intensity of the a. c. electric field.
ω=the circular frequency of the a. c. electric field.
M=the mass of the DME.
g=the acceleration of gravity.
r=the radius of the DME.
η=the viscosity coefficient of the solution.
I=the moment of inertia of the DME.

amplitude can be evaluated by Eq. 5, i. e.,

$$(r\,\mathrm{d}\theta/\mathrm{d}t)_{\mathrm{mean}} = T/4 \cdot \int_0^{T/4} (r\,\mathrm{d}\theta/\mathrm{d}t)\,\mathrm{d}t$$
$$= 2\omega\alpha r(\beta-\omega^2+\gamma\omega)/\{(\beta-\omega^2)^2+\gamma^2\omega^2\} \quad (5)$$

where T is the period of the vibration.

Assuming that the concentration of the depolarizer at the vicinity of the electrode surface does not vary owing to the successive vibration, the treatment of Okinaka-Kolthoff's theory[2] developed for the limiting current of the rotated dropping mercury electrode can be applied to this case.

Thus, the following equation is given for the mean limiting current of the VDME;

$$\bar{i}_l = \bar{i}_d + knCD^{1/2}(m\tau)^{1/2}(r\mathrm{d}\theta/\mathrm{d}t)^{1/2}{}_{\mathrm{mean}} \quad (6)$$

where $\bar{i}_d$ is the mean diffusion-controlled current in μA, n is the number of electrons transferred per an ion, C is the bulk concentration of the depolarizer in mF, D is the diffusion constant in cm^2/sec., τ is the life-time of the DME in sec. and k is a numerical constant. In Eq. 6, it is assumed that the streaming velocity of the solution on and near the electrode surface is proportional to the velocity of the vibration. It is noteworthy that the actual surface velocity, and accordingly, the constant, k, are unknown.

Combining Eqs. 3, 5 and 6, one can obtain an expression for the relation between the limiting current and the surface charge of the DME;

$$\bar{i}_l = \bar{i}_d + k'(qE)^{1/2} \quad (7)$$

where k' is a proportionality factor.

The surface charge, q, of the DME in Eq. 7 can be evaluated by the following equation. Assuming Helmholtz's electrical double layer, we get

$$q = \varepsilon\varphi/4\pi\delta \quad (8)$$

where ε is the dielectric constant, φ is the potential of the DME and δ is the thickness of the electrical double layer.

Eqs. 7 and 8 lead to the following expression:

$$\bar{i}_l - \bar{i}_d = k''E^{1/2}(\varphi_{\mathrm{DME}} - \varphi_{\mathrm{max}})^{1/2} \quad (9)$$

where k'' is a proportionality factor, φ_{DME} is the potential of the DME and φ_{max} is the potential of the electrocapillary maximum.

From Eq. 9 it can be forecast that $(\bar{i}_l - \bar{i}_d)$ becomes practically zero at the potential of the electrocapillary maximum, and that the current-voltage curve of the VDME consists of two parabolas which intersect at the potential of the electrocapillary maximum. This curvilinear relation of the current and the potential can be transferred to the linear relation by plotting the square of the $(\bar{i}_l - \bar{i}_d)$ versus the potential of the DME.

The accurate determination of the Lippmann-potential will be carried out by evaluating the intersecting point of two straight lines of the $(\bar{i}_l - \bar{i}_d)^2$ versus φ_{DME} plot in the positive polarization and in the negative polarization, respectively.

Experimental

The current-voltage curve was recorded by a Shimadzu Model RP-2 polarograph. The DME used was of an appreciably long life-time and of the slow rate of mercury flow (τ=ca. 10 sec., $m \leq 1$ mg./sec.). It is because the mercury flow on the surface of the DME owing to the rapid growth of the mercury droplet presumably affects the ζ-potential of the mercury-solution interface.

The a. c. source was supplied from a C-R oscillater, and was amplified by a power tube (6L6G) and the cathode-follower out-put was applied to the platinum plate electrodes (Fig. 2).

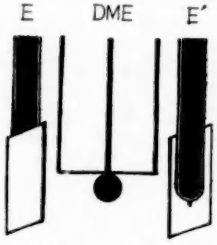

Fig. 2. VDME: E and E' are the platinum plate electrodes to which the a. c. voltage is applied.

Since the impedance of the solution was small, the cathode resistor as small as 30 ohms was used in order to avoid the voltage drop of the out-put. The a. c. voltage was measured by a vacuum tube voltmeter.

All the reagents were of analytical grade. The test solution contained 10^{-3} F Hg^{2+} as the depolarizer. The concentration of the supporting electrolyte ranged from 10^{-3} to 1 F. In the case of the low saline concentration, the depolarizer concentration as small as 10^{-4} F was preferable in order to avoid the migration current. Under these conditions the mercuric ion develops a well-defined wave by a conventional polarograph, and the diffusion-controlled current gives a plateau ranging from -0.1 to -1.7 volts vs. S. C. E. The trace of dissolved oxygen was carefully removed by adding a small quantity of the sodium sulfite solution after the sufficient

2) Y. Okinaka and I. M. Kolthoff, *J. Am. Chem. Soc.*, **79**, 3326 (1957).

bubbling of purified nitrogen. The presence of trace oxygen in the test solution causes the fatal deformation of the current-voltage curve, especially near the potential of the electrocapillary maximum in question.

Results and Discussion

The current-voltage curve of 0.77×10^{-3} F Hg^{2+} in 0.1 F KCl is illustrated in Fig. 3. In Fig. 3 the diffusion-controlled current gives a plateau covering the whole voltage span recorded.

In the region of the positive polarization, the vibration of the DME is gradually retarded as the applied potential is shifted toward more negative potentials, corresponding to the decrease of the surface charge of the DME, and this effect results in the decrease of the limiting current. At the zero-charge potential, that is, the potential of the electrocapillary maximum, the vibration entirely ceases, and accordingly the limiting current will be solely controlled by the diffusion of the depolarizer. Under the appreciably low intensity of the a. c. electric field, the limiting current coincides with the diffusion-controlled one at the potential of the electrocapillary maximum, while it is not so under the sufficiently intense electric field as is illustrated in Fig. 3. This reason is attributable to the fact that the rapid variation of the current at the potential close to the electrocapillary maximum can not be followed by the recorder owing to its damping. In the region of the negative polarization, the limiting current reincreases as the applied potential is shifted toward more negative potentials, corresponding to the increment of the surface charge of the DME. Thus, the limiting current gives a minimum at the potential of the electrocapillary maximum.

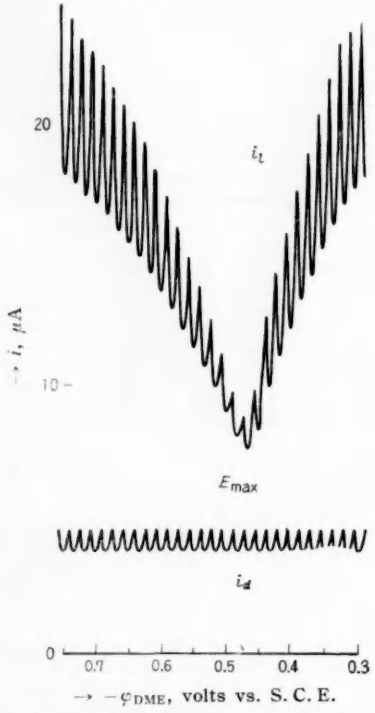

Fig. 3. The VDME current-voltage curve of 0.77×10^{-3} F Hg^{2+} in 0.1 F KCl. The a. c. frequency = 25 c. p. s. The intensity of the electric field = 0.55 volts/cm. $\tau = 9.9_4$ sec. (open circuit). $m = 0.85_5$ mg./sec. Temperature = 25°C. (The intensity of the a. c. electric field can be lowered when the trace of surface active materials is removed by adding active charcoal).

The square of $(\bar{i}_l - \bar{i}_d)$ is plotted versus the potential of the DME in Fig. 4. In Fig. 4, the parabolic curvilinear relation of the current-voltage curve in Fig. 3 is transferred to the linear relation as is predicted in Eq. 9. The mean value** of the potential at the intersecting point of

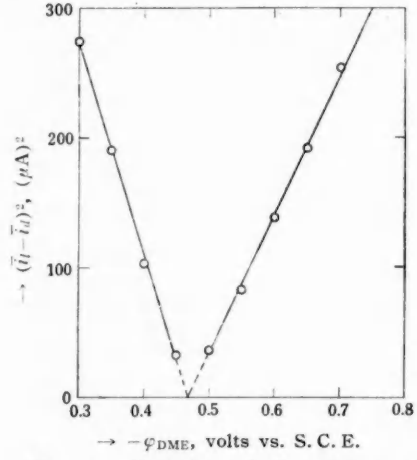

Fig. 4. Variation of the square of $(\bar{i}_l - \bar{i}_d)$ with the potential of the DME. The current was evaluated at the middle point of the saw-tooth oscillation in Fig. 3.

** This value was evaluated as the mean of the data obtained when the applied voltage sweeps toward more negative potentials and when the applied voltage sweeps toward less negative potentials.

two straight lines is -0.467 ± 0.001 volts vs. S.C.E. (in 0.1 F KCl solution). This value shows a very good agreement with the datum obtained by Grahame[3].

This method of determining the Lippmann-potential seems to be better than any other method[4] from the standpoints of the ease and rapidness of the recording, and of its good reproducibility and accuracy.

The authors wish to express their hearty gratitutde to Professor Mutsuaki Shinagawa for his advice and encouragement.

Laboratory of Chemistry, Minami College
Hiroshima University, Hiroshima

3) D. C. Grahame, *Chem. Revs.*, **41**, 441 (1947).
4) D. C. Grahame, R. P. Larson and M. A. Poth, *J. Am. Chem. Soc.*, **71**, 2978 (1949); T. I. Popova and T. A. Kryukova, *J. physik. Chem.*, **25**, 283 (1951); J. A. V. Butler, "*Electrocapillarity*", Methuen & Co., Ltd., London (1940), p. 56.

Visible and Ultraviolet Absorption Spectra of Red Complexes of 1,3,5-Trinitrobenzene and its Derivatives with Ammonium Hydroxide

By Takehiro Abe

(Received February 10, 1959)

Trinitrobenzene and its derivatives give red colors with ammonia and with aqueous alkalies. In 1902, Meisenheimer[1] already suggested the following formulae I and II like intermediates in aromatic substitutions, for structures of red products of 1,3,5-trinitrobenzene and trinitroanisole with sodium methoxide or sodium ethoxide, respectively.

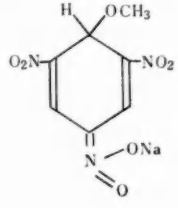

I

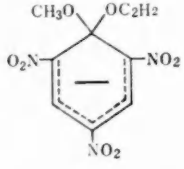

II

By means of the infrared or visible absorption spectra for the red complex of trinitroanisole Meisenheimer's structure II has recently been supported by Hammick and Foster[2,3], by Caldin et al.[4,5], and by Nagakura and Tsubomura[6]. In the previous papers[7,8] the present author also reported the visible absorption spectra of the red colors produced by trinitrobenzene, trinitrotoluene, and tetryl in dilute aqueous solutions of sodium hydroxide. These red colors were reversibly decolorized by addition of weak acids. All the above spectra have been measured directly for the red solutions prepared by adding alkaline solutions into solutions of the nitro compounds, and consequently have been subjected to be influenced by alkalies in the solutions, giving no precise molar absorbancies. In the present study, an attempt has, therefore, been made to determine molar extinction coefficients for the spectra of the red complexes of 1,3,5-trinitrobenzene, 2,4,6-trinitrotoluene, tetryl, and picryl chloride with ammonium hydroxide without the effect of alkali.

Experimental

Solvents.—All commercial guaranteed solvents were fractionally distilled after usual treatments.

Preparation of the Red Complexes of the Nitro Compounds with Ammonium Hydroxide.—A red-colored solution was prepared by

1) J. Meisenheimer, *Ann.*, **323**, 205, 214, 241 (1902).
2) D. L. Hammick and R. Foster, *J. Chem. Soc.*, **1954**, 2153.
3) R. Foster, *Nature*, **175**, 746 (1955).
4) E. F. Caldin and G. Long, *Proc. Roy. Soc.*, **A228**, 263 (1955).
5) J. B. Ainscough and E. F. Caldin, *J. Chem. Soc.*, **1956**, 2528, 2540, 2546.
6) S. Nagakura and H. Tsubomura, Personal Communication; at the Symposium on Electonic States in Tokyo on May 17, 1958.
7) T. Abe, This Bulletin, **31**, 904 (1958).
8) T. Abe, ibid., **32**, 339 (1959).

adding a little of guaranteed ammonia water (28%) into a solution made by dissolving each of the nitro compounds into acetone. This red solution was evaporated slowly at room temperature by a vacuum pump to remove acetone, ammonia and water, and a dark red residue was obtained. However, the red substance obtained

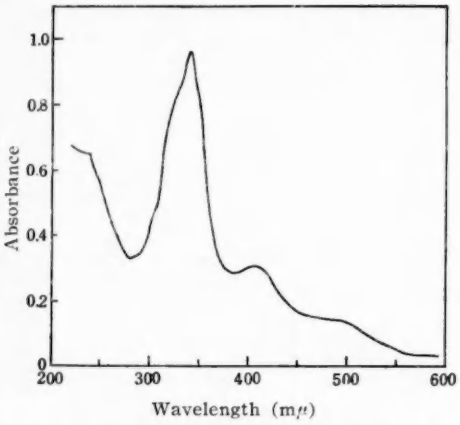

Fig. 1. An absorption spectrum of the red complex of trinitrotoluene with ammonium hydroxide, obtained by evaporation on a water bath, in water.

by evaporation not at room temperature but on a water bath gives an absorption curve illustrated in Fig. 1, which is very different from that indicated in Fig. 2, possibly owing to the further reaction. After being washed with a small quantity of acetone to remove the nitro compound contained, the red substance was dried again at room temperature by a vacuum pump. The powdered dark red product obtained is considered to be the colored complex of the nitro compound with ammonium hydroxide, which is more soluble in water than in acetone, while the nitro compound readily dissolves in acetone but not easily in water. By the above procedure, the red complex of picryl chloride could be obtained easily, although the red color produced by picryl chloride with sodium hydroxide in water disappeared in a few minutes[8].

Spectra.—The spectra of the solutions were measured with a Hitachi quartz spectrophotometer, Model EPU-2 at room temperature. The path length of absorption cells was 1 cm.

Trinitrobenzene forms with sodium methoxide a red product of the empirical composition, trinitrobenzene · CH_3ONa · $1/2H_2O$[9] and with sodium hydroxide a red one having the empirical composition, trinitrobenzene · NaOH[10], respectively. In the present work, the red complexes of the nitro compounds with ammonium hydroxide are assumed to have compositions of nitro compound·NH_4OH in calculating molar extinction coefficients for their spectra. This point is returned to below.

9) L. de Bruyn and van Leent, *Rec. trav. chim.*, **14**, 150 (1895).
10) Giua, *Gazz. chim. ital.*, **45**, II, 351 (1915).

Results and Discussion

The Spectra of the Red Complexes of the Nitro Compounds with Ammonium Hydroxide in Water (Fig. 2).—An absorption spectrum for the red complex of trinitrotoluene is similar to that for the

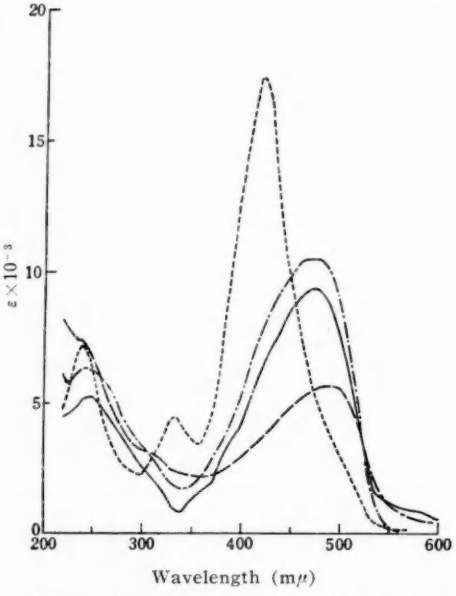

Fig. 2. Absorption spectra of the red complexes of trinitrobenzene (——), trinitrotoluene (— — —), tetryl (— · —), and picryl chloride (- - - -) with ammonium hydroxide, all in water.

complex of trinitrobenzene, showing an intense absorption maximum band at about 475 mμ, although a whole molar absorbancy for the former is slightly greater than that for the latter. This similarity implies that both the red complexes are structurally analogous. The red complex of tetryl also shows an analogous absorption curve with those of trinitrobenzene and trinitrotoluene, giving a weaker absorption maximum at about 490 mμ as compared with those for the latter. Only the red complex of picryl chloride shows an intense absorption maximum band at about 420 mμ as compared with those for the other complexes, and a weak band clearly at about 330 mμ. The 330 mμ band seems possibly to be attributed to the complex, although it has not been decided whether the band is due

to the complex itself or to picric acid formed by the further reaction[8], because the band lies at the wavelength close to that of the maximum for the picrate ion. All these red complexes give distinct bands at about 240 mμ.

The Spectra of the Red Complexes in Ethanol (Fig. 3).—These red comlexes in ethanol roughly show the similar spectra

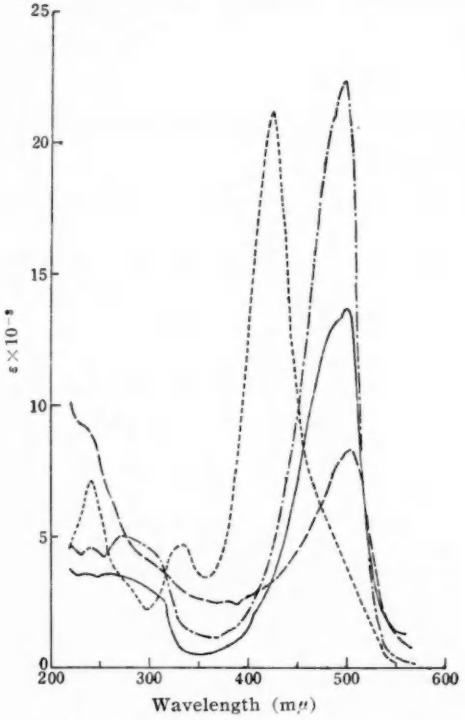

Fig. 3. Absorption spectra of the red complexes of trinitrobenzene (——), trinitrotoluene (—·—), tetryl (— —), and picryl chloride (----) with ammonium hydroxide, all in ethanol.

as in water. Both in ethanol and in water, the intense visible absorption bands for these complexes shift to the red in the order of picryl chloride, trinitrotoluene, trinitrobenzene, and tetryl with their molar absorbancies decreasing in the same order, except the molar absorbancy for picryl chloride in ethanol. The molar absorbancies for the 240 mμ bands increase in the order of trinitrobenzene, trinitrotoluene, picryl chloride, and tetryl. All the visible bands shift to the red and have greater molar absorbancies in ethanol as compared with those in water. Each of the wide visible bands for the red complexes of trinitrobenzene, trinitrotoluene, and tetryl in water is expected to consist of more than two absorption bands, because a shoulder is observed for the corresponding one in ethanol.

The red complexes between these nitro compounds and ammonium hydroxide may be regarded as the same complexes as those of the nitro compounds with sodium hydroxide or sodium methoxide. Accordingly, the red complexes with ammonium hydroxide can be presumed to have compositions of nitro compound · NH_4OH by analogy with the empirical compositions of trinitrobenzene · CH_3ONa[9], trinitrobenzene · $NaOH$[10], and trinitroanisole · CH_3ONa[11], as mentioned above. On standing in the cold with dilute aqueous solution of sodium hydroxide, 1,3,5-trinitrobenzene yields 3,5-dinitrophenol[12] through a red intermediate. Considering only this reaction, the red intermediate seems to be more like the following structure IV than like the structure III presented by Meisenheimer, as mentioned in the previous paper[8].

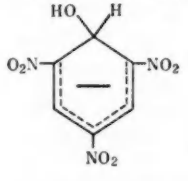

III

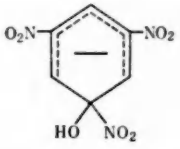

IV

The red color of the complex is certainly owing to transitions of its π-electrons. On the other hand, the complex of tetryl with sodium hydroxide finally produces a product indicating an absorption curve analogous to that for picric acid[8]. The red complex of tetryl with hydroxide anion is, therefore, expected to have Meisenheimer's structure V.

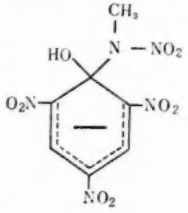

V

11) Jackson, *Am. Chem. J.*, **20**, 448 (1898); **23**, 294 (1901).
12) L. de Bruyn and van Leent, *Rec. trav. chim.*, **13**, 151 (1894).

However, Figs. 2 and 3 indicate that the spectra for the red complex of trinitrobenzene resemble those for the red complex of tetryl, as in the case of the red complexes with sodium hydroxide[8]. This similarity between their spectra can be explained by assuming the structure III for the red complex of trinitrobenzene, since the structure IV is hardly expected to be able to give the similar spectra as those for structure V owing to difference between their π-electron systems. In dilute aqueous solution of sodium hydroxide, picryl chloride finally gives an absorption curve analogous to that of picric acid after the red coloration[8], as in the case of tetryl. The red complex of picryl chloride with ammonium hydroxide is, therefore, expected to have the structure VI such as that for tetryl.

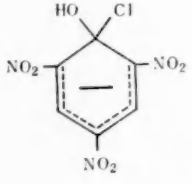

VI

Figs. 2 and 3, though not decisive, appear to be in favor of Meisenheimer's structures such as III, V and VI for all the above red complexes with ammonium hydroxide. Their structures are, however, to be determined hereafter by means of X-rays and infrared spectroscopy.

The difference between the spectra for the red complexes of tetryl and picryl chloride, which both seem to have the same π-electron structures indicated in V and VI, can be interpreted in terms of hyperconjugation of $-Cl$ and $-N(CH_3)NO_2$ to their π-electron systems.

Effect of Sodium Hydroxide on the Spectrum of the Red Complex of 2, 4, 6-Trinitrotoluene with Ammonium Hydroxide in Water (Fig. 4).—As the concentration of sodium hydroxide increases, the molar absorbancy for the spectrum of the red complex of trinitrotoluene with ammonium hydroxide decreases in water, and the decolorization of the red color becomes faster. On the other hand, all these red complexes of the nitro compounds are very stable both in water and in ethanol in absence of alkali. The negative ion OH^- is, therefore, considered

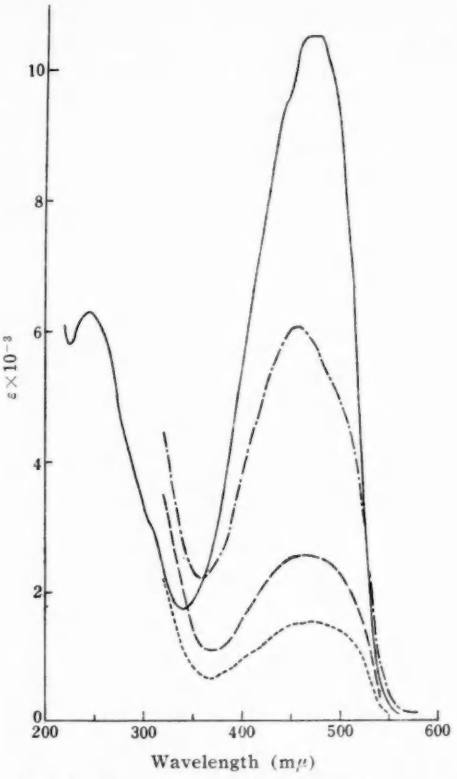

Fig. 4. Absorption spectra of the red complex of trinitroluene with ammonium hydroxide (4.96×10^{-5} M) in water (——) and in aqueous sodium hydroxide solution (0.103 N: – – –, 0.516 N: ——, 1.03 N: – – –).

to play an important role for the further decolorization reaction of the red complex. At a low concentration of sodium hydroxide, 0.103 N, the red complex of trinitrotoluene shows an absorption curve similar to that for trinitrotoluene in an aqueous solution of sodium hydroxide[7,8]. This leads to the suggestion that the absorption curves for the red complexes of the nitro compounds, reported in the previous papers[7,8], are somewhat affected by sodium hydroxide.

Summary

The red complexes of trinitrobenzene, trinitrotoluene, tetryl and picryl chloride with ammonium hydroxide, regarded as intermediates in aromatic substitutions, were obtained. Each of these red complexes roughly shows a similar spectrum

both in water and in ethanol. All their visible bands, however, shift to the red and have greater molar absorbancies in ethanol as compared with those in water. The red complex of trinitrobenzene shows an absorption curve analogous to that for the complex of tetryl, although they yield different products after further reactions. As the concentration of sodium hydroxide increases, the molar absorbancy for the spectrum of the red complex of trinitrotoluene decreases in water, probably owing to the action of OH^-.

The author is particularly indebted to Professor Y. Nomura for his suggestion and encouragement throughout this work. Thanks are also due to Dr. S. Maeda for the use of the spectrophotometer.

Department of Chemistry
Defense Academy
Yokosuka

SHORT COMMUNICATIONS

Infrared Spectroscopic Study on Hydrogen Bond Formation between Acetylene and Donor Solvents

By Shunsuke MURAHASHI*,
Bunkichi RYUTANI and Koichi HATADA*

(Received June 5, 1959)

It was previously reported by Copley[1], Huemer[2], and Mckinnis[3] that a donor solvent showed a high solvent power for acetylene. They suggested that this could be attributed to hydrogen bond formation between a hydrogen atom of methine group and a donor group of solvent. Any direct experimental evidence, however, has not been given.

In the course of our studies on the solubility of high pressure acetylene in various solvents at low temperature, some evidences which show the hydrogen bond formation have been accumulated by the measurements of the solubility in mixed solvents and of infrared spectra of acetylene. This communication deals with some results obtained from spectroscopic measurements[4].

The spectra were measured by means of a Perkin-Elmer model 21 double beam spectrophotometer equipped with a rock salt prism. The wave numbers of the absorption bands were corrected by the spectral data of a thin film of polystyrene measured right after each run. The error range of the observed wave numbers was about $\pm 5\,cm^{-1}$ at $3000\,cm^{-1}$ and about $\pm 1\,cm^{-1}$ at $700\,cm^{-1}$. Two cells of 0.1 mm. thickness filled with solution and with pure solvent respectively, were used in order to avoid interference of strong bands of the solvent. All the measurements were carried out at 20~25°C.

The spectral data of the acetylene dissolved in various solvents are given in Table I. As shown in Table I, the C–H stretching bands of acetylene in these solutions shift toward lower frequencies and the C–H deformation bands toward higher frequencies than those of gaseous acetylene. The largest shifts of the C–H stretching and deformation frequencies were found for ethyleneglycol dimethyl ether solution. On the other hand, the solution in *n*-octane, which shows the lowest solubility of acetylene, gives negligibly small shifts of the C–H stretching and deformation bands. The last column of Table I shows that the solubility of acetylene in donor solvents can be related to the magnitudes of the shifts of the C–H stretching and deformation frequencies. Therefore, it appears that a close relationship exists between the solubility of acetylene and the donating power of solvent molecules.

Further evidences of these arguments were also obtained by the absorption

* Present address: Department of Chemistry, Faculty of Science, Osaka University, Nakanoshima, Osaka.

1) M. J. Copley et al., *J. Am. Chem. Soc.*, **61**, 1599 (1939).

2) H. Huemer, Library of Congress, Washington 25, D. C., Microfilm file PB. 73508, (1942) p. 7274.

3) A. C. Mckinnis, *Ind. Eng. Chem.*, **47**. 850 (1955).

4) The results of the study of solubility will be reported in *J. Chem. Soc. Japan, Pure Chem. Sec.* (*Nippon Kagaku Zasshi*).

TABLE I. INFRARED ABSORPTION SPECTRA OF ACETYLENE IN VARIOUS SOLUTIONS*

Solvents	C-H stretching vibration		C-H deformation vibration		Solubility of acetylene at 0°C, 6.8 atm. C_2H_2 press., molefractions
	ν cm^{-1}	$\Delta\nu$** cm^{-1}	ν cm^{-1}	$\Delta\nu$** cm^{-1}	
n-Octane	3278	− 5	731	0	0.100
Benzene	3257	−26	742	11	—
n-Hexyl ether	3229	−54	—	—	0.303
Ethyleneglycol dimethyl ether	3205	−78	766	35	0.541

* Saturated solutions were prepared by bubbling dry acetylene through the solvents at 20°C under atmospheric pressure.

** $\Delta\nu = \nu - \nu_0$

ν_0: the value for gaseous acetylene

ν_0(for C-H stretching) = 3282.5 cm^{-1} [5]

ν_0(for C-H deformation) = 730.74 cm^{-1}

TABLE II. INFRARED ABSORPTION SPECTRA OF MONOSUBSTITUTED ACETYLENES AND THEIR SOLUTIONS IN ETHYLENEGLYCOL DIMETHYL ETHER

Monosubstituted acetylenes	ν_{C-H} or ν_{C-D} cm^{-1}			$\Delta\nu$* cm^{-1}
	Liq. substances	CCl_4 solutions (5 vol. %)	$CH_3OCH_2CH_2OCH_3$ solutions (5 vol. %)	
-C≡C-H	3281	3313	3241	− 72
-C≡C-D	2564	2583	2545	− 38
H-C≡C-$CO_2C_2H_5$	3238	3300	3196	−104
H-C≡C-C≡N	3238	3304	3151	−153

* $\Delta\nu = \nu_{C-H(or\ C-D)}$ (in $CH_3OCH_2CH_2OCH_3$ solution) $- \nu_{C-H(or\ C-D)}$ (in CCl_4 solution)

measurement of four monosubstituted acetylene derivatives as shown in Table II. The spectra of these compounds are somewhat complicated on account of an interaction between methine group and substituted group in the molecule. It is, however, of interest to see great differences between the frequencies of their C-H stretching bands in ethyleneglycol dimethyl ether solution and those in carbon tetrachloride solution. In these cases it is seen that the magnitude of the shift of the C-H stretching band depends upon the electronegativity of the substituted groups. All of the above results show that a hydrogen bond is formed between the solute and the donor solvent molecules.

Furthermore some additional evidences of the presence of these intermolecular interaction were also obtained. As shown in Table II, the absorption bands of pure liquid propiolic and cyanoacetylene considerably shift to lower frequencies than those in dilute carbon tetrachloride solution. These shifts may be attributed to the formation of intermolecular hydrogen bond.

Similar shifts were also observed for phenyl acetylene and its deuterated one. The shifts are, however, not so large as those of the above mentioned substances. Therefore, these small shifts may be caused by the "hydrogen-bond-like interaction" between π bonds of benzene nucleus and methine hydrogen[6].

The C-H deformation band was not observed in the rock salt region for the acetylene derivatives except for the case of cyanoacetylene where the frequency of the C-H deformation band was 671 cm^{-1} for the carbon tetrachloride solution and 736 cm^{-1} for the ethyleneglycol dimethyl ether solution. These results of the deformation band may also support the presence of hydrogen bond between the solute and the solvent.

The authors are grateful to Dr. H. Tadokoro in their laboratory for his helpful discussions and to the Research Laboratory

5) E. E. Bell and H. H. Nielsen, *J. Chem. Phys.*, **18**, 1382 (1950).

6) A. W. Baker and A. T. Shulgin, *J. Am. Chem. Soc.*, **80**, 5358 (1958); P. B. Schleyer et al., ibid., **80**, 6691 (1958).

of Dainippon Celluloid Co., Ltd., for the use of the spectrometer.

Institute of Scientific and Industrial Research
Osaka University
Sakai, Osaka

Polarographic Half-Wave Reduction Potentials of Vinyl Compounds and their Molecular Orbital Computation

By Takayuki Fueno, Kameo Asada, Keiji Morokuma and Junji Furukawa

(Received June 25, 1959)

The polarographic half-wave reduction potentials of several vinyl compounds have been determined under essentially identical condition*, and it has been found that these potentials are linearly related to the heights of the lowest vacant π-electronic energy levels of these compounds calculated by the LCAO MO method.

The reduction potentials were determined in a 3:1 dioxane-water mixture containing 0.05 M tetra-*n*-butylammonium iodide as a supporting electrolyte. All the compounds were purified by appropriate methods before use. A measured amount of vinyl compound was dissolved into the electrolyte solution so that its concentration was in the region ranging from 10^{-3} to 5×10^{-3} M.

The electrolysis-cell was immersed in a thermostat maintained at 25.0±0.1°C, and any oxygen dissolved in the solution was removed by passing through it a slow stream of oxygen-free and solvent-saturated nitrogen. The dropping-mercury electrode was polarized against a saturated calomel electrode (S. C. E.) connected to the mercury cathode through a pin-hole in the wall of the cell, and the current-voltage curve was recorded. Maxima of the current-voltage curves were suppressed by 10^{-5} M methylene blue incorporated in the sample solution. The half-wave potentials, $E_{1/2}$, were read against S. C. E. and were all corrected for *iR* drop. When tetra-*n*-butylammonium hydroxide was used as the supporting electrolyte, the potentials did not appreciably deviate from those determined in the iodide solution. All the obtained data on $E_{1/2}$ are listed in Table I.

In calculating the energies of the lowest vacant π-levels, the simple LCAO MO method (neglecting overlap integrals) was employed. For each vinyl compound $x_{l\nu}$, defined as $\varepsilon_{l\nu}=\alpha+x_{l\nu}\beta$, was obtained from the required secular equation. Here α and β are the Coulomb integral of a carbon atom and the resonance integral of a carbon-carbon π-bond, respectively, and $\varepsilon_{l\nu}$ is the energy of the lowest vacant π-level. To empirical integral parameters associated with heteroatoms, were assigned the same values that had previously been used to calculate the localization energies of vinyl compounds[1,2]: $\alpha_O=\alpha+2\beta$ (for carbonyl oxygens), $\alpha_O=\alpha+\beta$ (for ethereal oxygens), $\alpha_N=\alpha+\beta$, $\alpha_{Cl}=\alpha+1.8\beta$, $\alpha_C=\alpha-0.2\beta$ (for carbons bearing a methyl group), $\beta_{CO}=\sqrt{2}\beta$ and $\varepsilon=0.1$**. The

TABLE I. THE INTERRELATION AMONG $E_{1/2}$, $x_{l\nu}$ AND L_β FOR VINYL COMPOUNDS

Vinyl compound	$-E_{1/2}$ a) With Bu_4NI	$-E_{1/2}$ a) With Bu_4NOH	$-x_{l\nu}$	L_β b)
Acrylonitrile	2.01	1.95	0.314	1.240
Acrolein	1.53	—	0.315	1.214
Methyl vinyl ketone	1.67	1.63	0.386	1.299
Methyl acrylate	1.95	1.94	0.500	1.428
Methyl methacrylate	2.01	2.00	0.511	1.511
Styrene	2.35	2.35	0.662	1.704
α-Methylstyrene	2.39	2.39	0.692	1.843
β-Methylstyrene	2.54 c)	—	0.735	—
Phenyl vinyl ether	3.0	3.0	0.960	2.196
Ethylene	NW	NW	1.000	2.000
Vinyl acetate	NW	NW	1.065	2.130
Vinyl chloride	NW	NW	1.087	2.173
Propylene	NW	NW	1.105	2.210
n-Butyl vinyl ether	NW	NW	1.194	2.387
i-Butyl vinyl ether	NW	NW	1.194	2.387
Isobutylene	NW	NW	1.220	2.440

a) Given in volt vs. S. O. E. The mark NW means "no reduction wave".
b) Given in units of $-\beta$. The values are taken from Ref. 2.
c) H. A. Laitinen and S. Wawzonek, *J. Am. Chem. Soc.*, **64**, 1765 (1942).

* Some experimental data determined under different conditions are available, which can not be directly compared.

1) T. Fueno, T. Tsuruta and J. Furukawa, *J. Chem. Soc. Japan, Pure Chem. Sec.* (*Nippon Kagaku Zasshi*), **78**, 1075 (1957).
2) T. Fueno, T. Tsuruta and J. Furukawa, ibid., **78**, 1080 (1957).

** A carbon atom bearing one or more heteroatoms was assumed to have the Coulomb integral of $\alpha+\epsilon\beta\geq k_X\beta$. Here $\alpha+k_X\beta$ is the Coulomb integral of the heteroatom X.

resonance integrals for π-bonds other than carbonyl bonds were all assumed equal to β. The calculated values of x_{lv} are also listed in Table I. Since both α and β are negative quantities, the lowest vacant level ought to be more stable as x_{lv} takes a smaller negative value.

Inspection of the data given in Table I shows that, the smaller the value of x_{lv} for a vinyl compound, the more easily it can be reduced. Phenyl vinyl ether was found to have the highest reduction potential (ca. -3.0 V.) of all the compounds which could be reduced under the present experimental condition. At about -3.0 V. the residual current began to increase markedly owing to reduction of the supporting electrolyte. Vinyl acetate, vinyl chloride, *n*-butyl vinyl ether, *i*-butyl vinyl ether, ethylene, propylene and isobutylene gave no reduction waves in the range of the applied potential less negative than -3.0 V. vs. S. C. E. The situation may reasonably be explained by their relatively large values of $-x_{lv}$.

The half-wave potentials, $E_{1/2}$, determined with the ammonium iodide as the supporting electrolyte were found to be linearly correlated to x_{lv}'s by

$$E_{1/2} = 2.33\,x_{lv} - 0.80$$

the correlation coefficient being 0.995. The linear equation gives $\beta = -2.33$ eV., if it is assumed that, as in the case of unsaturated hydrocarbons[3,4], the electron transfer step from the electrode to vinyl compounds would be potential-determining. This value of β is in reasonable agreement with -2.23 eV.[4] for unsaturated hydrocarbons.

It seems interesting to note that the value of $-x_{lv}$ increases with increasing magnitude of the anionic β-carbon localization energy, L_{β}[-2)], of vinyl compounds, as seen in Table I. Thus, the polarographic reducibility of vinyl compounds may roughly parallel to their anionic polymerizability. This is to be expected, because vinyl compounds probably possess parallel susceptibilities toward an electron as well as basic substances. The detailed discussion on the present results will be published elsewhere.

Department of Industrial Chemistry
Faculty of Engineering
Kyoto University
Sakyo-ku, Kyoto

3) H. A. Laitinen and S. Wawzonek, *J. Am. Chem. Soc.*, **64**, 1765 (1942).
4) G. J. Hoijtink and J. van Schooten, *Rec. trav. chim.*, **72**, 903 (1953).

*The Abnormal Relation between the Viscosities and the Temperatures of Sodium Carbonate Solution**

By Kazuo FUJITA

(Received June 29, 1959)

It has been reported that the ultrasonic velocity and electric conductivity of the dilute solution of sodium sulfate present the abnormalities at the temperatures near the transition points of the saturated solution coexisting with the solid states[1,2].

But the reason why these abnormalities are caused is not fully explained in these reports. Therefore, this communication is to report that the abnormal relation between the viscosities and the temperatures was discovered in sodium carbonate solution.

The author believes that this result is a clue to the behavior of the aqueous solution, containing the inorganic compounds which have the transition-points in the saturated solutions.

In the viscosity measurements was used Ubbelohde suspended level viscometer,

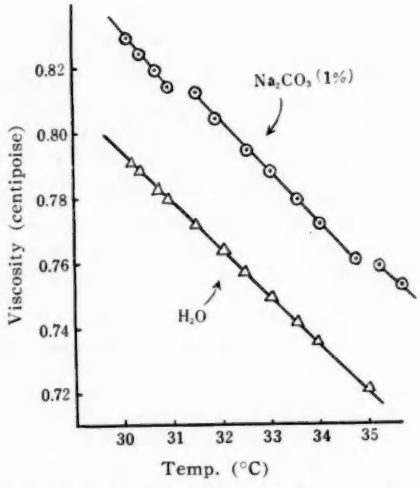

Fig. 1. Plot of viscosity against temperature for 1% Na_2CO_3 aqueous solution and distilled water.

* Presented at 12th Annual Meeting of the Chemical Society of Japan, Kyoto, April 2, 1959.
1) T. Sasaki and T. Yasunaga, *Chem. and Chem. Ind. (Kagaku to Kogyo)*, **7**, 146 (1954).
2) K. Hirano, *J. Chem. Soc. Japan, Pure Chem. Sec. (Nippon Kagaku Zasshi)*, **79**, 648 (1958).

the length and diameter of whose capillary are 20 cm. and 0.33 mm., respectively, and this viscometer being used, the flow time of distilled water 7 cc. was 2280 seconds at 25°C, and in this determination a kinetic energy correction was negligible. The temperature measurements were made with accuracy of ±0.01°C. At intervals of 0.5°C from 25 to 40°C, the flow time of 1% sodium carbonate solution and distilled water were measured using a stop watch. The results were shown in Fig. 1. From these results, it is seen that the changes of viscosity with temperatures were not smooth at about 31 and 35°C.

TABLE I. ENTHALPIES OF ACTIVATION FOR VISCOUS FLOW OF Na_2CO_3

Temp. range (°C)	Enthalpy of activation for viscous flow (kcal./mol.)
Below 30.93	5.11
31.43~34.90	3.11
35.29 and over	2.63

These two points of temperature correspond to the two transition points of the saturated sodium carbonate coexisting with the solid.

Eyring and coworkers[3] have applied the theory of absolute reaction rates to viscous flow and obtained following relation

$$\eta = hN/V \cdot \exp \Delta F^*/RT$$

where ΔF^* is the free energy of activation for viscous flow, V is the molar volume and the other constants have the usual significance. By using this relation the enthalpies of activation for viscous flow were calculated. The values of the enthalpies at below 30.9°C, 31.4~34.9°C and above 35.3°C are different from each other, and the data are shown in Table I.

The viscosity measurements are being made on solutions of sodium carbonate with various concentrations and dilute solutions of other compounds (e.g., Na_2HPO_4).

Department of Chemistry
Wakayama Medical College
Misono-cho, Wakayama

3) S. Glasstone, K. J. Laidler and H. Eyring, "The Theory of Rate Processes", McGraw-Hill Book Co., Inc., New York (1941).

The Syntheses and Exhaustive Methylation of cis- and trans-1,2,3,4,5,6,4a,4b-Octahydrobenzo[f]quinoline[1]

By Tadashi MASAMUNE
and Masato KOSHI*

(Received July 10, 1959)

A recent paper[2] has described the preparation and also Hofmann's exhaustive methylation of 4-methyl-1,2,3,4,5,6,4a,4b-octahydrobenzo[f]quinoline (II) R=Me. The stereochemistry of the ring fusion is tentatively assigned as *cis*.

The present paper undertakes to report the syntheses and exhaustive methylation of *cis*- and *trans*-1,2,3,4,5,6,4a,4b-octahydrobenzo[f]quinoline (II) R=H and (IV). These bases are interesting as 5,6-benzo-derivatives of decahydroquinoline.

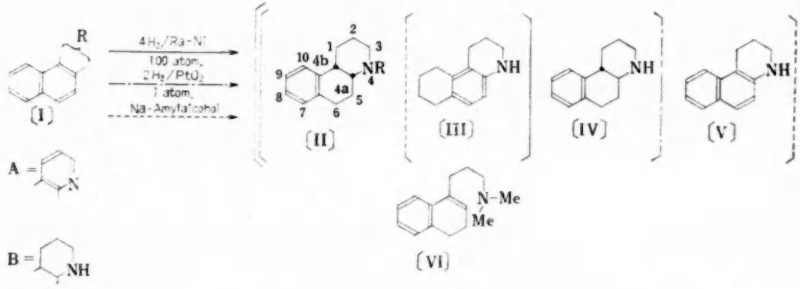

* Present address: Central Research Laboratory of Tōyōkōatsu Industries, Inc., Totsuka-ku, Yokohama.

1) Part X of "The Condensed Polynuclear Perhydrocompounds Containing Nitrogen"; Part IX, T. Masamune, This Bulletin, **30**, 491 (1957).

2) N. A. Nelson, J. E. Ladbury and R. S. Hsi, *J. Am. Chem. Soc.*, **80**, 6633 (1958).

Hydrogenation of benzo[f]quinoline[3] (I) R=A using a catalyst of Raney nickel (150°C) under 100 atm. initial pressure resulted in conversion into the mixture of octahydrobenzo[f]quinoline, consuming four molecular equivalents of hydrogen. From the ethereal solution of oily mixture, *cis*-octahydrobenzo[f]quinoline (II) R=H was isolated as carbonate. *cis*-1,2,3,4,5,6,4a,4b-Octahydrobenzo[f]quinoline[4], which was analyzed as the hydrochloride (Found: C, 64.46; H, 8.09. Calcd. for $C_{13}H_{17}N \cdot HCl \cdot H_2O$; C, 64.65; H, 8.28%.), can be regenerated from the carbonate by adding aqueous caustic alkali. Overall yield, 4.8%. The evaporation of the solvent from mother ethereal solution gave 1,2,3,4,7,8,9,10-octahydrobenzo[f]quinoline (III) in yield of 88%, but no *trans* isomeride could be isolated. On the other hand, hydrogenation of 1,2,3,4-tetrahydrobenzo[f]quinoline[5] (I) R=B in glacial acetic acid with platinum oxide as a catalyst at ordinary pressure, gave the mixture of *cis* and *trans* isomers of octahydrobenzo[f]quinoline in poor yield (*cis* and *trans* 2.4% each). The main product was 1,2,3,4,7,8,9,10-octahydrobenzo[f]quinoline. Yield, 86%. The separation of *cis* and *trans* isomerides was carried out most conveniently by means of the difference between the speed of carbonate formation of the *cis*- and *trans*-bases; thus, on exposing the mixture of *cis* and *trans* isomerides to air for a few hours the *cis* isomeride forms the carbonate preferentially.

Furthermore, the reduction of benzo[f]-quinoline to octahydro-derivatives by sodium and amylalcohol, which has been first described by Bamberger and Müller[3] was reexamined. In this case, *trans*-1,2,-3,4,5,6,4a,4b-octahydrobenzo[f]quinoline (IV) (2.9%) (Found: C, 83.25; H, 9.12; Calcd. for $C_{13}H_{17}N$: C, 83.43; H, 9.08%.), 1,2,3,4,7,8,9,10-octahydrobenzo[f]quinoline (III) (29%) and 1,2,3,4-tetrahydrobenzo-[f]quinoline (V) (39%) were obtained respectively from the reaction mixture.

Though no rigid proof can be given for the configuration of the above isomers,

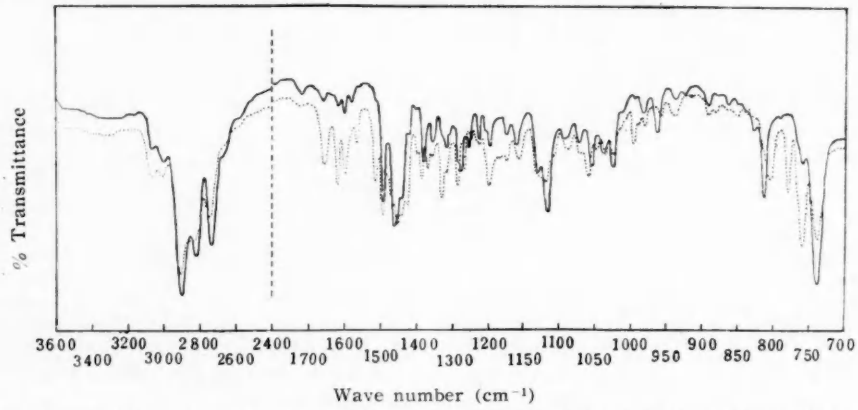

Fig. 1. The infrared spectra of *cis*- and *trans*-4-methyl-1,2,3,4,5,6,4a,4b,-octahydrobenzo[f]-quinolines.
cis: ------ *trans*: ——

TABLE I. PHYSICAL CONSTANTS OE THE *trans* AND *cis* ISOMERS AND THEIR DERIVATIVES

	cis, (°C)	*trans*, (°C)
1,2,3,4,5,6,4a,4b-Octahydrobenzo[f]quinoline	b. p. 160~165/5 mm.	m. p. 88~90[b]
Benzoate	m. p. 96~97	m. p. 100~102
Picrate	m. p. 197~198.5	m. p. 189~190
Hydrochloride	m. p. 258~259	m. p. 251~253[c]
N-Methylate picrate	m. p. 165~167	m. p. 210~212
Methiodide	m. p. 295[a]	m. p. 238~240

a) N. A. Nelson et al.[2] record m. p. 295°C (decomp.).
b) E. Bamberger et al.[3] record m. p. 91°C.
c) E. Bamberger et al.[3] record m. p. 252°C.

3) E. Bamberger and R. Müller, *Ber.*, **24**, 2648 (1891).
4) Analysis of free base was difficult, owing to rapid absorption of atmospheric carbon dioxide.
5) E. Bamberger and R. Müller, *Ber.*, **24**, 2641 (1891).

in view of the reduction conditions and other considerations[2] there is little doubt that the higher melting product resulting from the reduction with sodium-alcohol system is the *trans* isomeride. The infrared spectra of *cis*- and *trans*-*N*-methyl-octahydrobenzo[f]quinoline are shown in the figure. Physical constants of the *cis* and *trans* isomers and their derivatives are given in Table I.

Exhaustive methylation of *cis*-octahydrobenzo[f]quinoline has been recently carried out by Nelson et al.[2] who found that distillation of *cis*-octahydro-4-methylbenzo[f]quinoline methohydroxide produced 1-(3-dimethylaminopropyl)-3,4-dihydronaphthalene (VI). In the present investigation the Hofmann degradation of *cis*- and *trans*-octahydro-4-methylbenzo[f]-quinoline methohydroxides gave the same oily product in yields of 43% and 32%, respectively, boiling at 150~155°C/4 mm. (picrate m.p. 87~88°C), which was identified as 1-(3-dimethylaminopropyl)-3,4-dihydronaphthalene (VI), and no other compound could be isolated.

Examination of a model of the feasible structures for *cis*- and *trans*-*N*-methyl-octahydrobenzo[f]quinoline shows that in *cis* configuration the necessary conformational requirement for easy Hofmann fission is satisfied by elimination of any one of the equatorial 2-hydrogen, 4b-hydrogen and 5-hydrogen and in *trans* configuration by elimination of the equatorial 2-hydrogen.

Thus, in the exhaustive methylation of both *cis*- and *trans*-octahydrobenzo[f]-quinolines the preferential elimination of a β-proton on C 4b shows vividly that the influence of the electronic character of aromatic substituent at position C 4b is superior to the necessary co-planar *trans*-arrangement for easy Hofmann fission. Several examples[6] of this type of elimination have already been reported. Detailed results of the matters discussed in the present paper will be reported elsewhere.

Department of Chemistry
Faculty of Science
Hokkaido University
Sapporo

6) T. Masamune, This Bulletin, **30**, 491 (1957) and references given there; H. Booth, F. E. King and J. Parrick, *J. Chem. Soc.*, **1958**, 2302.

Thermal Homopolymerization of Lysine and Copolymerization with Neutral and Acidic Amino Acids[1]

By Kaoru HARADA

(Received July 15, 1959)

Glutamic acid and aspartic acid characteristically yield copolymers[2,3] with unsubstituted amino acids which fail to form polymers when heated individually. By using an excess of acidic amino acids, it is furthermore possible to copolymerize eighteen common amino acids into a *proteinoid*[4].

The special effects of basic amino acids, particularly lysine, are also interesting. Free DL-lysine was converted to its liquid lactam at 150~170°C with vigorous evolution of water vapor and it homopolymerized at 180~230°C.

The free lysine also copolymerized easily with glycine, alanine and other neutral amino acids, glutamic acid, aspartic acid, caprolactam, succinic acid, terephthalic acid and other carboxylic acids. After acidic hydrolysis, component amino acids were identified by paper chromatography. Infrared absorption spectra of lysine homopolymer, lysine-neutral amino acid copolymers and lysine-glutamic acid copolymer indicated that these are typical polypeptides. The salient maxima at 3080, 3280, 1630 and 1540 cm^{-1}; however, lysine-aspartic acid copolymer shows additional bands at 1720 and 1780 cm^{-1} which indicate the 5 membered cyclic imide structure[5],

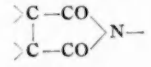

Some of the yield and amino acid composition of typical polymers are as follows:

DL-Lysine homopolymer*

Temp., °C	Yield after dialysis, g.
180	0.07
190	0.15
200	0.17
210	0.18

1) Contribution No. 116 of the Oceanographic Institute, aided by Grant C-3971 of the National Institutes of Health, U. S. Public Health Service.

2) K. Harada and S. W. Fox, *J. Am. Chem. Soc.*, **80**, 2694 (1958).

3) S. W. Fox, K. Harada and A. Vegotsky, *Experientia*, **15**, 81 (1959).

4) S. W. Fox and K. Harada, *Science*, **128**, 1214 (1958).

5) A. Vegotsky, K. Harada and S. W. Fox, *J. Am. Chem. Soc.*, **80**, 3361 (1958).

DL-Lysine-glycine copolymer**

Reaction conditions °C	hr.	Yield after dialysis g.	Amino acid composition*** Gly %	Lys %
180	2	0.65	77	23
190	1	0.68	62	38
200	1/2	0.64	60	40

DL-Lysine-DL-aspartic acid copolymer****

Temp. °C	Yield after dialysis g.	Amino acid composition*** Asp %	Lys %
170	0.09	33	67
180	0.19	31	69
190	0.99	25	75
200	1.13	24	76
210	1.23	22	78

* DL-Lysine (0.01 mol.) was heated for 2 hr.

** DL-Lysine (0.01 mol.) and glycine (0.01 mol.) were heated.

*** Amino acid compositions were determined by DNP method using column chromatography.

**** DL-Lysine (0.01 mol.) and DL-aspartic acid (0.01 mol.) were heated for 2 hr.

Lysine monohydrochloride did not homopolymerize but did copolymerized with glutamic acid, and with other amino acids in the presence of orthophosphoric acid. Lysine homopolymer was water-soluble (it contained some gel-like material), but it was nondiffusible through cellophane tubing. Lysine-glutamic acid and lysine-glycine copolymers were gel-like materials and lysine-aspartic acid copolymer was sponge-like. The amphoteric polymers of lysine-glutamic acid and also lysine-aspartic acid swelled in alkali and acid, and did not dissolve in either alkali or acid. It is likely that these polymers have a high degree of branching and have a quasi three-dimensional structure. α,ω-Linkage studies of lysine and acidic amino acid residues are now in progress. The lactam formation of lysine is very interesting as is copolymerization of glutamic acid with other amino acids[2]. The lactams serve as reactive intermediates, solvents for the reactions and also basic or acidic catalysts for peptide bond formation. At this time, the studies have revealed a new property of lysine and presented an easy way to prepare lysine-containing polymers.

The Chemistry Department and Oceanographic Institute of the Florida State University Tallahassee, Florida, U.S.A.